

University of Warwick institutional repository: <http://go.warwick.ac.uk/wrap>

A Thesis Submitted for the Degree of PhD at the University of Warwick

<http://go.warwick.ac.uk/wrap/57155>

This thesis is made available online and is protected by original copyright.

Please scroll down to view the document itself.

Please refer to the repository record for this item for information to help you to cite it. Our policy information is available from the repository home page.

**PHENAZINE ANTIBIOTIC PRODUCTION
IN LIQUID CULTURE, ON SURFACE AGAR,
AND ON PLANT ROOTS BY
PSEUDOMONAS AUREOFACIENS PGS12**

Nadine Antoinette SEVENO

A thesis presented for the degree of Doctor of Philosophy.

Department of Biological Sciences,
University of Warwick.

September, 2000.



CONTENTS

SECTION	TITLE	PAGE
	Summary	i
	Abbreviations	ii
	List of figures	iii
	List of tables	iv
	Declaration	v
	Acknowledgements	vi
	Publication	vii
<u>Chapter 1</u> <u>General Introduction</u>		
1.1	Fluorescent pseudomonads: Biological control agents	2
1.1.1	The genus <i>Pseudomonas</i>	2
1.1.2	Habitat and function	6
1.2	Biological control	7
1.2.1	Definitions	7
1.2.2	Biological control by rhizobacteria: Mechanisms and applications	8
1.2.3	Phenazine antibiotics and their biosynthetic pathway in <i>P. aureofaciens</i>	10
1.3	Quorum sensing in Gram-negative bacteria	10
1.3.1	Definitions	10
1.3.2	The <i>luxI/luxR</i> paradigm	12
1.3.3	Genetics and biochemistry of phenazine production	14
1.3.4	Regulation of phenazine production	15
1.3.5	Quorum sensing and starvation: Signals for entry into stationary phase	17
1.3.6	Biosensors of autoinducer signal molecules	20
1.3.7	Quorum sensing in other Proteobacteria	20

1.3.8	Novel families of intercellular signalling molecules	21
1.4	The use of reporter genes in microbial ecology	22
1.4.1	Detection of bacteria in environmental samples	22
1.4.1.1	Marker genes	22
1.4.2	Reporter genes of transcriptional activity	24
1.4.2.1	The <i>lux</i> reporter system	25
1.4.2.2	Ice nucleation genes	27
1.5	Aims of this study	28

Chapter 2 Materials and Methods

2.1	Media, reagents, and solutions	30
2.2	Bacterial strains and plasmids	30
2.2.1	Growth and maintenance of strains	30
2.3	Measurement of bacterial growth	33
2.3.1	Colony forming units (CFU)	33
2.3.2	Total cell counts (TCC) as measured by the CellFacts particle analyser	33
2.4.	Standard DNA manipulations	35
2.4.1	Electrophoresis of nucleic acids	35
2.4.1.1	Non-denaturing agarose gels	35
2.4.2	Recovery and purification of DNA fractionated on agarose gels	35
2.4.3	Nucleic acid extraction	35
2.4.3.1	Small scale preparation and purification of plasmid DNA	35
2.4.3.2	Large scale extraction of DNA	36
2.5	The polymerase chain reaction (PCR) and automated sequencing of PCR products	36
2.5.1	Standard PCR reaction	36
2.5.1.1	Design of oligonucleotide primers	38
2.5.2	Automated sequencing of PCR products	38

2.6	Mini-Tn5 transposon mutagenesis of <i>P. aureofaciens</i> PGS12	38
2.7	Detection and quantification of PCA	39
2.7.1	Extraction of total phenazines	39
2.7.2	Analysis of samples by HPLC	39
2.7.3	Quantification of PCA by spectrophotometry	40
2.7.4	Quantification of PCA with <i>Bacillus subtilis</i> 6051a	40
2.8	Measurement of <i>luxAB</i> expression	40
2.8.1	Measuring bioluminescence from liquid cultures	40
2.9	Monitoring gene expression on nutrient agar	40
2.9.1	Measurement of bioluminescence by luminometry	40
2.9.2	Measurement of bioluminescence using a CCD-camera	41
2.10	Monitoring gene expression in sterile rhizosphere of bean	41
2.11	Monitoring gene expression on sterile wheat seedlings	43
2.12	Statistical analysis	44

Chapter 3 **Selection of *LuxAB*-Marked *P. aureofaciens* Strains and Development of Bioassays**

3.1	Introduction	46
3.2	Aims	47
3.3	Mini-Tn5 transposon mutagenesis of <i>P. aureofaciens</i> PGS12	47
3.3.1	Recovery frequency of transconjugants	47
3.3.2	Phenotypic classification of <i>luxAB</i> -marked strains	47
3.3.2.1	Classification according to phenazine and HHL production	49
3.3.2.2	Classification according to pyoverdinin and mucus production	49
3.3.3	Genotypic characterisation of [HHL ⁺ , Phz ⁻] strains by PCR	49
3.3.3.1	Screening for insertion within the biosynthetic genes of the phenazine operon	49
3.3.3.2	Screening for insertion within <i>phzB</i>	53
3.3.4	Genotypic characterisation of [HHL ⁻ , Phz ⁻] strains by PCR	60
3.4	Bioluminescence measurements following decanal addition to liquid culture	60

3.5	Development of a <i>luxR</i> -based bioassay for detection and quantification of HHL	64
3.5.1	Dose-response curves	64
3.6	Extraction, detection, quantification, and biological activity of PCA	66
3.6.1	PCA extraction and analysis by HPLC	66
3.6.2	Quantification of PCA by spectrophotometry	68
3.6.3	Quantification of PCA with <i>Bacillus subtilis</i> 6051a	68
3.7	Conclusions and discussion	68
3.8	Future work	75

Chapter 4 Phenazine and HHL Production in Liquid Culture by *P. aureofaciens* PGS12

4.1	Introduction	78
4.2	Aims	79
4.3	Growth phases, cell density, and growth rates	79
4.3.1	Growth curve of <i>P. aureofaciens</i> PGS12 in NB	79
4.3.2	Comparing CFU and TCC	80
4.3.3	Growth phases and associated mean cell size	87
4.3.4	Influence of the inoculum concentration on the phases of growth culture and on cell diameter	87
4.4	Phenazine and HHL production by <i>P. aureofaciens</i> PGS12 in NB	91
4.4.1	Phenazine accumulation	91
4.4.2	HHL accumulation	92
4.5	Conclusions and discussion	97
4.5.1	Results: Summary	97
4.5.2	Discussion	97
4.6	Future work	101

Chapter 5 **Transcriptional Activity of the Phenazine Operon Studied with *luxAB*-Reporters in Liquid Culture**

5.1	Introduction	104
5.2	Aims	105
5.3	Selection of a strain with constitutive luciferase expression	105
5.4	Growth rates and bioluminescence from <i>P. aureofaciens</i> I17	107
5.4.1	Compared growth characteristics of strains I17 and PGS12	107
5.4.2	Bioluminescence profile of strain I17	107
5.4.3	Minimum detectable bioluminescence from strain I17 in liquid culture	110
5.5	Growth and bioluminescence profile of strain B103, reporter of phenazine gene expression	110
5.5.1	Compared growth characteristics and HHL accumulation from strains B103 and PGS12	110
5.5.2	<i>PhzB::luxAB</i> gene expression from strain B103	110
5.5.3	Comparison of bioluminescence from strains B103 and I17	113
5.5.4	Bioluminescence level and HHL concentration at the induction of the phenazine operon	117
5.6	Conclusions and discussion	117
5.6.1	Results: Summary	117
5.6.2	Discussion	118

Chapter 6 **Transcriptional Activity of the Phenazine Operon Studied with *luxAB*-Reporters on Solid Surface Agar**

6.1	Introduction	124
6.2	Aims	125
6.3	Growth of <i>P. aureofaciens</i> on nutrient agar	125
6.4	Production of phenazine and HHL on nutrient agar	128
6.4.1	Production of HHL	128
6.4.2	Production of phenazine	128
6.5	<i>LuxAB</i> -reporter activity	131

6.5.1	<i>LuxAB</i> -reporter activity measured with a CCD-camera	131
6.5.1.1	<i>LuxAB</i> -reporter activity monitored over time	131
6.5.1.2	<i>LuxAB</i> -reporter activity within colonies	131
6.5.2	<i>LuxAB</i> -reporter activity measured with a luminometer	134
6.6	Conclusions and discussion	134
6.7	Future work	143

Chapter 7 **Transcriptional Activity of the Phenazine Operon Studied with *luxAB*-Reporters on Bean Roots and Wheat Seedlings**

7.1	Introduction	145
7.2	Aims	146
7.3	Colonisation and luciferase activity on bean seedlings	147
7.3.1	Colonisation of bean roots	147
7.3.1.1	Total cell counts and density	147
7.3.1.2	Colonisation as seen with a CCD-camera	147
7.3.2	Luciferase activity and cell diameter on bean roots	151
7.3.2.1	Luciferase activity per TCC	151
7.3.2.2	Cell diameter	153
7.3.3	HHL and PCA detection	153
7.3.3.1	Testing HHL and phenazine detection in vermiculite	153
7.4	Colonisation and luciferase activity on wheat seedlings	153
7.4.1	Colonisation of wheat seedlings	156
7.4.1.1	Total cell counts	156
7.4.2	Luciferase activity and cell diameter on wheat seedlings	156
7.4.2.1	Luciferase activity measured with a luminometer	156
7.4.2.2	Cell diameter	156
7.4.2.3	Bioluminescence measured with a CCD-camera	156
7.4.2.4	Colonisation of wheat seedlings visualised using a CCD-camera	163
7.5	Comparison of bioluminescence from cells growing in liquid culture, colonies, on bean roots, and on wheat seedlings	163

7.6	Conclusions and discussion	165
7.7	Future work	168
<u>Chapter 8</u>	<u>Concluding Discussion</u>	169
<u>Chapter 9</u>	<u>References</u>	182

SUMMARY

The growth of *P. aureofaciens* PGS12 was followed in nutrient broth, on nutrient agar, and on plant roots by monitoring cell numbers, the production of the autoinducer *N*-acyl-L-hexanoyl homoserine lactone (HHL), and the antibiotic phenazine-1-carboxylic acid (PCA). In nutrient broth, as the growth rate declined, HHL synthesis increased rapidly. Up to 38% more HHL was produced compared to the increase in cell numbers indicating that transcription of the phenazine operon was autoinduced. As the bacterial culture entered stationary phase, HHL concentration declined rapidly while PCA concentration continued to accumulate at a high rate. In stationary phase, HHL concentration continued to decline while PCA accumulated slowly. A promoterless mini-Tn5-*luxAB* transposon was used to generate isogenic strains of *P. aureofaciens* PGS12. Strain B103 was shown to have the *luxAB* reporter gene inserted in the *phzB* gene within the phenazine operon. Phenazine transcriptional activity (bioluminescence) was compared with the light output from a constitutive reporter, strain I17. Levels and pattern of bioluminescence from strain B103 followed closely HHL production and indicated that gene expression was maximal in transition phase and silenced in stationary phase. PCA production continued in stationary phase suggesting that the protein products of the phenazine operon were maintained in the cell after down regulation. The induction of the phenazine operon started in nutrient broth when cell density was ca. 2×10^8 cells ml⁻¹ and HHL had accumulated to a threshold concentration of $0.63 \times 10^{-6} \pm 0.3 \times 10^{-6}$ ng cell⁻¹.

On NA, cells were in a transition phase of growth for at least 9 h. The cell density was 55 to 75 times higher within a colony than in liquid culture. The maximal production of HHL and light output per calculated equivalent volumes were also between 50 and 65 times higher on NA than in broth. The maximal light output and maximal HHL accumulation per cell were similar on both media. Therefore, the increased levels on NA may be mainly due to a higher cell number in the colony. The production of the antibiotic PCA per cell was ca. 7 times higher in a colony than in NB, and the production in an equivalent volume was ca. 360 times higher in a colony. Therefore, the higher PCA concentration in the colony cannot be explained solely on the basis of an increase in cell density. The autoinducer concentration remained high within a colony for a prolonged period of time compared to the burst seen in NB. A high concentration of HHL per cell for a longer period of time may have sustained the greater production and accumulation of PCA in the colony. Similarly the transcriptional activity of the phenazine operon, as reflected by *phzB::luxAB* expression in strain B103, remained maximal during this time.

In contrast to laboratory culture studies, in all the experiments where *P. aureofaciens* PGS12 was inoculated onto roots, neither HHL nor PCA was detected, although the bacteria colonised the bean roots and wheat seedlings efficiently. On wheat seedlings, the transcriptional activity from both reporter strains decreased during the experiment. On bean roots, bioluminescence per cell from strains I17 and B103 increased 25-fold during the first 3 days and the ratio of bioluminescence from strains B103 over I17 indicated an up to 5 times greater transcriptional activity from strain B103 than from strain I17. The minimum levels for the detection of HHL and PCA were low. Therefore, either these compounds were produced in minute amounts, or HHL and phenazine were degraded or adsorbed onto the plant material lowering their levels below the detection limit.

ABBREVIATIONS

AHL	<i>N</i> -acyl-L-homoserine lactone
bp	Base pair
BSA	Bovine serum albumine
CCD	Charge coupled device
CFU	Colony forming unit
°C	Degrees Celsius
DNA	Deoxyribonucleic acid
DSW	Distilled sterilised water
EDTA	Ethylenediaminetetraacetic acid
g	Gram
G + C	Guanine and Cytosine
h	Hour
μ	micro
min	Minute
M	Mole
NB	Nutrient agar
NA	Nutrient broth
n	Nano
OD	Optical density
PBS	Phosphate buffer solution
PCA	Phenazine-1-carboxylic acid
PCR	Polymerase chain reaction
PIA	<i>Pseudomonas</i> isolation agar
RLU	Relative light unit
RNA	Ribonucleic acid
rpm	Revolution per minute
SDS	Sodium dodecyl sulphate
s	Second
sp.	Species

spp.	Species (plural)
TBE	Tris-borate EDTA
TE	Tris-EDTA
T _m	Melting temperature
Tris	Tri-hydroxymethyl-aminomethane
V	Volts
v/v	volume per volume
w/v	weight per volume
xg	Centrifugal force

LIST OF FIGURES

1.1	Inferred phylogenetic relationships among species of <i>Pseudomonas (sensu stricto)</i> and other members of the γ sub-division of the Proteobacteria.	5
1.2	Structures and numbering system of phenazine antibiotic compounds (from Turner and Messenger, 1986).	11
1.3	Structures of <i>N</i> -acyl-L-homoserine lactones (AHLs), the <i>Pseudomonas</i> Quinolone Signal (PQS), a diketopiperazine (DKP), and a butyrolactone (A-factor).	13
1.4	Proposed pathway for the biosynthesis of PCA and 2-OH-PCA in <i>P. aureofaciens</i> spp.	18
2.1	Example of a cell size distribution profile of a bacterial culture obtained with a CellFacts instrument.	34
3.1	Colonies of <i>P. aureofaciens</i> PGS12 (in orange) and of an isogenic <i>lux</i> -marked [HHL ⁺ , Phz ⁻] strain on nutrient agar after 24 h of growth at 30°C.	48
3.2	PCR amplification of <i>phzA</i> with <i>phzAfd</i> and <i>phzArv</i> primers.	54
3.3	PCR product from <i>phzB</i> obtained with <i>phzBfd</i> and <i>phzBrv</i> primers.	55
3.4	PCR products obtained with the <i>luxAB3rv</i> primer.	56
3.5	Alignments results from BlastA database with the sequence IRB2.	57
3.6	Localisation of the miniTn5 <i>luxAB</i> insertion within <i>phzB</i> .	59
3.7	PCR amplification of <i>phzI</i> with <i>I3fd</i> and <i>Irv</i> primers for [HHL ⁻ , phz ⁻] strains.	61
3.8	Bioluminescence following addition of decanal ($\mu\text{l ml}^{-1}$) to <i>P. aureofaciens</i> B103.	62
3.9	Description of the bioassay for detection and quantification of AHLs.	65
3.10	Construction of a calibration curve for HHL quantification: Effect of the incubation time (Fig. 3.10a) and the concentration of the test	

	organism, <i>E. coli</i> JM107 (pSB401) (Fig. 3.10b and 3.10c).	67
3.11a	Chromatogram overlay plot of a phenazine sample (extracted phenazine) and a pure standard of PCA.	69
3.11b	Phenazine calibration curve obtained by HPLC analysis of a PCA standard.	70
3.12	Calibration curve of PCA concentrations against absorbance at OD ₃₆₉ in 5% (w/v) NaHCO ₃ , pH7.	71
3.13	Growth inhibition of <i>B. subtilis</i> 6051a against <i>P. aureofaciens</i> PGS12 (Fig. 3.13a) and PCA calibration curve obtained against the growth of <i>Bacillus subtilis</i> 6051a (Fig. 3.13b).	72
4.1	Growth curve for <i>P. aureofaciens</i> PGS12 in NB at 28°C.	81
4.2	Volumetric and specific growth rate for <i>P. aureofaciens</i> PGS12 in NB at 28°C.	82
4.3	Growth curve for <i>P. aureofaciens</i> PGS12 in NB at 28°C.	84
4.4	Growth curve A of <i>P. aureofaciens</i> PGS12 and associated cell size profile (Fig 4.4a) and specific growth rate (Fig 4.4b).	86
4.5	Time course of 3 cultures of <i>P. aureofaciens</i> PGS12 from 3 inoculum concentrations and associated mean cell size distribution.	88
4.6	Changes in cell size in relation to cell density (TCC) in growth cultures A, B, and C started at 3 different inoculum concentrations.	90
4.7	Time course of the growth of <i>P. aureofaciens</i> PGS12 and volumetric (Fig. 4.7a) or specific (Fig. 4.7b) phenazine accumulation.	93
4.8	Time course of the growth of <i>P. aureofaciens</i> PGS12 and volumetric (Fig. 4.8a) or specific HHL accumulation (Fig. 4.8b).	94
4.9	Accumulation of phenazine (Fig. 4.8a) and HHL (Fig. 4.8b) and cell size variation during the culture of <i>P. aureofaciens</i> PGS12 started at three inoculum concentrations in NB at 28°C.	95
4.10	Rate of PCA and HHL accumulation from <i>P. aureofaciens</i> PGS12	

	(Fig. 4.10a), relative growth and accumulation of PCA and HHL as a function of time (Fig. 4.10b), and as a function of growth (Fig. 4.10c).	106
5.1	Selection of a constitutive <i>luxAB</i> -reporter: Growth and bioluminescence per cell of <i>luxAB</i> -marked strains.	108
5.2	Growth curves and associated cell size profiles (Fig. 5.2a) and accumulation of PCA and HHL (Fig. 5.2b) for <i>P. aureofaciens</i> strains PGS12 and I17.	109
5.3	Growth and bioluminescence curves for <i>P. aureofaciens</i> I17.	
5.4	Growth cultures of <i>P. aureofaciens</i> B103 and PGS12 and associated cell size profiles (Fig. 5.4a) and relative HHL accumulation (Fig. 5.4b).	111
5.5	Growth curve of <i>P. aureofaciens</i> B103 (Fig. 5.5a), specific growth rate (Fig. 5.5b) and pattern of <i>phzB::luxAB</i> activity.	112
5.6	Relative growth, accumulation of HHL and bioluminescence as a function of time (Fig. 5.6a and 5.6b) and as a function of growth (Fig. 5.6c).	114
5.7	Bioluminescence per cell as a function of cell density from strain I17 (Fig. 5.7a) and strain B103 (Fig. 5.7b, 5.7d, and 5.7e) from cultures started at 3 different inoculum concentrations, and ratio of bioluminescence from strain B103 (culture B) over strain I17.	115-116
5.8	Luciferase activity from the <i>phzB::luxAB</i> gene fusion in strain B103 reports the transcription of the phenazine operon and the autoinduction process.	119
6.1	Growth of <i>P. aureofaciens</i> PGS12, I17, and B103 in colonies on NA and associated cell diameter (Fig. 6.1a) and generation time (Fig. 6.1b).	126
6.2	Colonies of <i>P. aureofaciens</i> PGS12 growing on NA after 0, 3, 6, 9, 12 and 24 h incubation at 21°C.	127
6.3	Production of HHL per colony (Fig. 6.3a) and per cell (Fig. 6.3b) by <i>P. aureofaciens</i> PGS12, B103 and I17 on NA.	129

6.4	Production of PCA per colony (Fig. 6.4a) and per cell (Fig. 6.4b) by <i>P. aureofaciens</i> PGS12 and I17 on NA.	130
6.5	Gene expression from <i>P. aureofaciens</i> B103 and I17 measured from video-images taken with a CCD-camera.	132
6.6	Colonies of <i>P. aureofaciens</i> B103 and I17 expressing the <i>luxAB</i> reporter genes on NA.	133
6.7	Bioluminescence per ml and per cell from <i>P. aureofaciens</i> strain I17 (Fig. 6.7a) and strain B103 (Fig. 6.7b) in colonies growing on NA at 21°C and ratio of luminescence from strain B103 over I17 (Fig. 6.7c).	135
6.8	Luminescence and HHL accumulation by <i>P. aureofaciens</i> B103 on NA per cell as a function of time (Fig. 6.8a and Fig. 6.8b with relative values) and as a function of cell density (Fig. 6.8c).	136
7.1	Colonisation of bean roots in sterile vermiculite by <i>P. aureofaciens</i> strains PGS12, B103 and I17.	148
7.2	Colonisation of bean roots by strain B103 carrying a <i>phzB::luxAB</i> gene fusion taken with a CCD-camera after 24 h (A) and 3 days (B) (Fig. 7.2a, Fig. 7.2aref), after 5 days (Fig. 7.2b, 7.2bref), and after 9 days (Fig. 7.2c, 7.2cref).	149-150
7.3	<i>LuxAB</i> -reporter activity from <i>P. aureofaciens</i> strains B103 and I17 on bean roots and ratio of bioluminescence from strain B103 over the average value of bioluminescence from strain I17 (Fig. 7.3c).	152
7.4	Average cell diameter of <i>P. aureofaciens</i> strains PGS12, B103, and I17 colonising sterile bean roots over 9 days.	154
7.5	Colonisation of wheat seedlings by <i>P. aureofaciens</i> strain B103, I17, and PGS12.	157
7.6	Bioluminescence from <i>P. aureofaciens</i> strains B103 and I17 on wheat seedlings.	158
7.7	Ratio of bioluminescence (Fig. 7.7a) from <i>P. aureofaciens</i> strain B103 over the average bioluminescence level from strain I17 and cell diameter (Fig. 7.7b) on wheat seedlings.	159

7.8	<i>LuxAB</i> -reporter activity from <i>P. aureofaciens</i> B103 and I17 on wheat seedlings video-imaged with a CCD-camera.	160
7.9	Wheat seedlings after 68 h of colonisation by <i>P. aureofaciens</i> strain B103 (top 15 seedlings) and strain I17 (bottom 15 seedlings) as seen by a CCD-camera.	161-162
8.1	Model for control of phenazine regulation in <i>P. aureofaciens</i> PSG12 (adapted from Chancey <i>et al.</i> , 1999).	175

LIST OF TABLES

1.1	Species currently classified as members of the genus <i>Pseudomonas</i> (Kerstens <i>et al.</i> , 1996).	3
1.2	Characteristics of the phenazine gene cluster in <i>P. aureofaciens</i> 30-84 (from Pierson III <i>et al.</i> , 1994, 1995; Wood <i>et al.</i> , 1996).	16
2.1	Media, reagents, and solution used in this study.	31
2.2	Bacterial strains and plasmids used in this study and relevant characteristics.	32
2.3	Standard PCR reaction.	37
3.1	Classification of <i>luxAB</i> -marked <i>P. aureofaciens</i> strains for HHL and phenazine production.	50
3.2	Classification of <i>luxAB</i> -marked <i>P. aureofaciens</i> strains for HHL, phenazine, mucus ¹ and siderophore production.	51
3.3	Primers and conditions for PCR amplification.	52
3.4	Viability of <i>P. aureofaciens</i> B103 following a 10-min incubation with decanal.	62
4.1	Growth rates and cell density in two growth cultures of <i>P. aureofaciens</i> PGS12 in NB at 28°C.	83
4.2	Comparison of growth rates in the growth culture of <i>P. aureofaciens</i> PGS12 in NB obtained as TCCs or CFUs (detailed in Fig. 4.3).	85
4.3	Growth characteristics of cultures A, B, and C of <i>P. aureofaciens</i> PGS12 in NB at 28°C (detailed in Fig. 4.5).	89
6.1	Comparison of values obtained in NB and on NA.	139
7.1	Detection of PCA and HHL in Hoagland solution mixed with vermiculite.	155
7.2	Bioluminescence per cell from strains B103 and I17 on laboratory media and on plant roots.	164

DECLARATION

This thesis has been composed by myself and has not been used in any previous application for a degree. The results presented here were obtained by myself and all sources of information have been specifically acknowledge by reference.

Nadine A. Seveno.

ACKNOWLEDGEMENTS

I would like to thank my supervisors, Prof. Liz Wellington and Dr. Alun Morgan, for their enthusiasm, encouragement and academic input that has made this work possible and for financial support that has enabled me to present my work at conferences.

I would like to thank Jane Green and Margaret Ousley for their technical assistance respectively at the University of Warwick and at Horticulture Research International.

Numerous people in the departments, at Warwick University and at HRI, past and present, have proven friendly and helpful. I would not have been able to succeed in this research without the continuous help from everyone in the labs where I worked. I would like to thank especially people in the laboratory of Dr C. Dow and of Dr A. Millar.

PUBLICATION

Authors: Seveno N.A., Morgan J.A.W., Wellington E.M.H.

Title: Growth of *Pseudomonas aureofaciens* PGS12 and the dynamics of HHL and phenazine production in growth media and on plant roots.

Date submitted: 26/07/2000.

Returned: 24/09/2000.

Editors comments: The paper has been accepted for publication with minor modifications.

CHAPTER ONE

GENERAL INTRODUCTION

CHAPTER ONE

GENERAL INTRODUCTION

1.1. FLUORESCENT PSEUDOMONADS: BIOLOGICAL CONTROL AGENTS

1.1.1. *The genus Pseudomonas*

Migula proposed the genus *Pseudomonas* in 1884 and its description has been since thoroughly revised on several occasions. The general, and still valid characteristics, as described by Palleroni (1984) are: straight or slightly curved rod shaped Gram-negative cells (approximately 0.5 to 1.0 μm by 1.5 to 5 μm in length); many species accumulate poly- β -hydroxybutyrate (PHB) as carbon reserve material; motile by one or more polar flagella, rarely non-motile; aerobic, having a strictly respiratory type of metabolism with oxygen as terminal electron acceptor (in some cases nitrate can be used as an alternative electron acceptor); some species are facultative chemolithotrophs and are able to use H_2 or CO as energy sources. The first well-documented arguments for the multigeneric nature of *Pseudomonas* came from the pioneering studies of Palleroni and collaborators (1973) at Berkeley. By measuring the percentage similarity of various *Pseudomonas* species by rRNA:DNA hybridisation, they were able to subdivide the genus into five distantly related so-called rRNA groups (rRNA groups I to V). The combined data from 16S rRNA sequence analysis, rRNA-DNA hybridisation and polyphasic taxonomic studies (including DNA:DNA hybridisation) contributed to the present knowledge of the phylogenetic distribution of the pseudomonads. The genus *Pseudomonas* belongs to the γ -subclass of the *Proteobacteria*, and is now restricted to the rRNA group I. It encompasses 36 genuine *Pseudomonas* species which display genomic and phenotypic characteristics similar to the type species *Pseudomonas aeruginosa* (Kerstens, 1996; Table 1.1). The majority of the other species have been reclassified as the genera *Burkholderia*, *Ralstonia*, *Brevundimonas*, *Sphingomonas*, *Xanthomonas*, *Stenotrophomonas* and as members of the family *Comamonadaceae* comprising the genera *Acidovorax*, *Comamonas* and *Hydrogenophaga* (Kerstens *et al.*, 1996).

Table 1.1. Species currently classified as members of the genus *Pseudomonas* (Kerstens *et al.*, 1996).

<i>P. aeruginosa</i> (type strain)	<i>P. fuscovaginae</i>
<i>P. agarici</i>	<i>P. lundensis</i>
<i>P. alcaligenes</i>	<i>P. marginalis</i> (various pathovars)
<i>P. amygdali</i>	<i>P. meliae</i>
<i>P. anguilliseptica</i>	<i>P. mendocina</i>
<i>P. asplenii</i>	<i>P. mucidolens</i>
<i>P. avellanae</i>	<i>P. oleovorans</i>
<i>P. balearica</i>	<i>P. pseudoalcaligenes</i>
<i>P. caricapapaye</i>	<i>P. putida</i> (2 biovars)
<i>P. chlororaphis</i>	<i>P. resinovorans</i>
<i>P. chichorii</i>	<i>P. savastanoi</i>
<i>P. citronellolis</i>	<i>P. stanieri</i>
<i>P. coronofaciens</i>	<i>P. stutzeri</i>
<i>P. corrugata</i>	<i>P. synxantha</i>
<i>P. fiscurectae</i>	<i>P. syringae</i> (various pathovars)
<i>P. flavescens</i>	<i>P. taetrolens</i>
<i>P. fluorescens</i> (various biovars)	<i>P. tolaasii</i>
<i>P. fragi</i>	<i>P. viridiflava</i>

The phylogenetic relationships of *Pseudomonas* (*sensu stricto*) and some members of the γ sub-division of *Proteobacteria* derived by comparison of 16S rRNA gene sequences and inferred phylogenetic relationship between 24 species of the genus *Pseudomonas* are indicated in Fig. 1.1 (Moore *et al.*, 1996). The species formed 2 intrageneric divisions; Division 1: the *P. aeruginosa* cluster which includes *P. aeruginosa*, *P. alcaligenes*, *P. balearica*, *P. citronellolis*, *P. mendocina*, *P. oleovorans*, *P. pseudoalcaligenes*, *P. resinovorans*, *P. flavescens*, and *P. stutzeri*; and Division 2: the *P. fluorescens* cluster which includes *P. fluorescens*, *P. agarici*, *P. amygladali*, *P. asplenii*, *P. aureofaciens*, *P. cichorii*, *P. coronafaciens*, *P. ficuserectae*, *P. marginalis*, *P. putida*, *P. syringae*, *P. tolaasii* and *P. viridiflava*. The division of *Pseudomonas* spp. into 2 major intrageneric clusters is also largely supported by the studies of Vancanneyt *et al.* (1996) who performed chemotaxonomic analysis using whole-cell fatty acid methyl ester (FAME) and phospholipid fatty acid profilings.

Some of the *Pseudomonas* species do not accumulate PHB and produce, when grown under iron deficiency, a yellow-green pigment that fluoresces under UV radiation. This substance, first observed by Gessard (1892), was called bacterial fluorescein and more recently pyoverdin. They are, for this reason, referred to as fluorescent pseudomonads. In Bergey's Manual of Systematic Bacteriology (Palleroni, 1984), the following species are included in this group: *Pseudomonas aeruginosa*, *P. aureofaciens*, *P. cichorii*, *P. fluorescens*, *P. putida*, *P. syringae* and *P. viridiflava*. Thus, production of pyoverdinin is found among members of the 2 intrageneric clusters.

P. aureofaciens Kluver (1956) is a later subjective synonym of *P. chlororaphis* (Guignard and Sauvageau, 1894) and Palleroni *et al.* (1984) suggested to reclassify *P. aureofaciens* as *P. chlororaphis*. However, for this study, as in the current literature, the species name "*aureofaciens*" was used. In this project, research has focused on the bacterium *P. aureofaciens* PGS12, originally isolated from roots of corn, and inhibitory to numerous plant pathogens *in vitro* and *in situ* (Georgakopoulos, 1994a).

Fig. 1.1.

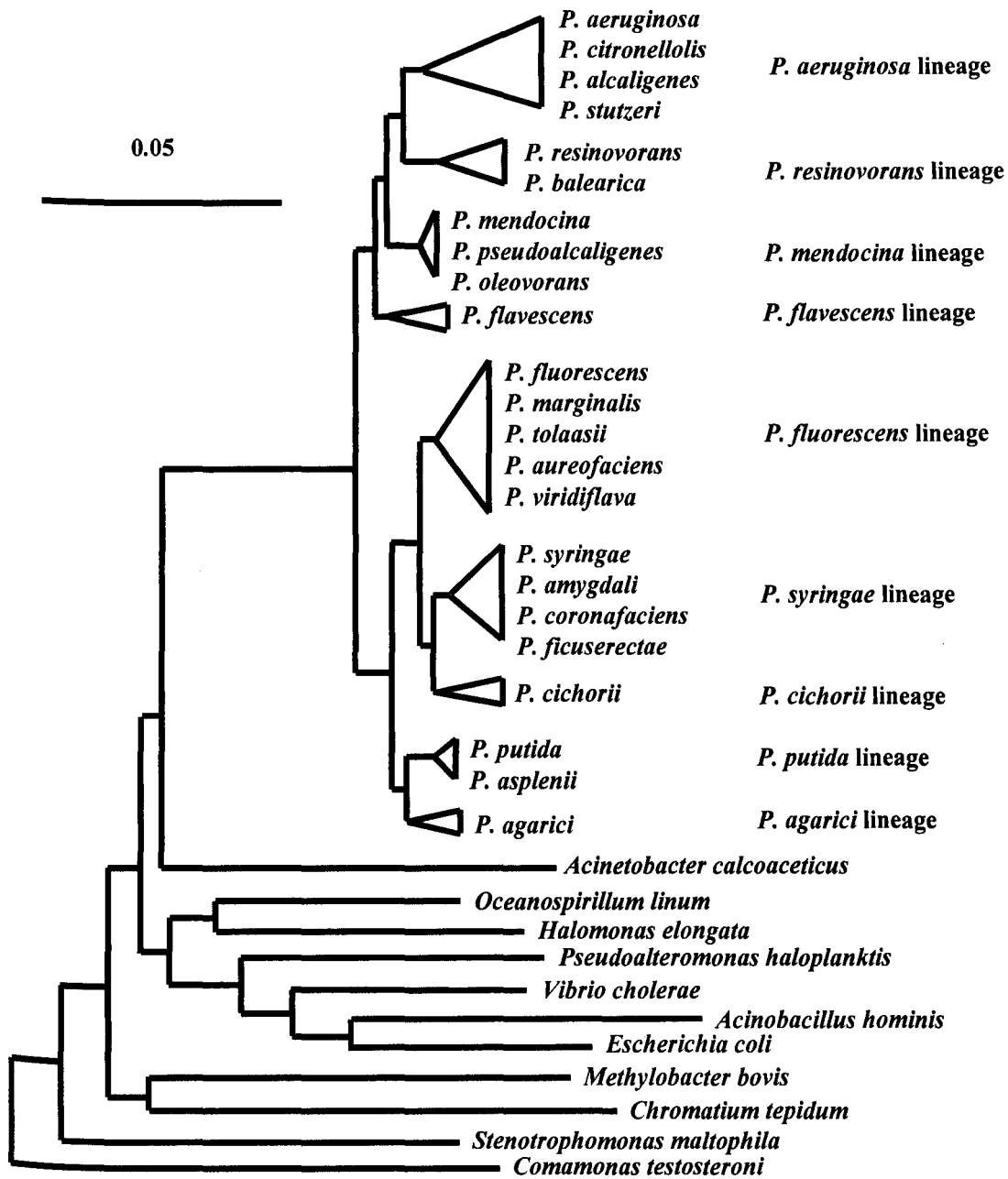


Fig. 1.1. Inferred phylogenetic relationships among species of *Pseudomonas* (*sensu stricto*) and other members of the γ sub-division of the Proteobacteria. Evolutionary distances were derived from pairwise dissimilarities of the 16S rRNA gene sequences (after Moore *et al.*, 1996).

1.1.2. *Habitat and function*

Pseudomonads are widespread in nature, being common inhabitants of soil or of fresh water and marine environments. The genus *Pseudomonas* includes species with a variety of functions with ecological, economic and health related importance (Palleroni, 1992). Members of this genus play important roles in the biosphere (e.g. denitrification processes in soil) and many are endowed with the capacity to degrade a large variety of organic compounds (Palleroni *et al.*, 1973). The catabolic diversity of pseudomonads makes them attractive candidates for use in bioremediation studies, in particular because of the ability of various species to degrade aromatic compounds, halogenated derivatives, and numerous recalcitrant organic residues that are seldom or rarely degraded by other groups of microorganisms (Palleroni, 1993).

The great majority of pseudomonads are strictly saprophytic and as such are beneficial to humans because they help decompose enormous quantities of organic matter. Most pathogenic *Pseudomonas* spp. infect plants, only *P. aeruginosa* is an important opportunistic human pathogen (Agrios, 1988). Most pathogenic bacteria, including pseudomonads, are facultative saprophytes; they develop mostly in the host plant as parasites and partly in plant debris or in soil as saprophytes. They may also survive in or on seeds, other plant parts, or insects found in soil. On the plant, they may survive epiphytically, in buds, on wounds, in their exudate, or inside the various tissues or organs that they infect (Agrios, 1988). The dissemination of plant pathogenic bacteria is carried out primarily by water, insects, other animals, and humans. Even pseudomonads with their flagella can move only very short distances under their own power. Flagella may help bacteria to spread over short distances, to colonise plant roots for example (Agrios, 1988; de Weger *et al.*, 1987).

Phytopathogenic bacteria exist as distinct pathovars belonging to one species but distinguishable from each other by the host plants they infect. There are now listed over 50 different pathovars of *P. syringae* (Agrios, 1988; Clerc *et al.*, 1998). *P. syringae* is an epiphytic bacterium that causes mainly necrotic lesions on aerial parts of plants (Clerc *et al.*, 1998). For example, *P. syringae* pv. *tabaci* is responsible for wildfire of tobacco resulting in important economic loss in all parts of the world where tobacco is grown, *P. syringae* pv. *phaseolicola* causes halo blight of common bean, whereas *P. syringae* pv. *glycines* causes blight of soybean (Agrios, 1988). Some fluorescent *Pseudomonas* bacteria can cause soft rot in a large number of plants such

as potatoes, lettuce and tobacco, and are important factors in pre- and post-harvest crop loss (Janse *et al.*, 1992). Several pathovars are also recognised in *P. marginalis*, and *P. cichorii* whereas *P. agarici* and *P. tolaasii* cause diseases in mushrooms (Agrios, 1988).

Fluorescent pseudomonads aggressively colonise root systems and, when inoculated onto seeds and other plant parts, may cause substantial increases in plant growth and yield. This is why they are also often referred to as plant growth-promoting rhizobacteria (PGPR) (Schroth and Hancock, 1982). Rhizobacteria do not only promote growth, they can also protect the plant against soil-borne diseases, and hence are potential biological control agents. For these reasons they are also termed plant health-promoting bacteria (Schippers *et al.*, 1993). *P. aureofaciens* PGS12 in greenhouse tests caused growth promotion of celery cultivars and was inhibitory to celery wilt caused by *Fusarium oxysporum* f. sp. *apii*. However, in fields infested with the pathogen, PGS12 showed variable inhibitory capacity (Becker *et al.*, 1990; Georgakopoulos, 1994a).

1.2. BIOLOGICAL CONTROL

1.2.1. Definitions

Current practices for controlling plant disease are based largely on synthetic pesticides, management of the plant and its environment, and genetic resistance in the host plant (Strange, 1993). However, there is an increasing demand for a “greener” approach to agriculture. Due to revised safety regulations (Duke *et al.*, 1993) and development of resistance in pathogen populations (Elmholt, 1991) some synthetic pesticides currently in use will be replaced while applications will have to be reduced (MAFF Regulation). Biological control, using microorganisms to suppress plant diseases, offers a powerful alternative to the use of synthetic chemicals. Biological control of plant pathogens, which may be described as “the use of living organisms to control a crop disease or prevent the establishment of a pest”, is frequent in the environment (Dowling and O’Gara, 1994). There are several diseases that cannot develop because the suppressive soil contains microorganisms antagonistic to the pathogen. The three fungi studied most intensively with the disease they are responsible for are: (i) *Gaeumannomyces graminis* var. *tritici* (Ggt) (take-all of wheat); (ii) *Fusarium oxysporum* (Fusarium wilt diseases in a variety of crops); and

(iii) *Thielaviopsis basicola* (root rot of tobacco) (Agrios, 1988; Schippers, 1993). In all three types, strains of fluorescent *Pseudomonas* spp. were shown to play an important role in disease suppression. The other most studied PGPR are in the genus *Bacillus* (Emmert and Handelsman, 1999; Schippers, 1993).

1.2.2. Biological control by rhizobacteria: Mechanisms and applications

Understanding the mechanisms underlying biocontrol of plant disease is critical to the eventual improvement and wider use of biocontrol agents. Included among the control mechanisms of soilborne pathogens by fluorescent pseudomonads are substrate competition and niche exclusion (Defago and Haas, 1990), effective root colonisation (Lugtenberg and Dekkers, 1999), releases of specific and non-specific metabolites such as antibiotics (Fravel, 1988), and induced resistance (Van Loon *et al.*, 1998). The most effective *Pseudomonas* strains have a variety of mechanisms suppressing pre-infection activities of the fungal pathogen (such as propagule germination) but also infection and post-infection development (Schippers *et al.*, 1987).

The principal antibiotics produced by pseudomonads are pyroles (e.g., pyrrolnitrin, pyoluteorin), phloroglucinols (2,4-diacetylphloroglucinol), oomycin A and phenazines (Dowling and O'Gara, 1994; Thomashow, 1996; Weller, 1988). *P. aureofaciens* PGS12 produces a number of compounds with antimicrobial properties such as phenazine and pyrrolnitrin antibiotics, hydrogen cyanide, siderophores (collectively termed pyoverdins in fluorescent pseudomonads), and proteases (Georgakopoulos *et al.*, 1994a; Hamdan *et al.*, 1991). Phenazines produced by the root-colonising and biological control agents *P. fluorescens* 2-79 and *P. aureofaciens* 30-84 inhibit take-all of wheat caused by *Ggt* (Pierson III and Thomashow, 1992; Thomashow and Weller, 1988). Mutants of these bacteria, unable to synthesise phenazines, are not only defective in pathogen inhibition and disease control but are also impaired in their ability to persist on plant roots in competition with indigenous microflora (Mazzola *et al.*, 1992). These results highlighted the importance of antibiotics in the ecology of bacteria in the rhizosphere.

Any time an antibiotic is used, careful measures must be taken to delay the development of antibiotic resistance. Indeed, studies have demonstrated that the use of antibiotics in animal feed leads to antibiotic resistance in humans (Levy, 1978).

However, microorganisms used for biocontrol are likely to produce *in situ* minute amounts of antibiotic, compared with the amounts of chemical fungicides used to control diseases, and microbes deliver the antibiotic to the exact location needed, as opposed to the blanket approach used with fungicides (Thomashow and Weller, 1990; Thomashow, 1996). Phenazine-1-carboxylic acid (PCA) produced by *P. fluorescens* 2-79 and *P. aureofaciens* 30-84 was isolated from the roots and rhizosphere soil of wheat seedlings grown in steamed and natural soils, and with or without *Ggt*. Roots from which PCA was recovered had significantly less take-all than roots with no PCA, and as little as 20 to 30 ng per seedling conferred protection (Thomashow *et al.*, 1990). The risk of emergence of antibiotic resistance is further lessened because disease suppression by biocontrol agents often results from the associations of several microbial mechanisms and from the co-operation of several pathogen-suppressing microorganisms (Schipper, 1993). For example, mutants of *P. fluorescens* 2-79 unable to synthesise phenazine antibiotics, anthranilic acid and siderophores provided significantly less but still some suppression of the take-all disease compare to the wild-type strain (Thomashow and Weller, 1990). Co-inoculation of two biocontrol agents, based on detailed knowledge of the mechanisms involved, is still in its infancy and ought to be explored further. Mazzola *et al.* (1995) showed that several isolates of *G. graminis* var. *tritici* and var. *avenae* are sensitive to various degrees to PCA and 2,4-diacetylphloroglucinol produced by *P. fluorescens* strains 2-79 and Q2-87 respectively. Carefully selected co-inoculation of suppressive microorganisms combined with other control practices (Integrated Pest Management) may be the way forward for a modern and less polluting agriculture. This could be implemented within the context of organic farming or not. Improved methods for strain production and formulation to increase delivery and long term survival in the environment of the biological control agents are also needed. However, the cost associated with biological control is high and, so far, *P. aureofaciens* (strain Tx-1) has only been used professionally on golf courses in the US. In this system, large quantities of microbes are grown in a special production system that connects directly to the sprinkler system. As the golf courses are watered, they are also spread with the biocontrol agent (<http://www.epa.gov/pesticides/biopesticides/factsheets/fs006473e1.html>).

1.2.3. Phenazine antibiotics and their biosynthetic pathway in *P. aureofaciens*

The natural occurrence of phenazine pigments has been known since the late nineteenth century (Turner and Messenger, 1986). All of these pigments contain the same basic dibenzopyrazine structure for which the nucleus and numbering system is outlined in Fig. 1.2. Over fifty different naturally occurring phenazine compounds are produced by *Pseudomonas* and *Streptomyces* species. All are pigmented and many exhibit broad-spectrum antibiotic activity against bacteria and fungi (Brisbane *et al.*, 1987; Gurusiddaiah *et al.*, 1986; Toohey *et al.*, 1965; Turner and Messenger, 1986). Their proposed modes of action include DNA intercalation (Perrin *et al.*, 1999), as well as the disruption of energy-dependent membrane associated metabolic processes due to their ability to undergo oxidation-reduction reactions and generate cytotoxic peroxides (Picker and Fridovich, 1984).

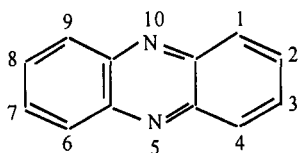
Kluyver (1956) and Haynes *et al.* (1956) first described, in simultaneous publications, the production of phenazine-1-carboxylic acid (Fig. 1.2) by *P. aureofaciens*. More recent studies, aimed at the formulation improvement of biocontrol agents, showed that PCA accumulation was very sensitive to the culture pH and temperature; high PCA production was observed at 25-27°C and pH7 (Sliniger and Jackson, 1992; Slininger *et al.*, 1995). *P. aureofaciens* strains PGS12 and 30-84 were shown to produce mainly PCA and lesser quantities of 2-hydroxyphenazine-1-carboxylic acid (2-OH-PCA) and 2-hydroxy-phenazine (2-OH-Phz) (Fig. 1.2). PCA has a yellow-green colour and the hydroxylated compounds give cultures their characteristic orange-red colour. The latter also inhibit *Ggt in vitro* and were shown to contribute to disease suppression on wheat seedlings (Thomashow and Pierson III, 1991).

1.3. QUORUM SENSING IN GRAM-NEGATIVE BACTERIA

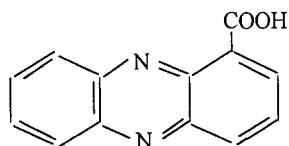
1.3.1. Definitions

Synthesis of phenazine antibiotics in *P. aureofaciens* is under the control of the autoinducer hexanoyl-L-homoserine lactone (HHL; Wood *et al.*, 1997). Autoinducers are signal molecules that regulate diverse biochemical processes in a density-dependent manner referred to as quorum sensing. Swift *et al.* (1996) defined quorum sensing as “a phenomenon in which a low molecular weight pheromone accumulates

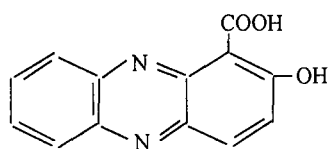
Fig. 1.2. Structures and numbering system of phenazine antibiotic compounds (from Turner and Messenger, 1986).



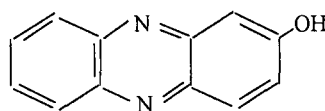
Structure and numbering system of the phenazine (Phz) nucleus



Phenazine-1-carboxylic acid (PCA)



2-hydroxy-phenazine-1-carboxylic acid (2-OH-PCA)



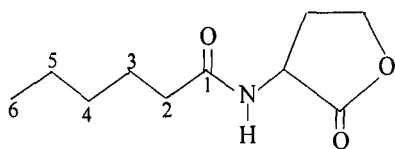
2-hydroxy-phenazine (2-OH-Phz)

extracellularly, allowing individual cells to sense when the minimal population unit or quorum of bacteria has been achieved for a concerted population response to be initiated". The signal components, the autoinducers *N*-acyl-L-homoserine lactones (AHLs; Fig. 1.3), activate diverse biochemical and physiological functions (reviewed by Dunlap, 1997; Dunny and Winans, 1999). AHLs exhibit functional similarity to pheromones, self-produced compounds released from cells that have specific effects on other cells of the same or other species (Pierson III *et al.*, 1999). Pheromone-like compounds are used as signals in many bacteria and the chemical structure of butyrolactones (A-factors), which regulate antibiotic production and the formation of aerial mycelia in *Streptomyces* spp., is very close to the chemical structure of AHLs (Horinouchi and Beppu, 1992; Fig. 1.3).

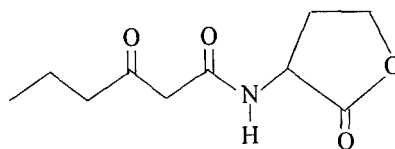
1.3.2. *The luxI/luxR paradigm*

The basic framework for quorum sensing was established in the early 1970s by Nealson and collaborator (1977; 1999). They showed that the marine luminescent bacteria, *Vibrio fischeri* and *Vibrio harveyi*, produce diffusible compounds, termed autoinducers, that accumulated to high concentrations only when, in confined environments, a critical cell concentration was achieved. The signals from *V. fischeri* and *V. harveyi* do not cross-react, showing the species specificity of some of these compounds. Luminescence by *V. fischeri*, the light organ symbiont of pinecone fish, requires the autoinducer *N*-(3-oxohexanoyl)-L-homoserine lactone (OHHL; Fig. 1.3) which activates transcription of the luminescence genes (*luxICDABEG* operon). Cells are permeable to OHHL, so that it accumulates within *V. fischeri* and in the external medium at equal concentrations (Kaplan and Greenberg, 1985). In the light organ, *V. fischeri* is found at densities of 10^9 to 10^{10} cells per ml of organ fluid. In environments in which *V. fischeri* density is low, such as seawater ($<10^3$ cells per ml), OHHL does not accumulate and luminescence does not occur (Dunlap and Greenberg, 1991; Ruby *et al.*, 1980). The *lux* operon is organised as two divergently transcribed units. One transcriptional unit contains *luxR*, which encodes LuxR an autoinducer-responsive transcriptional activator. The other transcriptional unit contains *luxA* and *luxB*, which encodes the α and β subunits of luciferase; *luxC*, *luxD* and *luxE*, which encode proteins involved in the synthesis of the aldehyde substrate for luciferase; and *luxI*, (adjacent to *luxR*, divergently transcribed) encodes the autoinducer synthase, LuxI.

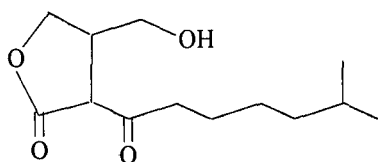
Fig. 1.3. Structures of *N*-acyl-L-homoserine lactones (AHLs), the *Pseudomonas* Quinolone Signal (PQS), a diketopiperazine (DKP), and a butyrolactone (A-factor).



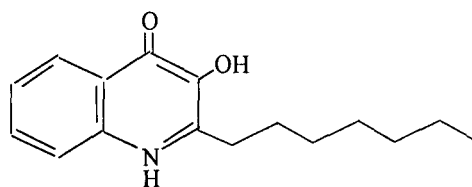
N-(hexanoyl)-L-homoserine lactone (HHL or C6-HSL)



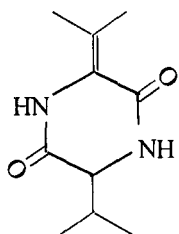
N-(3-oxohexanoyl)-L-homoserine lactone (OHHL or 3-oxo-C6-HSL)



Butyrolactone (A-factor) from *Streptomyces griseus*



2-heptyl-3-hydroxy-4-quinolone (PQS)



cyclo(Δ -Ala-L-Val)
(cyclic dipeptides, DKP)

At low cell densities, *luxI* is transcribed at a basal level leading to a slow accumulation of OHHL. When at a sufficiently high concentration, OHHL interacts with LuxR, forming a complex that facilitates association of σ^{70} -RNA polymerase with the *lux* operon promoter situated between *luxR* and *luxI*, it activates transcription of the *luxICDABEG* operon (Dunlap and Greenberg, 1988; 1991). This results in the positive autoregulation of *luxI* and a 1,000- to 10,000-fold increase in luminescence over pre-induction levels (Dunlap and Greenberg, 1988). Expression of *luxR* is controlled both positively and negatively (Shadel and Baldwin, 1991). Cyclic AMP (cAMP) and cAMP receptor protein (CRP) activate transcription from the *luxR* promoter (Devine *et al.*, 1988; Dunlap and Greenberg, 1988). Expression of *luxR* is controlled negatively at the level of translation by LuxR, and this translational negative autoregulation is dependent on autoinducer (Engebrecht and Silverman, 1986). In addition, the expression of *luxR* is subject to negative autoregulation at the transcriptional level, which also involves the autoinducer OHHL (Dunlap and Ray, 1989). *LuxR* transcriptional negative autoregulation is dependent on the 20-bp palindromic *lux* box and a regulatory site in *luxD* (Shadel and Baldwin, 1992).

1.3.3. Genetics and biochemistry of phenazine production

Pierson III *et al.* (1995) determined the complete nucleotide sequence of both strands of a 5.7 kb EcoRI-HindIII fragment containing the phenazine biosynthetic region of *P. aureofaciens* 30-84. The region contains five ORFs, named *phzF*, *phzA*, *phzB*, *phzC* and *phzD* (Genbank accession number L48339). The regulatory genes *phzR* (Genbank accession number L32729) and *phzI* (Genbank accession numbers L33724) were identified respectively by Pierson III *et al.* (1994) and Wood and Pierson III (1996). The characteristics of each ORF and its deduced protein product are summarised in Table 1.2. The expression of the phenazine biosynthetic operon (*phzFABCD*) is regulated by PhzI and PhzR, members of the LuxI/LuxR family of quorum-sensing regulators. Wood *et al.* (1997) identified the signal molecule, the autoinducer HHL. Expression of *phzFAB* (but not *phzD*) from strain 30-84 is required for production of PCA in *E. coli*, and *phzC* is implicated in the conversion of PCA to 2-OH-PCA (Pierson III *et al.*, 1995). Levitch and Stadtman (1964) first showed that phenazines are products of the shikimic acid pathway. Chorismate is the probable branch point intermediate, and the amide group of glutamine is the primary source of

ring nitrogen (Turner and Messenger, 1986). PhzF resembles 3-deoxy-D-arabino-heptulosonate-7-phosphate synthase, and could direct substrate into the shikimate pathway. PhzA and PhzB resemble isochorismatase and anthranilate synthase respectively; these enzymes may modify and condense chorismate, yielding the heterocyclic nitrogen ring of phenazines (Pierson III and Thomashow, 1992; Pierson *et al.*, 1995). A proposed pathway by Pierson III (1995) for the biosynthesis of PCA and 2-OH-PCA in *P. aureofaciens* is outlined in Fig. 1.4.

1.3.4. Regulation of phenazine production

Antibiotic synthesis is tightly linked to the overall metabolic status of the cell, which in turn is dictated by nutrient availability and other environmental stimuli. Georgakopoulos *et al.* (1994a, 1994b) used a reporter gene fusion to the ice nucleation gene *inaZ* to assess environmental effects on antibiotic gene expression. They showed that nutrient availability is the major determinant of expression of the *phz* locus of *P. aureofaciens* PGS12 *in vitro*, and that *in situ* expression varies among seeds from different plant species. The highest expression was found on wheat seedlings (Georgakopoulos, 1994b).

Antibiotic biosynthesis is also controlled at the cellular level by regulatory systems that co-ordinate metabolic processes during growth and in response to environmental changes (Haas *et al.*, 2000). Chancey *et al.* (1999) were the first to describe, in *P. aureofaciens*, a mechanism for direct linkage between a two-component sensory transduction system, the GacS/GacA (Global Antibiotics and Cyanide control) regulon, and an AHL-mediated regulatory system. GacS (formerly LemA) is a sensor kinase and GacA a cytoplasmic response regulator. GacS and GacA regulate the expression of multiple phenotypes, and therefore this system is known as a global regulatory system (Laville *et al.*, 1992; Willis *et al.*, 1990). Chancey and collaborators demonstrated that GacS/GacA controls AHL production via transcriptional regulation of *phzI*. Because AHL is required for phenazine gene expression, GacS/GacA mutants of *P. aureofaciens* 30-84 were not able to produce phenazine antibiotics. Furthermore, the data suggested that the GacS/GacA regulon also controls phenazine production in an AHL-independent manner. One hypothesis is that a second transcriptional activator regulates phenazine gene expression. The two-

Table 1.2. Characteristics of the phenazine gene cluster in *P. aureofaciens* 30-84
(from Pierson III *et al.*, 1994, 1995; Wood *et al.*, 1996).

Gene	Size (bp)	Protein	M _r ^a	Similarity ^b	Similarity (%) ^c
<i>phzR</i>	726	PhzR	29.0	LuxR	45.0
<i>phzI</i>	591	PhzI	22.3	LuxI	49.0
<i>phzF</i>	1200	PhzF	43.9	AroF	58.5
<i>phzA</i>	621	PhzA	23.1	EntB	72.0
<i>phzB</i>	1911	PhzB	69.6	TrpE(G)	53.8
<i>phzC</i>	834	PhzC	30.2	ThyA	50.2
<i>phzD</i>	666	PhzD	25.0	PdxH	53.4

^aPredicted protein mass in kDa.

^bGene product in the database with the highest amino acid similarity: LuxR/I from *Vibrio fischeri*; AroF from *Nicotiana tabacum* (DAHP synthase); EntB from *Escherichia coli* (dihydroxybenzoate synthase); TrpE(G) from *Rhizobium melitoli* (anthranilic synthase); ThyA from *Mycobacterium tuberculosis* (no obvious functional similarity); PdxH from *Escherichia coli* (role of PhzD currently unknown).

^cDetermination based upon predicted amino acid sequence.

component system GacS/GacA provides a global switch which is turned on only during the transition phase leading to the production of extracellular metabolites such as biocontrol factors in bacteria (Haas *et al.*, 2000). Integrated regulatory schemes may allow bacteria to regulate expression of a wide array of genes in a co-ordinated manner in response to multiple environmental signals.

Pierson *et al.* (1998) demonstrated that naturally co-existing, non-isogenic bacterial populations interact with *P. aureofaciens* 30-84 at the level of gene expression *via* the exchange of AHLs on wheat roots. Out of 700 wheat root-associated isolates, 8% were able to activate phenazine gene expression *in vitro*. Inconsistent control of take-all by strain 30-84 in the field may be explained by this regulatory mechanism. However, *in situ* studies to determine the environmental factors that regulate the expression of the phenazine operon (on plant roots or in the rhizosphere) are still lacking. Recently, Teplitski *et al.* (2000) found that exudates from pea seedlings, and various species of higher plants, contained several separable compounds that mimicked AHL signals in LuxR-based quorum-sensing systems. Cell density-dependent regulation of genes responsible for pathogen inhibition in the rhizosphere has important practical implications for biological control. The AHL signal-mimic compounds could prove important in the interactions between higher plants, biological control agents, and fungal plant pathogens. Secretion of AHLs by a root system may enable the density-dependent requirement for antibiotic production to be by-passed. This would lead to early accumulation of the antibiotic in the root system and to early prevention of the establishment of a soil-borne disease.

1.3.5. Quorum sensing and starvation: Signals for entry into stationary phase

Microorganisms produce secondary metabolites in the transition phase, between exponential growth and stationary phase. Entry into stationary phase dramatically alters patterns of gene expression to allow extended cell survival in the absence of nutrients. Thus, starvation is thought to be the major signal regulating entry into stationary phase (Lazazzera, 2000). In Gram-negative bacteria, the key transcription factor for entry into stationary phase seems to be RpoS. Products of *rpoD* and *rpoS* encode the housekeeping and stationary phase sigma factors α^{70} and α^{38} (α^S) respectively. In *E. coli*, stationary phase results in increased resistance to a number of

Fig. 1.4.

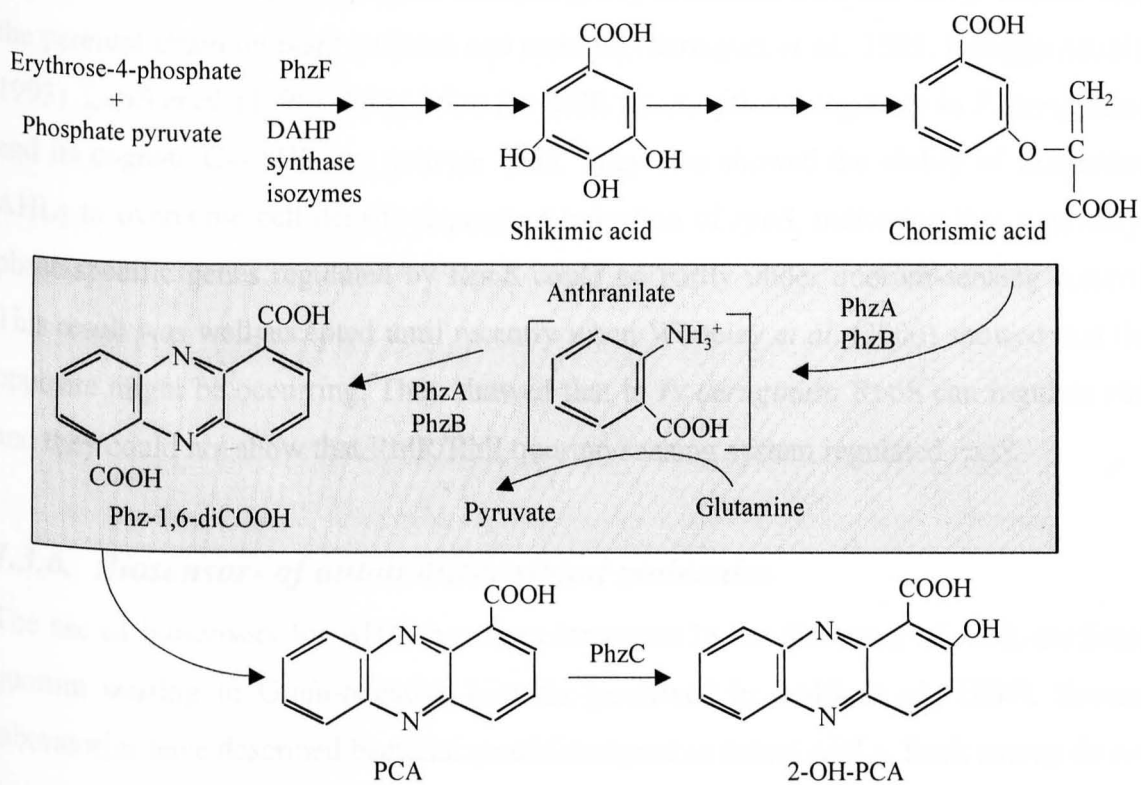


Fig. 1.4. Proposed pathway for the biosynthesis of PCA and 2-OH-PCA in *P. aureofaciens* spp.

PhzdiPCA (phenazine-1,6-dicarboxylic acid) is the proposed basic phenazine structure that most other phenazines are believed to be derived from. The grey box represents a putative phenazine macromolecular synthesis complex (the PhzA-PhzB complex; from Pierson III *et al.*, 1995).

environmental stresses, such as high osmolarity, oxidative agents and high temperature (Huisman and Kolter, 1994). *RpoS* mutants of *P. fluorescens* Pf-5 are less persistent than the parental strain on plant surfaces and residues (Sarniguet *et al.*, 1995; Hengge-Aronis, 1993). Latifi *et al.* (1996) showed that the RhlR transcriptional regulator in *P. aeruginosa* and its cognate C4-AHL can activate *rpoS*. They also showed the ability of exogenous AHLs to overcome cell density-dependent induction of *rpoS*, indicating that stationary-phase-specific genes regulated by RpoS could be partly under quorum-sensing control. This result was well accepted until recently when Whiteley *et al.* (2000) showed that the opposite might be occurring. They showed that in *P. aeruginosa* RpoS can regulate *rhlI* and they could not show that RhlR/RhlI quorum sensing system regulated *rpoS*.

1.3.6. Biosensors of autoinducer signal molecules

The use of biosensors for AHLs has been important in the discovery of AHL-mediated quorum sensing in Gram-negative bacteria (reviewed in Swift *et al.*, 1999). Several laboratories have described bacterial strains designed to detect AHLs. Such strains do not express an AHL synthase (LuxI homologues), but do express an AHL-responsive transcriptional activator (LuxR homologues), and contain an AHL-activated promoter fused to reporter genes such as *LacZY* or *luxCDABE*. The strength of activation of the reporter genes for the given AHL is dependent upon the LuxR homologue. For this study, a bioassay based upon the reporter strain *E. coli* JM107 containing a *luxR*-based plasmid sensor for AHLs (pSB401) was developed. The plasmid pSB401 carries a fusion of *luxRI* regulatory genes (from *V. fischeri*) to the complete biosynthetic gene cluster *luxCDABE* (from *Photobacterium luminescens*) on a pRK415 plasmid (Winson *et al.*, 1998). The *luxR* gene codes for a functional transcriptional regulator while the *luxI* gene, the AHL synthase, is mutated and not functional. The enzymes encoded by the *luxCDABE* operon are functional at temperatures as high as 45°C. The transcription of the operon from the *luxI* promoter, mediated by the AHL-activated LuxR transcriptional regulator, results in light emission from the LuxAB luciferase. The construct was shown to detect a range of AHL molecules with acyl side chains of C-6, C-8, C-10 and C-12 (Winson *et al.*, 1998). The development of a bioassay with *E. coli* JM107(pSB401) for the quantification of AHL production is described in Chapter 3.

1.3.7. *Quorum sensing in other Proteobacteria*

Within the last 10 years, several groups have made key discoveries that have led to the current view that quorum sensing is common to many Gram-negative bacterial species (Swift *et al.*, 1993). Several bacterial species were shown to produce AHLs using AHL-biosensors (section 1.3.6; Swift *et al.*, 1999) and there are now over 15 LuxI and LuxR homologues in the protein sequence databases. Furthermore, the *lux* box-like sequence is found in the promoter regions of many of the genes regulated by LuxR homologues (England *et al.*, 1999). A number of beneficial and pathogenic plant-associated bacteria utilise AHL signals. Examples of pathogenic plant-associated bacteria comprise *Agrobacterium tumefaciens*, *Erwinia carotovora*, *Pantoea stewartii* subsp. *Stewartii*, and *Ralstonia solanacearum*, and among beneficial bacteria, *Rhizobium leguminosarum*, *Pseudomonas fluorescens*, and *Pseudomonas aureofaciens* (reviewed in Pierson III, 1999). In *P. aeruginosa*, an important opportunistic human pathogen, the expression of many virulence factors is controlled through a hierarchy of quorum-sensing systems in co-ordination with other regulatory mechanisms (Pesci and Iglewski, 1997). *P. aeruginosa* contains two quorum-sensing systems: The LasR/I system, which uses 3-oxo-C12-HSL, and the RhlR/I system, which uses C4-HSL. The quorum-sensing hierarchy begins with basal production of LasR and 3-oxo-C12-HSL. At a high culture density, *lasR* is induced by Vfr, and 3-oxo-C12-HSL reaches a threshold concentration where it binds to LasR. LasR-3-oxo-C12-HSL can then activate genes controlled by the *las* system including *rhlR*. Speculatively, 3-oxo-C12-HSL may block the binding of C4-HSL to RhlR until enough RhlR and/or C4-HSL are produced to overcome the blocking effect (Pesci *et al.*, 1997). Once RhlR associates with C4-HSL, autoinduction of *rhlI* occurs, and the remainder of the RhlR-C4-HSL-controlled genes are activated. This would provide *P. aeruginosa* with two mechanisms to ensure that the *rhl* system is activated after the *las* system, implying that only the *las* system directly “senses a quorum”. The virulence factors controlled by the *las* quorum-sensing systems include: Elastase (*lasB*), LasA protease (*lasA*), alkaline protease (*apr*), exotoxin A (*toxA*), and general secretory pathway proteins (*xcpP*, *xcpR*). The *rhl* system controls rhamnosyltransferase (*rhlAB*), elastase (*lasB*), the stationary-phase sigma factor (*rpoS*), alkaline protease (*apr*), and pyocyanin (phenazine antibiotic) (Pesci and Iglewski, 1999). The demonstration that

RhlR-C4-HSL regulates *rpoS* positively could explain the multiple control levels that exist to regulate RhlR (Latifi *et al.*, 1996).

1.3.8. *Novel families of intercellular signalling molecules*

A wide range of bacteria produce autoinducers, however, not all bacteria communicate using AHLs alone. *Ralstonia solanacearum* uses a 3-hydroxypalmitic acid methyl ester in conjunction with AHLs to modulate pathogenicity (Flavier *et al.*, 1997). A novel family of intercellular signalling molecules, the diketopiperazines (DKPs; Fig. 1.3) has recently been described (Holden *et al.*, 1999). In *P. aeruginosa* two DKPs, and a third DKP in *P. fluorescens* and *P. alcaligenes*, have been identified. Although DKPs are structurally distinct from AHLs, at high concentration they can activate or antagonise several different LuxR-based quorum-sensing systems (Holden *et al.*, 2000). DKPs exhibit a remarkable spectrum of biological and pharmacological activities and they might have a role in modulating prokaryotic-eukaryotic interactions (Holden *et al.*, 2000). Apart from AHLs and DKPs, *P. aeruginosa* was recently been shown to produce another small diffusible signal molecule, a 4-quinolone named the *Pseudomonas* Quinolone Signal, PQS (Pesci *et al.*, 1999; Pesci, 2000; Fig. 1.3). PQS recovered from spent culture supernatant of a *lasI rhlI* double mutant can induce *lasB* expression, and its production is LasR dependent. The discovery of these new classes of chemical compounds implies that the boundaries of quorum sensing in *P. aeruginosa* may not be defined by, nor limited to, AHLs. Finally, Surette *et al.* (1999) identified a new family of autoinducer production genes that are necessary for synthesis of the autoinducer-2 (AI-2) by *V. harveyi*. The chemical structure of AI-2 is unknown and AI-2 does not interact with the *luxR/I* system that produces AI-1 (OHHL). The gene involved, termed *luxS*, was mapped on the *V. harveyi* genome and homologues were identified in *Escherichia coli*, *Salmonella typhimurium* and *Helicobacter pylori*. It is now becoming clear that a given organism might employ multiple quorum-sensing signal molecules belonging to the same and/or different chemical classes.

1.4. THE USE OF REPORTER GENES IN MICROBIAL ECOLOGY

1.4.1. *Detection of bacteria in environmental samples*

Quantification of microbial populations and of their activities is a primary goal for microbial ecology. Traditional techniques for measurement of microbial numbers and activity generally lack the specificity required for risk assessment following environmental release of genetically modified organisms (GMOs). Tracking techniques are required to provide information regarding the survival, growth, activity and dispersal of a released organism. Quantification of total, viable, culturable and non-culturable components of the released strain is needed to evaluate actual and potential activities of the organism. The method of detection depends primarily upon the aims of the research and a combination of methods may be needed to obtain all the desirable information. Something like 10^3 distinct microbial genotypes may be present in a single gram of soil (Torsvik *et al.*, 1990). Methods must therefore aim at the detection of unique features of the target microorganism such as surface proteins, unique DNA sequences (including rRNA genes) or unique phenotypic characteristics. These may be possessed naturally by the target bacteria or, for GMOs, can be introduced as a marker gene that endows a specific tractable phenotype and/or unique DNA sequence. Commonly used methods for detecting microorganisms in environmental samples include culture techniques, immunological assays, and molecular-based techniques such as DNA probing, genetic tagging, use of fluorescent probes and quantitative PCR. These methods may be coupled with advanced cell detection techniques such as confocal laser scanning microscopy and flow cytometry (Jansson and Prosser, 1997).

1.4.1.1. **Marker genes**

Dilution plate counting remains the most common method for estimation of viable cell concentration. Viability is in this context assessed as the ability to grow on laboratory media and under given culture conditions. However, in environmental studies, the methods largely underestimate cell numbers as it has been reported that only 1% of bacteria present in environmental samples may be grown on laboratory media (Lee and Fuhrman, 1990). This subpopulation is termed “viable but non-culturable” (Bloomfield *et al.*, 1998). However, the selectivity of media can also be an advantage if one needs to

track a specific microbe. Media currently available for the specific isolation of *Pseudomonas* spp. include Pseudomonas Isolation Agar (Difco), CN Agar (Oxoid), and CFC Agar (Oxoid). However, rather than designing media that will select a particular group, more commonly the organisms are selected for, or provided with, a phenotype that will be selected by previously determined conditions. The earliest examples of this approach were laboratory selection of strains with resistance to specific antibiotics or heavy metals. For example, *P. aureofaciens* PGS12 is naturally resistant to several antibiotics and notably to at least $75 \mu\text{g ml}^{-1}$ of tetracycline and could be selected from soil samples on this criterion.

Currently, the most common markers are those conferring antibiotic resistance, which greatly increase the sensitivity of enumeration techniques, and because of their ease of use, antibiotic resistance is also a component of other marker systems. Three other markers, *lacZY* (coding for β -galactosidase and lactose permease), *xylE* (encoding catechol 2,3-dioxygenase), and *gusA* (β -glucuronidase) have been used for viable cell enumeration by detection of coloured colonies on laboratory media (Drahos *et al.*, 1986; Morgan *et al.*, 1989; Wilson, 1995). One of the main advantages of the *xylE* system is that a temperature inducible expression system minimises the reduction of host fitness due to metabolic burden of *xylE* gene expression. The marker gene *gusA* has been used extensively in plant sciences and with *Rhizobium*, to detect and quantify the bacterium in root nodules (Wilson *et al.*, 1995). One of the advantages of the GUS enzyme is that it acts on a very wide range of glucuronide substrates to give coloured or fluorescent products.

Green fluorescent proteins (GFPs) are presently attracting interest. They emit a green fluorescence without the need for any co-factors, substrates, or additional gene products. The absorbance and fluorescence properties of GFP are due to the formation of a chromophore through a unique post-translational modification of the protein. The utility of the original GFP cloned from *Aequorea* has been improved by construction of new GFPs that are more soluble in the cell, have spectrally shifted excitation and emission wavelengths, creating different colours and new applications (de Lorenzo *et al.*, 1998). Cells marked with the *gfp* gene can be detected using fluorescence microscopy and fluorimetry and colonies can be identified using a UV light source.

Bacteria tagged with *lux* or *luc* genes can be detected as light-emitting colonies (Grant *et al.*, 1991). Luminescence from colonies of most marked strains can be detected by the naked eye in a darkened room, whereas exposure to X-ray film or photography of luminescent colonies improves sensitivity. CCD systems provide even greater sensitivity and enable detection and enumeration of microcolonies and of luminescent bacteria mixed with non-marked organisms (Jansson and Prosser, 1997). However, luminescence is more frequently used to report gene expression (section 1.4.2.1). Combinations of methods can be used for very sensitive and specific detection. For example, Bailey *et al.* (1995) marked *P. fluorescens* SBW25 with kanamycin resistance and with *lacZY* and *xylE* to enable tracking of the organism.

1.4.2. Reporter genes of transcriptional activity

Many of the genes used as markers of bacterial presence and survival can be used in a different context by fusion to specific promoters as indicators of the specific gene activity. Many traits that microbes might exhibit cannot be directly assessed in natural habitats such as in soil, in the rhizosphere, or in and on plants. It is generally impossible, and always very difficult, to detect the presence of specific enzymes, antibiotics, or other compounds elaborated by microorganisms *in situ*. For this reason, the behaviour of microbial strains in natural habitats is usually inferred from studies of these strains in culture. Many studies have demonstrated that microbes can exhibit quite habitat-specific patterns of gene expression (Wilson and Lindow, 1993). A better understanding of gene expression in the environment is necessary to effectively utilise microorganisms to perform such functions as bioremediation, biocontrol, and plant growth promotion.

Reporter genes are introduced in an organism either on a plasmid or as an insertion on the chromosome. A suitable delivery system is required in order to mark the strain of choice, and the strain must be amenable to basic genetic manipulation. The question of plasmid versus chromosomal insertion is important notably because of the possibility of losing the plasmid and horizontal gene transfer, and because of the effects of changes in the copy number of the gene per cell (Smit *et al.*, 1992). The basic strategy for analysing transcriptional regulation using reporter gene fusions is to insert the promoterless reporter gene downstream from the promoter of the gene of interest to

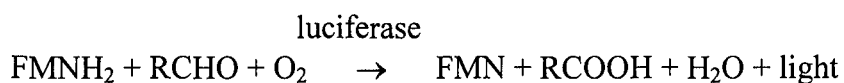
generate a construct in which the regulatory elements of the gene of interest controls the expression of the reporter gene. The transcriptional activity of the gene of interest is measured by assaying the abundance of the reporter gene product or its enzymatic activity. Transposon mutagenesis enables random insertion into the chromosome of the target strains. The promoterless mini-Tn5-*luxAB* transposon, engineered by de Lorenzo *et al.* (1990), was used for this research to generate isogenic strains of *P. aureofaciens* PGS12 (Chapter 3). Insertions of mini-Tn5s bearing promoterless reporter genes generate random chromosomal transcriptional fusions. After selection and genetic characterisation of the strains of interest, the gene fusion provides information on the promoter activity of the target gene or operon. Reporter genes serve as ‘amplifiable’ reporters of the transcriptional activity of genes to which they are fused (Stewart and Williams, 1992).

While the absolute amount of a protein product which contributes to a particular phenotype is determined by the inherent stability of its corresponding mRNA and by the turnover kinetics of the protein itself, regulation of a phenotype is often determined by modulating the rate of transcription (Lindow *et al.*, 1995). Thus, reporter gene fusions cannot provide absolute estimates of the steady-state amount of mRNA from a target gene, nor of the abundance of the corresponding protein. When comparisons of estimates of transcription are made in reference to a standard gene or constitutive reporter, accurate estimates of transcription *relative to* that of other genes may be provided. Most reporter gene fusions used to evaluate the transcriptional activity of a target gene are transcriptional fusions, leading to the production of a chimeric mRNA, and not translational fusions. Promoterless reporter genes are often placed at random positions downstream from the promoter of a target gene, and to avoid chimeric proteins, vectors used to produce reporter gene fusions usually introduce translational stop signals 5’ from the translational initiation codons of the reporter gene (Lindow *et al.*, 1995).

1.4.2.1. The *lux* reporter system

Luminescence genes from *V. fischeri* and *V. harveyi* were the first to be cloned and are among the most commonly used reporter genes in bacterial ecology. The *lux* genes required for bioluminescence are organised in two divergently transcribed operons, *luxICDABE* and *luxR*, the transcriptional regulator (section 1.3.2). The active form of

luciferase is a dimer formed from the *luxAB* gene products, whereas *luxCDE* codes for a long-chain aldehyde substrate, which may be added externally. The light-emitting reaction requires flavin mononucleotide (FMNH₂), oxygen, and a long chain aliphatic aldehyde (Stewart and Williams, 1992):



Because light does not accumulate, the major attraction of bioluminescence is the ability to measure transcriptional activity in real time (Schauer, 1988). A major advantage for environmental studies is that extraction of cells from the environment is not necessary, hence, direct *in situ* visualisation of microbial colonisation of the roots or rhizosphere is possible (Killham *et al.*, 1998). The sensitivity of detection of light output, by luminometry measurement or by using CCD imaging techniques, makes *lux*-reporter genes a very attractive system (Rattray *et al.*, 1990, 1995). The *lux* system also provides the ability to quantify and localise the activity of a specific organism in the presence of indigenous microbial communities (Prosser, 1994; Prosser *et al.*, 1996a and 1996b; White *et al.*, 1996).

Another major advantage of *lux* technology is that it can be used to assess cell metabolic activity. This characteristic has been used successfully to optimise rhizobacteria for biological control (White *et al.*, 1996). Successful biocontrol agents must be able to survive and to show activity at the required target site, that is, at the site of the root susceptible to fungal attack, and their metabolic activity should also be enhanced upon fungal attack. *In situ* visualisation of *lux*-marked microbial colonisation showed that bacteria colonised the rhizosphere and rhizoplane as single cells and microcolonies (de Weger *et al.*, 1991; Beauchamp *et al.*, 1993; Prosser *et al.*, 1996a). Measurement of microbial activity using bioluminescence can be used to indicate either actual or potential activity. Bacteria introduced into rhizosphere and non-rhizosphere environments can enter into a viable but non-culturable state. The addition of nutrients indicates the potential of strains to recover from periods of starvation or nutrient stress (Meikle *et al.*, 1994). However, the dependence of bioluminescence upon abundant O₂ and FMNH₂ may also be disadvantageous when studying gene expression from cells in anaerobic environments or cells with relatively low metabolic activity. In these cases,

light emission may not be proportional to the rate of transcription of *lux* gene fusions and it may prove difficult to estimate absolute rates of transcription of the reporter gene. Constitutive *lux*-reporters can act as a control to determine the importance of these factors.

Fusions of *lux* genes to genes responsive to specific environmental constituents have also proven useful for estimating the natural abundance of such compounds. For example, several studies on the development and use of bacteria that report the presence and bioavailability of naphthalene have been published (King *et al.*, 1990). Bacterial cells containing fusions of the naphthalene-catabolic operon, *nah*, with *lux* genes emit light in the presence of naphthalene and bioluminescence is proportional to exogenous naphthalene concentrations. The same principle allows for the detection of AHLs described in section 1.3.5.

1.4.2.2. Ice nucleation genes

A few bacterial species including various strains of *P. syringae* are ice nucleation active (Ice⁺) and catalyze ice formation in water at temperatures as warm as -2°C; in the absence of ice nucleating agents, water can supercool to nearly -40°C (Lindow *et al.*, 1990; Lindow, 1995). Bacterial ice nucleation activity has been successfully introduced and expressed in many Gram-negative bacteria. Ice-nucleation is rapidly measured by a droplet-freezing assay (Lindow *et al.*, 1990). A promoterless *inaZ* reporter gene was used in studies of phenazine antibiotic production by *P. aureofaciens* PGS12 in culture and on the surface of seeds grown in soil (Georgakopoulos *et al.*, 1994a, 1994b). Analysis of the effects of some culture parameters on the expression of the phenazine operon indicated that expression was affected by substrate concentration and specificity. In soil, the highest expression level was found on wheat seeds and the lowest on cotton seeds. The authors found that the nutritional value of seed exudates was a primary factor responsible for the differences in expression levels among seeds. In these studies, phenazine biosynthesis was only slightly affected by soil type and by soil matric potentials.

1.5. AIMS OF THIS STUDY

This research project focused on the regulation of the phenazine operon by *P. aureofaciens* PGS12. The aim was to study the role of the autoinducer HHL and cell density in regulating phenazine production when cells are growing under different conditions, in liquid culture, on a solid surface in colonies, and on plant roots. The production of the phenazine antibiotics was quantified *in vitro* and *in situ*. The reporter genes *luxAB* were fused to a phenazine gene to study the transcriptional activity of the operon and its regulation by HHL

CHAPTER TWO

MATERIALS AND METHODS

CHAPTER TWO

MATERIALS AND METHODS

2.1. MEDIA, REAGENTS, AND SOLUTIONS

Unless otherwise stated, all chemicals were from Sigma (Poole, Dorset, UK), BDH (Merk Ltd., Lutterworth, Leicestershire, UK), or Fisher (Fisher Scientific UK, Loughborough, Leicestershire, UK). Media, reagents, and solutions are shown as constituents per litre unless otherwise stated (Table 2.1). Items in rounded brackets were added in sterile solution after autoclaving. All growth media were sterilised by autoclaving at 121°C for 15 min. All reagents were stored at room temperature unless otherwise stated.

2.2. BACTERIAL STRAINS AND PLASMIDS

2.2.1. *Growth and maintenance of strains*

All bacterial cultures were grown routinely in Nutrient Broth (NB, Oxoid) or on Nutrient Agar (NA, Oxoid), unless otherwise stated. To ensure the maintenance of plasmids, *E. coli* strains were incubated at 37°C in media containing the antibiotic tetracycline (Tc) at a concentration of 12 µg ml⁻¹ (Tc¹²). *P. aureofaciens* strains were incubated at 30°C unless otherwise stated. For selection purposes, they were grown on PIA (Pseudomonas Isolation Agar, Difco) and because PGS12 is naturally resistant to high levels of tetracycline, *P. aureofaciens* PGS12 tetracycline resistant mutants were grown in media containing 75 µg ml⁻¹ of tetracycline. Liquid cultures were grown in conical flasks at 1/4 total volume and shaken in an orbital shaker (200 rpm). For long term storage of strains, colonies were preserved in Protect Vials (Technical Service Consultants Ltd., UK) at -70°C.

All bacterial strains used in this study are listed in Table 3.1. *P. aureofaciens* PGS12 was a gift from Dr Dimitri Georgakopoulos from the TEI of Heraklion, (Crete). *E. coli* JM107(pSB401) was a gift from Dr Briget Laue from the Applied Biochemistry

Table 2.1. Media, reagents, and solution used in this study.

Medium/ Reagent	Constituent per litre
AHL stock solution	50% (v/v) acetonitrile, stored at 4°C
Ringers solution (1/4 strength)	2.25 g NaCl, 0.10 g KCl, 0.12 g CaCl ₂ , 0.05 g sodium hydrogen carbonate
Phosphate Buffer Solution (PBS)	8 g NaCl, 0.2 g KCl, 1.44 g Na ₂ HPO ₄ , 0.42 g KH ₂ PO ₄ , [pH 7.4]
10 × TBE buffer	0.9 M Tris-borate, 20 mM EDTA, [pH 8.0]
DNA loading buffer	60% (w/v) sucrose, 0.25% (w/v) bromophenol blue, 100 mM EDTA
T ₁₀ E ₁	10 mM Tris-Cl, 1 mM EDTA, [pH 8.0]
T ₅₀ E ₂₅	50 mM Tris-Cl, 25 mM EDTA, [pH 8.0]
Tetracycline stock solution	50 mg ml ⁻¹ in 50 % (v/v) ethanol; kept at -20°C
Kanamycin stock solution	50 mg ml ⁻¹ in SDW
Lysosyme solution	4 mg ml ⁻¹ in T ₅₀ E ₂₅
Kanner Minimum Media	0.4% Na ₂ HPO ₄ , 0.15% KH ₂ PO ₄ , 0.1% NH ₄ Cl, 0.02% MgSO ₄ .7H ₂ O, 0.0005% FeNH ₄ .citrate, 2% glycerol

Table 2.2. Bacterial strains and plasmids used in this study and relevant characteristics.

Strain or plasmid	Characteristics	Reference
<i>E. coli</i>		
JM109	<i>recA1 endA1 gyrA96 thi hsdR17 supE44 relA1 Δ(lac-proAB) mcrA [F' traD36 proAB lacI^f lacZ ΔM15]</i>	Winson <i>et al.</i> (1998)
SM10 (λ pir)	<i>thi-1 thr leu tonA lacY supE recA::RP4-2-Tc::Mu, Km^r, λpir</i>	Miller <i>et al.</i> (1988)
<i>P. aureofaciens</i>		
PGS12	wild-type	Georgakopoulos <i>et al.</i> (1994a)
B103	<i>phzB::miniTn5luxAB, Phz⁻ HHL⁺</i>	This study
B105	<i>phzB::miniTn5luxAB, Phz⁻ HHL⁻</i>	This study
I17	<i>PGS12::miniTn5luxAB, Phz⁺ HHL⁺</i>	This study
B21	<i>phzI::miniTn5luxAB, Phz⁻ HHL⁻</i>	This study
I18Y	<i>phz::miniTn5luxAB, Phz⁻ HHL⁻</i>	This study
I18W	<i>phz::miniTn5luxAB, Phz⁻ HHL⁺</i>	This study
EH5	<i>phz::inaZ, Phz⁻ HHL⁺</i>	Georgakopoulos <i>et al.</i> (1994a)
W	spontaneous mutant of PGS12, <i>Phz⁻ HHL⁻</i>	Georgakopoulos <i>et al.</i> (1994a)
<i>Bacillus subtilis</i>		
6051a	Test organism against phenazine antibiotics	Stead <i>et al.</i> (1996)
Plasmids		
pSB401	<i>luxR-P_{luxI}-luxCDABE, Tc^R</i>	Winson <i>et al.</i> (1998)
pUT/Tc	<i>Ap^R, tnp</i> gene of Tn5-IS50 _R inserted in <i>SalI</i> site of pGP704, <i>luxAB, Tc^R</i>	de Lorenzo <i>et al.</i> (1990)
pLAFR3: <i>phzI::Km</i>	<i>pLAFR-20H2.7RVΔ3:I::Km^R+RV, Tet^R</i>	Wood and Pierson III (1996)

and Food Science Laboratory, University of Nottingham (UK) and *E. coli*(pUT) was collected from the Plant Pathology Department, Horticulture Research International (UK).

2.3. MEASUREMENT OF BACTERIAL GROWTH

2.3.1. Colony forming units (CFU)

Triplicate samples were serially diluted in sterile ¼ strength Ringer's solution to reduce the microbial number sufficiently to obtain separate colonies when plating. 100 µl was spread out on NA and plates incubated overnight. Samples yielding between 25 and 250 colonies were counted.

2.3.2. Total cell counts (TCC) as measured by the CellFacts particle analyser

Electronic counting is based on the principle that the electric conductivity of a bacterial cell is less than that of a saline solution. An electronic particle counter consists of two chambers connected through a small hole of 30 µm in diameter. Each chamber is provided with an electrode, so that the electrical conductivity across the hole can be monitored. Then bacteria are added to one of the chambers and pumped to the other. Each time a bacterium passes through the hole, the conductivity of the circuit decreases momentarily causing a pulse of voltage. These pulses are then counted and analysed by the attached computer to yield information on concentration of bacteria in the suspension. Moreover, the size of the voltage pulse is proportional to the size of the bacterium traversing the hole (or, more precisely, to the volume of solvent displaced). Therefore an electronic cell counting device gives the number and distribution of the diameters – more precisely spherical equivalent diameter – of the cells suspended in the sample.

For this research, total cell count and cell-size distribution data were generated using the CellFacts instrument (Microbial System Ltd., Coventry) combined with CellFacts Industrial software in discrete sample analysis mode. The analysis procedure entails delivery of the sample (typically 100 µl) to the measurement chamber via the instrument wand which concomitantly discharges a fixed 0.9 ml volume of electrolyte (CellLyte,

Fig. 2.1

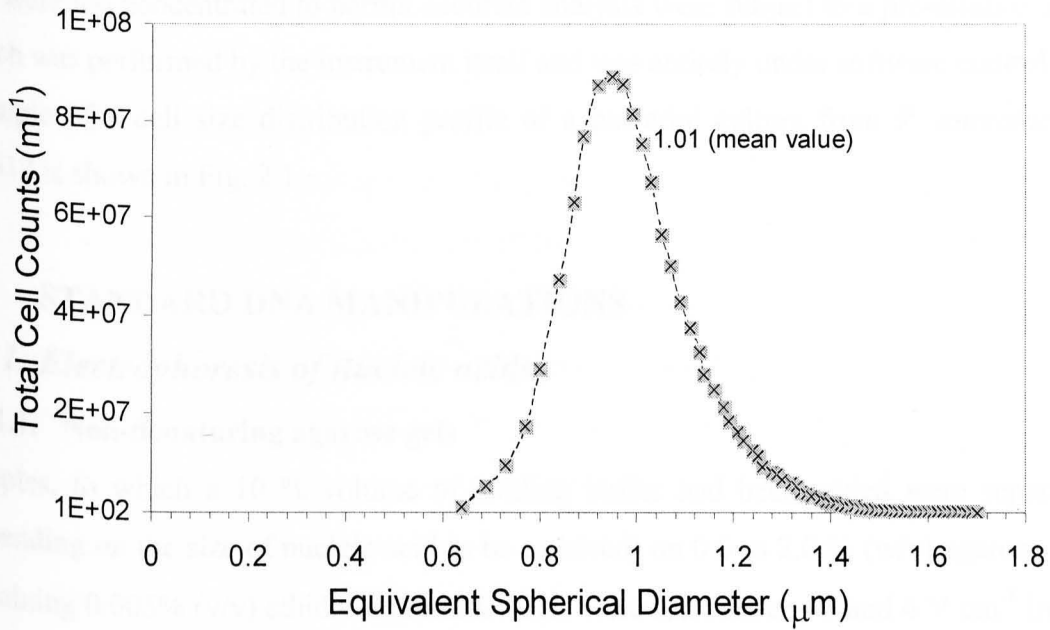


Fig. 2.1. Example of a cell size distribution profile of a bacterial culture obtained with a CellFacts instrument.

The sample consisted of an 8 h culture of *P. aureofaciens* PGS12 in NB. The overall cell number (Total Cell Count, TCC) and cell diameter (equivalent spherical diameter) were given on a separate spreadsheet by the CellFacts Industrial software.

Microbial Systems Ltd.) thus diluting the sample in the measurement chamber. Samples that were too concentrated to permit accurate analysis were subject to a pre-dilution step, which was performed by the instrument itself and was entirely under software control. An example of a cell size distribution profile of a bacterial culture from *P. aureofaciens* PGS12 is shown in Fig. 2.1.

2.4. STANDARD DNA MANIPULATIONS

2.4.1. Electrophoresis of nucleic acids

2.4.1.1. Non-denaturing agarose gels

Samples, to which a 10 % volume of loading buffer had been added were separated (depending on the size of nucleic acid to be resolved) on 0.6 to 2.0 % (w/v) agarose gels containing 0.005% (v/v) ethidium bromide. Gels were run between 1 and 4 V cm⁻¹ in 1 × TBE buffer, examined using a short wave transilluminator (UVP International, Model TS35) and gel images were recorded using UVP Life Sciences Grab It 2.0 Synoptics Ltd. The product size was estimated using a 1 kb molecular weight marker (BCL) for comparison.

2.4.2. Recovery and purification of DNA fractionated on agarose gels

DNA samples were electrophoresed on an agarose gel until the DNA fragments of interest had separated sufficiently to be cut from the gel without any other contaminating fragments. The fragment of interest was visualised using an UV light box and cut from the gel. QIAquick Spin Columns (QIAGEN) were used according to the manufacturer's instructions to purify DNA from the gels.

2.4.3. Nucleic acid extraction

2.4.3.1. Small scale preparation and purification of plasmid DNA

E. coli strains were grown overnight and 1 to 5 ml was transferred into a conical sterile tube and the cells pelleted by centrifugation at 10,000xg for 1 min. The supernatant was discarded and plasmid DNA was then isolated using a QIAprep Spin Plasmid miniprep

column according to the manufacturer's instructions. The preparation yielded up to 10 μg of plasmid DNA.

2.4.3.2. Large scale extraction of DNA

Pseudomonas spp. and *E. coli* spp. were grown for 16 h at 28°C and 37°C respectively and 5 ml was centrifuged at 5,000xg for 10 min. The pellet was resuspended in 500 μl sterile distilled water containing 5 μl 10% (w/v) SDS in T₅₀E₂₅. To break the bacterial cell membrane, the cell suspension was snap frozen in dry ice bubbling in 100% ethanol and immediately thawed at 65°C for 20 min. The proteins were precipitated by the addition of 1.5 ml ice cold 5M potassium acetate keeping the suspension at -20°C for 15 min. The precipitate was centrifuged at 10,000xg for 15 min and the supernatant transferred to a sterile 1.5 ml Eppendorf tube. DNA was precipitated by adding 10% (w/v) sodium acetate (3M) and 2.5 volume of 95% (v/v) ethanol. This was kept at room temperature for 15 min. The tubes were centrifuged for 20 min at 10,000xg and the supernatant discarded without disturbing the DNA pellet. The pellet was washed with 70% (v/v) cold ethanol, dried at 65°C for 15 min, and dissolved in 50 μl TE buffer at 65°C for 30 min. The preparation yielded on average 2 $\mu\text{g } \mu\text{l}^{-1}$ of pure DNA (OD₂₆₀ of 0.8-1.0). The extracted DNA was stored at -20°C.

2.5. POLYMERASE CHAIN REACTION (PCR) AND AUTOMATED SEQUENCING OF PCR PRODUCTS

2.5.1. Standard PCR reaction

Each component of the PCR reaction was kept constant unless otherwise stated. Amplification reactions were performed in 0.5 ml Eppendorf tubes and sterile distilled water was added to a final 50 μl per reaction mixture. The PCR components and their working concentrations are listed in Table 2.3.

Reactions were carried out in a Hybaid Express thermal cycler. A typical PCR reaction comprised: (i) A hot start: 1 cycle at 94°C for 1 min and 80°C for 5 min (the Taq polymerase was added at the end of this cycle); (ii) 35 cycles comprising a denaturation step at 94°C for 30 sec, an annealing step usually at 50°C for 30 sec, and an extension

Table 2.3. Standard PCR reaction.

Components	Stock concentration	Volume for 50 μ l PCR reaction	Working concentration
Buffer	$\times 10$	5 μ l	$\times 1$
DNTPs	10 mM	1 μ l	0.2 mM each
MgCl ₂	50 mM	1 μ l	1 mM
Forward primer	15 μ M	2 μ l	0.6 μ M
Reverse primer	15 μ M	2 μ l	0.6 μ M
BSA	1 mg ml ⁻¹	2.5 μ l	50 μ g ml ⁻¹
DMSO	50%	5 μ l	5%
DNA	50 ng μ l ⁻¹	1 μ l	1 ng μ l ⁻¹
Taq polymerase	0.5 U μ l ⁻¹	2 μ l	1 U μ l ⁻¹

step at 72°C for usually 45 sec; and (iii) a final extension of 72°C for 5 min. The optimal annealing temperature for each primer set was determined using a gradient system integrated into the Hybaid Express thermal cycler. The extension lasted 45 s for a 1 kb PCR product, and was adjusted accordingly for longer or shorter PCR products.

2.5.2. Design of oligonucleotide primers

Primers (supplied by GIBCO BRL) were designed using the program Primer3 present on the Internet site: <http://www-genome.wi.mit.edu/cgi-bin/primer/primer3.cgi>. Melting temperature (T_m) was always chosen to be approximately 60°C. Primers were dissolved in SDW ($1 \mu\text{g } \mu\text{l}^{-1}$) and a 50 μl working stock solution ($0.1 \mu\text{g } \mu\text{l}^{-1}$) was aliquoted and stored at -20°C. The primers used in this study are listed in Chapter 3 (Table 3.3).

2.5.3. Automated sequencing of PCR products

PCR products (30–90 ng) purified from an agarose gel (QIAquick column) and 1.6 pmol of primer were mixed with 4 μl of Big Dye ready reaction mix (Applied Biosystems) and SDW to a final volume of 10 μl . The dye was incorporated into the mix during sequencing which was performed with a thermal cycler (Hybaid) at the following program: 96°C for 30 s, 50°C for 15 s, 60°C for 4 min for a total of 30 cycles. Samples were analysed on an Applied Biosystems Model 373A automatic sequencer run by the University of Warwick sequencing service.

2.6. MINI-TN5 TRANSPOSON MUTAGENESIS OF *P. AUREOFACIENS* PGS12

The donor strain, *E. coli* SM10 (λpir), harboured the delivery plasmid pUT/Tc carrying the mini-Tn5*luxAB* elements from *Vibrio harveyi* (de Lorenzo *et al.*, 1990). The recipient strain was *P. aureofaciens* PGS12. The donor and recipient strains were grown separately for 10 h in 250 ml flasks in NB, with $12 \mu\text{g ml}^{-1}$ Tc for the donor strain. 1 ml of both cultures was centrifuged at 10,000 $\times g$ for 1 min, the cell pellets were washed twice in 0.85% (v/v) NaCl, each resuspended in 600 μl NB, and mixed together thoroughly. 200 μl of the mixture was plated on NA and incubated at 30°C for 14 h to allow conjugation

to take place. All growth was scraped from the NA plate and resuspended in 1 ml 0.85% (v/v) NaCl. Selection for transconjugants was made on PIA, on which *E. coli* SM10 λ pir (pUT) could not grow and PIA containing 75 $\mu\text{g ml}^{-1}$ Tc (PIA Tc⁷⁵), the minimum growth inhibitory concentration against *P. aureofaciens* PGS12. Dilutions of the bacterial suspension were spread on PIA and PIA Tc⁷⁵ and the plates incubated at 30°C for 48 h. The recovery frequency of transconjugants was estimated from the ratio of the colony number on PIA Tc⁷⁵ over the colony number on PIA.

The parent strain, *P. aureofaciens* PGS12, is orange due to phenazine production, hence selection was made for white colonies not expected to produce phenazine ([phz⁻] phenotype). White colonies were subcultured twice on PIA Tc⁷⁵ and tested for light emission under a CCD camera.

2.7. DETECTION AND QUANTIFICATION OF PCA

2.7.1. Extraction of total phenazines

P. aureofaciens PGS12 was grown in NB and 10 ml samples were centrifuged at 10,000xg for 10 min. The supernatant was kept and acidified to pH2 with 1N HCl. Each sample was shaken with 10 ml of dichloromethane for 2 h. The aqueous and organic phases were separated by centrifugation at 5,000xg for 3 min. The inactive aqueous phase was discarded and the active dichloromethane phase was evaporated to dryness overnight in a fume hood. Phenazine antibiotics present in the residue were dissolved in 5 ml of 5% aqueous (w/v) NaHCO₃.

2.7.2. Analysis of samples by HPLC

Analysis of samples was conducted with a HPLC system (Kontron 300 series) fitted with a Lichrospher 100 RP-18 (5 μm) column. The mobile phase consisted of 70% (v/v) acetonitrile in sterile distilled water acidified with 1 ml H₃PO₄ added per litre (pH 2.5). The elution profiles (chromatograms) were monitored at 249 nm and the spectrum of the eluted peak were UV scanned with a Kontron Instruments, Uvikon 930. The flow rate was set at 1 ml min⁻¹ and the sample injection volume was 20 μl .

2.7.3. Quantification of PCA by spectrophotometry

UV scans of pure PCA presented 2 characteristic peaks at 250 and 369 nm. A calibration curve was made with PCA standards (Maybridge Chemical Company Ltd., UK) dissolved in 5% NaHCO₃ (pH7). PCA was diluted in NB from 50 ng ml⁻¹ to 50 µg ml⁻¹ and the OD (optical density) was measured at 369 nm. The OD against the dilution range gave a linear relationship. PCA in liquid samples was measured against this calibration curve (Fig. 2.2). Since absorbance is affected by pH, care was taken to measure samples at pH7.

2.7.4. Quantification of PCA with *Bacillus subtilis* 6051a

A bioassay based on the tube (or turbidity) method (Hewitt, 1977) was developed. A spore suspension of *B. subtilis* 6051a was prepared to a concentration of 12×10⁴ CFU ml⁻¹ and 0.5 ml was added to 4 ml of half strength NB. A dilution series of PCA was prepared and 0.5 ml of each concentration added to the spore suspension. The 5 ml samples were incubated at 30°C on a rotary shaker for 12 h and the growth of the test organism was measured by recording the optical density at 600 nm (turbidity measurement).

2.8. MEASUREMENT OF *LUXAB* EXPRESSION

2.8.1. Measuring bioluminescence from liquid cultures

Bioluminescence was measured after addition of 1 µl decanal to 1 ml triplicate samples of cell solution in scintillation vials. Samples were shaken for 4 min at 28°C and light emission recorded using a luminometer (Model 20e, Turner Designs Photometer). Emission of light was integrated for 5 s and converted to Relative Light Units (RLU) per ml.

2.9. MONITORING GENE EXPRESSION ON NUTRIENT AGAR

2.9.1. Measurement of bioluminescence by luminometry

Bacteria were grown on NA at 21°C for 17 h, the time at which colonies became visible to the naked eye. Bioluminescence, cell counts, and HHL and phenazine production were

monitored from 5 individual colonies that were randomly picked up with an agar plug (7 mm). The agar plug was placed in 1 ml PBS and vortexed vigorously for 30 s to detach bacteria. Bioluminescence was measured by mixing 100 µl of the bacterial suspension with 0.1 µl decanal for 4 min. Samples were shaken for 4 min at 28°C and light emission recorded using a luminometer (Model 20e, Turner Designs Photometer). Emission of light was integrated for 5 s and converted in Relative Light Units (RLU) per ml. 100 µl was used to estimate the bacterial cell count with a CellFacts Instrument (Microbial Systems Ltd.). The agar plug was then crushed with a pellet mixer in the remaining 800 µl of PBS. The bacterial and agar mixture was centrifuged and the supernatant retained to quantify HHL and phenazine as described above in respectively section 2.8 and 2.9.3.

2.9.2. Measurement of bioluminescence using a CCD-camera

Overnight cultures of bacteria were diluted to get approximately 25 colonies per plate. The plates were incubated for 17h at 21°C. Gene expression from colonies was monitored continuously in a non-destructive manner by growing bacteria in the presence of decanal vapour, which was obtained from 150 µl of a decanal solution (3% v/v) in mineral oil dispensed in two 1 cm agar-wells cut in each plate. Bioluminescence was measured by low-light video imaging using a liquid-nitrogen cooled CCD-camera (Princeton Instruments, Trenton, NJ, LN/CCD-512-TKB). Images were automatically taken every hour for 48 h, integrated for 25 min and the luminescence expressed as “photons per colony”. The images were processed with Metamorph Software, which transformed luminescence into numerical data that were further analysed in Excel.

2.10. MONITORING GENE EXPRESSION IN STERILE RHIZOSPHERE OF BEAN

Bean seeds of *Phaseolus vulgaris* were surface sterilised in 1.5% (v/v) sodium hypochlorite for 5 min and washed 5 times in sterile distilled water. The surface sterilised seeds were placed on ½ strength Hoagland’s salt solution (macronutrients only; Hoagland and Arnon, 1950) in large plates and covered with a moistened Whatman filter paper. The plates were incubated in the dark at 26 °C for 2 days to ensure sterility before planting.

Germinated seedlings with 1-2 cm long radicals and with no visible contamination were inoculated with bacterial cultures. *P. aureofaciens* PGS12, B103, and I17 were grown individually in NB for 20 h, the cell pellet washed in 0.85% saline solution, and diluted to 10^7 and 10^8 cells per ml to give a final seed inoculation of ca. 1×10^7 and 1×10^9 cells per seedling (Expt. 2 and Expt. 1 respectively). The seedlings were immersed in the bacterial solutions for 20 min, blotted briefly, and planted immediately in 25-ml culture tubes (20 cm long x 2.5 cm diameter) containing sterile vermiculite (to a 6 cm depth) moistened with 5 ml of sterile $\frac{1}{2}$ Hoagland's salts solution (macronutrients only; Hoagland and Arnon, 1950). The seedlings were covered lightly with sterile vermiculite and the glass tubes were wrapped with a sterile plastic bag that stopped evaporation from the vermiculite. Holes covered with a 3M micro-perforated tape allowed circulation of air. Plants were incubated in a growth chamber (26°C with a 12 h light/dark regime). The control consisted of seedlings immersed in 0.85% (v/v) saline solution without bacteria. There were 9 replicates for each of the time points for each bacterial strain and the control.

Plants were harvested aseptically every 48 h for 9 days, and the root with tightly adhering vermiculite excised (excluding the remaining cotyledons) and transferred into 15-ml sterile plastic tubes containing 10 ml PBS at 26°C. Bacteria were removed from roots by vortexing the tubes vigorously for 1 min. Bacterial numbers were measured in each sample batch from 100 μ l triplicates with a CellFacts Instrument. Bioluminescence was assayed immediately after harvest by placing 1 ml of the PBS mixture with 1 μ l of decanal in scintillation vials. The samples were shaken for 4 min at 26°C, light emission recorded using a luminometer (Model 20e, Turner Designs Photometer). Emission of light was integrated for 5 s and converted to Relative Light Units (RLU) per ml. Axenic conditions were verified at each time point by plating PBS dilutions on NB from non-inoculated control seedlings. The roots were further washed and dried in glass vials in an oven at 70°C for 24 h to obtain a dry weight measurement. The vermiculite and the bacterial cells from the PBS mixtures were pelleted at 10,000 g for 10 min and the supernatant was kept. Phenazine and HHL were assayed from suspension as described in section 2.9.3 and 2.8.

For image analysis, excised roots and seedlings were placed in a closed Petri dish in the presence of vapour of decanal obtained from 100 µl of 3% (v/v) decanal in mineral oil. Root colonisation was monitored by low-light video imaging, using a liquid-nitrogen cooled CCD-camera (Princeton Instruments, Trenton, NJ, LN/CCD-512-TKB). Images were integrated for 25 min and processed with Metamorph Software, which transformed luminescence into numerical data that were further analysed in Excel.

2.11. MONITORING GENE EXPRESSION ON STERILE WHEAT SEEDLINGS

Wheat seedlings (Hereward variety) were surface sterilised by suspending the seeds in 100% ethanol for 20 min and 25% sodium hypochlorite for 1 h with gentle shaking. Seeds were washed 5 times for 2 min each with sterile distilled water. Surface sterilised seeds were placed in Petri dishes 0.7% w/v agar (Difco), covered with a moistened Whatman filter paper, and pre-germinated at 21°C for 24 h. *P. aureofaciens* PGS12, B103, and I17 were grown individually for 18 h at 28°C in 1/5 strength NB (500 ml) in which little or no phenazine was produced. The cultures were centrifuged, the pellets washed twice in 0.85% (v/v) NaCl and re-suspended in 50 ml 0.85% (v/v) NaCl to give a final bacterial suspension at ca. 1×10^7 cells ml⁻¹. Surface sterilised pre-germinated seedlings were immersed in the bacterial suspensions for 20 min and blotted briefly. Control treatments consisted of seedlings dipped for 20 min in 0.85% (v/v) NaCl. The inoculation resulted in a bacterial population at 10^7 cells per seedling. The treated seedlings were placed immediately onto 0.7% (w/v) agar containing ½ strength Hoagland salt's solutions (macronutrients only; Hoagland and Arnon, 1950) in PBS (pH 7.4) in Petri dishes. Nine seedlings for each time point and for each bacterial strain and the control were placed in a Petri dish. The plates were sealed with 3M micro-perforated tape and the seedlings grown at 21°C with 12-h light/dark regime. Axenic conditions were verified at each time point by plating PBS dilutions on NB from uninoculated control seedlings.

The seedlings after 0, 24, 48 and 72 h were placed individually in 5 ml PBS (at 21°C) in plastic sterile tubes and vortexed for 30 s to detach the bacteria. Bioluminescence was assayed immediately by adding 0.1 µl decanal to 100 µl of the PBS

suspension in Eppendorf tubes. The tubes were shaken for 4 min at 28°C and light emission recorded using a luminometer (Model 20e, Turner Designs Photometer). Emission of light was integrated for 5 s and converted to Relative Light Units (RLU) per ml. Cell counts were obtained with a CellFacts Instrument. The seedlings were then discarded and the PBS suspension centrifuged at 10,000 g for 10 min. Phenazine and HHL were assayed from the supernatant as described above in section 2.9.3 and 2.8.

For image analysis, 15 seedlings inoculated with the reporter strains I17 or B103 were grown on 0.7% (w/v) agar containing ½ strength Hoagland salt's solutions (macronutrients only) in PBS (pH 7.4) and with vapour of decanal obtained from 100 µl of 3% (v/v) decanal in mineral oil. Bacterial gene expression was monitored by low-light video imaging, using liquid-nitrogen cooled CCD-camera (Princeton Instruments, Trenton, NJ, LN/CCD-512-TKB). Images were taken every hour for 72 h and transformed into numerical data using Metamorph Software and Excel.

2.12. STATISTICAL ANALYSIS

All data are presented as an average plus or minus (\pm) a confidence interval (C.I.) calculated from at least 3 replicates. The standard errors for each data point were plotted on the graphical representations of the data, and the significance of the result is reported in the text. All data were subject to statistical analysis using Microsoft Excel 97, Analysis toolpack (Microsoft Corporation).

CHAPTER THREE

SELECTION OF *LUXAB*-MARKED *P. AUREOFACIENS* STRAINS AND DEVELOPMENT OF BIOASSAYS

CHAPTER THREE.

SELECTION OF *LUXAB*-MARKED *P. AUREOFACIENS* STRAINS AND DEVELOPMENT OF BIOASSAYS

3.1. INTRODUCTION

Bacterial bioluminescence provides a real-time reporter for measuring gene expression, a sensitive marker for bacterial detection, and a measure of cellular activity and viability. Another advantage of bioluminescence is that it may be used to detect and monitor gene expression *in vitro* and *in situ* in a non-invasive and non-destructive manner (Prosser *et al.*, 1996; Stewart and Williams, 1992; Chapter 1).

Experiments by Amin-Hanjani *et al.* (1993) showed that introduction of a *luxABE* construct on the chromosome was more stable than on a multicopy plasmid. They constructed a luminescent strain of *P. fluorescens* 10586 in which luciferase activity was constitutive. They showed that the maximum growth rate of the chromosomally marked strain was unaffected compared to the wild-type but was reduced in the plasmid marked strain. The chromosomally encoded marker was stable in both liquid culture and in soil, whereas the plasmid was unstable during continuous subculturing in liquid medium and in soil. For these reasons, it was decided to mark *P. aureofaciens* PGS12 on the chromosome with the *luxA* and *luxB* genes. For this, a mini-Tn5 *luxAB* delivery system engineered by Lorenzo *et al.* (1990) to generate random gene fusions into a variety of Gram-negative bacteria was used. Transposon mutagenesis was followed by the selection of strains of interest. The selection focused on 2 types of strain: One with constitutive expression of luciferase and one marked with the *luxAB* genes in the phenazine operon able to report the transcriptional activity of the operon. In this chapter are described the ways in which the characterisation and selection of the *luxAB* strains were undertaken, the development of a *luxR*-based bioassay for the detection and quantification of AHL, and the optimisation of the parameters needed for measurement of luciferase activity.

3.2. AIMS

1. Construction of *luxAB::phz* gene fusions in order to study the transcriptional activity of the phenazine operon. After transposon mutagenesis of *P. aureofaciens* PGS12, strains were classified phenotypically as [HHL[±], Phz[±]], and genotypically characterised by PCR and sequencing of the PCR products, and finally a [HHL⁺, Phz⁻, LuxAB⁺] was selected. The selection of constitutively-luciferase-expressing strains is described in Chapter 5.
2. Optimisation of the amount of aldehyde and the period of incubation necessary to quantify luciferase activity from a selected *P. aureofaciens* strain.
3. Development of a bioassay for the detection and quantification of the autoinducer HHL.

3.3. MINI-TN5 TRANSPOSON MUTAGENESIS OF *P. AUREOFACIENS* PGS12

3.3.1. Recovery frequency of transconjugants

The recovery frequency of transconjugants was estimated from the ratio of the colony number on Pseudomonas Isolation Agar containing 75 µg ml⁻¹ tetracycline (PIA Tc⁷⁵) and PIA, after incubation at 30°C for 48 h. The total number of bacteria counted on PIA was $43.34 \times 10^9 \pm 1.88 \times 10^9$ CFU ml⁻¹, and the total number of transconjugants counted on PIA Tc⁷⁵ was $26.74 \times 10^2 \pm 8.57 \times 10^2$ CFU ml⁻¹. Therefore, Tc^R transconjugants of strain PGS12 were recovered at a frequency of 6.16×10^{-7} per final recipient. On average, 10 white colonies per ml were recovered on PIA Tc⁷⁵ at a frequency of 3.74×10^{-4} per Tc^R transconjugant.

3.3.2. Phenotypic classification of *luxAB*-marked strains

The wild-type strain *P. aureofaciens* PGS12 is orange due to the accumulation of phenazine antibiotics. After transposon mutagenesis, white strains were selected as they hold the potential to have a *luxAB* insert within the phenazine operon. Fig. 3.1 shows colonies of the wild-type strain PGS12 and of an isogenic *lux*-marked [HHL⁺, Phz⁻] strain on nutrient agar. Strains were subcultured on PIA and tested for light production

Fig. 3.1

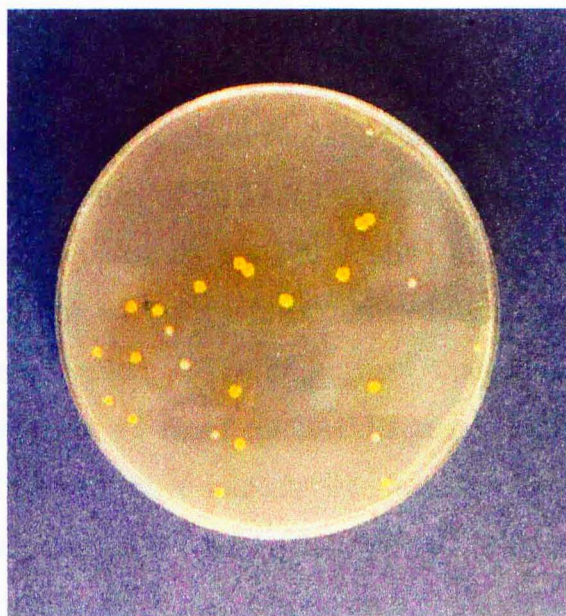


Fig. 3.1. Colonies of *P. aureofaciens* PGS12 (in orange) and of an isogenic *lux*-marked [HHL⁺, Phz⁻] strain on nutrient agar after 24 h of growth at 30°C.

with a CCD-camera after addition of decanal to the lid of the petri dishes. One colony per plate emitting the highest level of light was selected. All strains were also tested for auxotrophy on Kanner minimum medium with glycerol as a carbon source and the selected [*LuxAB*⁺] strains grew on minimum medium.

3.3.2.1. Classification according to phenazine and HHL production

Strains were tested for production of HHL and phenazine in liquid culture. They were grown in NB using for the inoculum a 1/100 dilution of an overnight culture. HHL production was measured after 6 h using a filter sterilised supernatant using the *lux*-AHL-bioassay (This chapter, section 3.4). Phenazine production was measured by spectrophotometry at OD₃₆₉ in 48 h old cultures. Bacterial cell numbers were counted after 6 and 48 h. A total of 65 white mutants were selected. 80% were [*HHL*⁻, *Phz*⁻], 4.6% were [*HHL*⁻, *Phz*⁺] and 15.4% were [*HHL*⁺, *Phz*⁻] (Table 3.1). Strains with the wild-type phenotype [*HHL*⁺, *Phz*⁺], and expressing high levels of light on PIA plates, were also kept and further tested for constitutive expression of *luxAB* (Chapter 5).

3.3.2.2. Classification according to pyoverdinin and mucus production

Strains were subcultured on King's B medium (KB), incubated at 28°C for 72 h, and tested for the production of fluorescent pyoverdinin siderophores under longwave (365 nm) UV irradiation. Non-fluorescent mutants [*Flu*⁻] were detected by their failure to fluoresce. Colonies of non-mucus producers [*Muc*⁻] were transparent whereas colonies of mucus producers were white for the [*phz*⁻] strains and orange for the [*phz*⁺] strains. All [*HHL*⁻] strains were also [*Muc*⁻] and all [*HHL*⁺] were [*Muc*⁺] (Table 3.2). The [*Flu*⁻] phenotype did not seem to be related to the lack of autoinducer or phenazine production. Out of all selected strains, 17.74% were [*Flu*⁻].

3.3.3. Genotypic characterisation of [*HHL*⁺, *Phz*⁻] strains by PCR

3.3.3.1. Screening for insertion within the biosynthetic genes of the phenazine operon

White strains with [*HHL*⁺, *phz*⁻] phenotypes were screened for miniTn5-*luxAB* insertion within *phzF*, *phzA*, and *phzB* genes using a forward and a reverse primer designed to hybridise at the 5' and 3' end of each gene. Table 3.3 gives the complete sequences of

Table 3.1. Classification of *luxAB*-marked *P. aureofaciens* strains for HHL and phenazine production.

Phenotype ¹	Name of strains	% and (totals)
[HHL ⁻ , Phz ⁻]	I1, I5, I7, I9, I10, I11 (10% Phz), I12, I13, I15, I16 (10% HHL, 10% Phz), I18Y [*] , I19, B1, B2, B3, B4 (10% HHL, 10% Phz), B5, B6, B8, B9, B11, B12, B14, B15, B16, B17, B18, B19, B20, B21, B22, B105 [*] , A1, A2, A3, A4, A5Y [*] , A6 (5%HHL, 10% Phz), A7 (50% HHL), A8 (25% HHL), A11, A12, A13, A14, A15, A16, A17, A18, A19, ZO3, XBB1, ZB3	80% (52)
[HHL ⁺ , Phz ⁻]	I14, I15, I18W [*] , B103 [*] , A9, A5W [*] , A10, ZBC1, ZBA1, YA1	15.4% (10)
[HHL ⁻ , Phz ⁺]	I4, I11, A4	4.6% (3)

¹Strains were classified as [HHL⁺] or [PCA⁺] when light output or absorbance at OD₃₆₉ was equal to or not less than 25% of the level recorded from the parent strain, *P. aureofaciens* PGS12; and *vice versa*, strains were classified as [HHL⁻] or [PCA⁻] when the levels were 25% less than the parent strain.

*Strains I18Y, A5Y and B105 were spontaneous mutants of strains I18W, A5W and B103 respectively.

Table 3.2. Classification of *luxAB*-marked *P. aureofaciens* strains for HHL, phenazine, mucus¹ and siderophore production.

Phenotypes	Strains
HHL ⁺ , Phz ⁺ , Muc ⁺ , Flu ⁺	B23, I2, I3, I16, I6, I8,
HHL ⁺ , Phz ⁺ , Muc ⁺ , Flu ⁻	A20, B7
HHL ⁺ , Phz ⁻ , Muc ⁺ , Flu ⁺	I14, I15, I18W, A5W, A9, A10, B103, YA1, ZBC1, ZBA1,
HHL ⁻ , Phz ⁻ , Muc ⁻ , Flu ⁺	I1, I5, I7, I10, I11, I12, I13, I18Y, I19, A1, A2, A5Y, A6, A7, A8, A11, A12, A13, A14, A15, A16, A17, A18, A19, B2, B3, B4, B8, B9, B105, B11, B12, B14, B15, B16, B17, B18, B19, B21, B22
HHL ⁻ , Phz ⁻ , Muc ⁻ , Flu ⁻	I9, B1, B5 (10% Phz), B6, B20, XBB1, ZO3, ZB3, I16
HHL ⁻ , Phz ⁺ , Muc ⁻ , Flu ⁻	A4, I4

¹ Mucus phenotype is abbreviated as Muc and siderophore production is abbreviated as Flu (for fluorescence).

Table 3.3. Primers and conditions for PCR amplification.

Primers	Sequence	Target gene (Product size)	Annealing T°/ [MgCl ₂]/ [Primer] [*]
PhzFfd	ATCCCTCGTGAGAGTGATCG	<i>phzF</i> (1220 bp)	60°C/ 3 mM/ 0.9 μM
PhzFrv	GGTGAAGAGGGCTGGTTTT		
PhzAfd	TTCCATCGATCGTCCCTTAC	<i>PhzA</i> (550 bp)	63°C/ 3 mM/ 0.9 μM
PhzArv	ATCCAGTGGTGCTCTTTGCT		
PhzBfd	ACCTCATGGAACGCATCCT	<i>PhzB</i> (1880 bp)	63°C/ 2 mM/ 0.6 μM
PhzBrv	AAGCGTTGTTCTCGACAGGT		
PhzB2fd	CAAAAACAGATCGACCTGTTTG	<i>phzB</i>	60°C
I3fd	TACGACTACCTGGGCCAGAC	<i>phzI</i>	60°C
Irv	AGTTTGATGGCGAGGATTTTT	<i>phzI</i>	60°C
LuxAB3rv	AATCTTTATCGTACAAACCGCG	<i>luxA</i>	60°C

* The conditions for the annealing temperature (T°), magnesium chloride concentration and primer concentrations for the PCR reaction were determined using the HybaidTM Thermocycler or given by the Gibco BRL from where all primers were ordered.

primer sets and summarises general physical information. DNA from all 11 [HHL⁺, Phz⁻] strains was extracted and amplified by PCR.

With the phzFfd-phzFrv primer set, a 1210 bp PCR product was obtained for most of the strains but the amplification gave faint results even with the wild-type strain (figure not shown). With the phzAfd-phzArv primer set, a 550 bp PCR product was obtained from all strains (Fig. 3.2). With the phzBfd-phzBrv primer set, a 1880 bp PCR product was obtained from all strains except B103, I18W, B105 and I18Y (Fig. 3.3). This provided an early indication that in these strains the *luxAB* transposon may have inserted in *phzB*.

3.3.3.2. Screening for insertion within *phzB*

LuxAB3rv is a reverse primer designed to hybridise at 1025 bp from the start codon of the *luxA* gene. The luxAB3rv primer and the forward primers phzFfd, phzAfd, and phzBfd gave PCR products of 4000, 3300 and 2300 bp respectively (Fig. 3.4). No or faint PCR amplifications were obtained with strains I18Y and I18W, whereas strains B103 and B105 gave sufficient PCR product for sequencing. The PCR product obtained with strain B103 with the primers phzBfd and luxAB3rv was sequenced using both primers for the start of the sequencing reaction. A 450 bp sequence was generated with each primer and the sequences were searched for homology with cloned and published sequences in BlastA (<http://www.ncbi.nlm.nih.gov/blast/blast.cgi>). The sequence from phzBfd showed 92% identity with *phzB* from *Pseudomonas aureofaciens* 30-84 (GenBank accession no L48339) and the sequence from luxAB3rv showed 86% identity with *luxAB* from *Vibrio harveyi* (GenBank accession no M10961). From these results, the insertion within *P. aureofaciens* B103 was located about 1000 bp from the 5' end of *phzB*. In an attempt to localise more precisely the point of insertion of the *luxAB* genes, another forward primer, phzB2fd, was designed. It hybridised 1623 bp from the start codon of *phzB* and was used to start a sequencing reaction using the PCR product generated with phzBfd and luxAB3rv primers. A sequence overlapping *phzB* and *luxA* was obtained. Fig. 3.5 summarises the highest homology with known sequences found in Blast A. The insertion was localised 1865 bp from the start codon of *phzB* (Fig. 3.6).

Fig. 3.2. PCR amplification of *phzA* with *phzAfd* and *phzArv* primers.

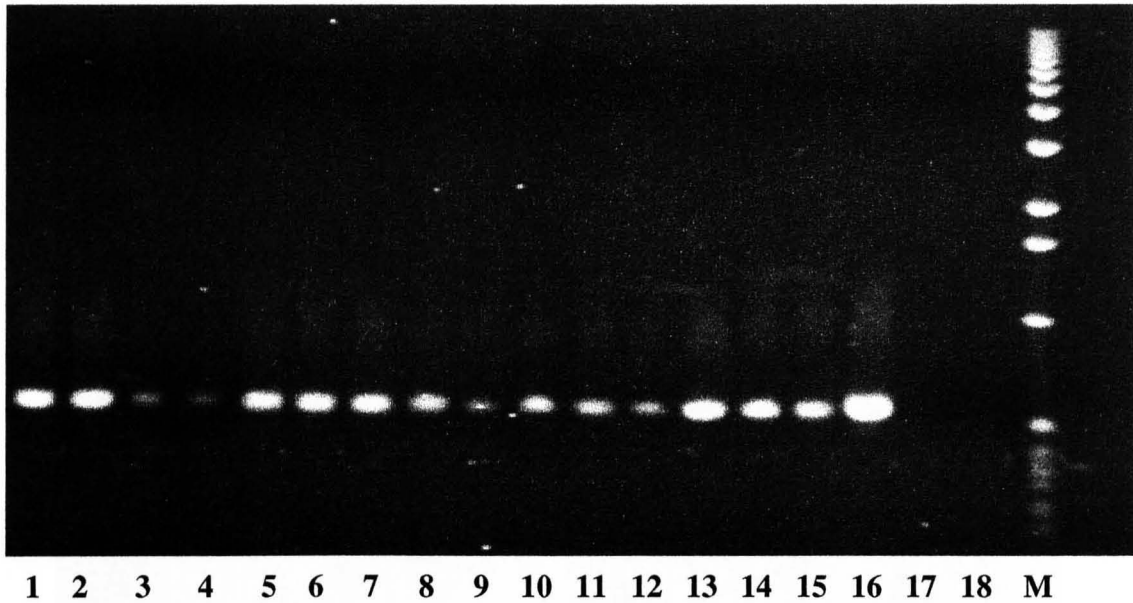


Fig. 3.2. Lanes: 1 to 11: eleven [HHL⁺, phz⁻] *luxAB*-marked strains; 12: wild-type strain PGS12; 13: strain B105; 14: strain I18W; 15: strain EH5; 16: strain W; 17: *E. coli* JM107; 18: no target DNA; M: 1 kb ladder.

All PCR products were around 550 bp. Strain EH5 is a [HHL⁺, phz⁻] *inaZ*-marked strain and strain W a spontaneous mutant [HHL⁻, phz⁻] of the wild-type strain PGS12 (Georgakopoulos, 1994a).

Fig. 3.3. PCR product from *phzB* obtained with *phzBfd* and *phzBrv* primers.

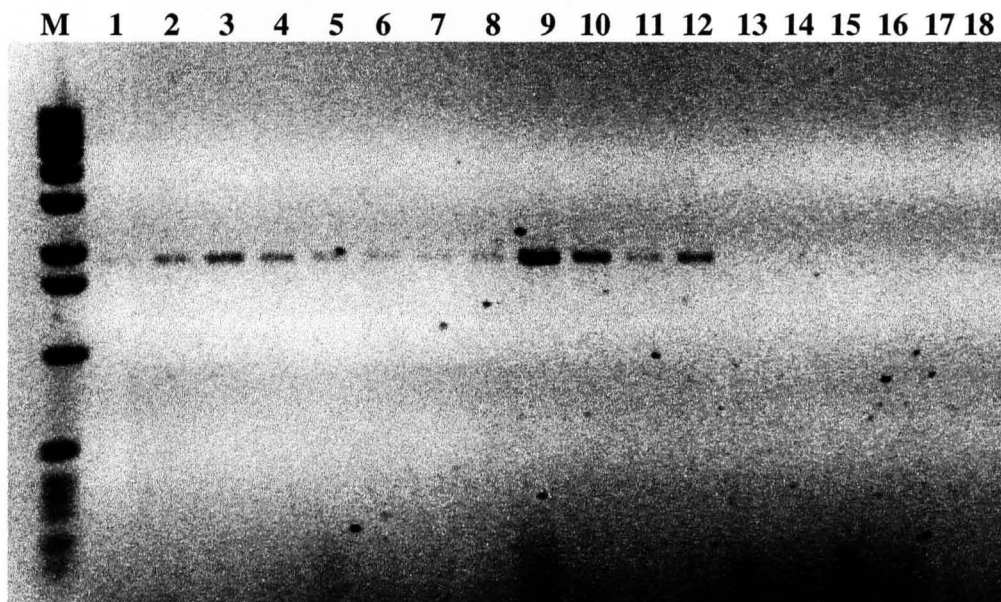


Fig. 3.3. Lanes: 1 to 9: nine [HHL⁺, *phz*⁻] *lux*-marked strains; 10: strain PGS12; 11: strain EH5; 12: strain W; 14: strain I18W; 15: strain I18Y; 16: strain B105; 17: strain B103; 18: *E. coli* JM107; M: 1 kbp ladder.

All PCR products were around 1880 bp. Strain EH5 is a [HHL⁺, *phz*⁻] *inaZ*-marked strain and strain W a spontaneous mutant [HHL⁻, *phz*⁻] of the wild-type strain PGS12 (Georgakopoulos, 1994a).

Fig. 3.4. PCR products obtained with the luxAB3rv primer.

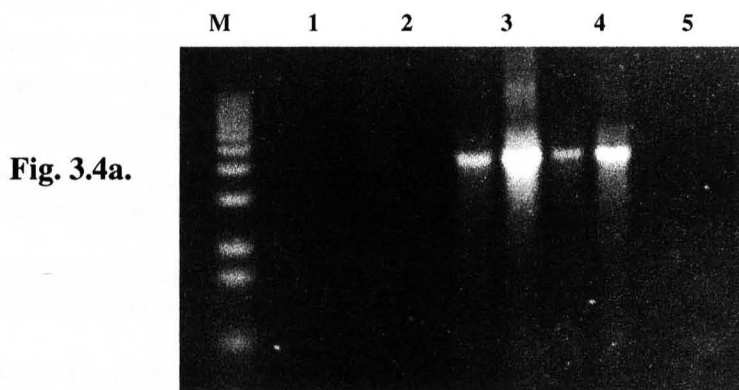


Fig. 3.4a.

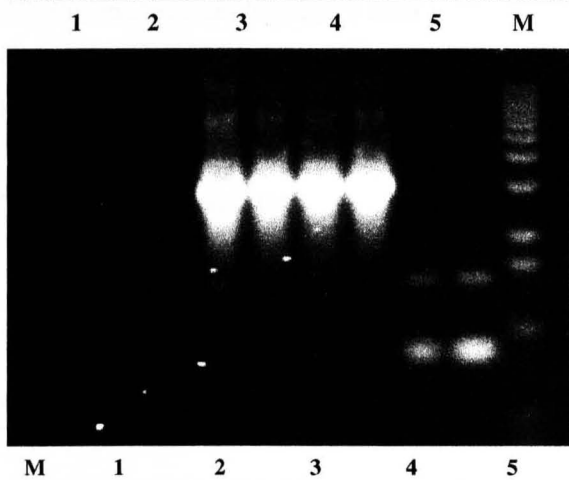


Fig. 3.4b.

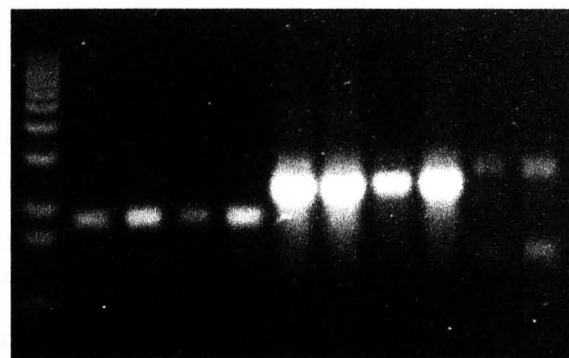


Fig. 3.4c.

Fig. 3.4. PCR products obtained with the primer luxAB3rv and either the primer phzFfd (Fig. 3.4a), or phzAfd (Fig. 3.4b), or phzBfd (Fig. 3.4c).

All PCR reactions were done in replicates. Lanes 1: strain I18Y; 2: I18W; 3: B105; 4: B103; 5: PGS12; M: 1 kb ladder.

The PCR products from strains B103 and B105 measured: with the primer phzFfd 4000 bp, with the primer phzAfd 3300 bp, with the primer phzBfd 2300 bp.

The PCR products from strains I18Y and I18W measured with phzBfd 1500 bp (no product was obtained with the other primers).

Faint false positive products were obtained from strain PGS12.

Fig. 3.5. Alignments results from BlastA database with the sequence IRB2.

Pseudomonas chlororaphis autoinducer synthase PhzI (phzI), transcriptional activator PhzR (phzR), PhzA (phzA), PhzB (phzB), PhzC (phzC), PhzD (phzD), PhzE (phzE), PhzF (phzF), PhzG (phzG), and PhzH (phzH) genes, complete cds Length = 10508

Score = 121 bits (61), Expect = 2e-25
Identities = 64/65 (98%)
Strand = Plus / Plus

Query: 52 ggcacatggcaccgtcgaatcagccgacagcagaccggcgaagtgcacgccctgcgtggacc 116
Sbjct: 6589 ggcacatggcaccgtcgaatcagccgacagcagaccggcgaagtgcacgccctgcgtggacc 6653

Query: 116 ccgagtcgctgctgaaccaggaaggtccgcgcatcatcgccgatctgctgcggcacgccc 176
Sbjct: 6680 ccgagtcgctgctga-cccaggaaggtccgcgcatcatcgccgatctgctgcggcacgccc 6739

Query: 15 ccgaacgggtgggtttctacaacaccttcgccgccc 50
Sbjct: 6524 ccgaacgggtgggtttctacaacaccttcgccgccc 6559

V. harveyi luciferase alpha and beta subunit (luxA and luxB) genes, complete cds Length = 3141

Score = 117 bits (59), Expect = 3e-24
Identities = 66/67 (98%), Gaps = 1/67 (1%)
Strand = Plus / Plus

Query: 192 gtcgactttatcgagcctgattttgaacaactca-catcgcgactgtgaatgaacgtcgcttgaag 257
Sbjct: 571 gtcgactttatcgagcctgattttgaacaactcaccatcgcgactgtgaatgaacgtcgcttgaag 637630

Query: 258 taggtcttatcgtaat-ccaacaaataaggaa 288
Sbjct: 670 taggtcttatcgtaataccaacaaataaggaa 701

Pseudomonas aureofaciens phzFABCD genes, complete cds's Length = 5698

Score = 115 bits (58), Expect = 1e-23
Identities = 61/62 (98%)
Strand = Plus / Plus

Query: 52 ggcacatggcaccgtcgaatcagccgacagcagaccggcgaagtgcacgccctgcgtgg 113
Sbjct: 3659 ggcacatggcaccgtcgaatcagccgacagcagaccggcgaagtgcacgccctgcgtgg 3720

Query: 116 ccgagtcgctgctgaaccaggaaggtccgcgcatcatcgccgatctgctgcggcacgccc 176
Sbjct: 3750 ccgagtcgctgctga-cccaggaaggtccgcgcatcatcgccgatctgctgcggcacgccc 3809

Query: 16 cgaacgggtgggtttctacaacaccttcgccgcccag 52
Sbjct: 3595 cgaacgggtgggtttctacaacaccttcgccgcccag 3631

Pseudomonas fluorescens autoinducer synthase (phzI) gene, positive regulator protein (phzR), phzABCDEFG genes, complete cds Length = 8505

Score = 85.7 bits (43), Expect = 9e-15
Identities = 55/59 (93%)
Strand = Plus / Plus

Query: 55 atcggcaccgtcgaatcagccgcgacagcgagaccggcgaagtgcacccctgcgtgg 113
Sbjct: 6417 atcggcaccgtggaatcagtcgacagcgagaccggcgaagtgcacccctgcgtgg 6475

Score = 75.8 bits (38), Expect = 9e-12
Identities = 44/46 (95%)
Strand = Plus / Plus

Query: 131 acccaggaaggtccgcatcatcgccgatctgctgcccacgccc 176
Sbjct: 6519 acccaggaaggtccgcatcatcgccgatctgctgcccacgccc 6564

Score = 38.2 bits (19), Expect = 1.9
Identities = 28/31 (90%)
Strand = Plus / Plus

Query: 15 ccgaacgggtgggtttctacaacaccttcgc 45
Sbjct: 6349 ccgaacgagtaggtttctacaacacgttcgc 6379

***Pseudomonas aeruginosa* pyocyanine biosynthesis operon, complete sequence Length = 6720**

Score = 60.0 bits (30), Expect = 5e-07
Identities = 42/46 (91%)
Strand = Plus / Plus

Query: 65 tcgaaatcagccgcgacagcgagaccggcgaagtgcacccctgcg 110
Sbjct: 5020 tcgagatcagccgcgaccgagaccggcgaagtgcacccctgcg 5065

Query: 140 ggtccgcatcatcgccgatctgctgcccacgc 174
Sbjct: 5121 ggtccgcatcatcgccgatctgctgcccacgc 5155

***Vibrio harveyi* gene luxA fragment encoding lucifer alpha subunit Length = 163**

Score = 48.1 bits (24), Expect = 0.002
Identities = 31/32 (96%), Gaps = 1/32 (3%)
Strand = Plus / Plus

Query: 258 taggtctatcgtaat-ccaacaataaggaa 288
Sbjct: 43 taggtctatcgtaatccaacaataaggaa 74

Fig. 3.5. Alignments results from BlastA database with the sequence IRB2.
IRB2 is the sequence (started with the primer phzB2fd) of the PCR product generated with the phzBfd and luxAB3rv primers.

Fig. 3.6. Localisation of the miniTn5luxAB insertion within *phzB*.

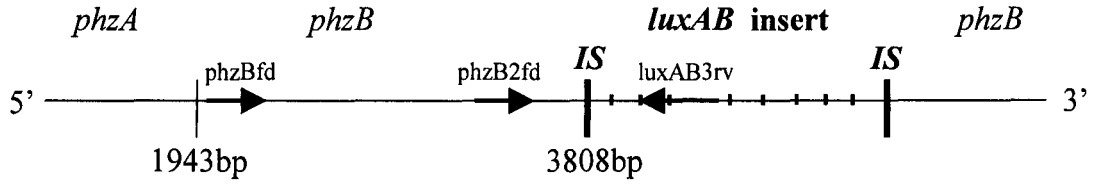


Fig. 3.6. The *phzB2fd* primer was used to start a sequencing reaction that led to the identification of the insertion of the *luxAB* genes within *phzB*. The sequencing reaction was made from the PCR product obtained with the *phzBfd* and *luxAB3rv* primers. The *phzB* gene in *P. aureofaciens* 30-84 (accession number L48339) is at 1943 bp from the first start codon of the phenazine operon and the *luxAB* insertion is at 3808 bp.

3.3.4. Genotypic characterisation of [HHL⁻, Phz⁻] strains by PCR

Two primers, I3fd and Irv, hybridising at each end of *phzI* gene were designed using the sequence provided by GenBank (Accession number: L33724) for *P. aureofaciens* 30-84 as a template. DNA from [HHL⁻, Phz⁻] strains was extracted and PCR amplification undertaken. PCR products were generated for all strains apart for strain B21 (Fig. 3.7). PCR amplification using I3fd and luxAB3rv was attempted but it was not possible to obtain a single product. Phenazine production was restored in colonies of strain B21 grown on NA close to an HHL producer such as strain PGS12.

3.4. BIOLUMINESCENCE MEASUREMENTS FOLLOWING DECANAL ADDITION TO LIQUID CULTURE

Strains marked with *luxAB*, and not the entire *luxABCDE* operon, require the addition of exogenous aldehyde to produce light. When assaying for any enzyme, care has to be taken to establish that, firstly, the measured rate is the true initial rate of reaction, and, secondly, the substrate concentration is not a limiting factor. The level of light emitted by a bacterial cell depends on the concentration of O₂, FMNH₂, aldehyde and luciferase within the cell. The availability of excess O₂ to the bioluminescent bacteria was ensured by shaking the culture during growth and by continuous mixing during light measurement. To obtain reproducible results, the temperature was kept constant throughout the measurements. The *V. harveyi* enzyme is stable up to 37°C, and luminescence was recorded at 28°C for optimal growth of the *P. aureofaciens* strains marked with *luxAB*. Fig. 3.8 shows the light output from strain B103 following the addition of different volumes of decanal. To test the toxicity of decanal, viable cell counts were determined after recording light output for 10 min (Table 3.4).

In the presence of excess substrate, the initial rate of the enzyme catalysed reaction is calculated for the part of the curve of product formation against time that is linear. Because light does not accumulate, the initial rate of reaction catalysed by luciferase was determined when a constant amount of light per unit of time was emitted from the culture. When undiluted decanal was added to B103, luminescence first increased rapidly during the first 2 min, and then remained stable or increased slowly (Fig. 3.8). Addition of 3 µl ml⁻¹ decanal did not increase the level of luminescence

Fig. 3.7. PCR amplification of *phzI* with I3fd and Irv primers for [HHL⁻, phz⁻] strains.

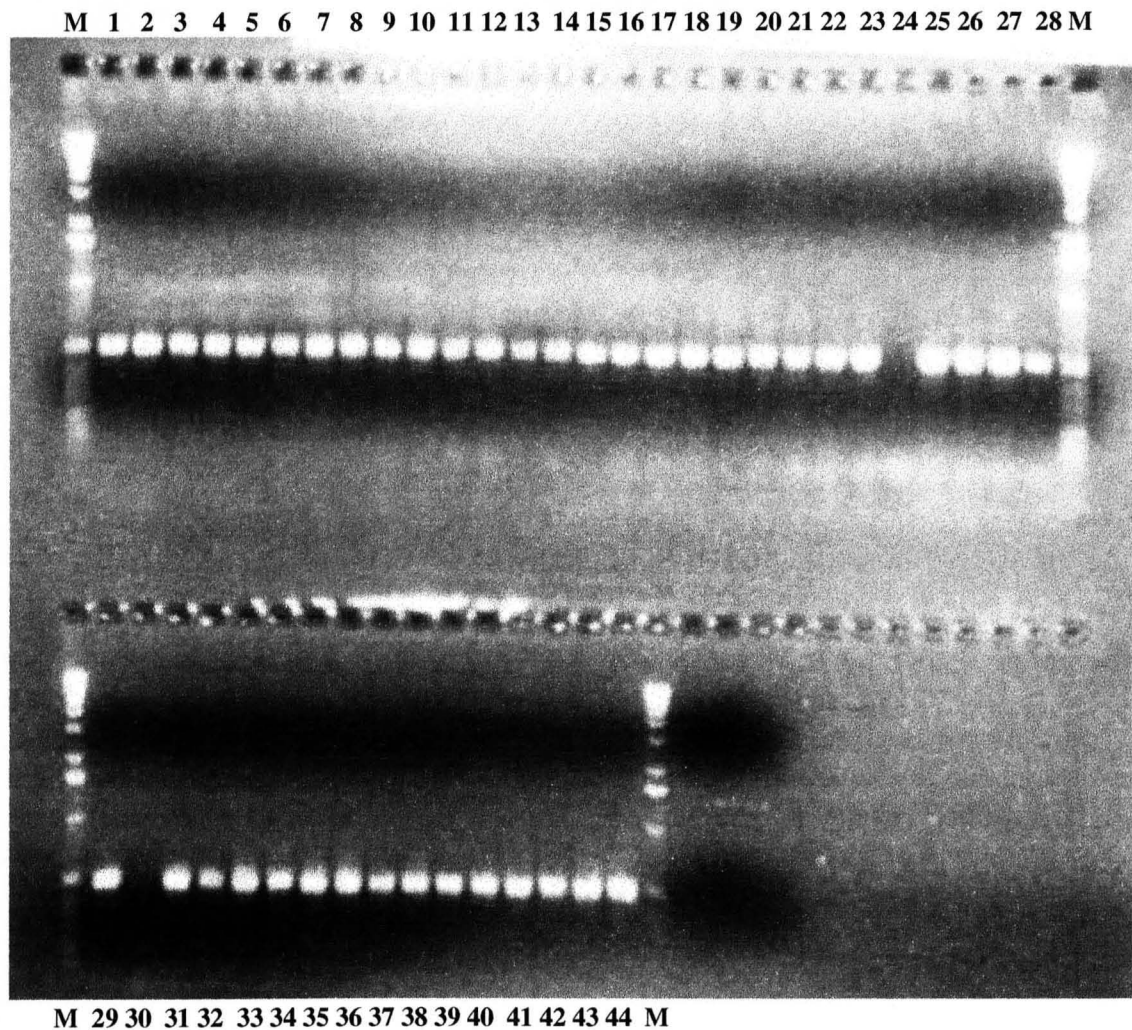


Fig. 3.7. Lanes: 1 to 23: Strains PGS12, I1, I4, I5, I7, I10, I11, I12, I13, I16, I19, B1, B2, B3, B4, B5, B6, B8, B9, B11, B12, B14, B15; lane 24: control, no DNA; lane 25 to 29: strains B16, B17, B18, B19, B20; lane 30: strain B21; lane 31 to 44: strains B22, A1, A2, A4, A6, A11, A12, A13, A14, A15, A16, A17, A18, A19; lane M: 1 kb ladder. All PCR products were around 500 bp.

Fig. 3.8

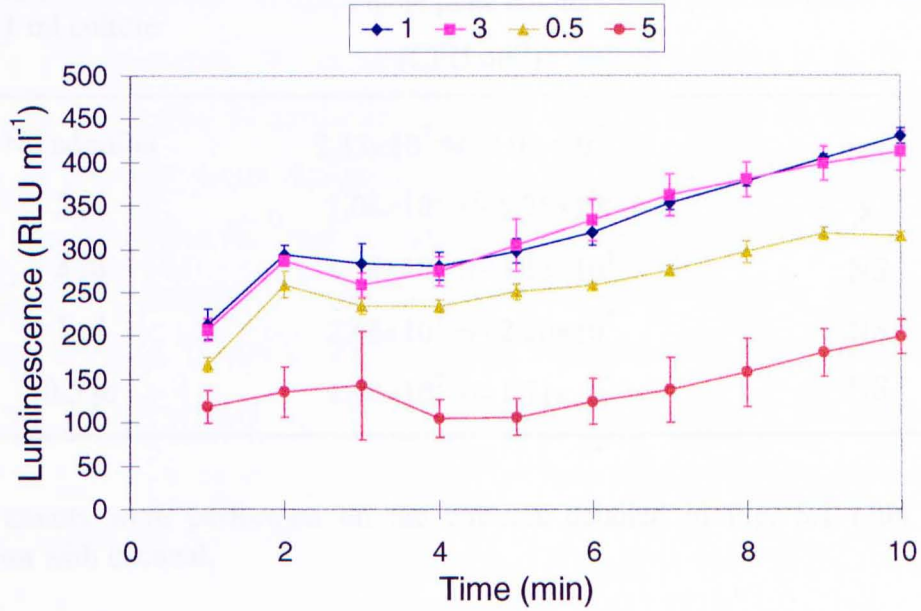


Fig. 3.8. Bioluminescence following addition of decanal ($\mu\text{l ml}^{-1}$) to *P. aureofaciens* B103.

A culture of strain B103 was inoculated at 7×10^7 TCC ml^{-1} and grown in NB for 2 h. Bioluminescence was measured at 1 min intervals from 1 ml samples of culture following the addition of 5, 3, 1 or 0.5 μl decanal. The culture was shaken and kept at 28°C throughout the measurements. Standard errors of means shown ($n = 3$).

Table 3.4. Viability of *P. aureofaciens* B103 following a 10-min incubation with decanal.

Decanal addition to 1 ml culture	Viable plate counts ^a (CFU ml ⁻¹)	Significance ^b
No addition	2.43×10 ⁷ +/- 2.03×10 ^{7(c)}	NS
5 µl	1.08×10 ⁶ +/- 5.76×10 ⁵	S
3 µl	1.19×10 ⁷ +/- 3.13×10 ⁶	NS
1 µl	2.66×10 ⁷ +/- 2.20×10 ⁷	NS
0.5 µl	1.90×10 ⁷ +/- 1.71×10 ⁷	NS

^a Plate counts were performed on the cultures detailed in Fig. 5.1 after a 10 min incubation with decanal.

^b Significance levels were determined using the Student T-test to compare the viability of a culture to which no decanal was added to cultures with various additions of the aldehyde. Values significant at the $P \leq 0.05$ level are indicated by S and those not significantly different at the $P \leq 0.05$ level are indicated by NS.

^c The confidence intervals were determined from 3 replicates using T-test_(0.05).

obtained with $1 \mu\text{l ml}^{-1}$, suggesting that with $1 \mu\text{l ml}^{-1}$ the aldehyde substrate was already in excess. With the addition of $0.5 \mu\text{l ml}^{-1}$ decanal, the level of luminescence remained lower than with $1 \mu\text{l ml}^{-1}$ throughout the 10-min determination period, suggesting that the aldehyde was at a limited concentration. Addition of more decanal ($5 \mu\text{l ml}^{-1}$) led to a reduction in light output. This corresponded to a similar decrease in viable cell counts (Table 3.4), which may be attributed to a toxic effect of decanal on the cells. T-test_{0.05} analysis of the light output emitted between 3 and 6 min, after addition of $1 \mu\text{l ml}^{-1}$ decanal, confirmed that the level of luminescence was not significantly different during this 3 min incubation period. This indicated that the initial rate of the luciferase reaction was being recorded. Therefore, for subsequent experiments, undiluted decanal was used at $1 \mu\text{l ml}^{-1}$ of cell solution and bioluminescence was measured 4 min after addition of aldehyde. This was in accordance with what has been used in other bacterial species such as *E. coli* (Rattray *et al.*, 1990).

3.5. DEVELOPMENT OF A LUXR-BASED BIOASSAY FOR DETECTION AND QUANTIFICATION OF HHL

A bioassay based upon the reporter strain, *E. coli* JM107 containing a *luxR*-based plasmid sensor for AHLs (pSB401) was developed. The plasmid pSB401 engineered by Winson *et al.* (1998) carries a fusion of *luxRI'* regulatory genes (from *V. fischeri*) to the complete biosynthetic gene cluster *luxCDABE* (from *Photobacterium luminescens*) on a pRK415 plasmid. The construct is further described in Chapter 1 (section 1.3.5).

3.5.1. Dose-response curves

The concentrations of hexanoyl homoserine lactone (HHL) produced by *P. aureofaciens* were quantified by comparing light emitted from samples with light emitted from a dilution series of pure HHL. The purified HHL compound was kindly provided by Prof. Paul Williams, Department of Biological Sciences, University of Nottingham, UK. The bioassay is described in Fig. 3.9. In order to establish the optimal parameters to obtain a calibration curve for a large range of HHL concentrations, the *E. coli* JM107 (pSB401) culture was diluted in NB, and incubated (at 37°C with shaking) with a serial dilution of

Fig. 3.9.

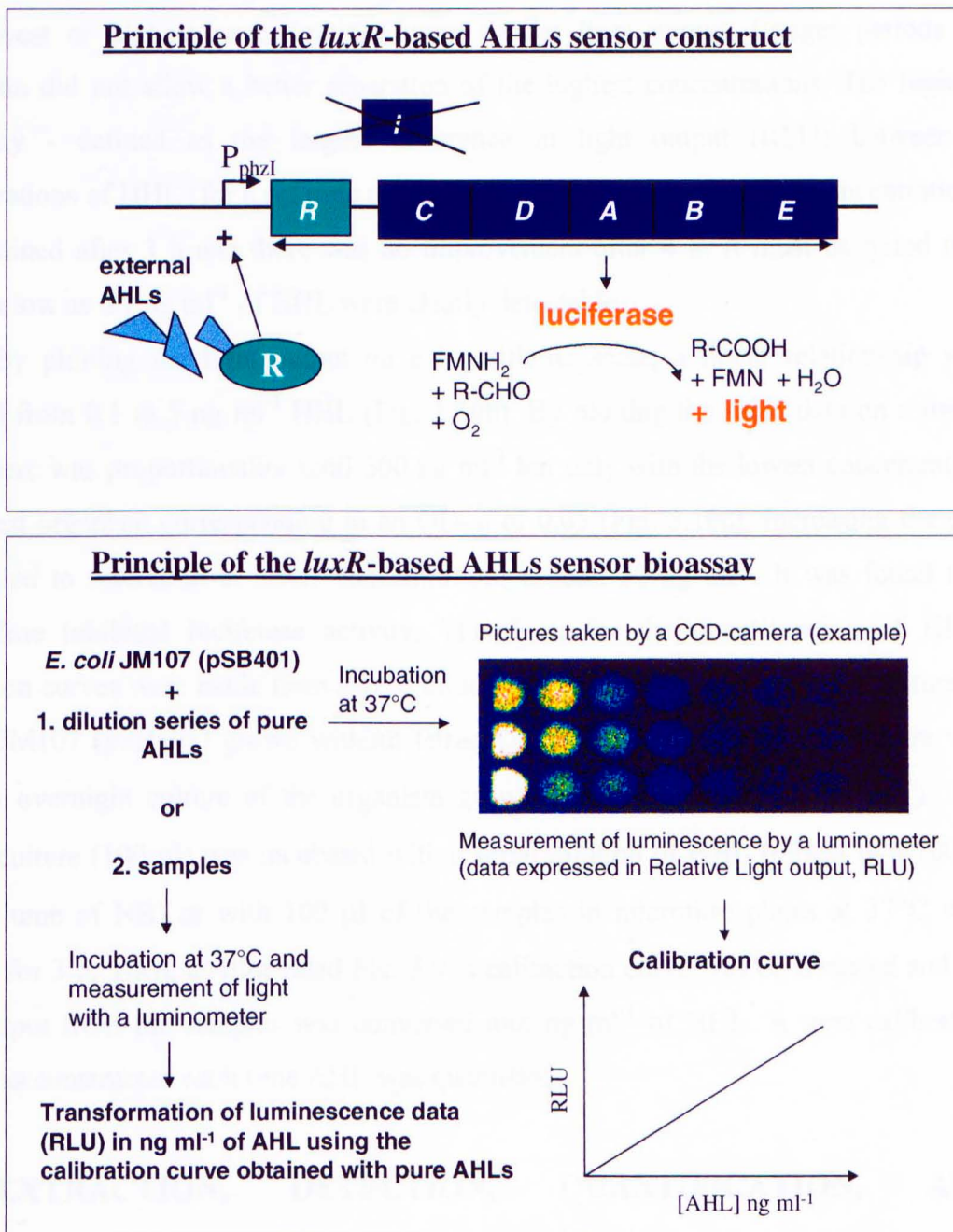


Fig. 3.9. Description of the bioassay for detection and quantification of AHLs.

100 μ l of a 1/10 of a 5 h culture of the sensor strain was added to a microtitre plate with 100 μ l of the filter sterilised bacterial suspensions to be tested for HHL production, or with 100 μ l of a dilution series of pure AHL in NB. The plates were incubated for 3.5 h at 37°C with gentle shaking. The level of bioluminescence was recorded from both plates with a Labsystem Luminoskan luminometer. A calibration curve was constructed from the light output recorded with pure AHLs. The AHL concentrations in the samples were calculated from this calibration curve.

HHL. Several incubation times and concentrations of the test organism were tested. The results showed an increase in luminescence with time and with HHL concentrations (Fig. 3.10a). After 1 h incubation, the different HHL concentrations were discernible; only the very lowest or highest concentrations gave similar light output. Longer periods of incubation did not allow a better separation of the highest concentrations. The highest sensitivity - defined as the largest difference in light output (RLU) between 2 concentrations of HHL (for a set time of incubation) - for the lowest HHL concentrations was obtained after 3 h and there was no improvement after 4 h. It must be noted that levels as low as 0.1 ng ml^{-1} of HHL were clearly detectable.

By plotting the light output on a logarithmic scale, a linear relationship was obtained from 0.1 to 5 ng ml^{-1} HHL (Fig. 3.10b). By plotting the same data on a linear scale, there was proportionality until 500 ng ml^{-1} but only with the lowest concentration of the test organism corresponding to an OD_{600} of 0.05 (Fig. 3.10c). Increasing the cell density led to saturation at lower concentrations around 50 ng ml^{-1} . It was found that tetracycline inhibited luciferase activity. Therefore, for the quantification of HHL, calibration curves were made from a $1/10$ dilution in NB ($\text{OD}_{600} 0.05$) of a 5 h culture of *E. coli* JM107 (pSB401) grown without tetracycline. The inoculum of this culture was from an overnight culture of the organism grown with tetracycline ($12 \mu\text{g ml}^{-1}$). The diluted culture ($100 \mu\text{l}$) was incubated with a serial dilution of HHL (mixed in a $100 \mu\text{l}$ final volume of NB) or with $100 \mu\text{l}$ of the samples in microtitre plates at 37°C with shaking for 3 h. Then, as illustrated Fig. 3.9, a calibration curve was constructed and the light output from the samples was converted into ng ml^{-1} of HHL. A new calibration curve was constructed each time AHL was quantified .

3.6. EXTRACTION, DETECTION, QUANTIFICATION, AND BIOLOGICAL ACTIVITY OF PCA

3.6.1. PCA extraction and analysis by HPLC

PCA was extracted from liquid culture of *P. aureofaciens* PGS12 using an adaptation of a method described by Thomashow *et al.* (1990) which was used to extract PCA from liquid culture and also from the rhizosphere of wheat. The extracted and pure PCA

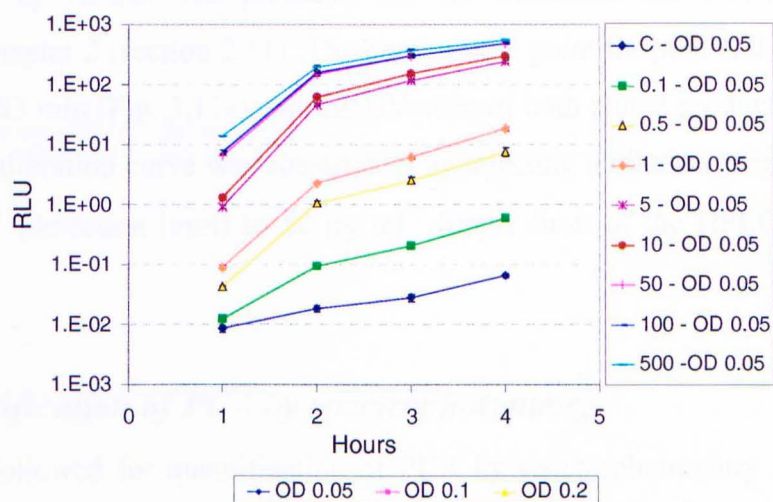
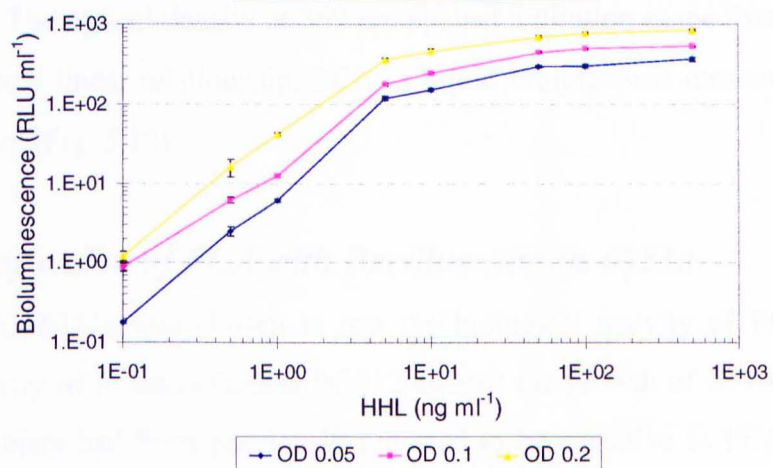
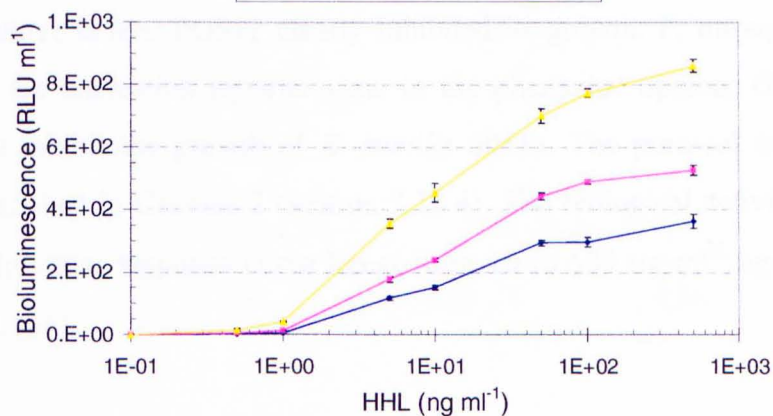
Fig. 3.10a**Fig. 3.10b****Fig. 3.10c**

Fig. 3.10. Construction of a calibration curve for HHL quantification: Effect of the incubation time (Fig. 3.10a) and the concentration of the test organism, *E. coli* JM107 (pSB401) (Fig. 3.10b and 3.10c).

In Fig. 3.10a, a serial dilution of pure HHL (from 0.1 to 500 ng ml⁻¹) was incubated at 37°C with the reporter strain. Luminescence was recorded every 1 h. In Fig. 3.10b and 3.10c, the test organism was diluted in NB to 3 concentrations (measured at OD₆₀₀). Luminescence was measured after 3 h incubation. Fig. 3.10b and 3.10c correspond to the same data plotted on 2 different scales. Standard error of means shown ($n = 5$).

compounds (Maybridge Chemical Company Ltd., UK), both dissolved in 5% NaHCO₃, were analysed by HPLC. The protocols for the extraction and HPLC analysis are described in Chapter 2 (section 2.11). The elution time point for pure and extracted PCA coincided at 3.83 min (Fig. 3.11a) and the UV-scan of both eluted products showed 95% similarity. A calibration curve was constructed by injecting a dilution range of pure PCA from 5 ng ml⁻¹ (detection limit) to 50 µg ml⁻¹ (upper limit of the HPLC system) (Fig. 3.11b).

3.6.2. Quantification of PCA by spectrophotometry

The protocol followed for quantification of PCA by spectrophotometry is described in section 2.11.3. The optical density at 369 nm against a dilution range from 50 ng ml⁻¹ to 50 µg ml⁻¹ gave a linear relationship. PCA in liquid samples was measured against this calibration curve (Fig. 3.12).

3.6.3. Quantification of PCA with *Bacillus subtilis* 6051a

Bacillus subtilis 6051a was chosen to test the biological activity of PCA. Fig. 3.13a shows the activity of *P. aureofaciens* PGS12 against the growth of *B. subtilis* 6051a on NA. This organism had been previously reported to be sensitive to PCA (Stead *et al.*, 1996) and *P. aureofaciens* PGS12 clearly inhibited its growth. *P. aureofaciens* EH5 (a strain with an ice nucleation reporter gene in the phenazine operon; Georgakopoulos, 1994a) did not inhibit the growth of *B. subtilis* 6051a. The protocol followed for the bioassay is described in Chapter 2 (section 2.11.4). The biological activity of PCA was reflected in a log-dose response curve linear from 10 to 500 µg ml⁻¹ against the OD at 600 nm (Fig. 3.13b).

3.7. CONCLUSIONS AND DISCUSSION

After transposon mutagenesis, the resulting transconjugants had a single, stably integrated chromosomal copy of the *luxAB* genes, thereby avoiding potential gene dosage artefacts in subsequent studies of phenazine gene regulation. The transposition frequency of ca. 6×10^{-7} was close to frequencies given in the literature. Lorenzo *et al.* (1990)

Fig. 3.11a

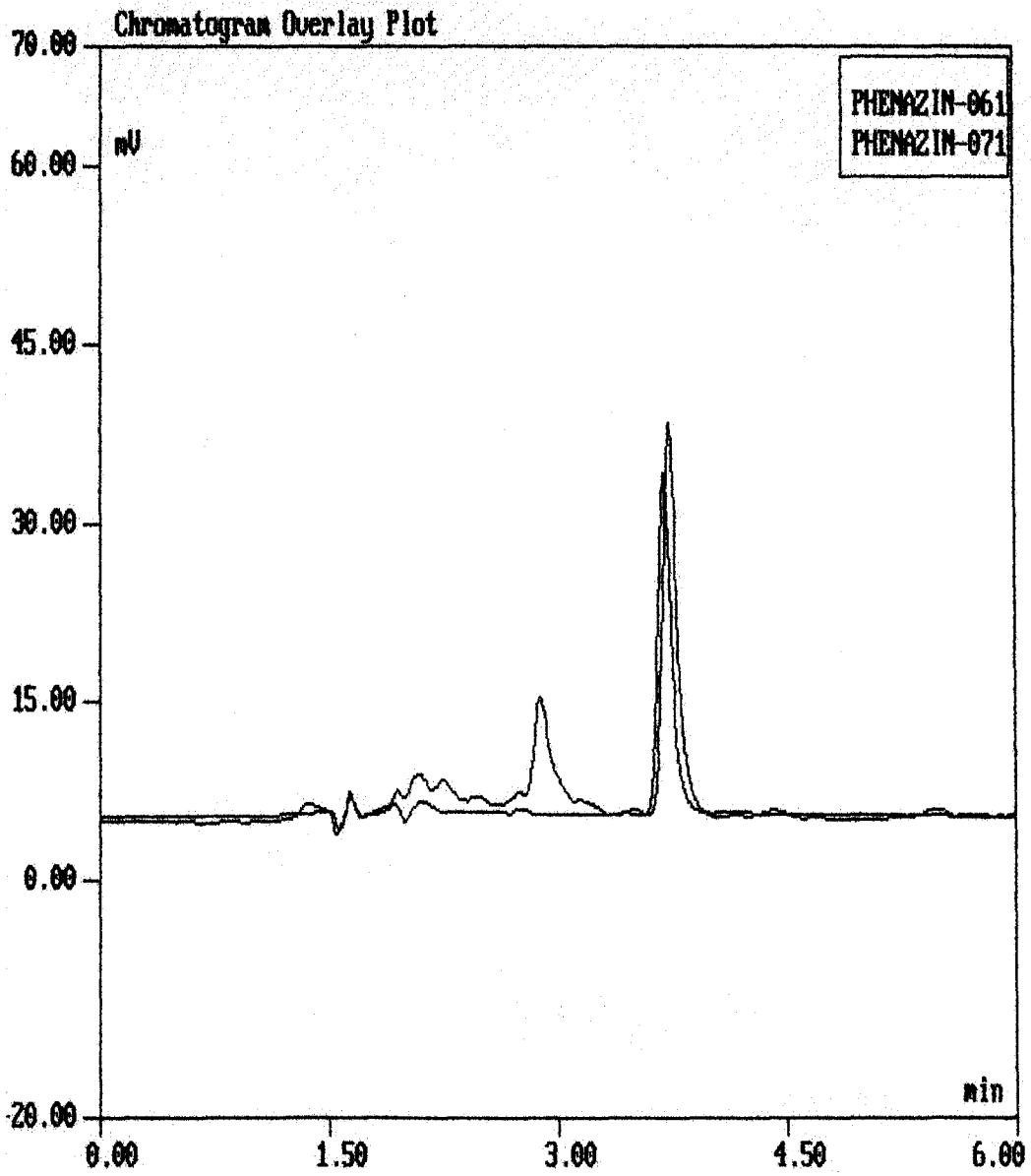


Fig. 3.11a. Chromatogram overlay plot of a phenazine sample (extracted phenazine) and a pure standard of PCA. Both products eluted at the same time at 3.83 min.

Fig. 3.11b

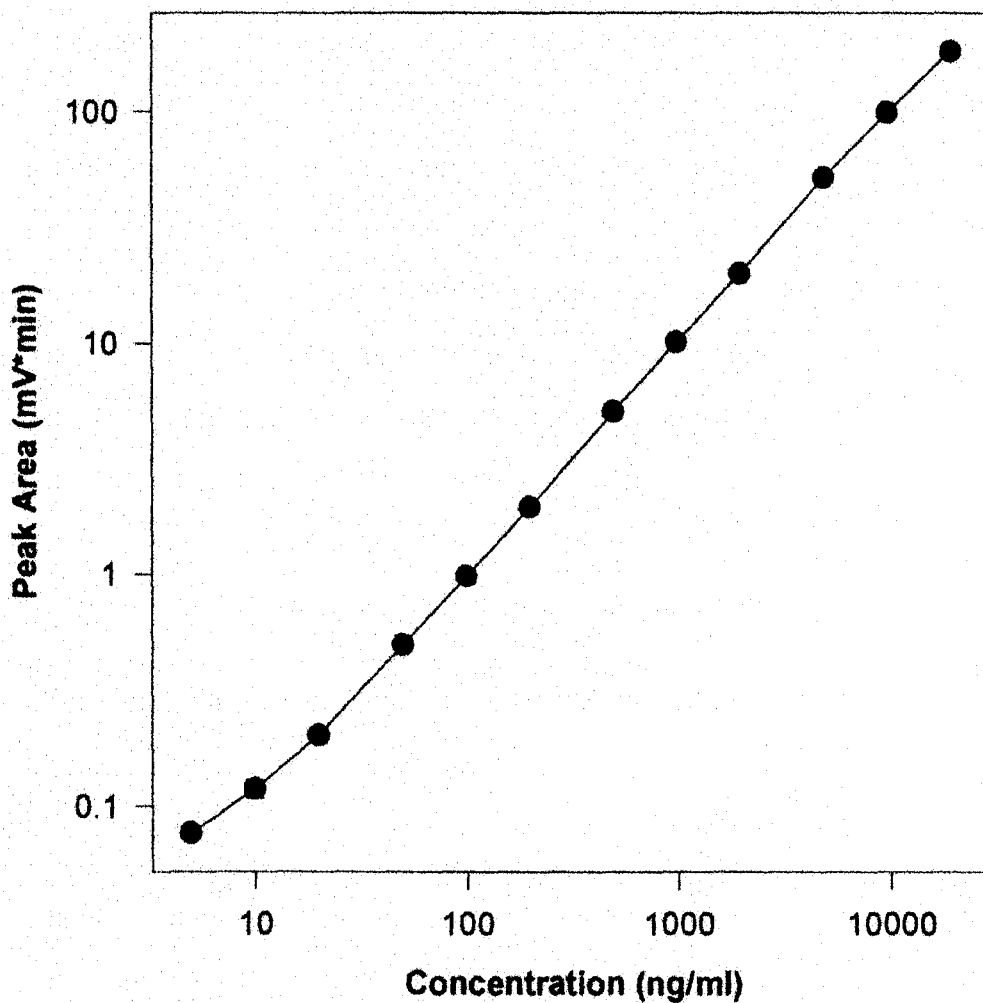


Fig. 3.11b. Phenazine calibration curve obtained by HPLC analysis of a PCA standard.

The standard errors of means ($n = 3$) were comprised within the line symbols.

Fig. 3.12

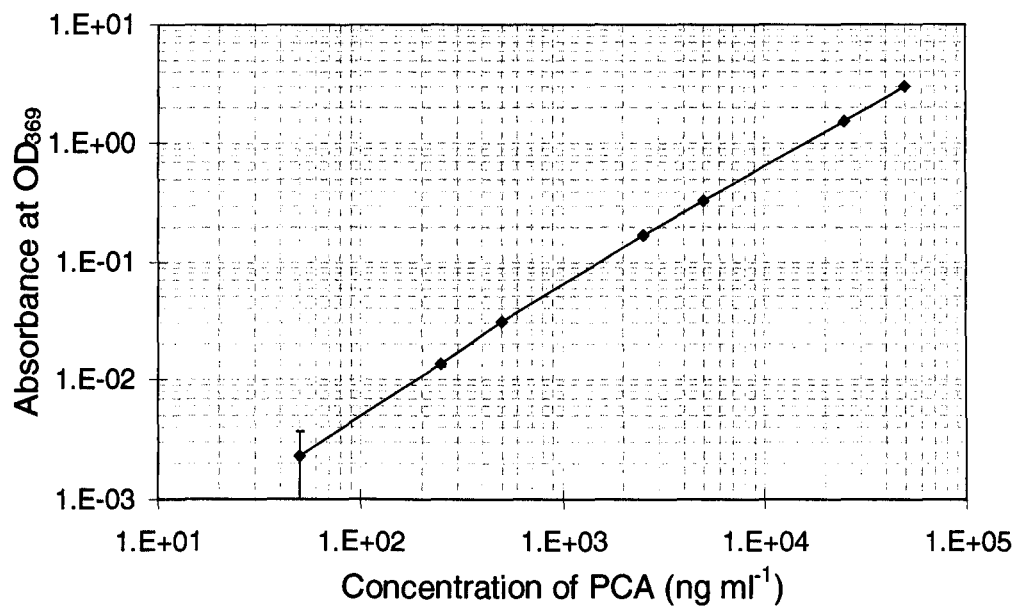


Fig. 3.12. Calibration curve of PCA concentrations against absorbance at OD₃₆₉ in 5% (w/v) NaHCO₃, pH7.
Standard errors of means shown ($n = 3$).

Fig. 3.13a

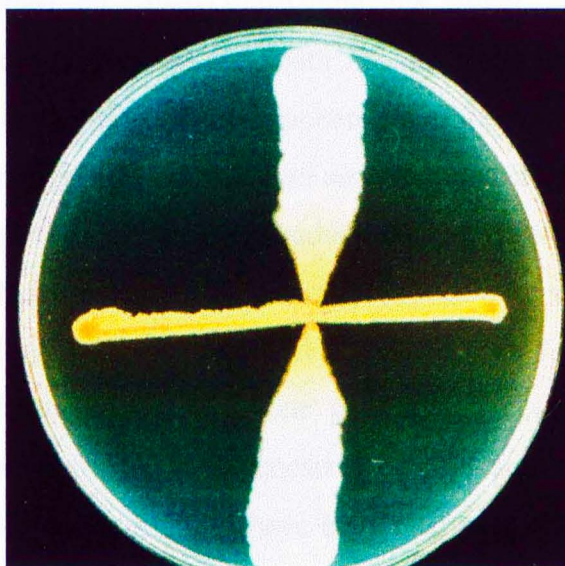


Fig. 3.13b.

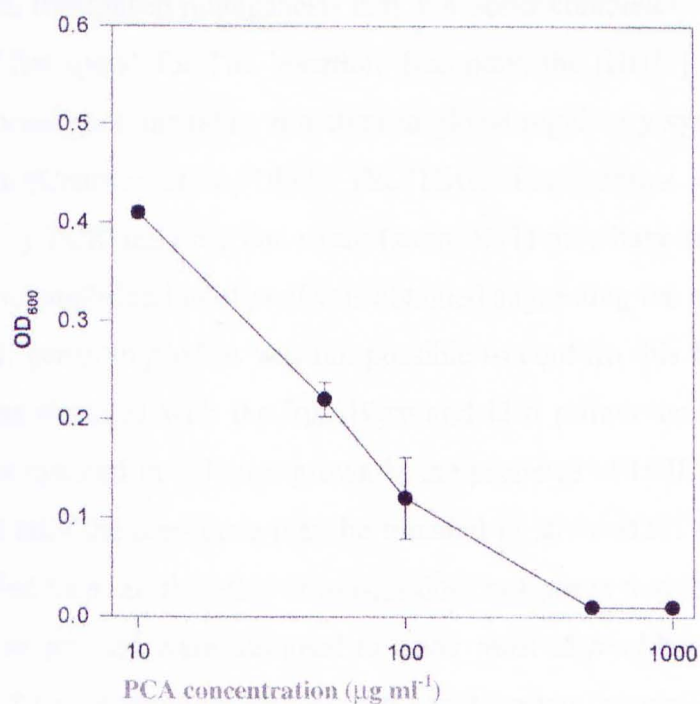


Fig. 3.13. Growth inhibition of *B. subtilis* 6051a against *P. aureofaciens* PGS12 (Fig. 3.13a) and PCA calibration curve obtained against the growth of *Bacillus subtilis* 6051a (Fig. 3.13b).

The orange halo surrounding *P. aureofaciens* PGS12 is due to the pigmentation of the hydroxylated phenazine. The inhibition is thought to be due mainly to the production of phenazine-1-carboxylic acid (PCA). The bacteria were grown for 48 h on NA at 30°C for 48 h before taking the picture. The bioassay for quantification of PCA using *B. subtilis* 6051a is described in section 2.7.4. Standard errors of means shown ($n = 3$).

recovered transconjugants of *P. putida* at a frequency of ca. 10^{-6} per final recipient. Thomashow and Weller (1988) recovered transconjugants of *P. fluorescens* at a frequency of 3×10^{-7} per initial recipient. Mating with *E. coli* could still be improved: Pierson *et al.* (1994) reported that addition of *p*-aminobenzoic to the mating plate inhibits phenazine production which may be harmful to *E. coli* and increases the transfer rate.

Mutants defective in phenazine antibiotic production [Phz^-] were recovered after transposon mutagenesis. Of these mutants, the majority (80%) were also deficient in HHL production [HHL^-] and only 15.4% were [HHL^+ , Phz^-]. Yet, 5 genes code for phenazine biosynthesis (*phzFABCD*) and only one gene (*phzI*) codes for the HHL synthetase. It is expected that transposon mutagenesis occurs at random, thus, 5 times more [HHL^+ , Phz^-] than [HHL^- , Phz^-] ought to have been recovered. Two reasons may explain these results. First, transposon mutagenesis may not occur completely at random and there may be some “hot spots” for Tn5 insertion. Secondly, the [HHL^-] phenotype may result from several genotypes, including mutation in global regulatory systems such as the GacA/GacS system (Chancey *et al.*, 1999). The [HHL^- , Phz^-] strains were tested for Tn5 insertion in *phzI* by PCR and only one strain (strain B21) may have an insertion in *phzI*. From this strain no amplification of *phzI* was obtained suggesting the presence of the insertion of the *luxAB* genes in *phzI*. It was not possible to confirm this because no positive amplification was obtained with the *luxAB3rv* and *I3fd* primer set. However, phenazine production was restored in colonies grown in the presence of HHL producing strains. This showed that only the *phzI* gene may be mutated in strain B21. Although a PCR product was amplified from all the other strains, it does not prove that they did not have an insert in *phzI*. The primers were designed to cover most of *phzI* but they were designed using strain 30-84 as a template and discrepancy between the *phzI* sequences from strain PGS12 and strain 30-84 may exist. Chancey *et al.* (1999) demonstrated that HHL production in *P. aureofaciens* is regulated by the global regulatory GacA/GacS system. However, the level of production of AHL in the *gacA* and *gacS* mutants was ca. 10% of the level of production of AHL by the wild-type strain 30-84. It is possible that the mutants which show low levels of HHL production in our experiment resulted from mutation within *gacA* or *gacS*. Among the other [HHL^- , Phz^-] strains, there might be more *gacA* or *gacS* mutants that could have produced levels of HHL too low for

detection. Mutation(s) of new regulatory regions not yet known to regulate HHL synthesis may also be present. Furthermore, 3 [HHL⁻, Phz⁻] strains (strains B105, I18Y, and A5Y) were generated spontaneously from [HHL⁺, Phz⁻] by subculturing on NA. These strains must have undergone a second mutation. It is therefore possible that among the 80% of [HHL⁻, Phz⁻] there are some double mutants. These strains may have a *luxAB* insert within the phenazine biosynthetic genes and a second mutation leading to the [HHL⁻] phenotype and this would explain why PCR amplification was obtained from all strains.

The aim of this work was to construct and select a [Phz⁻] strain that may be used to study the transcriptional activity of the phenazine operon. The selected [HHL⁺, Phz⁻] strains were all prototrophic and produced fluorescent siderophores. While strains were tested for pyoverdinin production on KB medium, a new phenotype seemingly associated with HHL production was discovered. All [HHL⁻] strains were also deficient in the secretion of mucus whereas [HHL⁺] strains produced normal amount of mucus on KB medium. Although it has never been reported that the PhzI/PhzR system is involved in regulation of another phenotype other than phenazine biosynthesis, it cannot be excluded. Indeed in many other species quorum sensing systems regulate more than one phenotypes in the same species (as for example in *P. aeruginosa*; Pesci and Iglewski, 1997).

Strain B103 was shown to have a single insert in *phzB* and was used in the following parts of the research to study the transcription of the phenazine operon. The selected strains were tested for HHL production using a *luxRI'-luxABCDE* biosensor. After optimisation of the bioassay, high sensitivity to HHL was achieved: levels as low as 0.1 ng ml⁻¹ were detected. Higher sensitivity may still be achieved using a different reporter. Prof. Salmond (personal communication) was able to detect lower amounts of AHLs with a reporter based on a *traA-lacZ* fusion (*tra* is a regulon on the *Agrobacterium* Ti plasmid; Fuqua *et al.*, 1995). However, the best reporter system in terms of sensitivity may be created using a *phzR* gene from *P. aureofaciens* by constructing a *phzRI'-phzB::luxABCDE* reporter strain. This strain could be constructed by mutating the *phzI* gene in *P. aureofaciens* B103 by homologous recombination. Pierson *et al.* engineered the plasmid pLAFR3:*phzI::Km* in which the kanamycin gene was inserted into the *phzI* gene from *P. aureofaciens* 30-84. An attempt was made to introduce the *phzI::Km* allele

into the *P. aureofaciens* PGS12 chromosome via homologous recombination with the wild-type *phzI* allele but it was unsuccessful.

The percentage similarity of the UV-scan from the eluted product of the HPLC analysis between the extracted samples and the pure PCA and the identity of the elution time points indicate that the extracted material was PCA. For further confirmation of the identity of the sample, a different physical analysis would be necessary such as Mass Spectroscopy. The calibration curve for HPLC quantification of PCA showed the highest sensitivity (5 ng ml⁻¹). However, the spectrophotometric analysis had the advantage of not necessitating extraction of PCA from the samples, and sensitivity was reasonable (50 ng ml⁻¹). Furthermore, if the extraction plus HPLC method was to be used one would need to ensure that 100% of the PCA within the samples (or a high and constant percentage) could be extracted to allow quantification. Thus, for accurate quantification many replicates would have to be processed and this would make the process impractical. Quantification using *B. subtilis* 6051a did not afford any advantage compared to the spectrophotometric method but this organism could be used to test the biological activity (and by this the identity) of the extracted compound.

3.8. Future Work

1. Construction of a *P. aureofaciens* isogenic strains of PGS12, reporter of HHL. The construction of a *P. aureofaciens* B103 [Phz⁻] mutant (*P. aureofaciens* B103I) in an attempt to achieve higher sensitivity of HHL detection. *P. aureofaciens* B103I could also be used to monitor the production of HHL by the wild-type strain or other bacteria *in situ*. Further characterisation of strain B21 to test whether it could report HHL.
2. PCR or Southern analysis of the [HHL⁻, Phz⁻] mutants to look for GacA/GacS mutants. Further cloning of the other mutants to find the insertion points is needed. A new regulatory region influencing HHL synthesis may also be discovered.
3. HHL seems to control mucus secretion and more phenotypes may be under quorum sensing regulation. To discover the gene(s) under quorum-sensing regulation that code for the mucus phenotype, these steps could be followed: (i) Another round of transposon mutagenesis with insertion of a reporter followed by selection of [Muc⁻]

mutants; (ii) Analysis of *phzI* by Southern blot to select [Muc⁻; PhzI⁺] mutants; (iii) Tests on the transcriptional activity of the mutants to find whether the addition of HHL stimulates gene(s) expression; (iii) Cloning and characterisation of the gene(s).

CHAPTER FOUR

PHENAZINE AND HHL PRODUCTION IN LIQUID CULTURE BY *P. AUREOFACIENS* PGS12

CHAPTER FOUR

PHENAZINE AND HHL PRODUCTION IN LIQUID CULTURE BY *P. AUREOFACIENS* PGS12

4.1. INTRODUCTION

Evaluation of the physiological factors that are involved in antibiotic biosynthesis in culture may help to gain a better understanding of factors affecting antibiotic production in the environment. Because phenazine production is important for both pathogen inhibition and bacterial survival, practical implications for improving biological control of soil-borne plant diseases may arise from understanding the regulation of phenazine antibiotic production in liquid culture. The major limitation to the use of microbial strains for biological control is their inconsistent performance in the field (Weller, 1988). Phenazine antibiotic biosynthesis in *P. aureofaciens* is under quorum sensing control (Pierson III *et al.*, 1994). Specific environmental conditions may limit the autoinducer production or accumulation, resulting in little or no phenazine gene expression and affecting populations of *P. aureofaciens*.

Since the discovery of *P. aureofaciens* (Kluyver, 1956; Haynes *et al.*, 1956), liquid culture experiments have been aimed mainly at the understanding of the biosynthetic pathway of phenazines. Slininger *et al.* (1992, 1995) studied in detail the nutritional factors, liquid-culture pH and temperature regulating growth and accumulation of phenazine carboxylic acid (PCA) in *P. fluorescens* 2-79. Georgakopoulos (1994a) cloned the phenazine biosynthetic locus of *P. aureofaciens* PGS12 and analysed its expression *in vitro* with the ice nucleation reporter gene. However, the regulation of phenazine production by AHLs has not been thoroughly investigated. Pierson III *et al.* (1995) undertook a molecular analysis of the biosynthetic phenazine genes in *P. aureofaciens* 30-84 to understand the genetics and biochemistry of phenazine biosynthesis. Pierson III (1994) showed that phenazine accumulates in response to cell density and HHL accumulation by growing an HHL-deficient strain in a cell-free conditioned medium (medium in which strain 30-84 had grown). More recently studies

with strain 30-84 and isogenic derivatives were directed toward understanding the role of HHL as an intercellular and interspecies signalling compound for phenazine production on plant roots (Pierson *et al.*, 1998).

Therefore, this study is the first to attempt to analyse phenazine production in relation to growth rate and HHL accumulation in liquid culture by *P. aureofaciens*. During the different growth phases of a liquid culture, bacterial cells grow at different rates, and each doubling time defines a particular physiological state (cell size and macromolecular composition) of the cell (Schaechter *et al.*, 1958; 1962). Therefore, each phase of the bacterial life cycle corresponds to a specific cell size that defines the “cell size distribution of a bacterial life cycle”. Cell numbers were obtained with an electronic counter (CellFacts instrument, Microbial Systems) that also provided measurement of the bacterial cell volume. This study was made with the wild-type *P. aureofaciens* PGS12 originally isolated from a field of maize crop (Georgakopoulos, 1994).

4.2. AIMS

1. Establishing the onset of phenazine production in liquid culture in relation to growth rate, cell density and the accumulation of the autoinducer HHL;
2. Monitoring and quantifying the level of production of phenazine and HHL in relation to cell density and growth rate.

4.3. GROWTH PHASES, CELL DENSITY, AND GROWTH RATES

4.3.1. Growth curve of *P. aureofaciens* PGS12 in NB

The rate of growth in a batch culture can be expressed in terms of the specific growth rate (k). This is the number of generations per unit time, often expressed as the generations per hour.

$$k = \log (\text{CFU}_t) - \log (\text{CFU}_{t_1}) / 0.301(t_1-t)$$

k_{max} is the maximal specific growth rate during the exponential phase.

The time it takes a population to double in size – that is, the mean generation time or mean doubling time (g) is

$$g = 1 / k$$

The volumetric growth rate (r) is

$$r = \text{CFU}_t - \text{CFU}_{t_1} / (t_1 - t)$$

The maximal volumetric growth rate (r_{\max}) corresponds to the last time point of the exponential phase before entry into the transition phase.

Typical time courses for growth of *P. aureofaciens* PGS12 in NB at 28°C are shown in Fig. 4.1a and 4.1b. During the first 2 h, cells were in lag phase and no growth or little growth was detected. After 2 h, the culture entered exponential phase which lasted for approximately 6 h in both cultures. The maximal specific growth rate (k_{\max}) and associated generation time (g) corresponded to figures in the literature (Neidhart *et al.*, 1990). *P. aureofaciens* grew at 28°C with a doubling time of 34 ± 3 minutes. k_{\max} was found in mid-log phase as illustrated in Fig. 4.2a and 4.2b.

The end of the exponential phase coincided with the beginning of the transition, or deceleration phase. This was defined as the time point from which the volumetric growth rate starts to decrease. It corresponded to r_{\max} , the maximal volumetric growth rate. The transition phase started after 9 and 8 h of incubation and lasted between 1 and 4 h as illustrated in Fig. 4.2b and 4.2a respectively. Cells counts, k_{\max} , g , and r_{\max} from both growth curves are given in Table 4.1.

In the stationary phase the growth was constant (after about 10 h of growth). During stationary phase, the cell count remained constant up to 30 h of growth but declined afterwards as the culture entered a death phase (Fig. 4.1a).

4.3.2. Comparing CFU and TCC

The dilution plate counts (CFU) and CellFacts electronic cell counts (TCC), of a 12 h culture of *P. aureofaciens* PGS12 in NB at 28°C were compared (Fig. 4.3). The counts obtained from both methods were very close and were not significantly different (T-test_{0.05}). Two essential factors that characterise a growth curve, the maximal specific growth rate and the maximal volumetric growth rate, were also not significantly different (t-Test_{0.05}) in both curves as shown in Table 4.2. All cells counts throughout the thesis have been clearly labeled as being obtained by one or the other method.

Fig. 4.1a.

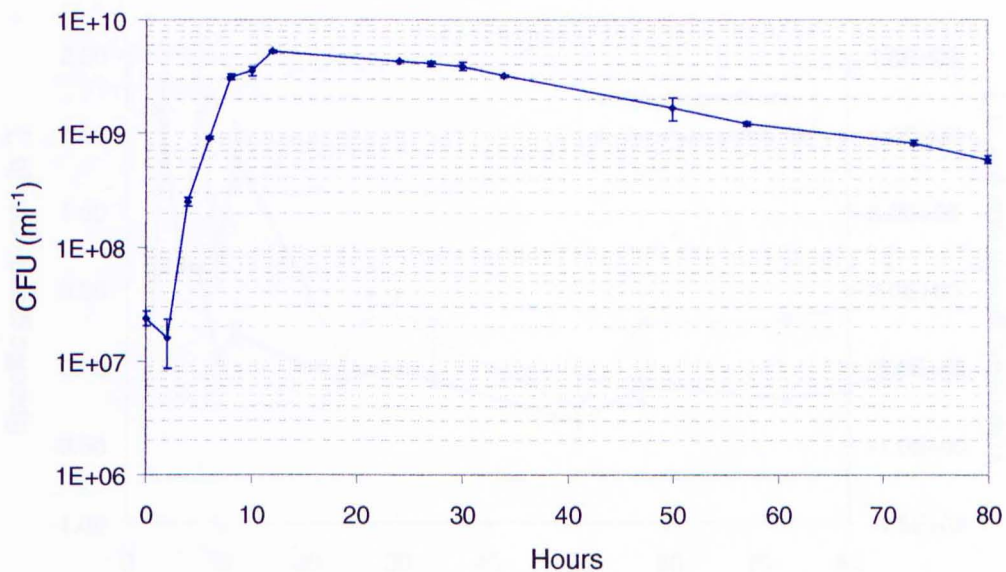


Fig. 4.1b.

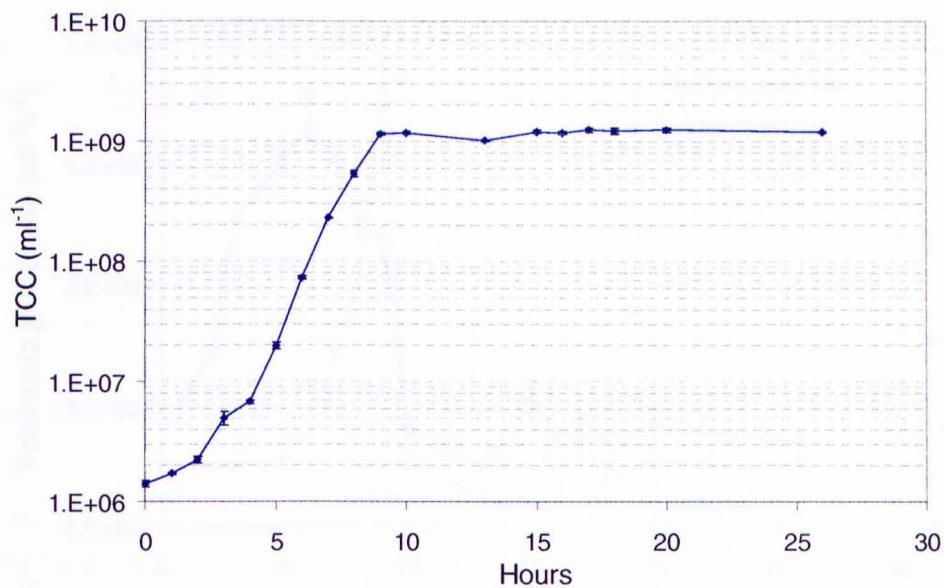


Fig. 4.1. Growth curve for *P. aureofaciens* PGS12 in NB at 28°C.

Colony Forming Units, CFU (Fig. 4.1a) were obtained by plate dilution technique and Total Cell Counts, TCC (Fig. 4.1b) with a CellFacts instrument. Standard errors of means shown ($n = 3$).

Fig. 4.2a.

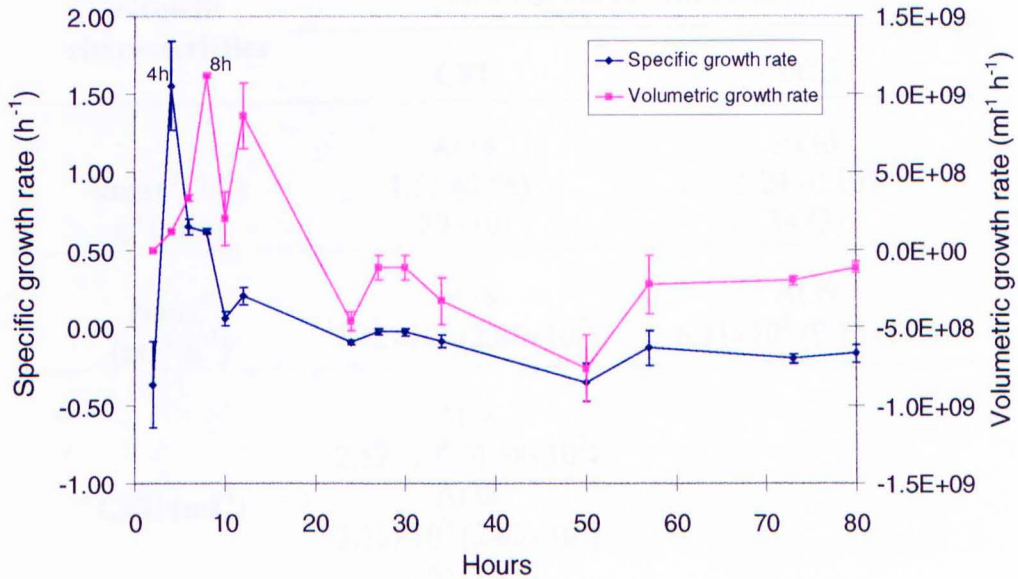


Fig. 4.2b.

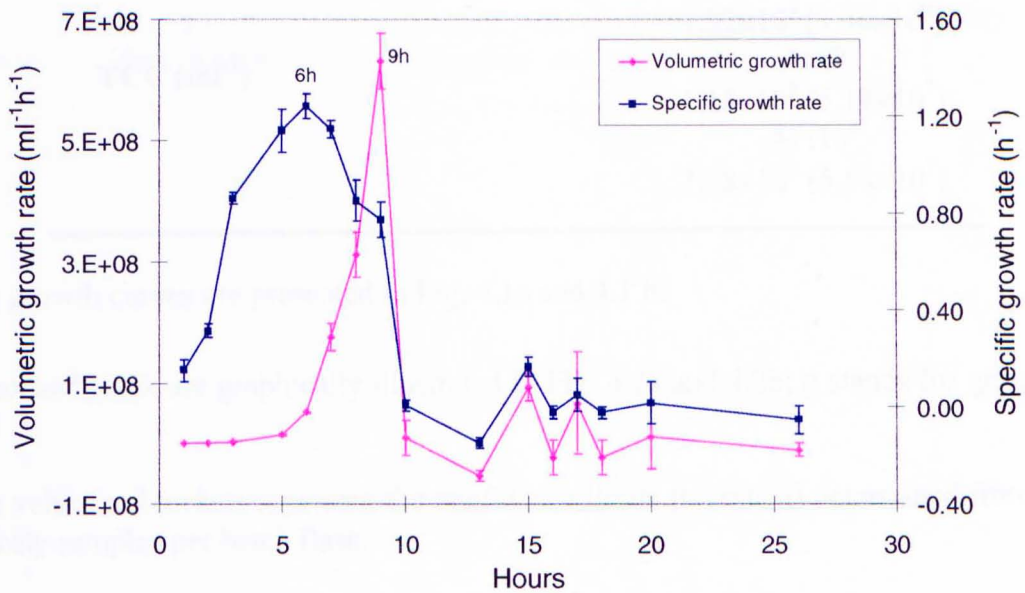


Fig. 4.2. Volumetric and specific growth rate for *P. aureofaciens* PGS12 in NB at 28°C.

Fig. 4.2a and Fig. 4.2b corresponds to the growth curves shown in Fig. 4.1a and 4.1b respectively. Standard errors of means shown ($n = 3$).

Table 4.1. Growth rates and cell density in two growth cultures of *P. aureofaciens* PGS12 in NB at 28°C.

Growth characteristics	Growth curve ^a obtained by	
	CFU	TCC
kmax^b (h⁻¹)	At t4 1.55 (0.56) ^c	At t6 1.24 (0.10)
g^b (min)	29 (10)	34 (3)
rmax^b (ml⁻¹ h⁻¹)	At t8 1.12×10 ⁹ (2.86×10 ⁷)	At t9 6.31×10 ⁸ (9.15×10 ⁷)
CFU (ml⁻¹)	At t4 2.52×10 ⁸ (4.38×10 ⁷) At t8 3.15×10 ⁹ (2.09×10 ⁸) At t12 ^d 5.27×10 ⁹ (3.46×10 ⁸)	
TCC (ml⁻¹)		At t6 7.32×10 ⁷ (3.30×10 ⁶) At t9 1.15×10 ⁹ (5.19×10 ⁷) At t10 ^d 1.18×10 ⁹ (5.58×10 ⁷)

^a The growth curves are presented in Fig. 4.1a and 4.1.b.

^b kmax and rmax are graphically illustrated in Fig. 4.2a and 4.2b; g stands for generation time.

^c The values in brackets represent the confidence limits (t-Test_{0.05}) determined from three replicate samples per batch flask.

^d Time point at which the cultures entered stationary phase (section 4.1.1.1)

Fig. 4.3.

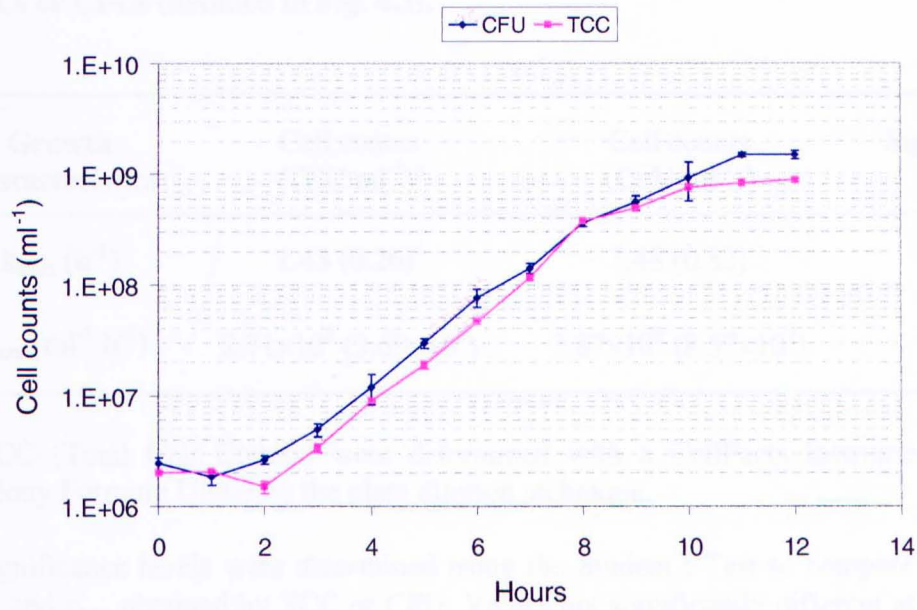


Fig. 4.3. Growth curve for *P. aureofaciens* PGS12 in NB at 28°C.

Two different cell counts were obtained from the same growth culture: TCC were measured using the CellFacts instrument and Colony Forming Units (CFU) were obtained by plate dilution technique. Standard errors of means shown ($n = 3$).

Table 4.2. Comparison of growth rates for *P. aureofaciens* PGS12 in NB obtained as TCCs or CFUs (detailed in Fig. 4.3).

Growth characteristics	Cell counts (TCC ml⁻¹)^a	Cell counts (CFU ml⁻¹)^a	Significance^b
k_{max} (h⁻¹)	1.43 (0.26) ^c	1.48 (0.82)	NS
r_{max} (ml⁻¹ h⁻¹)	2.71×10 ⁸ (3.69×10 ⁶)	2.87×10 ⁸ (8.57×10 ⁷)	NS

^a TCC (Total Cell Counts) were determined with a CellFacts instrument and CFU (Colony Forming Units) by the plate dilution technique.

^b Significance levels were determined using the Student t-Test to compare the mean of k_{max} and r_{max} obtained by TCC or CFU. Values not significantly different at the P ≤ 0.05 level are indicated by NS.

^c The values in brackets represent the confidence limits (T-test_{0.05}) determined from three replicate samples per batch flask.

Fig. 4.4a

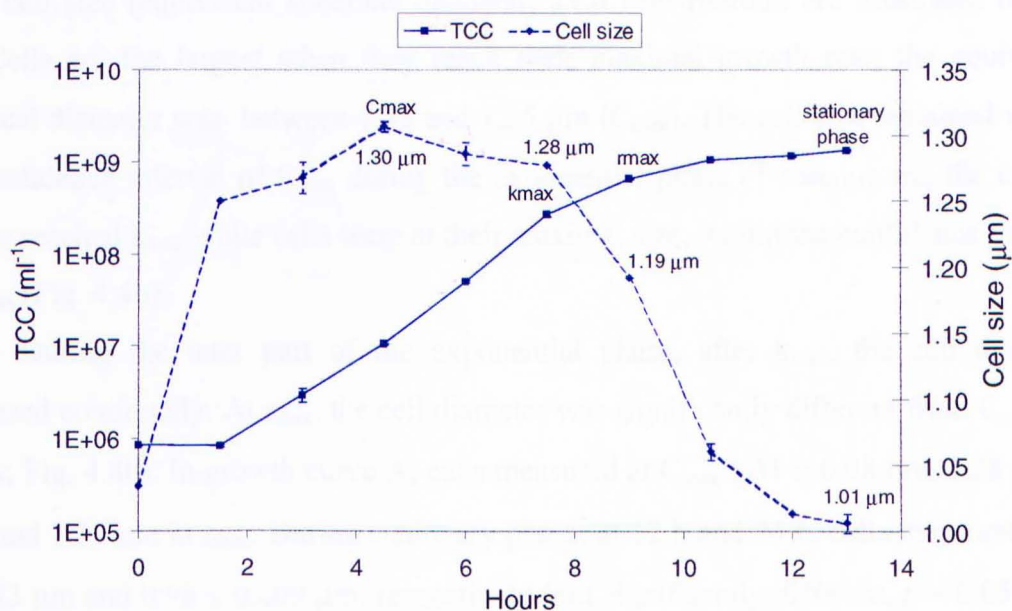


Fig. 4.4b

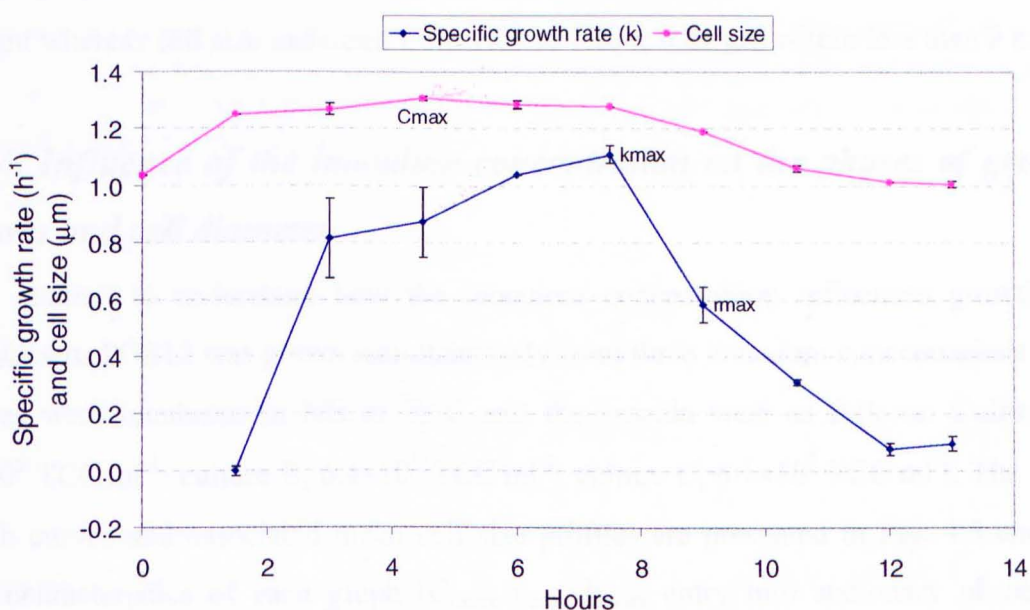


Fig. 4.4. Growth curve A of *P. aureofaciens* PGS12 and associated cell size profile (Fig 4.4a) and specific growth rate (Fig 4.4b).

P. aureofaciens PGS12 was grown in NB at 28°C. The cell size was determined with a CellFacts instrument. The decrease in specific growth rate between k_{\max} and r_{\max} was associated with a significant decrease in cell size diameter (T-test_{0.05}). Standard errors of means shown ($n = 3$).

4.3.3. Growth phases and associated mean cell size

A growth curve of *P. aureofaciens* PGS12 in NB at 28°C (culture A) and the associated mean cell size (equivalent spherical diameter, s.e.d.) distribution are illustrated in Fig. 4.4. Cells are the largest when they reach their maximal growth rate; the equivalent spherical diameter was between 1.35 and 1.25 μm (C_{max}). The cell size remained within the confidence interval of C_{max} during the exponential phase (T-test_{0.05}) and the culture always reached k_{max} while cells were at their maximal size, within the confidence interval of C_{max} (Fig. 4.4b).

During the later part of the exponential phase, after k_{max} , the cell diameter decreased continually. At r_{max} , the cell diameter was significantly different from C_{max} (T-test_{0.05}; Fig. 4.4b). In growth curve A, cells measured at C_{max} $1.31 \pm 0.08 \mu\text{m}$, $1.28 \mu\text{m}$ at k_{max} , and $1.19 \mu\text{m}$ at r_{max} . During stationary phase, at 12 h and 24 h, cells measured $1.01 \pm 0.023 \mu\text{m}$ and $0.98 \pm 0.009 \mu\text{m}$, respectively (not significantly different, $p = 0.05$). The lag phase corresponds to an increase in the rate of mass synthesis of the cells with a period of “rate maintenance” for cell number. Thus, in lag phase, cell numbers remained constant whereas cell size increased from 1.03 to $1.27 \pm 0.01 \mu\text{m}$ within less than 2 h.

4.3.4. Influence of the inoculum concentration on the phases of growth cultures and cell diameter

In an attempt to understand how the inoculum concentration influences growth, *P. aureofaciens* PGS12 was grown simultaneously from three inoculum concentrations. The cultures were incubated in NB at 28°C and the inocula were as follows: Culture A, 8.5×10^5 TCC ml^{-1} ; culture B, 6.4×10^6 TCC ml^{-1} ; culture C, 6.1×10^7 TCC ml^{-1} . The three growth curves and associated mean cell size profiles are presented in Fig. 4.5 and the main characteristics of each graph (C_{max} , r_{max} , k_{max} , entry into stationary phase and associated cell density) are summarised in Table 4.3.

The higher the inoculum concentration, the shorter was the exponential phase. The maximal cell density reached approximately 1×10^9 TCC ml^{-1} . Therefore, with the highest inoculum, the culture remained in log-phase for only 2 h and C_{max} was maintained only for 1.5 h (Fig.4.5). Consequently, the higher the inoculum concentration,

Fig. 4.5.

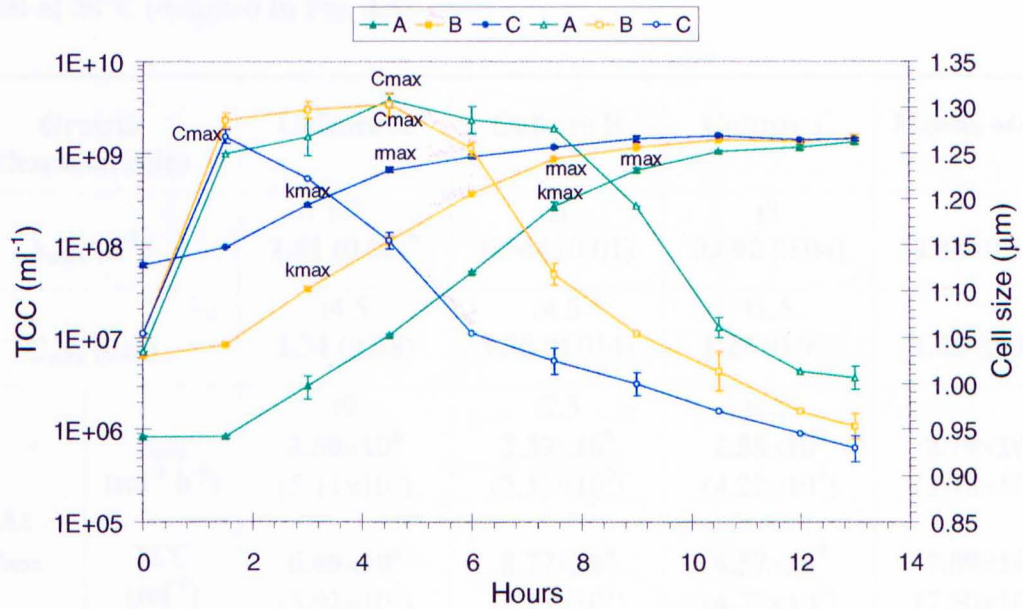


Fig. 4.5. Time course of 3 cultures of *P. aureofaciens* PGS12 from 3 inoculum concentrations and associated mean cell size distribution.

Inoculum A, 8.5×10^5 TCC ml⁻¹; Inoculum B, 6.4×10^6 TCC ml⁻¹; Inoculum C, 6.1×10^7 TCC ml⁻¹. The 3 cultures were grown simultaneously in NB at 28°C and the inoculum came from the same cultures. The values for C_{max} , r_{max} and k_{max} are given in Table 4.3. Standard errors of means shown ($n = 3$).

Table 4.3. Growth characteristics of cultures A, B, and C of *P. aureofaciens* PGS12 in NB at 28°C (detailed in Fig. 4.5).

Growth characteristics		Culture A	Culture B	Culture C	Means +/- CI
k_{max} (h^{-1})		t7 ^a 1.11 (0.06) ^b	t3 0.944 (0.01)	t3 0.692 (0.04)	0.88 (0.14)
C_{max} (μm)		t4.5 1.31 (0.08)	t4.5 1.30 (0.014)	t1.5 1.27 (0.09)	1.28 (0.03)
At r_{max}	r_{max} ($ml^{-1} h^{-1}$)	t9 2.50×10^8 (5.11×10^7)	t7.5 3.39×10^8 (2.55×10^7)	t4.5 2.58×10^8 (4.22×10^7)	2.79×10^8 (3.78×10^7)
	TCC (ml^{-1})	6.49×10^8 (3.02×10^7)	8.77×10^8 (1.67×10^7)	6.57×10^8 (4.77×10^7)	7.09×10^8 (7.50×10^7)
	Cell size (μm)	1.19	1.12 (0.017)	1.16 (0.016)	1.16 (0.02)
Entry into stationary phase ^c	TCC (ml^{-1})	t10.5 1.04×10^9 (5.11×10^7)	t10.5 1.40×10^9 (3.88×10^7)	t10.5 1.54×10^9 (8.32×10^7)	t1 1.32×10^9 (1.49×10^8)
	Cell size (μm)	1.06 (0.01)	1.01 (0.02)	0.97	1.01 (0.02)

^a The time points (tx) correspond to x hour(s) of incubation at 28°C in a rotary shaker at 180 rpm.

^b The means and confidence limits were determined from three replicate samples per batch flask.

^c The entry into stationary phase was calculated as the time point from which the cell counts remain constant (i.e., cell counts at t_{n+1} not significantly different from t_n , t-Test 0.05).

Fig. 4.6

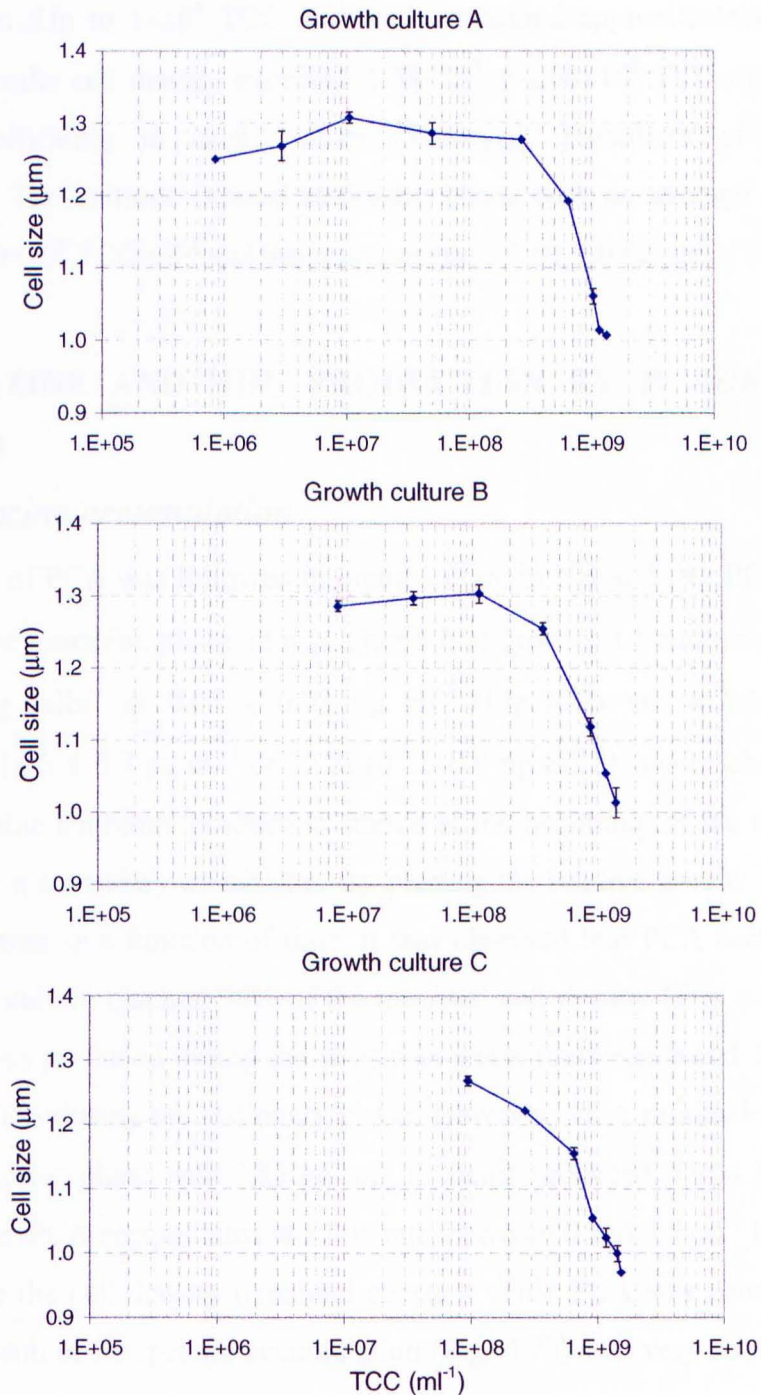


Fig. 4.6. Changes in cell size in relation to cell density (TCC) in growth cultures A, B, and C started at 3 different inoculum concentrations.

The growth curves are presented in Fig. 4.5. Up to 1×10^8 TCC ml⁻¹, the cell size was approximately 1.30-1.25 µm. The cell size decreased after 1×10^8 TCC ml⁻¹ in each culture regardless of the inoculum concentrations. At 1×10^9 TCC ml⁻¹, the cell size was between 1.10 and 1.00 µm. Standard errors of means shown ($n = 3$).

the faster the culture reached the transition phase. At r_{\max} , the cell density averaged $7.09 \times 10^8 \pm 7.50 \times 10^7$ TCC ml⁻¹ (from the 3 batch cultures), and cells measured on average 1.16 ± 0.02 μm . Up to 1×10^8 TCC ml⁻¹, cells measured approximately 1.30-1.25 μm (Fig.4.6). When the cell density exceeded $1.59 \times 10^8 \pm 1.08 \times 10^8$ TCC ml⁻¹, the cell size decreased significantly in each culture (T-test_{0.05}), regardless of the inoculum concentrations. The cultures entered stationary phase with an average cell density of $1.32 \times 10^9 \pm 1.49 \times 10^8$ TCC ml⁻¹ and the cells measured 1.01 ± 0.02 μm .

4.4. PHENAZINE AND HHL PRODUCTION BY *P. AUREOFACIENS* PGS12 IN NB

4.4.1. Phenazine accumulation

The production of PCA was followed in liquid culture in NB at 28°C. PCA was detected at the start of the transition phase, at r_{\max} , after 9 h of growth at a concentration $0.56 \times 10^{-6} \pm 0.03 \times 10^{-6}$ ng cells⁻¹ or 0.65 ± 0.03 $\mu\text{g ml}^{-1}$ (Fig. 4.7a and 4.7b). The maximal concentration (14.5 ± 0.7 $\mu\text{g ml}^{-1}$ or $12.2 \times 10^{-5} \pm 0.6$ ng cell⁻¹) was reached after 26 h of growth. Phenazine antibiotic production started at the beginning of the transition phase, as expected for a secondary metabolite. By plotting the relative growth and the relative PCA accumulation as a function of time, it was observed that PCA accumulated in the medium as the culture reached 94% of the maximal cell density (Fig. 4.10b and 4.10c). 30% of PCA was produced during the transition phase (between 9 and 10 h of growth), and the other 70% during the stationary phase. However, PCA production was maximal during the transition phase with 3.85 $\mu\text{g ml}^{-1} \text{ h}^{-1}$ being produced (Fig 4.10a). During the stationary phase, PCA accumulated at a low rate, between 0 and 0.5 ml⁻¹ h⁻¹.

Because the cell density remained constant while PCA was being produced, the shape of the graph of its specific accumulation (Fig. 4.7b) was very similar to the graph of volumetric accumulation (Fig. 4.7a). PCA was also measured in cultures A, B and C (Fig 4.9a). It was also first detected as the growth rate reached r_{\max} (culture B and C) or at the time point just after (culture A). Overall, PCA first appeared when cell size measured 1.11 ± 0.03 μm and the cell density was at $8.56 \times 10^8 \pm 2.15 \times 10^8$ TCC per ml. The maximal phenazine production was found in culture B (5.86 ± 0.22 ng 10^6 cell⁻¹).

4.4.2. HHL accumulation

HHL and PCA accumulated in a different manner. HHL was first detected during the mid-log period, between C_{\max} and k_{\max} (Fig. 4.8). The rate of production of HHL was maximal between $r_{\max-1}$ and r_{\max} ($2670 \text{ ng ml}^{-1} \text{ h}^{-1}$; Fig. 4.10a), and there was a 9.20 increase between $r_{\max-1}$ and r_{\max} . The rate of production of PCA was maximal between r_{\max} and $r_{\max+1}$ ($3850 \text{ ng ml}^{-1} \text{ h}^{-1}$; Fig. 4.10a). Using the bioassay based on the plasmid pSB401, the minimal HHL concentration detected was $0.4 \pm 0.02 \text{ ng ml}^{-1}$. The cell density was at that moment $2 \times 10^7 \pm 2.5 \times 10^6 \text{ cells ml}^{-1}$.

HHL production followed an exponential curve up to r_{\max} . The peak of HHL accumulation (HHL_{\max}) was recorded at the onset of the transition phase, concomitant or close to r_{\max} (HHL_{\max} was reached at r_{\max} in culture B and 1.5 h after r_{\max} in cultures A and C; Fig. 4.9b). The maximal accumulation was found in culture B with $57 \times 10^{-6} \pm 2.85 \times 10^{-6} \text{ ng cell}^{-1}$ ($50 \pm 2.5 \text{ } \mu\text{g ml}^{-1}$) and the average for culture A, B and C reached $32.4 \times 10^{-6} \pm 24.2 \times 10^{-6} \text{ ng cell}^{-1}$ ($30 \pm 20 \text{ } \mu\text{g ml}^{-1}$).

The relative accumulation of HHL as a function of time confirmed that HHL accumulated exponentially up to r_{\max} (time point 9; Fig. 4.10b). HHL accumulated more slowly than growth up to $r_{\max-1}$ and faster between $r_{\max-1}$ and r_{\max} (Fig. 4.10c). When the rate of the relative HHL accumulation (B) was subtracted from the relative growth rate (A), then the relative growth rate was always higher than the rate of relative HHL accumulation ($A - B < 0$) apart from ($A - B > 0$) between $r_{\max-1}$ and r_{\max} . For each growth culture studied, there was a switch from negative to positive values between $r_{\max-1}$ and r_{\max} . During this one hour, there was 23% more HHL produced (per cell) than growth (Fig 4.10c). In cultures A, B and C there was respectively 25%, 38% and 28% increases in the rate of HHL accumulation compare to growth (Figures not shown).

HHL concentration decreased between r_{\max} and $r_{\max+1}$ at the same rate as it built-up between r_{\max} and $r_{\max-1}$. The decrease in HHL concentration was translated as a negative rate of production (Fig. 4.10a), however, the decrease occurred at two different rates. First, a rapid decline took place between r_{\max} and $r_{\max+1}$ (at a similar rate

Fig. 4.7a.

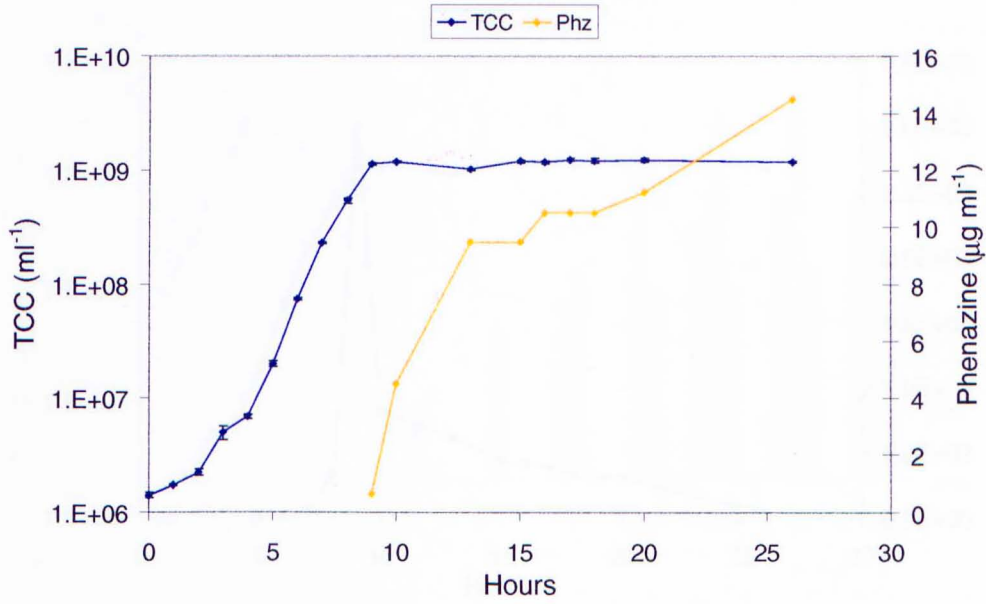


Fig. 4.7b.

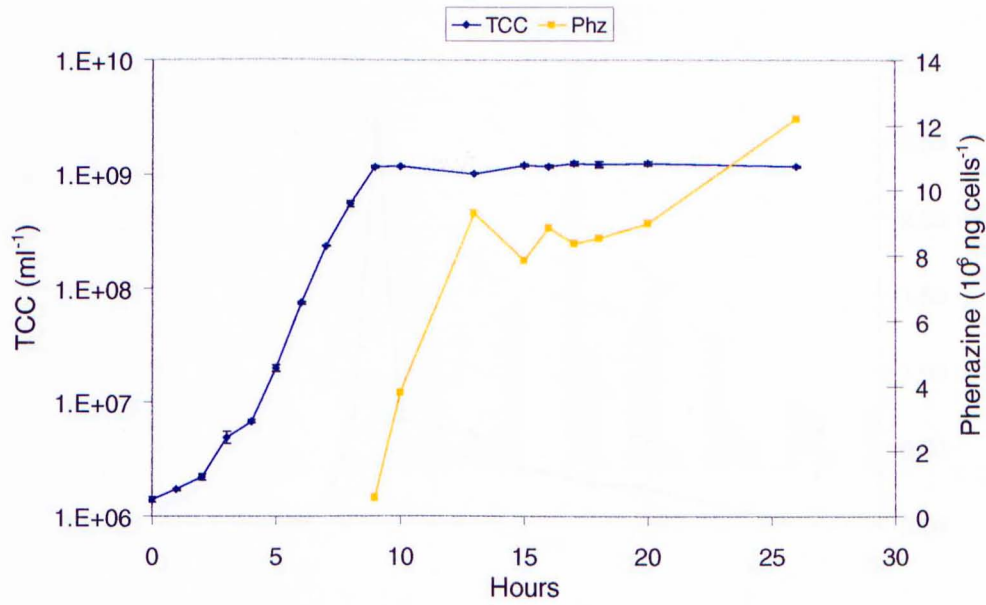


Fig. 4.7. Time course of the growth of *P. aureofaciens* PGS12 and volumetric (Fig. 4.7a) or specific (Fig. 4.7b) phenazine accumulation. Standard errors of means shown ($n = 3$).

Fig. 4.8a

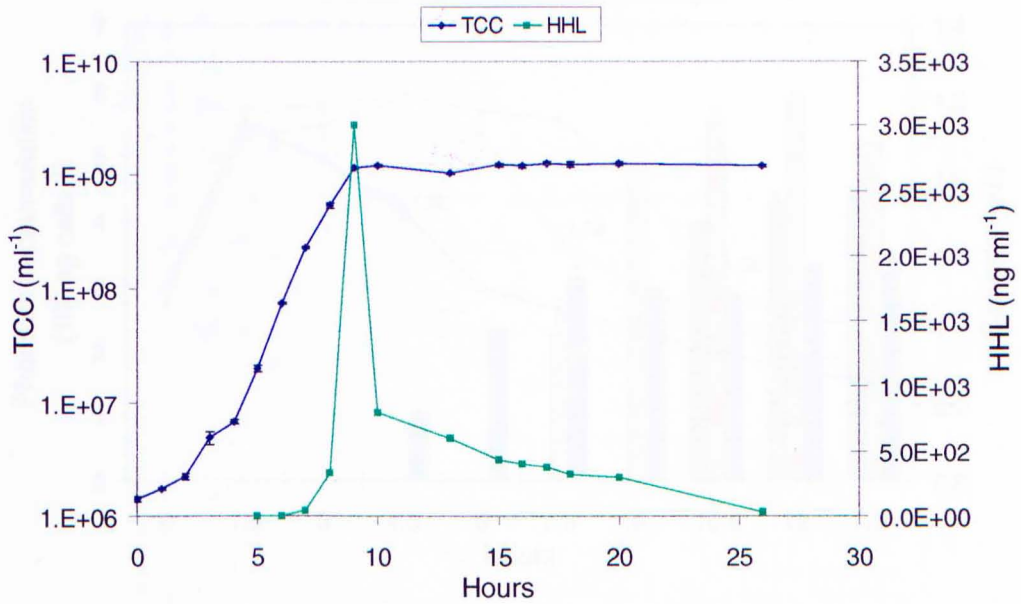


Fig. 4.8b

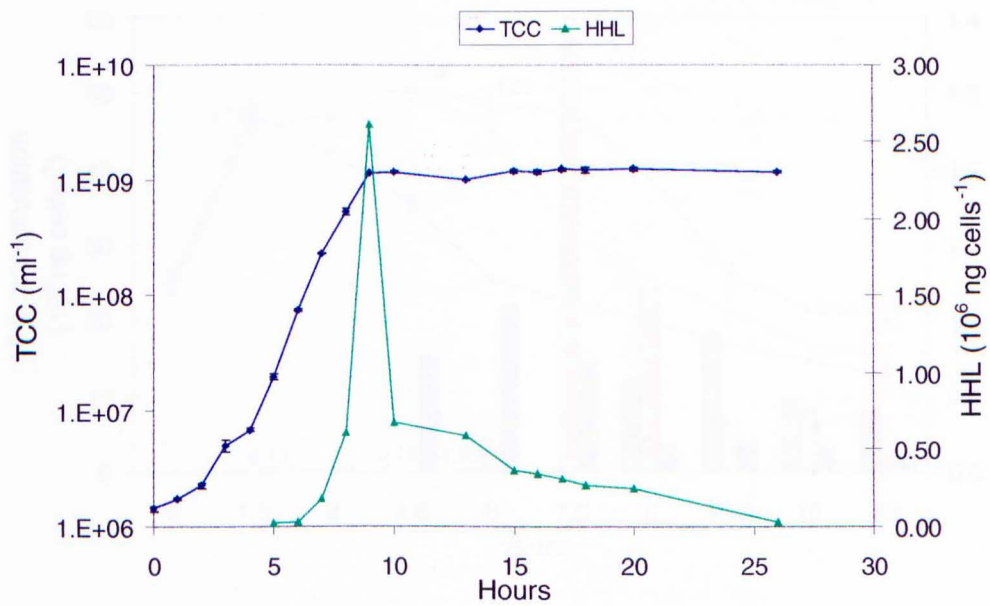


Fig. 4.8. Time course of the growth of *P. aureofaciens* PGS12 and volumetric (Fig. 4.8a) or specific HHL accumulation (Fig. 4.8b). Standard errors of means shown ($n = 3$).

Fig. 4.9a

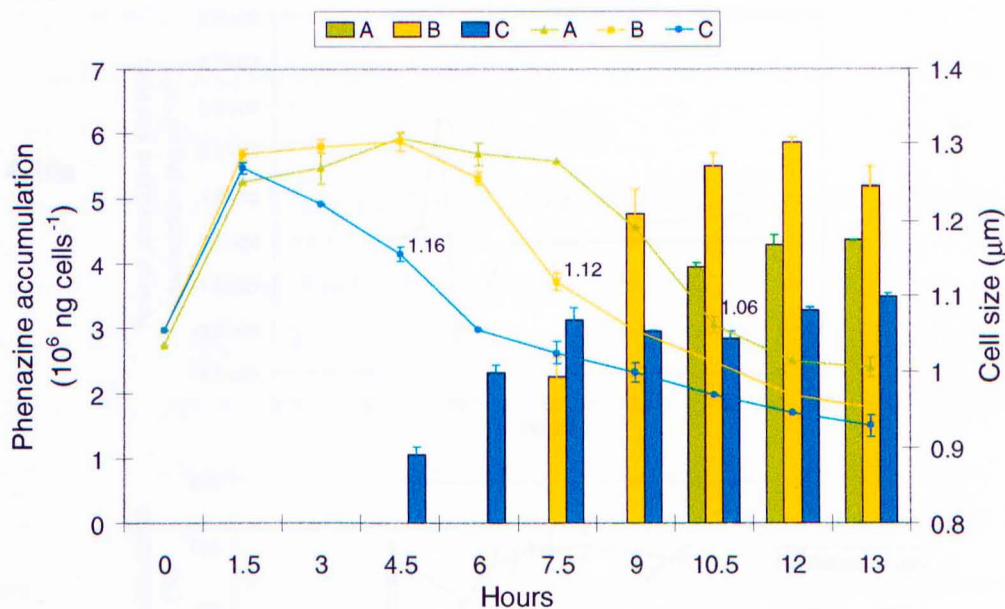


Fig. 4.9b

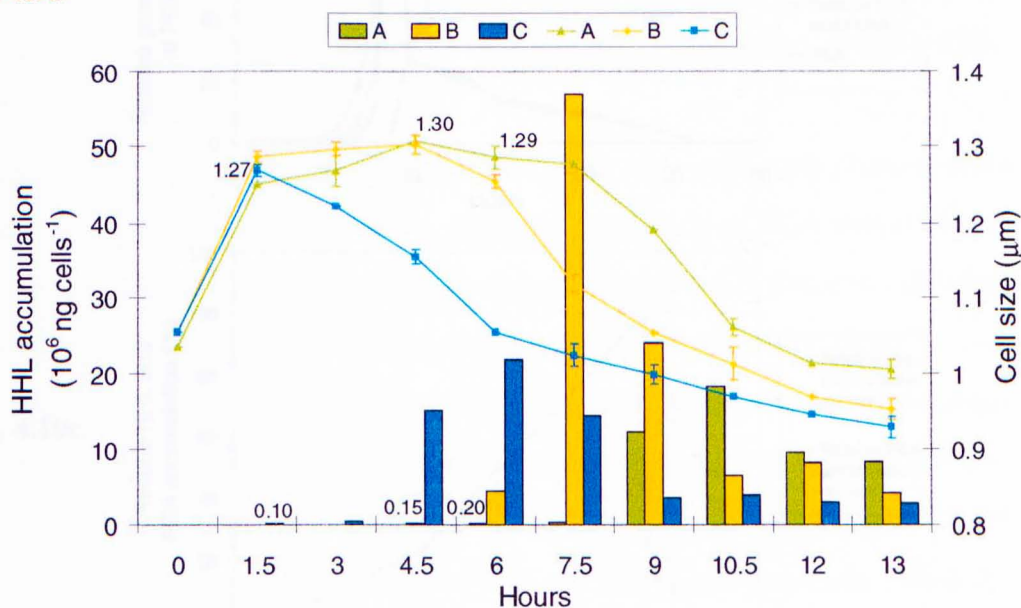


Fig. 4.9. Accumulation of phenazine (Fig. 4.8a) and HHL (Fig. 4.8b) and cell size variation during the culture of *P. aureofaciens* PGS12 started at three inoculum concentrations in NB at 28°C.

P. aureofaciens PGS12 was grown in NB at 28°C. The growth curves A, B, and C are detailed in Fig. 4.5. The inoculum concentrations were as follows (in TCC ml⁻¹): A, 8.5×10⁵; B, 6.4×10⁶; C, 6.1×10⁷. The values plotted correspond to the cell diameter at the first detection of PCA or HHL, which concentrations are also indicated. Standard errors of means shown ($n = 3$).

Fig 4.10a

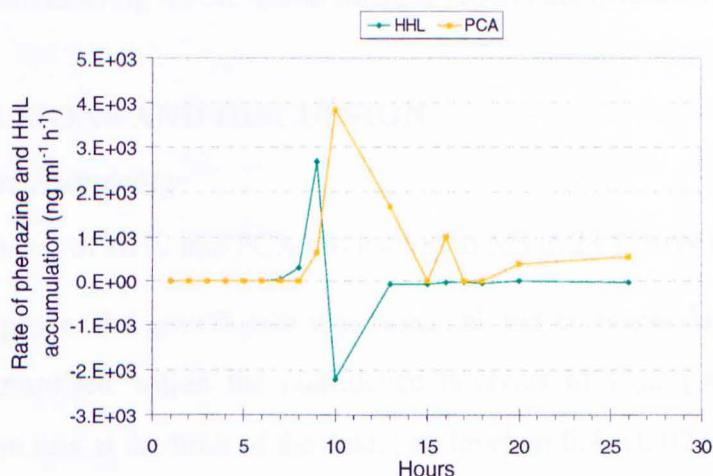


Fig. 4.10b

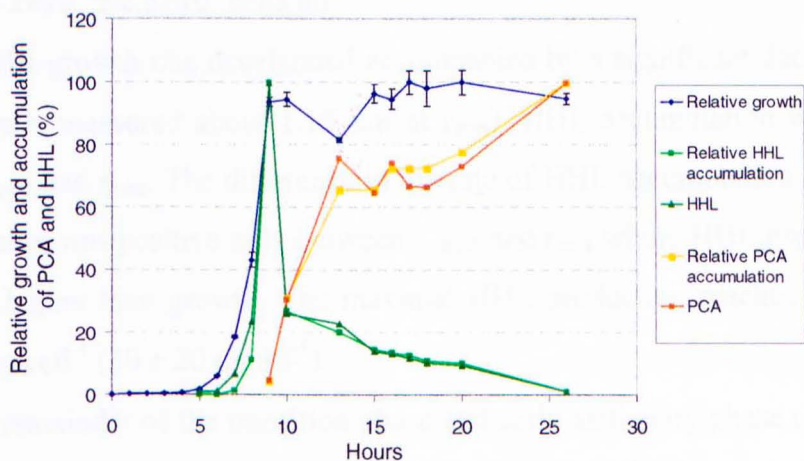


Fig. 4.10c

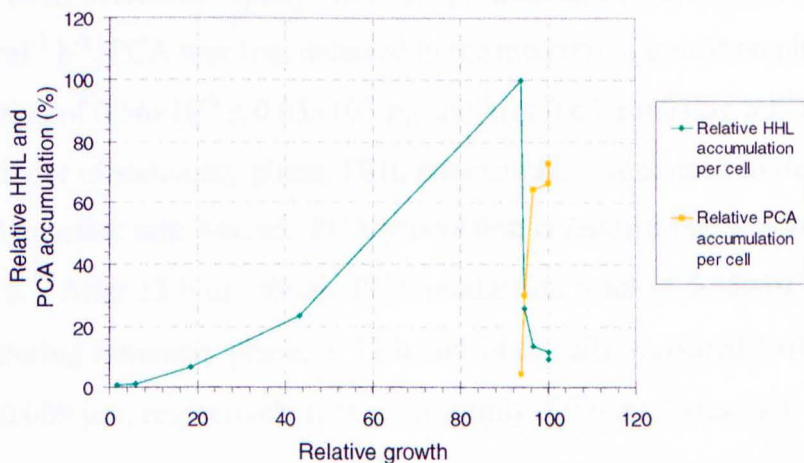


Fig 4.10. Rate of PCA and HHL accumulation from *P. aureofaciens* PGS12 (Fig. 4.10a), relative growth and accumulation of PCA and HHL as a function of time (Fig. 4.10b), and as a function of growth (Fig. 4.10c).

The values are relative values of growth, PCA or HHL accumulation, normalised to the maximum values obtained during the experiment. The corresponding growth curve of *P. aureofaciens* PGS12 grown in NB at 28°C is shown in Fig. 4.1b; r_{max} occurred at 9 h.

than the maximal production of HHL), then HHL concentration decreased at a slower but constant rate (around $45 \text{ ng ml}^{-1} \text{ h}^{-1}$), and finished around the detection limit after 26 h.

4.5. CONCLUSIONS AND DISCUSSION

4.5.1. Results: Summary

The different phases of HHL and PCA production in NB at 28°C may be outlined as follows:

1. In mid-log phase, the growth rate was maximal and corresponded to k_{max} . The cell size was comprised within the confidence intervals of C_{max} (ca. $1.30 \text{ }\mu\text{m}$). HHL concentration was at the limit of the detection level, at $0.4 \pm 0.02 \text{ ng ml}^{-1}$, and the cell density was $2 \times 10^7 \pm 2.5 \times 10^6 \text{ cells ml}^{-1}$.
2. After k_{max} , the growth rate decelerated accompanied by a significant decrease in cell diameter (cells measured about $1.15 \text{ }\mu\text{m}$ at r_{max}). HHL accumulation was maximal between $r_{\text{max}-1}$ and r_{max} . The difference in the rate of HHL accumulation compared to the growth rate was positive only between $r_{\text{max}-1}$ and r_{max} where HHL production was up to 38% higher than growth. The maximal HHL production reached $32.4 \times 10^{-6} \pm 24.2 \times 10^{-6} \text{ ng cell}^{-1}$ ($30 \pm 20 \text{ }\mu\text{g ml}^{-1}$).
3. During the remainder of the transition phase and early stationary phase (between r_{max} and $r_{\text{max}+1}$), HHL decreased rapidly while the production of PCA was at its maximum of ca. $4 \text{ ng ml}^{-1} \text{ h}^{-1}$. PCA was first detected in the medium in transition phase at r_{max} at a concentration of $0.56 \times 10^{-6} \pm 0.03 \times 10^{-6} \text{ ng cell}^{-1}$ (or $0.65 \pm 0.03 \text{ }\mu\text{g ml}^{-1}$).
4. In the remainder of stationary phase, HHL concentration continued to decrease but at a lower and constant rate whereas PCA production continued but at a low rate of ca. $0.5 \text{ ng ml}^{-1} \text{ h}^{-1}$. After 13 h of growth, PCA production reached $4.35 \times 10^{-6} \pm 0.65 \times 10^{-6} \text{ ng cells}^{-1}$. During stationary phase, at 12 h and 24 h, cells measured $1.01 \pm 0.023 \text{ }\mu\text{m}$ and $0.98 \pm 0.009 \text{ }\mu\text{m}$, respectively (not significantly different, T-test_{0.05}).

4.5.2. Discussion

This chapter outlines the basic cell growth and the production of HHL and phenazine by strain *P. aureofaciens* PGS12. This represents the first attempt to study this strain in detail and sets out the process for the work that follows. HHL production was first

detected in the mid-log phase probably due to activity of the previously produced PhzI protein, and to activity of a small amount of newly produced PhzI, the synthesis of which presumably resulted from the basal transcription of the phenazine operon. The point from which HHL per cell accumulates faster than growth is an indicator of the beginning of the autoinduction process. At that point, HHL concentration has reached a threshold concentration that enables the formation of active PhzR-HHL complexes (i.e., the substrate HHL has reached $1/K_m$, the affinity concentration for PhzR). The transcriptional regulator then activates transcription of the phenazine operon comprising the biosynthetic genes and *phzI*, the HHL synthase. This resulted in the autoinduction of HHL, and to a 100-300-fold increase in concentration over pre-induction levels. The relative growth rate was always higher than the rate of relative HHL accumulation ($A - B < 0$) apart from ($A - B > 0$) between $r_{\max-1}$ and r_{\max} . The autoinduction period may thereby be estimated to occur during this interval. At $r_{\max-1}$, the cell density calculated from several growth cultures was $3.62 \times 10^8 \pm 1.19 \times 10^7$ TTC ml⁻¹, and HHL concentration was at 173 ± 70 ng ml⁻¹, equivalent to 8.5×10^{-7} M. This is an estimation of the minimum HHL concentration (threshold) needed in liquid culture for autoinduction to occur. Eberhard *et al.* (1981) reported that levels as low as 3×10^{-10} M were sufficient to stimulate bioluminescence in *V. fischeri*. Hence, 3000 times more moles may be needed for induction of the phenazine operon in *P. aureofaciens* PGS12. Studies with radiolabelled *V. fischeri* (Kaplan and Greenberg, 1985) demonstrated that one to two molecules of autoinducer for each cell give some induction of luminescence, and that a maximal rate of induction requires only 40 molecules of autoinducer for each cell. The difference in the results may reflect a difference in regulation between the quorum-sensing system in *V. fischeri* and *P. aureofaciens* or/and a difference of methodology. However, Bainton *et al.* (1992) reported that the threshold concentration of OHHL for induction of carbapenem synthesis in *Erwinia carotovora* subsp. *carotovaora* was ca. 0.1 $\mu\text{g ml}^{-1}$, and synthetic HHL induced *phzB-lacZ* expression in *P. aureofaciens* 30-84Z at a concentrations as low as 1 nM *in vitro* (Wood *et al.*, 1997). The threshold level of 0.173 $\mu\text{g ml}^{-1}$ HHL required for induction of phenazine synthesis in *P. aureofaciens* PGS12 is very close to these values.

HHL accumulated as a consequence of cell density but the ability of exogenous AHL to overcome cell density-dependent induction is well known. It has been reported by Eberhard *et al.* (1981) in *V. fischeri*, by Williams *et al.* (1992) in *E. carotovora*, but also by Pierson III and Pierson (1996) in *P. aureofaciens* 30-84 where externally added AHLs or conditioned media overcame the cell-dependent induction of bioluminescence, carbapenem antibiotic, and phenazine antibiotic production respectively. You and colleagues (1998) observed that the addition of AHLs induced entry into stationary phase in *P. aeruginosa*. Addition of AHLs in the exponential phase, irrespective of cell density, could arrest cellular growth of *P. aeruginosa*, trigger a stationary phase-like morphological change, induce the expression of *rpoS*, and repress the transcription of *rpoD*. They therefore concluded that AHLs can act as a “growth controlling factor” to induce a rapid entry of cells into stationary phase. However, the effects were observed under levels of BHL (C4-HSL) 10^3 to 10^4 times that of the physiological concentration in *P. aeruginosa*.

Latifi *et al.* (1996) showed that in *P. aeruginosa* *rpoS* is regulated directly by RhlR/BHL. RhlR can activate *rpoS* transcription in an autoinducer BHL-dependent manner and *rpoS* expression can be abolished in *P. aeruginosa* mutants unable to generate AHL signal molecules. Furthermore, because BHL was added exogenously, the activation happened immediately rather than in late logarithmic or early stationary phase. This indicated that stationary-phase-specific genes regulated by RpoS might be partly under quorum-sensing control. This result, influence of *rpoS* expression by the RhlR-RhlI system (Latifi *et al.*, 1996), was well accepted until Whiteley *et al.* (2000) showed that RpoS can repress *rhlI* transcription. The percentage of identity shared between a sequence obtained from *phzB* gene in this study and the pyocyanine biosynthesis operon from *P. aeruginosa* was high (91%; Fig. 3.5). It is possible that if the pyocyanine biosynthetic genes and the phenazine biosynthetic genes share high identity then they might also share a common regulatory mechanism. However, a direct interaction between PhzR and *rpoS* remains to be established. A regulatory loop could exist in which RhlR-RhlI would activate *rpoS* and the *rpoS* product, in turn, would repress *rhlI*. However, Whiteley and colleagues could not show that the RhlR-RhlI quorum-sensing system regulates *rpoS* transcription.

In *E. coli*, *rpoS* regulates expression of at least 30 genes, some of which influence osmoprotection, cell morphology, or general stress resistance (Huisman and Kolter, 1994). It remains to be established among the multitude of phenotypes known to be subject to regulation by AHL in *Pseudomonas* spp. which ones are directly under RpoS influence. However, in *E. coli*, *rpoS* is under both transcriptional and translational control, which restricts the availability of functional RpoS to the stationary phase irrespective of the activity of P_{rpoS} (Muffler *et al.*, 1997). Swift *et al.* (1999) proposed that if this regulatory control was also present in *P. aeruginosa*, the fact that the addition of BHL could advance *rpoS* transcription would not necessarily result in RpoS availability. Genes hierarchically regulated via quorum sensing but directly regulated by RpoS could therefore be non-responsive to the addition of BHL.

Expression of RpoS may be induced by AHL signal molecules in *E. coli* but AHL-dependent synthesis of RpoS was prevented by over-expression of a newly identified protein, RspA (Huisman and Kolter, 1994). The similarity of the RspA sequence to that of catabolic enzymes led to the hypothesis that the effect of RspA on *rpoS* transcription could result from a degradation of homoserine lactones. RspA is similar to a lactonising enzyme (chloromuconate cycloisomerase) from *Pseudomonas putida* and shares active site residues. During the growth cycle of *P. aureofaciens*, HHL detection declined rapidly after r_{max} . HHL together with PhzR is thought to repress *phzR* expression posttranscriptionally and transcriptionally (Engebrecht and Silverman, 1986; Dunlap and Ray, 1989). However, the inactivation of transcription of *phzR* cannot explain on its own the sharp decrease in HHL concentration. Even if no more PhzR proteins were translated, and the transcription of *PhzI* stopped, the level of HHL could remain constant. The main hypothesis for the rapid decrease of HHL is a catabolic degradation or deactivation of HHL. RspA or RspA homologues in *Pseudomonas* are new potential candidates for a catabolic degradation of AHLs.

The transcription of *rpoS* is correlated with growth rate during transition from exponential phase to stationary phase: σ^S is not detected in the exponential phase but it increases four- to six-fold following the arrest of cell growth to enter into the stationary phase (Fujita, 1994). HHL started to accumulate in exponential phase but the decrease in HHL concentration was always correlated with a decline in growth rate. It is, therefore,

possible to hypothesise that there is a correlation between starvation signals and HHL degradation in *P. aureofaciens* PGS12. Cui *et al.* (1995a; 1995b) showed that *rsmA* (*rsm*, repressor of secondary metabolites) suppresses production of extracellular enzymes and synthesis of OHHL in several subspecies of *Erwinia carotovora*. In *E. carotovora* subsp. *carotovora*, *rsmA* reduced the levels of transcripts of *hslI*, a *luxI* homologue required for AHL synthesis. Whether RsmA elicits these responses by regulating *carR* and *expR*, the *luxR* homologues, has yet to be determined. *RsmA* has extensive homology with the *csrA* gene of *E. coli*, which specifies a negative regulator of carbon storage, and *csrA* is also notably involved in the control of gene expression for glycogen synthesis, cell morphology, and cell surface properties by affecting mRNA stability (Nogueira and Springer, 2000). *RsmA* homologues have so far been found in several enterobacteria but not in pseudomonads. The link between cell size, growth rate, HHL decline, and RsmA homologues is not yet obvious in pseudomonads.

A direct linkage between a two-component sensory transduction system and a quorum-sensing system was shown to control gene expression in *P. aureofaciens* (Chancey *et al.*, 1999) and in *P. aeruginosa* PAO1 (Reimann *et al.*, 1997). GacA/GacS can control AHL production via positive transcriptional regulation of *phzI* (Chapter 1). Recent evidence suggests that regulatory systems, such as two-component and quorum-sensing systems, are part of integrated regulatory networks (Latifi *et al.*, 1996; Chancey *et al.*, 1999). It is becoming clear that quorum sensing is a core and global regulatory system governing the gene expression of many crucial metabolic functions. Deciphering at the molecular level gene regulation via AHLs and the transduction cascades involving AHLs will permit a deep and global understanding of metabolism regulation in bacteria.

4.6. FUTURE WORK

1. An interesting area to follow on from this project may be to study phenazine gene expression, *RpoS*, and GacA/GacS in relation to one another and in relation to cell density. The insertion of another reporter gene such as *lacZ* in *rpoS* in strain B103 would permit parallel study of the gene expression of the phenazine operon and of the stationary phase factor. The use of a chemostat could prove valuable to control entry into stationary phase at different cell densities. Much more work remains to be done

to understand the positive transcriptional regulation of AHL by the GacA/GacS system. The strain B103 could be further mutated in its *GacA/GacS* genes or transcriptional activity may be followed by mRNA analysis (Northern blot or RT-PCR). Using a chemostat, interactions between quorum-sensing, stationary phase factors, and global regulator may be studied simultaneously under different conditions of cell density and/or starvation of carbon resource.

2. Very little is known about the silencing of the phenazine operon and the degradation of HHL. A homologue of RspA encoding for a lactonising enzyme has been found in *Pseudomonas putida*. It would be interesting to firstly discover if a RspA homologue exists in *P. aureofaciens*, and secondly to study the possible role of this protein in HHL degradation. Studies of over-expression and silencing of the RspA homologues would help to find whether a common, and may be universal, mechanism is at the origin of HHL degradation.

CHAPTER FIVE

TRANSCRIPTIONAL ACTIVITY OF THE PHENAZINE OPERON STUDIED WITH *LUXAB*- REPORTERS IN LIQUID CULTURE

CHAPTER FIVE

TRANSCRIPTIONAL ACTIVITY OF THE PHENAZINE OPERON STUDIED WITH *LUXAB*-REPORTERS IN LIQUID CULTURE

5.1. INTRODUCTION

P. aureofaciens is a potential biological control agent and disease suppression via this species depends largely on the production of phenazine antibiotics (Hamdan *et al.*, 1991). An obstacle to the commercialisation of biological control agents is inconsistent performance from one field to another. Part of the inconsistency may be due to variability in the levels of phenazine produced in the environment. Two approaches are available to study phenazine production. One that follows the accumulation of the compound, the other that monitors the expression of the phenazine operon with a reporter gene. PCA is readily measured *in vitro* and can also be monitored directly on plant roots (Thomashow *et al.*, 1990). However, to do this an extraction is required which demands multiple replications and a lot of time and space is needed for this approach. Gene fusion offers a simpler experimental approach, especially *in situ*. In this research, the *luxAB*-reporter was chosen to study the expression of the phenazine operon. Among all the transcriptional reporters currently available, the *luxAB*-reporter together with luminescence technology (luminometry and CCD-camera) has the unique advantage of enabling quantitative and real time study of *in situ* and *in vitro* gene expression. In this chapter, reporter strains were used, firstly, to obtain general information about the *luxAB* system in *P. aureofaciens* and, secondly, to study the transcriptional activity of the phenazine operon in liquid culture. Chapter 6 describes the study of the transcription of the phenazine operon on nutrient agar and chapter 7 describes the study on plant roots and seedlings.

Two isogenic strains of *P. aureofaciens* PGS12 were generated by transposon mutagenesis (Chapter 3). Strain B103 has a promoterless *luxAB* cassette fused to *phzB*, one of the two genes with *phzA* which are part of the structural region required for PCA production. Thus, strain B103 reports the transcriptional activity of the phenazine operon.

Strain I17 has a *luxAB* cassette integrated randomly in the genome, and expressed light output constitutively. This chapter describes the expression of *phzB::luxAB* from strain B103 compared to the light output from the constitutive strain I17. Using the pattern of phenazine gene activity and the production of HHL and PCA, a model for the chain of events leading to phenazine production for strain PGS12 is presented.

5.2. AIMS

The aims of this study are to provide information on:

1. The pattern and level of the *phzB::luxAB* gene expression in *P. aureofaciens* B103 compare to a constitutive expression of luciferase by strain I17.
2. The timing of the expression of the phenazine operon within the growth cycle of *P. aureofaciens* in liquid culture, especially in relation to HHL and PCA production.

5.3. SELECTION OF A STRAIN WITH CONSTITUTIVE LUCIFERASE EXPRESSION

After transposon mutagenesis of *P. aureofaciens* PGS12 with the miniTn5-*luxAB*, strains with a wild-type phenotype [HHL⁺, Phz⁺] and expressing high levels of bioluminescence on PIA plates were further analysed to select a constitutive *luxAB* reporter. With constitutive *luxAB*-reporters, a constant level of light output per cell as a function of time or growth is expected. Hence, the pattern of gene expression of a non-constitutive reporter may be easily compared and measured against a constitutive reporter.

The selected strains were grown in NB at 28°C, and bioluminescence and cell number (TCC) recorded every 1 h 30 min (Fig. 5.1a). Strains I2, I3 and A20 did not express *luxAB* at a constant level per cell while strains I17, B23, B7 and I6 did. With this strains, bioluminescence was proportional to cell number during growth (Fig. 5.1b). Among all strains, I17 emitted the highest level of bioluminescence. Therefore, strain I17 was selected as a constitutive reporter of *luxAB* and further studied to verify that its growth characteristics and the production of PCA and HHL were similar to the parental strain.

Fig. 5.1a

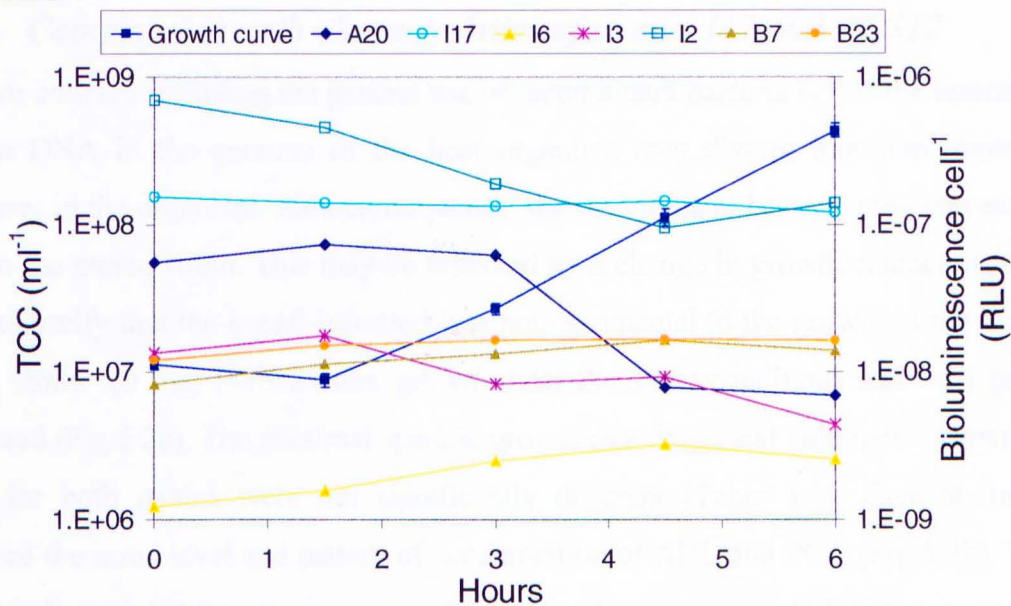


Fig. 5.1b

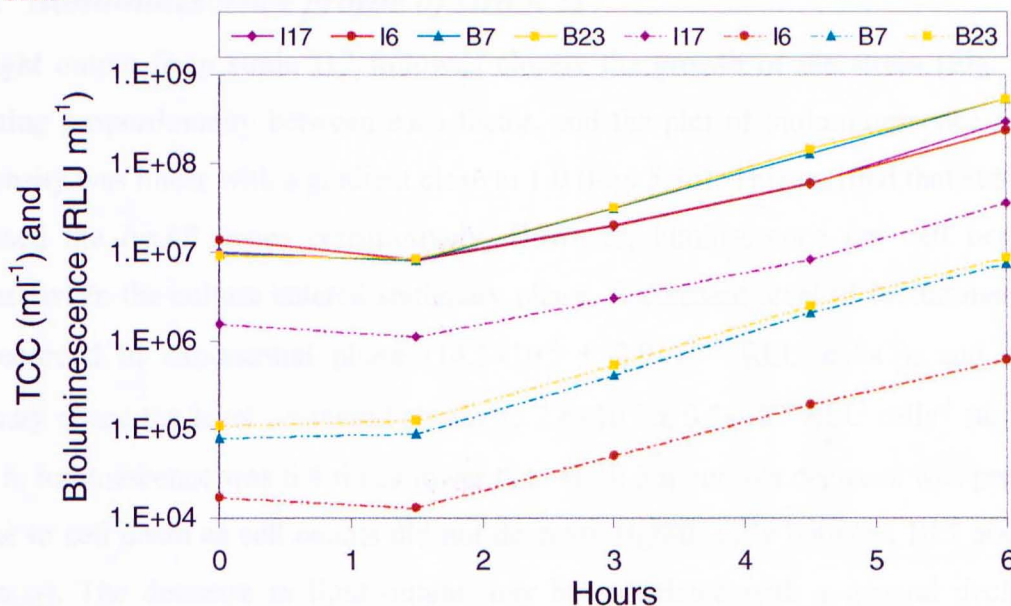


Fig. 5.1. Selection of a constitutive *luxAB*-reporter: Growth and bioluminescence per cell of *luxAB*-marked strains.

All strains were grown in the same conditions in NB at 28°C. The growth curves for all cultures were similar and only the averaged growth curve is shown (Fig. 5.1a). In Fig. 5.1b, the continuous lines represent the growth of 4 selected constitutive *luxAB*-reporter strains and the dotted lines represent bioluminescence from the same strains. Standard errors of means shown ($n = 3$).

5.4. GROWTH RATES AND BIOLUMINESCENCE FROM *P. AUREOFACIENS* I17

5.4.1. Compared growth characteristics of strains I17 and PGS12

A major concern regarding the general use of recombinant bacteria is that the insertion of foreign DNA in the genome of the host organism may disrupt important biological processes in the organism. As a consequence, the recombinant bacteria may become less fit than the parent strain. This may be reflected by a change in growth characteristics. In order to verify that the *luxAB*-insertion was not detrimental to the growth of the reporter strain, strain I17 and PGS12 were grown under the same conditions and their growth compared (Fig.5.2a). The maximal specific growth rate (k_{\max}) and volumetric growth rate (r_{\max}) for both strains were not significantly different (Table 5.1). Each strain also followed the same level and pattern of accumulation of AHL and PCA (Fig 5.2b). These results indicated that the reporter genes did not disadvantage strain I17 in its growth.

5.4.2. Bioluminescence profile of strain I17

The light output from strain I17 followed closely the growth of the strain (Fig. 5.3a), indicating proportionality between each factor, and the plot of bioluminescence against cell density was linear with a gradient close to 1.0 (Fig. 5.3b). This verified that strain I17 expressed the *luxAB* genes constitutively. However, luminescence per cell began to decrease when the culture entered stationary phase. A constant level of bioluminescence was recorded in exponential phase ($14.5 \times 10^{-6} \pm 2.0 \times 10^{-6}$ RLU cells⁻¹), and during stationary phase the level decreased slowly to $2.6 \times 10^{-6} \pm 0.5 \times 10^{-6}$ RLU cells⁻¹ (at 25 h). At 25 h, luminescence was 6.6 times lower than at 10.5 h but this decrease was probably not due to cell death as cell counts did not decrease significantly between 10.5 and 25 h (T-test_{0.05}). The decrease in light output may be associated with a general decline in metabolic activity of the cell and particularly with a decline in reducing equivalents, such as FMNH₂, that are necessary for luciferase activity.

Fig. 5.2a.

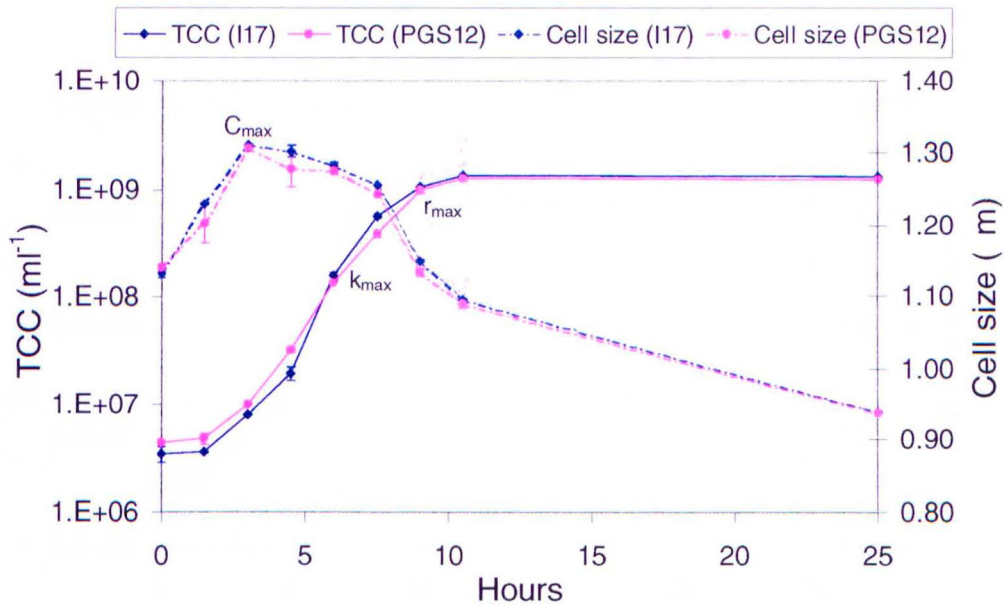


Fig. 5.2b.

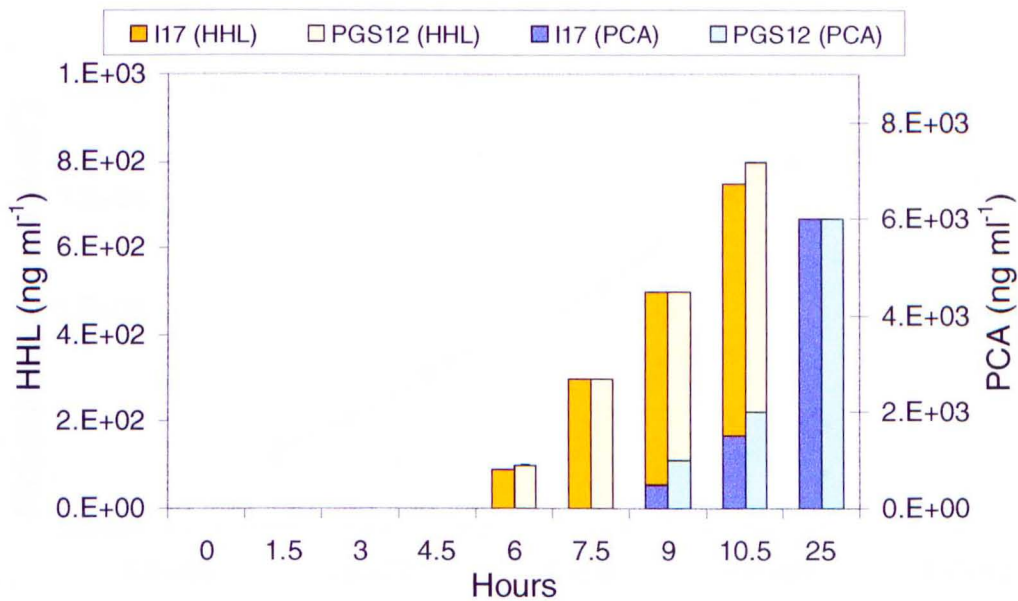


Fig. 5.2. Growth curves and associated cell size profiles (Fig. 5.2a) and accumulation of PCA and HHL (Fig. 5.2b) for *P. aureofaciens* strains PGS12 and I17.

Cultures were grown in the same conditions in NB at 28°C. Standard errors of means shown ($n = 3$).

Fig. 5.3a.

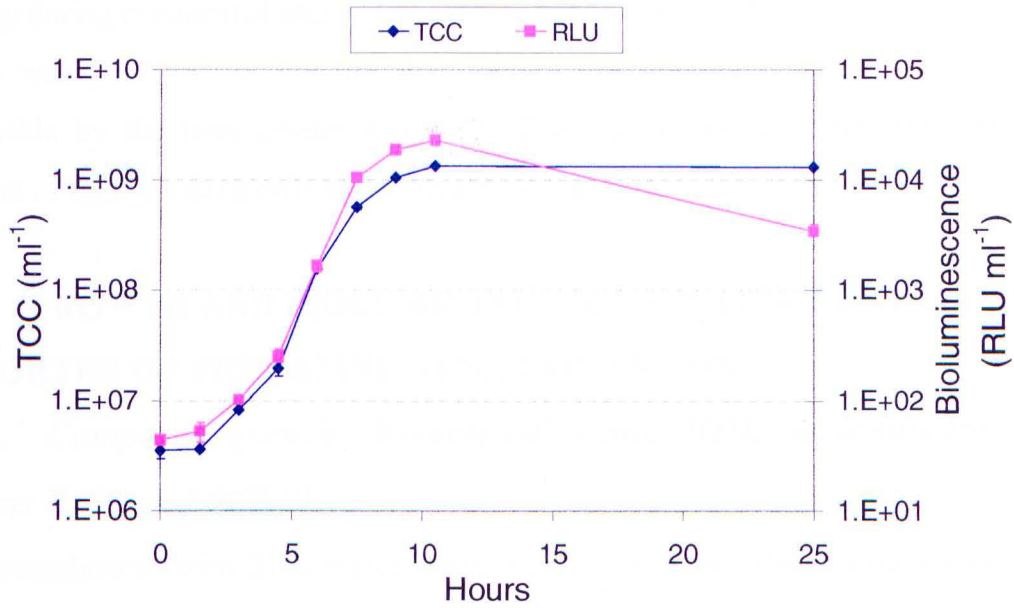


Fig. 5.3b.

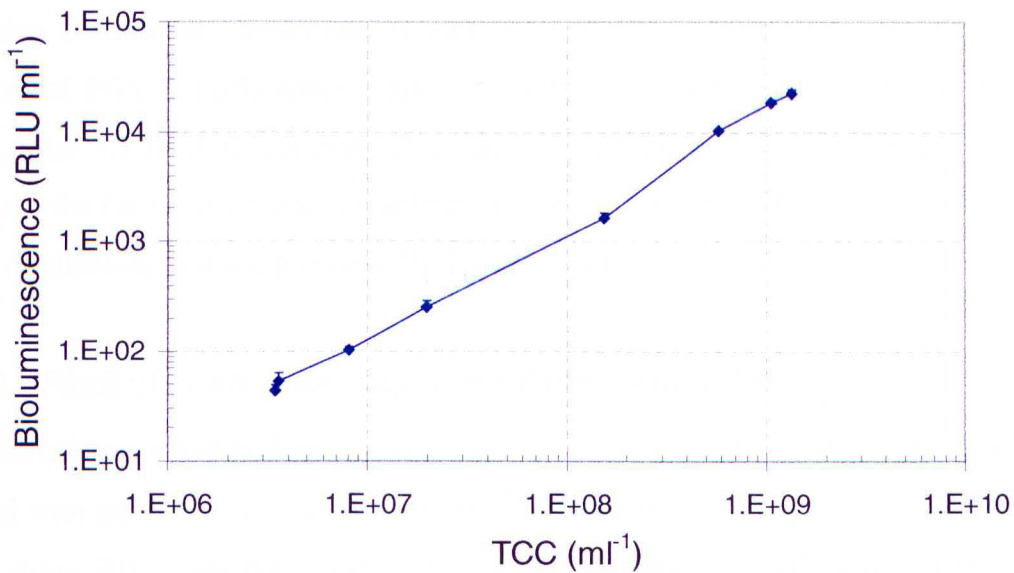


Fig. 5.3. Growth and bioluminescence curves for *P. aureofaciens* I17.

Fig. 5.3a shows bioluminescence and growth as a function of time, and Fig 5.3b shows bioluminescence as a function of cell density. Standard errors of means shown ($n = 3$).

5.4.3. Minimum detectable bioluminescence from strain I17 in liquid culture

Strain I17 expressed *luxAB* constitutively, and light output was proportional to cell density during exponential phase. The average light output emitted during the exponential phase was $14.5 \times 10^{-6} \pm 2.0 \times 10^{-6}$ RLU cell⁻¹. The minimum level of luminescence detectable by the luminometer was 0.005 RLU. Therefore, the minimum detectable number of light-emitting cells was estimated around 345.

5.5. GROWTH AND BIOLUMINESCENCE PROFILE OF STRAIN B103, REPORTER OF PHENAZINE GENE EXPRESSION

5.5.1. Compared growth characteristics and HHL accumulation from strains B103 and PGS12

The recombinant strain B103 marked with *luxAB* in *phzB* and the parental strain PGS12 showed no significant difference between their growth characteristics (Table 5.1; Fig. 5.4a). Thus, the *luxAB* insert did not have a deleterious effect on the growth of the host. However, HHL accumulation by each strain presented some differences (Fig. 5.4b). HHL detection declined at a lower rate in cultures of B103; 3 h after HHL_{max} was reached in cultures of PGS12, HHL concentration was only 7% of HHL_{max}, whereas in culture of B103, after 4.5 h, HHL concentration was still as high as 29% of HHL_{max}. Therefore, although the *luxAB* insert was not deleterious for the growth of B103, it possibly affected HHL production, or more precisely HHL degradation.

5.5.2. *PhzB::luxAB* gene expression from strain B103

The growth curve and bioluminescence profiles of strain B103 in NB at 28°C (culture B started with an inoculum of 4×10^6 cells ml⁻¹) are illustrated in Fig. 5.5a. The light output from strain B103 was not constant but varied in relation to cell density and with the phases of the growth culture. Luminescence per ml remained constant during the first 4.5 h of culture while cell numbers increased. Between $r_{\max-1}$ and r_{\max} , luminescence increased at a greater rate than growth, and until $r_{\max+1}$, it increased at a similar rate to

Fig. 5.4a.

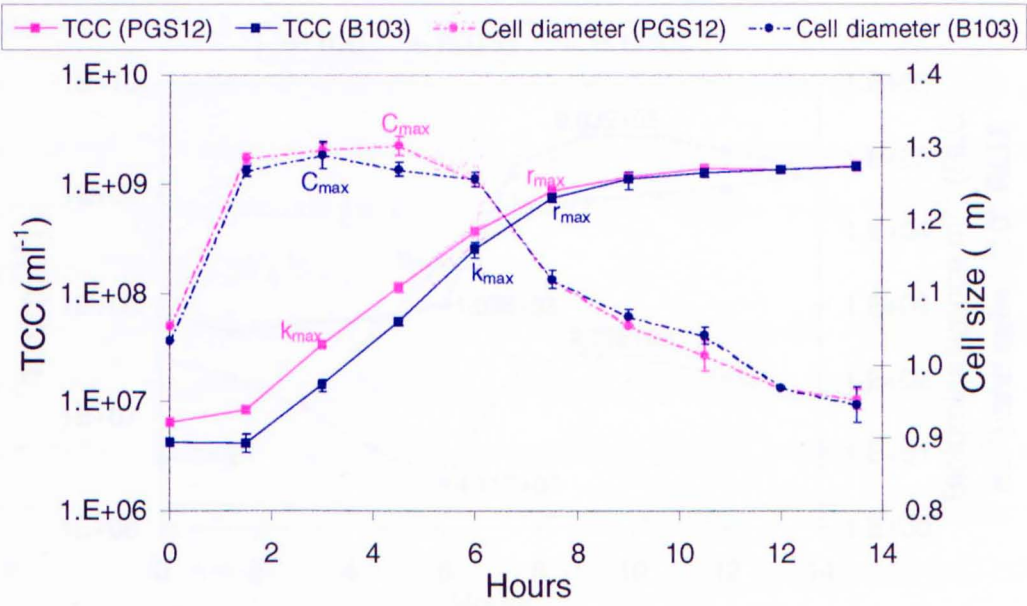


Fig. 5.4b

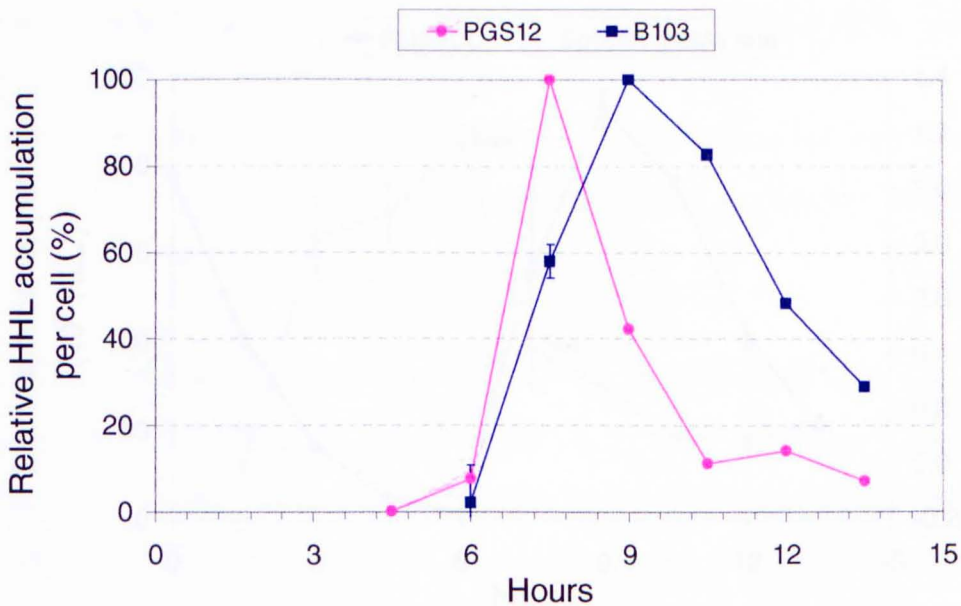


Fig. 5.4. Growth cultures of *P. aureofaciens* B103 and PGS12 and associated cell size profiles (Fig. 5.4a) and relative HHL accumulation (Fig. 5.4b).

Both strains were grown in the same conditions in NB at 28°C but not on the same day. The values were normalised to the maximal values obtained during the experiment. Standard errors of means shown ($n = 3$).

Fig. 5.5a

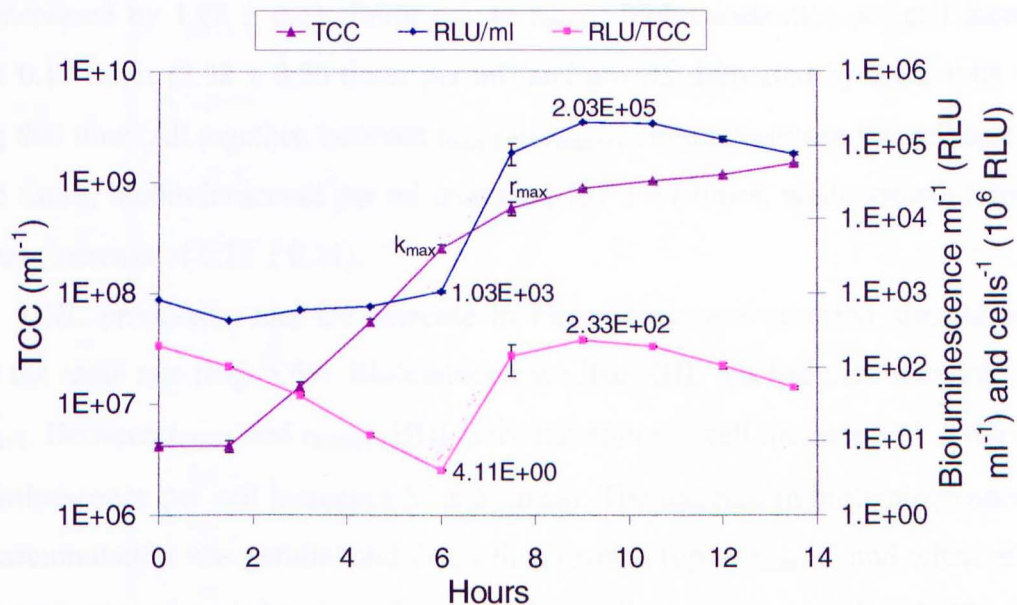


Fig. 5.5b

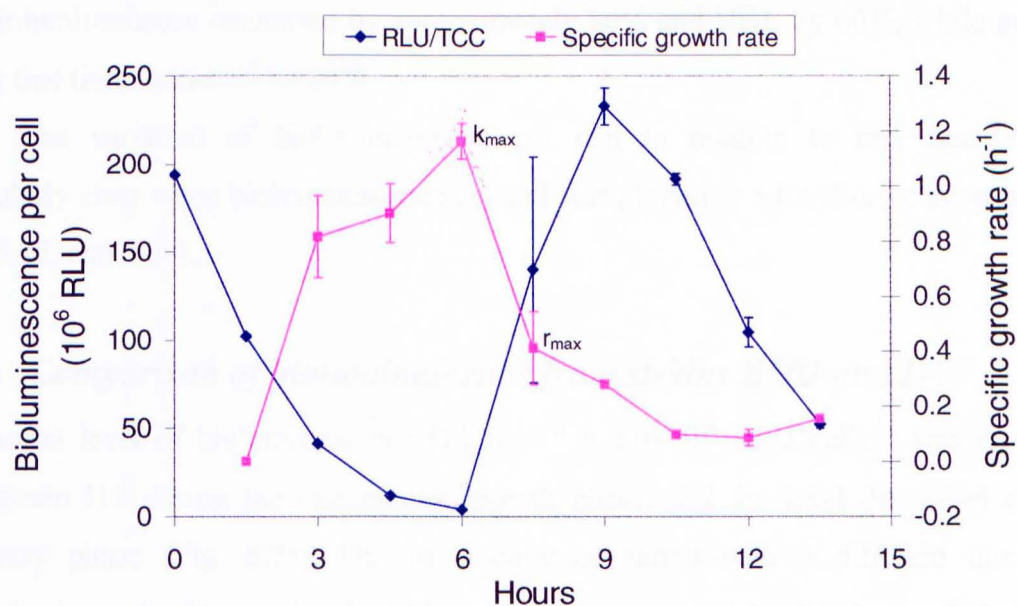


Fig. 5.5. Growth curve of *P. aureofaciens* B103 (Fig. 5.5a), specific growth rate (Fig 5.5b) and pattern of *phzB::luxAB* activity.

Bioluminescence is shown per ml and per cell on a logarithmic scale in Fig. 5.6a, and per cell on a linear scale in Fig. 5.6b. The maximal specific growth rate (k_{max}) occurred at t_6 and the maximal volumetric growth rate (r_{max}) occurred at t_9 . Standard errors of means shown ($n = 3$).

growth before declining during stationary phase. The increase in bioluminescence was concomitant with the decline in growth rate after k_{\max} (Fig. 5.5b). From $r_{\max-1}$ to r_{\max} , bioluminescence per cell increased 34 ± 18 times (77 ± 41 times per ml) while growth only increased by 1.88 ± 0.51 . From r_{\max} to $r_{\max+1}$, bioluminescence per cell increased 1.95 ± 0.17 times (2.98 ± 0.26 times per ml) and growth decreased by 0.4 ± 0.08 times during that time. All together, between $r_{\max-1}$ to $r_{\max+1}$, bioluminescence per cell increased 57 ± 5 times, bioluminescence per ml increased 197 ± 17 times, while growth remained constant (increase of 1.10 ± 0.21).

HHL production and the increase in bioluminescence occurred simultaneously and at the same rate (Fig. 5.6a). Bioluminescence like HHL reached their maximal value at $r_{\max+1}$. Between $r_{\max-1}$ and $r_{\max+1}$, HHL accumulation per cell increased 11 ± 0.6 times (bioluminescence per cell increased 57 ± 5 times). The increase in bioluminescence and HHL accumulation was parallel and faster than growth (up to $r_{\max+1}$), and when relative values were plotted as a function of growth, the gradient was greater than 1 (Fig. 5.6c). After $r_{\max+1}$, bioluminescence and HHL levels decreased. Bioluminescence decreased in average every 1.5 h by 24% and HHL by 20% (Fig. 5.6b). Altogether, between t_9 and t_{13} , bioluminescence decreased by approximately 80% and HHL by 60%, while growth during that time increased by 24%.

The variation of bioluminescence per cell in relation to cell density was particularly clear when bioluminescence per cell was plotted as a function of growth (Fig. 5.7b, 5.7d, and 5.7e).

5.5.3. Comparison of bioluminescence from strains B103 and I17

A constant level of bioluminescence ($14.5 \times 10^{-6} \pm 2.0 \times 10^{-6}$ RLU cells⁻¹) was recorded from strain I17 during the exponential growth phase, and the level decreased during stationary phase (Fig. 5.7a). Out of 3 cultures started with 3 different inoculum concentrations, the highest level of bioluminescence emitted by B103 was $799 \times 10^{-6} \pm 141 \times 10^{-6}$ RLU cell⁻¹ (culture A; Fig. 5.7d). This was 55 ± 9.8 times the level recorded from strain I17. The minimum level of light output was $2.99 \times 10^{-6} \pm 0.20 \times 10^{-6}$ RLU cell⁻¹ (culture A). It was recorded at k_{\max} and corresponded to 0.2 ± 0.01 times the level from

Fig. 5.6a

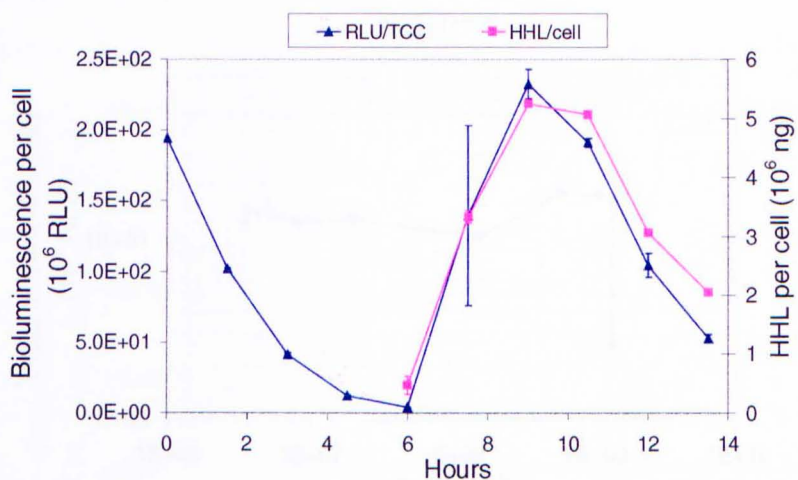


Fig. 5.6b

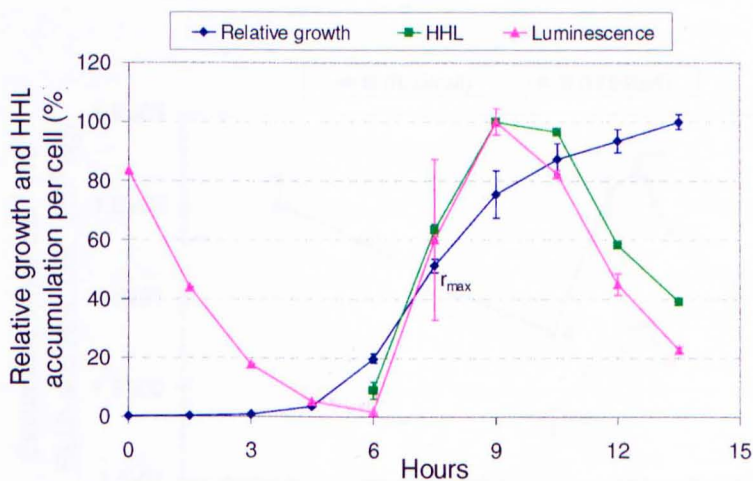


Fig. 5.6c

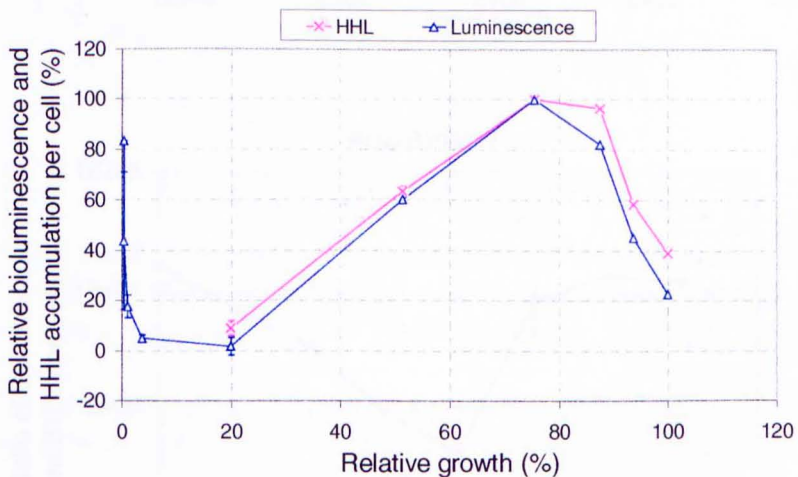


Fig. 5.6. Relative growth, accumulation of HHL and bioluminescence as a function of time (Fig. 5.6a and 5.6b) and as a function of growth (Fig. 5.6c).

The values are relative values of luminescence, growth, and HHL accumulation normalised to the maximum values obtained during the experiment. Standard errors of means shown ($n = 3$).

Fig. 5.7a

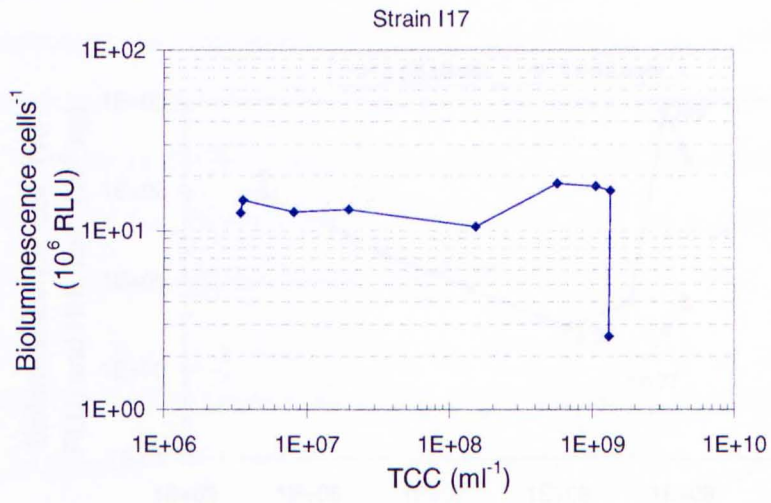


Fig. 5.7b

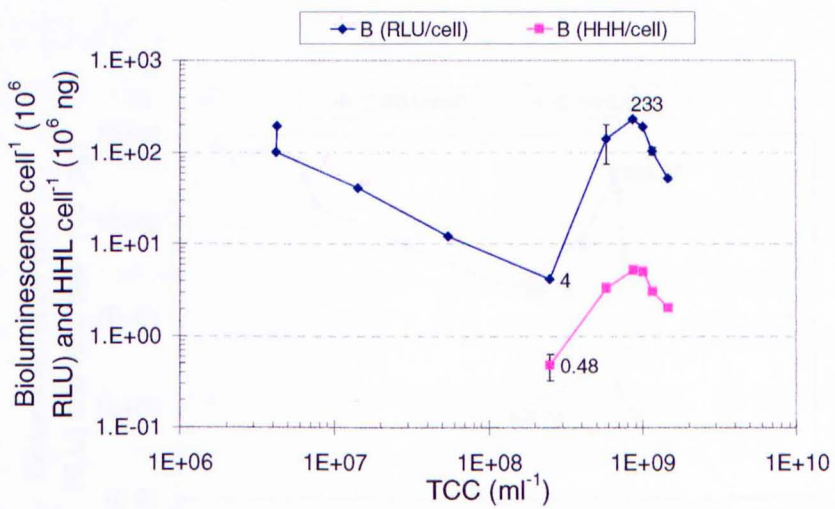


Fig. 5.7c

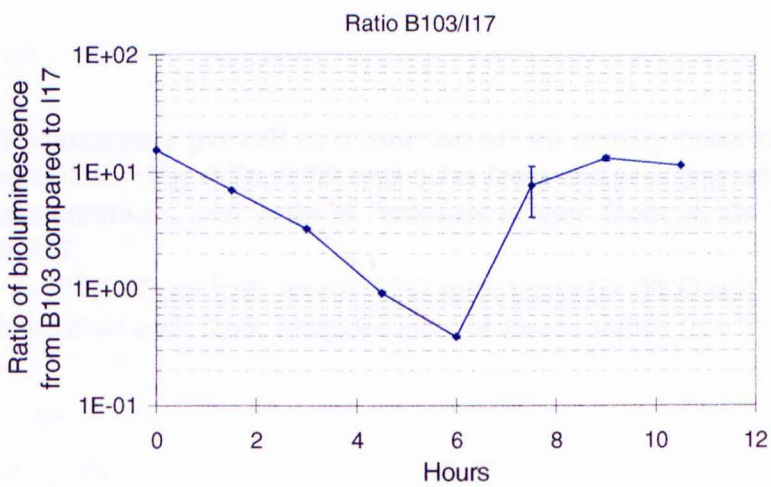


Fig. 5.7d

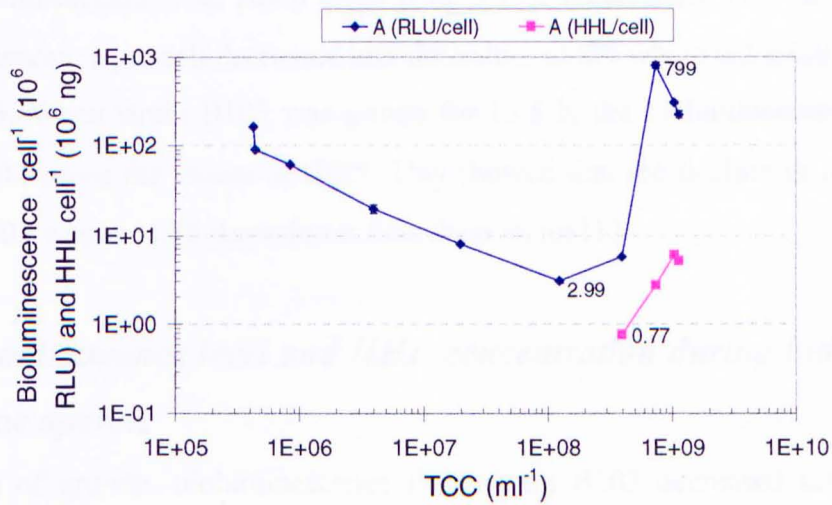


Fig. 5.7e

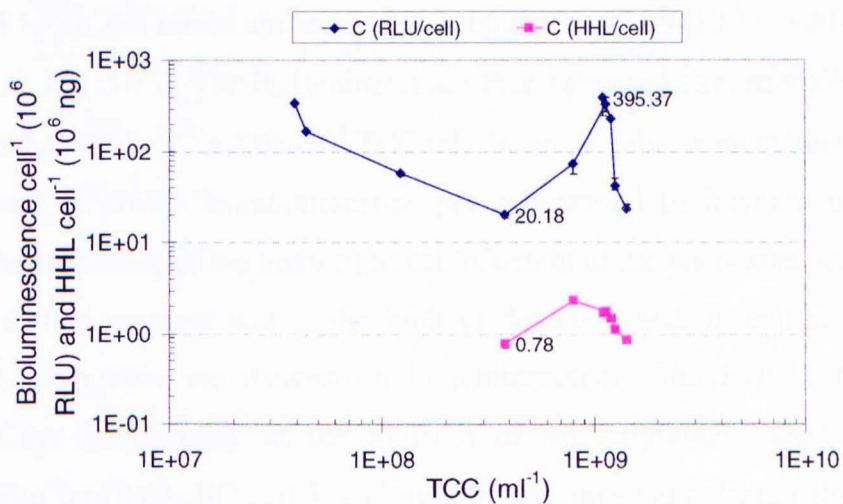


Fig. 5.7. Bioluminescence per cell as a function of cell density from strain I17 (Fig. 5.7a) and strain B103 (Fig. 5.7b, 5.7d, and 5.7e) from cultures started at 3 different inoculum concentrations, and ratio of bioluminescence from strain B103 (culture B) over strain I17.

Inoculum A: 4×10^5 TCC ml⁻¹; B: 4×10^6 TCC ml⁻¹; C: 4×10^7 TCC ml⁻¹. Samples were taken in triplicate from each flask. Standard error of means shown ($n = 3$).

strain I17. Because the level of bioluminescence from strain I17 was constant, the graph of the ratio of bioluminescence from strain B103 over I17 had the same shape as the graph of bioluminescence from strain B103 (Fig. 5.7c). When strain I17 was grown for 25 h, bioluminescence per cell decreased and the values at t25 were 0.2 ± 0.02 times the values at t10.5. When strain B103 was grown for 13.5 h, the bioluminescence per cell was 0.28 ± 0.02 times the values at t10.5. This showed that the decline in light output from strain B103 was ca. 6.76 times faster than from strain I17.

5.5.4. Bioluminescence level and HHL concentration during induction of the phenazine operon

As a function of growth, bioluminescence from strain B103 decreased until the cell density reached $2.7 \times 10^8 \pm 7.6 \times 10^7 \text{ ml}^{-1}$ (average value from culture A, B, and C; Fig. 5.7b, 5.7d, and 5.7e). The minimum level of light output was $2.99 \times 10^{-6} \pm 0.20 \times 10^{-6} \text{ RLU cell}^{-1}$ (culture A; Fig. 5.7d). The bioluminescence then increased exponentially until the cell density reached $9.04 \times 10^8 \pm 2.06 \times 10^8 \text{ TCC ml}^{-1}$ (average value from culture A, B, and C). The moment at which bioluminescence per cell started to increase may be an indication of the beginning of the transcriptional induction of the phenazine operon. HHL concentration at that moment was at the limit of detection and, in culture A, it was detected only 1.5 h after the increase in bioluminescence. The HHL concentration detected with the *lux*-bioassay at the moment of transcriptional induction of the phenazine operon was $0.63 \times 10^{-6} \pm 0.3 \times 10^{-6} \text{ ng cell}^{-1}$ (average value from cultures B and C; Fig. 5.7c, and 5.7d).

5.6. CONCLUSIONS AND DISCUSSION

5.6.1. Results: Summary

The different phases leading to PCA production in NB from these results are outlined:

1. Upon accumulation of HHL to a threshold concentration of $0.63 \times 10^{-6} \pm 0.3 \times 10^{-6} \text{ ng cell}^{-1}$, the autoinduction process was initialised most likely through the formation of an activated transcriptional regulator, the PhzR-HHL protein complex. At this moment, the cell density was at $2.7 \times 10^8 \pm 7.6 \times 10^7 \text{ ml}^{-1}$. The transcriptional activity

recorded from the expression of *phzB::luxAB* was at its minimum with a level of $2.99 \times 10^{-6} \pm 0.20 \times 10^{-6}$ RLU cell⁻¹, and the growth rate and cell diameter were maximal at ca. 1.30 μm .

2. After k_{max} , the growth rate and cell diameter decreased simultaneously (cells measured about 1.15 μm at r_{max} ; see chapter 4). In strain B103, the maximal HHL concentration ($5.25 \times 10^{-6} \pm 0.26 \times 10^{-6}$ ng cells⁻¹) and the maximum transcriptional activity from the *phzB::luxAB* reporter ($233 \times 10^{-6} \pm 10.5 \times 10^{-6}$ RLU cell⁻¹) occurred simultaneously at $r_{\text{max}+1}$. At the genetic level, the events leading to the simultaneous synthesis of HHL and bioluminescence are summarised in Fig. 5.8.
3. During stationary phase after $r_{\text{max}+1}$, HHL concentrations and luciferase activity from the *phzB::luxAB* fusion in strain B103 decreased rapidly. However, the decrease in HHL concentration did not occur as rapidly as it did in liquid culture of strain PGS12. In early stationary phase, in cultures of strain PGS12 (or strain I17), the production of PCA was at its maximum. PCA was first detected in the medium in transition phase at r_{max} with ca. 0.65 $\mu\text{g ml}^{-1}$ or 5.65×10^{-7} ng cells⁻¹. PCA production carried on during the remainder of the stationary phase. At 12 h, cells measured 1.01 ± 0.023 μm .

5.6.2. Discussion

The expression of *phzB::luxAB* gene fusion from strain B103 followed a pattern characteristic of genes under the influence of an autoinducer such as found in *V. fischeri* (Nealson, 1977). The bioluminescence profile during the growth of the organism varied with cell density and with the phases of growth. As described in Fig. 5.8, luciferase activity in strain B103 reflected the transcription and regulation of the phenazine operon. Upon accumulation of HHL to $0.63 \times 10^{-6} \pm 0.3 \times 10^{-6}$ ng cell⁻¹, the autoinduction process began and the transcription of the *luxAB* genes inserted into *phzB* occurred simultaneously to the transcription of *phzI*. Therefore, in strain B103, light formation reported in real time the accumulation of HHL and bioluminescence and both followed a similar pattern.

Fig. 5.8

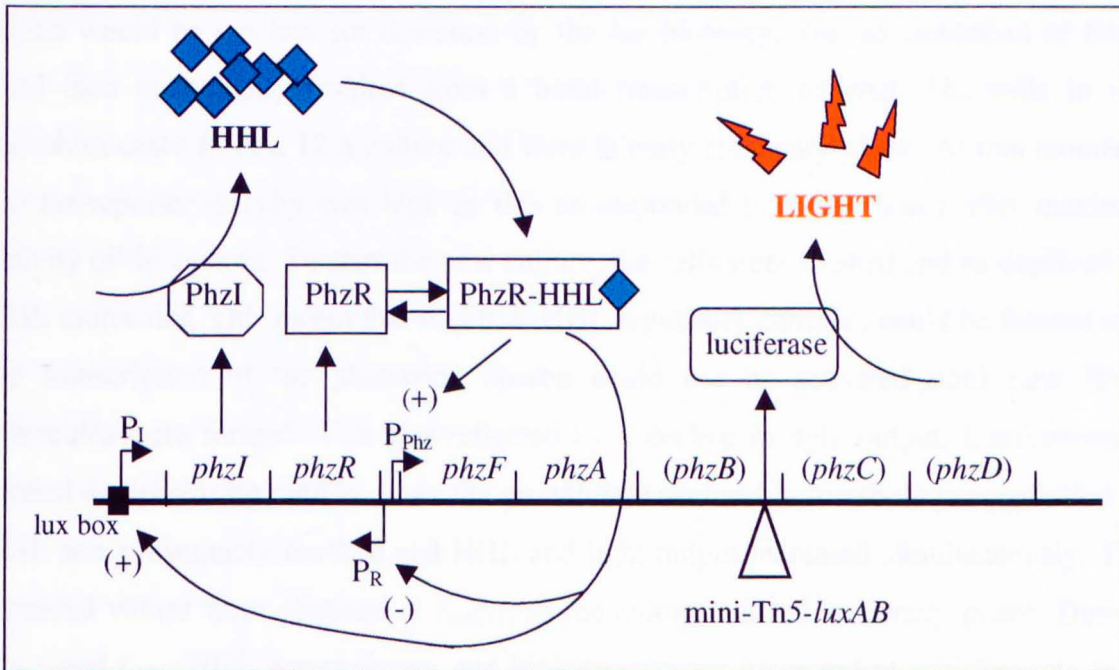


Fig. 5.8. Luciferase activity from the *phzB:luxAB* gene fusion in strain B103 reports the transcription of the phenazine operon and the autoinduction process.

Upon accumulation of HHL to a threshold concentration, the autoinduction process begins with the formation of an activated transcriptional regulator, the PhzR-HHL protein complex. The transcription of *phzI* is activated by the regulatory complex, inducing a positive feedback loop and leading to an exponential accumulation of HHL. The transcriptional regulator also triggers, through the P_{phz} promoter, the transcription of the biosynthetic genes and, in strain B103, the transcription of *luxA* and *luxB* genes inserted into *phzB*. Therefore, HHL accumulation and light formation are both under the same constraint, the regulation by PhzR-HHL complex, whose formation is itself dependent upon HHL synthesis. This implies that the level of luminescence from strain B103 is proportional to HHL accumulation, and that luminescence reports the transcription of phenazine operon in real time.

However, until the cell density reached approximately 2×10^8 TCC ml^{-1} , light output decreased while HHL was accumulating from about 0 to 0.63×10^{-6} ng cell^{-1} . The inoculum consisted of washed cells and only traces of HHL could remain, concentrations which would be too low for detection by the *lux* bioassay. The accumulation of HHL until then most likely resulted from a basal transcription of *phzI*. The cells in the inoculum came from a 12 h culture and were in early stationary phase. At this moment, the *lux*-reporter activity was high as this corresponded to a few hours after maximal activity of the operon. To start the new culture, the cells were washed and so deprived of HHL molecules. This meant that no PhzR-HHL regulatory complex could be formed and the transcription of the phenazine operon could not be activated until new HHL molecules were formed. This was reflected by a decline in light output. Luminescence carried on decreasing until k_{max} . As the growth rate declined, a threshold concentration of HHL was presumably reached and HHL and light output increased simultaneously. The maximal values were obtained at $r_{\text{max}+1}$, as the culture entered stationary phase. During $r_{\text{max}-1}$ and r_{max} , HHL accumulation and bioluminescence increased at a higher rate than growth indicating that autoinduction of the phenazine operon was taking place.

The dramatic decline of HHL concentration after approximately $r_{\text{max}+1}$ may be attributed to either its degradation, its binding to other molecules in the media, or to the negative autoregulation via PhzR. HHL together with PhzR is thought to repress *phzR* expression post-transcriptionally and transcriptionally. In *Vibrio fischeri*, the regulation can be positive or negative, depending upon the level of cellular LuxR and OHHL, and the presence or absence of a downstream element in the *luxD* open reading frame (Dunlap and Ray, 1989; Engebrecht and Silverman, 1986; Shadel and Baldwin, 1992). The discrepancy between B103 and the parental strain PGS12 regarding HHL decline may be attributed to changes in expression of coding regions downstream of the *luxAB*-insert, such as the *phzC* and *phD* genes which might be involved in the down regulation of phenazine operon. In strain B103, this downstream factor may not be transcribed, and the transcription of the whole operon may not be down regulated as efficiently as found for the wild-type strain.

As shown in Chapter 4, in cultures of the wild-type strain, PCA was first detected in the transition phase at approximately r_{max} , and the maximal rate of PCA production

corresponded to the sharp decrease in HHL concentration. Therefore, PCA was produced after the burst of HHL synthesis, after full autoinduction of the operon. PCA synthesis continued during stationary phase, and because it is stable (Turner and Messenger, 1986), it accumulated in the medium. The *luxAB* reporter system in the phenazine operon in strain B103 followed HHL production; this indicated that production of phenazine operon transcripts and promoter activity declined quickly after the peak of HHL production. Since PCA was still produced beyond this point, the protein products would appear to be relatively stable and continued to produce phenazine after the operon promoter had been silenced. If the PhzI protein behaved in a similar fashion, HHL synthesis would be expected to continue likewise for a longer period. Therefore, either PhzI is silenced or degraded in the cell relatively quickly.

The luciferase expression from strain I17 was proportional to cell density during the exponential growth of the organism and strain I17 may be referred to as a *luxAB* constitutive reporter. However, bioluminescence per cell declined when cells entered stationary phase. Rattray (1992) investigated whether luminometry could provide a measure of microbial activity by comparing activity provided by radiorespirometric and bioluminescence measurements. In liquid culture, during stationary phase, both respiration and luminescence decreased at a similar rate, whereas microbial biomass remained constant. This indicated that luminescence is related to microbial activity. Indeed luciferase activity may provide a direct assessment of the level of reducing equivalents (FMNH₂) in cells (Jablonski and DeLuca, 1978; Rattray, 1992). Hence, the decrease in bioluminescence during stationary phase reflects a general slow down of cell metabolism. Because in constitutive *luxAB*-reporters, bioluminescence is proportional to cell number, luminometry may be used to measure microbial biomass. Luminescence of dilutions of cells dividing exponentially is proportional to cell concentration over several orders of magnitude and the lower detection limit for cells of strain I17 by luminometry was around 345 cells ml⁻¹. Therefore, the *luxAB* reporter genes permitted a very sensitive detection of cells of strain I17. However, if luminometry is used for assessing biomass of starved cells, measurements of potential luminescence may be necessary (Rattray *et al.*, 1990; Meikle *et al.*, 1994). Potential luminescence consists of measurement of

luminescence after amendment of soil with nutrients. This technique is analogous to the substrate-induced respiration (SIR) method of Anderson and Domsch (1978).

Bioluminescence per cell from strain I17 can also be used without calculation of potential bioluminescence, whatever the physiological state of cells, to compare with the transcriptional activity from other non-constitutive *lux*-reporters. When cells entered the stationary phase, light output from strain B103 and I17 decreased but the decline in bioluminescence from strain B103 was approximately 6.8 times higher than the decline in bioluminescence from strain I17. If the decrease in bioluminescence from strain I17 represented a decrease in cell metabolism, then the difference in decrease between the 2 strains may represent more specifically a decrease in transcriptional activity from strain B103. This could be due to a down-regulation of the transcriptional activity of the phenazine operon by PhzR. In contrast, when cells are dividing exponentially, cell metabolism is close to a maximum. In NB at 28°C, the bioluminescence per cell corresponding to this active physiological state was $14.5 \times 10^{-6} \pm 2.0 \times 10^{-6}$ RLU cells⁻¹. At $r_{\max+1}$, light output from strain B103 was maximal and the level was up to 55 ± 9.8 times the level from the constitutive reporter. At $r_{\max-1}$ (or k_{\max}), the level of bioluminescence from strain B103 was only 0.2 ± 0.01 times the level from strain I17. All together, between $r_{\max-1}$ to $r_{\max+1}$, bioluminescence per cell increased 57 ± 5 times. These values showed clearly the power of the autoinduction process. The shift in the transcriptional activity of the phenazine operon happened in only 3 h. So when no HHL was present in the culture, the transcriptional activity decreased slowly and steadily, whereas when HHL reached the threshold concentration of ca. 0.6×10^{-6} ng cell⁻¹, the autoinduction of the operon started resulting in a large and fast increase in light output from the *phzB::luxAB* reporter. In view of these results, one could add the word “rapid” to the definition of quorum sensing, and this would become “rapid concerted bacterial population response upon accumulation of an autoinducer”.

CHAPTER SIX

TRANSCRIPTIONAL ACTIVITY OF THE PHENAZINE OPERON STUDIED WITH *LUXAB*- REPORTERS ON SOLID SURFACE AGAR

CHAPTER SIX

TRANSCRIPTIONAL ACTIVITY OF THE PHENAZINE OPERON STUDIED WITH *LUXAB*-REPORTERS ON SOLID SURFACE AGAR

6.1. INTRODUCTION

The well-agitated suspension culture is largely a laboratory artifice and many bacteria proliferate and survive attached to surfaces in the environment. Bacteria from attached cultures differentiate biochemically and morphologically from planktonic cells, and they interact in ways that produce spatially organised populations (Shapiro, 1983). Studies of colony formation in *E. coli* or *Pseudomonas* spp. indicate that the majority of cell division is localised at the edge of the colony throughout colony morphogenesis (Shapiro, 1983; Emerson, 1999; Newman and Shapiro, 1999). Colony development and collective motility phenomena in bacteria hold many parallels with the formation and development of biofilms, perhaps the most widespread multicellular prokaryotic structures in nature (Costerton *et al.*, 1995). The high cell concentration typically found in biofilms has led to the suggestion that AHL activity may be essential components of their physiology. Batchelor *et al.* (1997) showed that AHLs reduced significantly the lag phase of starved biofilm populations of ammonia-oxidising bacteria. McLean *et al.* (1997) gave the first evidence of autoinducer activity in naturally occurring biofilms. Davies *et al.* (1998) recently reported that AHLs play an essential role in the spatial organisation of *P. aeruginosa* biofilms. A *lasI* mutant produced a biofilm that was only 20% as thick as the one formed by the wild-type strain and was sensitive to the detergent sodium dodecyl sulfate. These results provide examples of complex multicellular traits in bacteria and make the study of colonies worthy of exploration. This chapter describes the production of HHL and phenazine by colonies of *P. aureofaciens* PGS12, B103 and I17 growing on nutrient agar. The transcriptional activity of the *phzB::luxAB* genes fusion from strain B103 was studied and compared to the constitutive luciferase activity from strain I17. The aim of this study was to provide information on the activity of the phenazine operon

from cells growing in colonies. This study provided a point of comparison with bacteria growing on plant roots where cells form microcolonies and a biofilm (Ratray *et al.*, 1995) and with planktonic cells.

6.2. AIMS

More specifically, this study was aimed at answering the following questions:

1. Do cells within colonies produce different amounts of AHLs and phenazine than planktonic, unattached cells? When does AHL and phenazine production occur during colony development?
2. What is the importance of AHL diffusion?
3. What are the major differences and similarities between cells in colony and planktonic cells?
4. What is the pattern of *phzB-luxAB* gene expression from strain B103 during colony development and does it follow AHL production? How does it compare with the constitutive luciferase expression from strain I17?

6.3. GROWTH OF *P. AUREOFACIENS* ON NUTRIENT AGAR

Bacterial cell counts were measured after bacteria were grown on NA at 21°C for 17 h. No data were available prior to that because colonies only became visible to the naked eye after about 17 h incubation. At t_0 the colonies contained, on average for all three strains, $3.1 \times 10^6 \pm 2.4 \times 10^5$ cells and cells measured $1.26 \pm 0.01 \mu\text{m}$ (Fig. 6.1a). This corresponded in liquid culture to the size for cells dividing exponentially. At t_3 , the average cell size had decreased to $1.20 \pm 0.002 \mu\text{m}$, indicating that cell growth was slowing down. Between t_3 and t_{12} , cells had the diameter of cells found in transition phase in liquid culture. At t_{24} , cells measured $1.02 \pm 0.004 \mu\text{m}$, which corresponded in liquid culture to cells in the stationary phase. From t_0 to 24, the specific growth rate decreased continuously as can be seen in Fig. 6.1b. At t_{24} , the cell numbers in colonies had reached $3.7 \times 10^8 \pm 1.7 \times 10^7$ cells (average for all 3 strains; Fig. 6.1a).

The growth of the colonies was also visible from pictures taken with a digital camera at t_0 , t_3 , t_6 , t_9 , t_{12} and t_{24} (Fig. 6.2). At each of these time points colony width

Fig. 6.1a

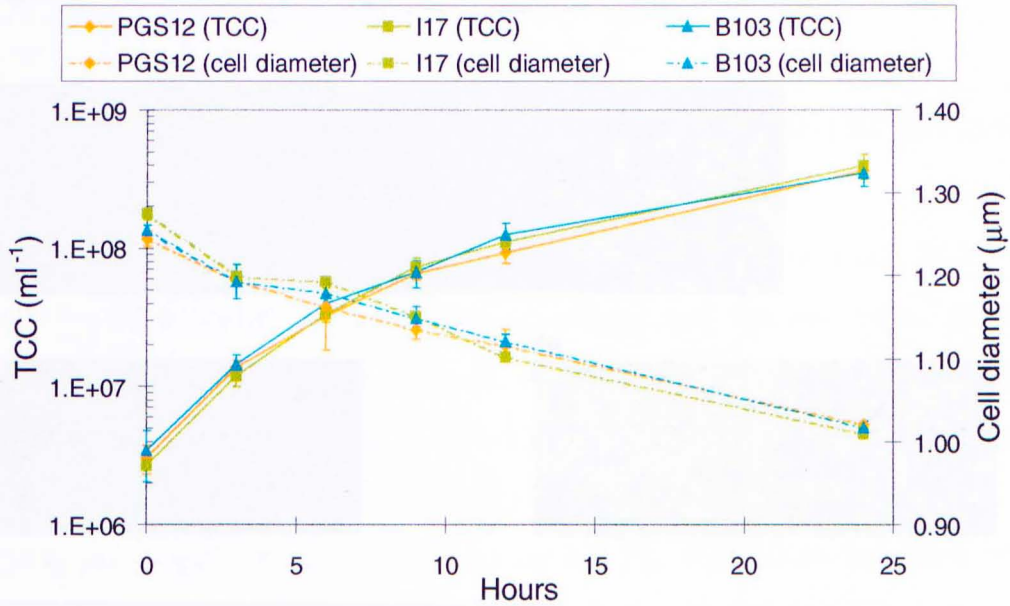


Fig. 6.1b

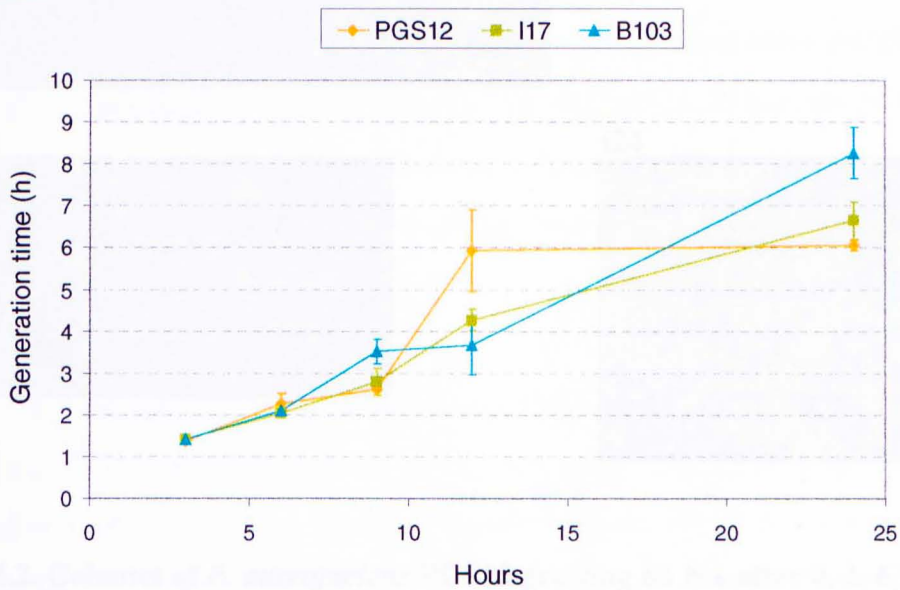


Fig. 6.1. Growth of *P. aureofaciens* PGS12, I17, and B103 in colonies on NA and associated cell diameter (Fig. 6.1a) and generation time (Fig. 6.1b).

The first time point (t_0) corresponds to a 17 h pre-incubation period (until colonies became visible on plates). The data were generated from 5 randomly picked colonies for each strain. Standard errors of means shown ($n = 5$).

Fig. 6.2

t0



t3



t6



t9



t12



t24



Fig. 6.2. Colonies of *P. aureofaciens* PGS12 growing on NA after 0, 3, 6, 9 12 and 24 h incubation at 21°C.

The pictures were taken with a digital camera. The cork borer delimited an agar plug of 7 mm that left about 2 mm around the largest colonies.

The colony diameters were: At t0, 0.6 mm; At t3: 1.25 mm; At t6: 2 mm; At t9: 2.25 mm; At t12: 3 mm; At t24: 3.5 mm. From measurements given by (Newman and Shapiro, 1999), the depth of a colony may be estimated to vary between 0.1 and 0.5 mm. Therefore, the volume of the colonies were estimated to be: At t0, 0.2 μ l; At t3: 0.8 μ l; At t6: 1.9 μ l; At t9: 2.5 μ l; At t12: 3.8 μ l; At t24: 5 μ l.

was also measured. From measurements given by (Newman and Shapiro, 1999), the depth of a colony may be estimated to vary between 0.1 and 0.5 mm. Hence, the volume of colonies was estimated to vary between 0.2 μl (at t_0) and 5 μl (at t_{24}).

6.4. PRODUCTION OF PHENAZINE AND HHL ON NUTRIENT AGAR

6.4.1. Production of HHL

HHL was only once detected at t_0 and in only one colony (of the strain B103) at the concentration of 0.34×10^{-6} ng cell⁻¹. The experiment was repeated twice and in the second replicate no HHL was detected at t_0 . At t_3 , HHL was found in all colonies at an average concentration for all strains of $2.14 \times 10^{-6} \pm 0.07 \times 10^{-6}$ ng cell⁻¹. This concentration was high, indicating that HHL was probably detectable in all colonies at t_1 or t_2 . Fig. 6.3a shows the overall accumulation per colony and Fig. 6.3b the accumulation of HHL per cell, for each strain, over time. There was little variation in HHL accumulation between each strain. HHL production was maximal during a 3 h time window (from t_6 to t_9) at ca. $6.30 \times 10^{-6} \pm 0.46 \times 10^{-6}$ ng cell⁻¹. After t_9 , HHL concentration per ml and per cell decreased and reached $0.22 \times 10^{-6} \pm 0.02 \times 10^{-6}$ ng cell⁻¹ at t_{24} . Within the 24 h experiment, HHL was not detected outside the perimeter delimited by the cork borer; it may thus be assumed that HHL did not significantly diffuse outside the colonies.

6.4.2. Production of phenazine

Accumulation of PCA within colonies of *P. aureofaciens* PGS12 and I17 was also monitored. PCA was first detected at t_6 , 3 h after HHL (Fig. 6.4a and 6.4b). The accumulation of PCA per cell increased rapidly between t_6 and t_9 , decreased between t_9 and t_{12} , and continued to accumulate between t_{12} and t_{24} . PCA concentration decreased between t_9 and t_{12} simultaneously with HHL concentration. There was little variation in PCA accumulation between strains PGS12 and I17. The final concentration at t_{24} reached $37 \times 10^{-6} \pm 5.0 \times 10^{-6}$ ng cell⁻¹ (on average for strain PGS12 and I17).

Fig. 6.3a

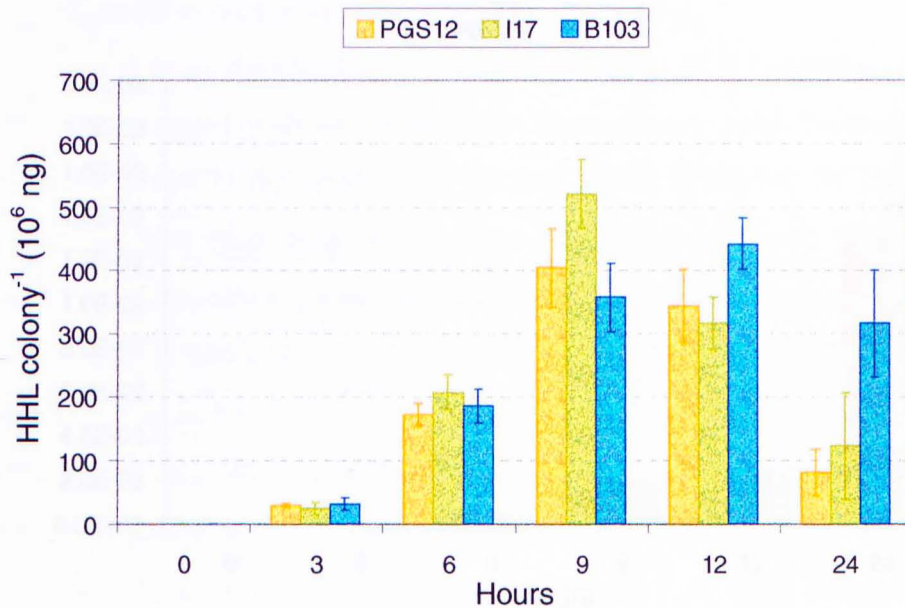


Fig. 6.3b

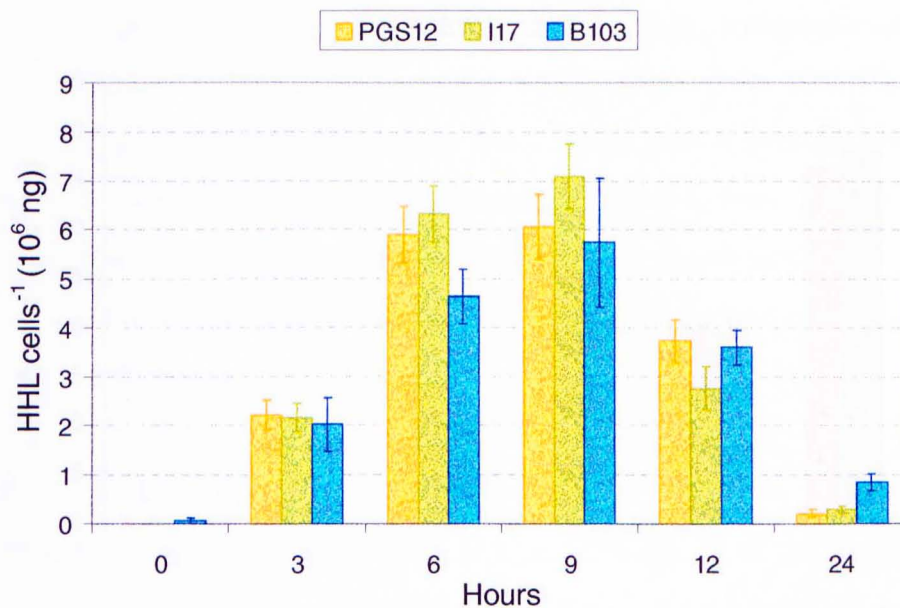


Fig. 6.3. Production of HHL per colony (Fig. 6.3a) and per cell (Fig. 6.3b) by *P. aureofaciens* PGS12, B103 and I17 on NA.

The time point t0 corresponded to a pre-incubation of 17 h. Standard errors of means shown ($n = 5$).

Fig. 6.4a

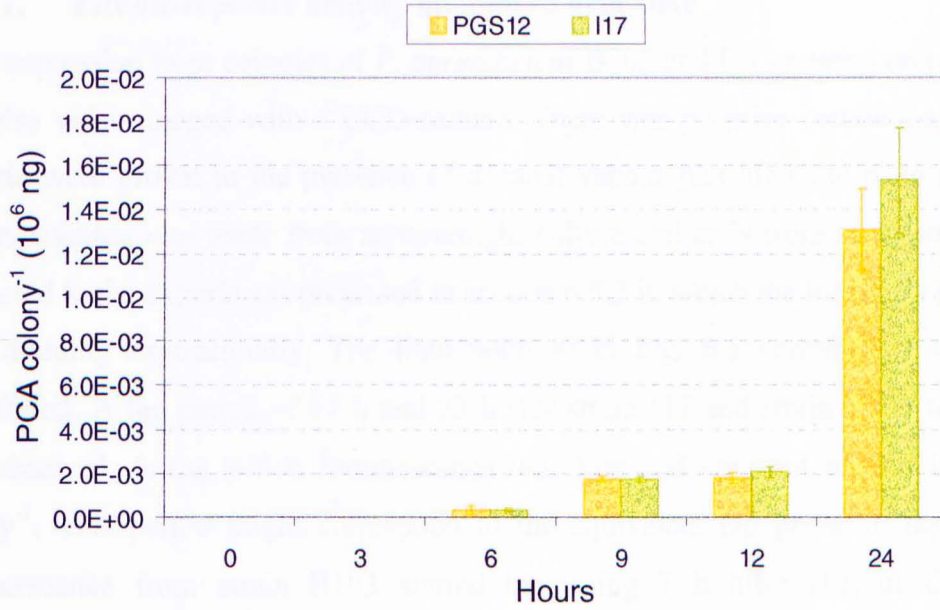


Fig. 6.4b

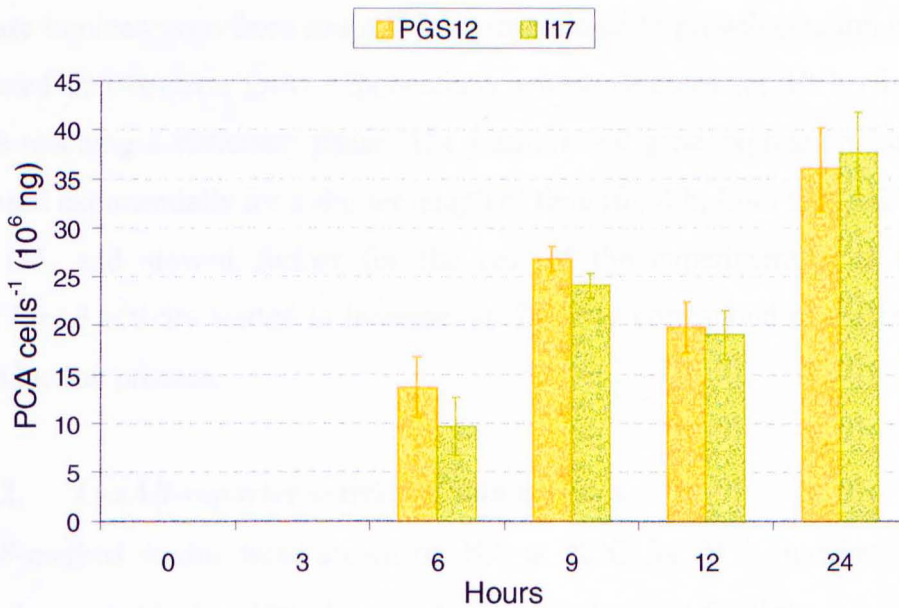


Fig. 6.4. Production of PCA per colony (Fig. 6.4a) and per cell (Fig. 6.4b) by *P. aureofaciens* PGS12 and I17 on NA.

The time point t0 corresponded to a pre-incubation of 17 h. Standard errors of means shown ($n = 5$).

6.5. LUXAB-REPORTER ACTIVITY

6.5.1. *LuxAB*-reporter activity measured using a CCD-camera

6.5.1.1. *LuxAB*-reporter activity monitored over time

Gene expression from colonies of *P. aureofaciens* B103 and I17 growing on nutrient agar was also video-imaged with a CCD-camera. There was no prior incubation period and bacteria were grown in the presence of decanal vapour just after the plate inoculation. The inoculation was made from an overnight culture and cells were in stationary phase, compared to the experiment presented in section 6.5.2 in which the inoculum consisted of cells dividing exponentially. The time point t_0 in Fig. 6.5 corresponds to the plate inoculation. A lag period of 17 h and 23 h (for strain I17 and strain B103 respectively) was observed during which luminescence was low and constant around $0.15 \text{ photon colony}^{-1}$. This period might correspond to the equivalent lag phase in liquid culture. Luminescence from strain B103 started increasing 7 h after I17, at t_{24} . At t_{26} , luminescence from both strains was not significantly different but it was at t_{27} (T-test_{0.05}). After 40 h, light output from strain B103 was 7-fold higher than from strain I17. Because luminescence from strain I17 is proportional to growth (section 6.5.2), it can be estimated that bacteria grow exponentially within colonies for 10 h (from t_{17} to t_{27}) before reaching a stationary phase. The *phzB::luxAB* gene expression from strain B103 increased exponentially for a shorter length of time (for 4 h, from t_{23} to t_{27}), then slowed until t_{35} , and slowed further for the rest of the experiment. The time at which *phzB::luxAB* activity started to increase, at t_{24} , may correspond to the beginning of the autoinduction process.

6.5.1.2. *LuxAB*-reporter activity within colonies

LuxAB-marked strains were grown on NA at 28°C for 24 h, incubated for 1 h with decanal vapour (3 μl in 100 μl mineral oil), and observed for light emission under close focus (Fig. 6.6). The light output was higher at the centre and/or between the centre and the edge of the colonies whereas the lowest light output was at the colony periphery. No difference in the pattern of luminescence between strain I17 and strain B103 could be detected at the moment the pictures were taken.

Fig. 6.5

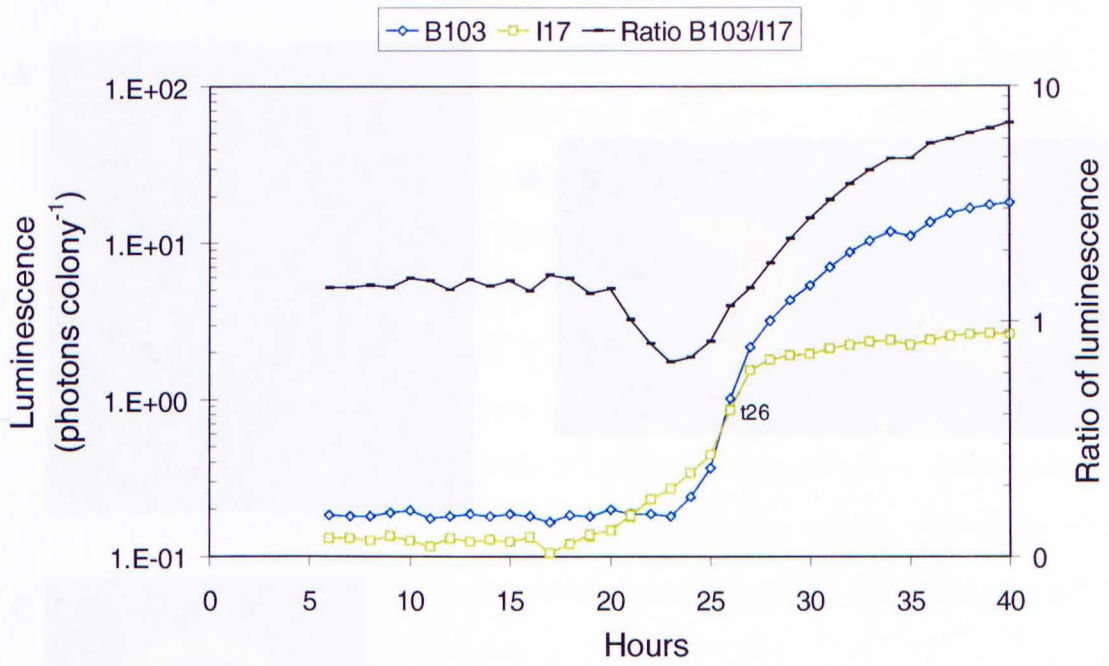


Fig. 6.5. Gene expression from *P. aureofaciens* B103 and I17 measured from video-images taken with a CCD-camera.

The time point t0 corresponded to the plate inoculation and the image analysis started at t6. Standard errors of means shown ($n = 55$).

Fig. 6.6

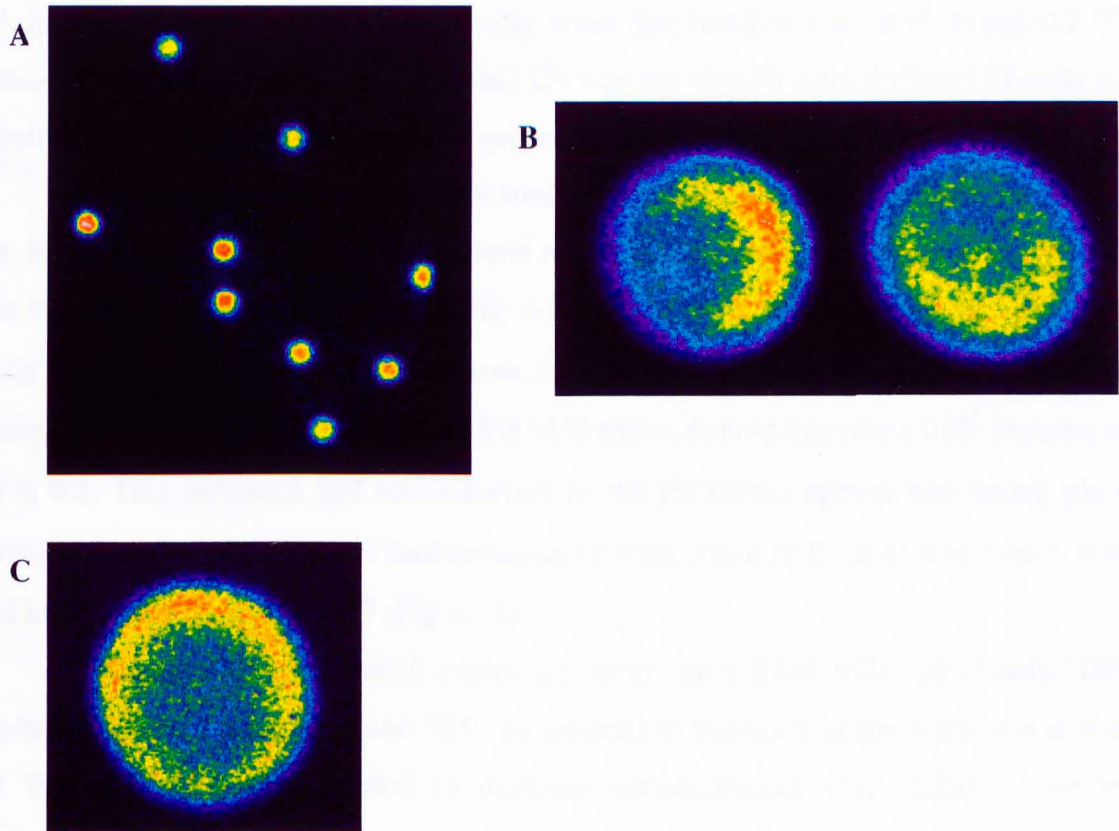


Fig. 6.6. Pictures of colonies of *P. aureofaciens* B103 and I17 expressing the *luxAB* reporter genes on NA.

A and B: Colonies of strain B103. C: Colony of strain I17. (B and C were magnified 8 times). All pictures were taken with a CCD-camera, integrated for 25 min, and image processed in Metamorph. Bacteria were grown for 24 h at 28°C and incubated with vapour of decanal prior to imaging. The gradient of intensity from the lowest levels is: purple, blue, green, yellow, orange, and red.

6.5.2. *LuxAB*-reporter activity measured with a luminometer

Bioluminescence per cell from strain I17 remained relatively constant during the experiment at an average of $54.2 \times 10^{-6} \pm 11.0 \times 10^{-6}$ RLU cell⁻¹ (Fig. 6.7a). At t0 and at t24, luminescence per cell was significantly lower than luminescence at t6, t9 and t12 (T-test_{0.05}). However, luminescence at t0 and t24 was not significantly different (T-test_{0.05}). Luminescence per colony followed the general growth pattern (Fig. 6.7a).

At t0, the light output from both strains was not significantly different (T-test_{0.05}; Fig. 6.7b). This time point may correspond to t26 in the experiment where luminescence was monitored with a CCD-camera (Fig. 6.5). Up to t9, bioluminescence per cell from strain B103 increased 21 ± 5 times whereas luminescence per cell increased 44 ± 2 times. During that time luminescence per cell from I17 showed comparatively a little increase of 1.9 ± 0.2 . This indicated that autoinduction of the phenazine operon was taking place between t0 and t9. The peak of bioluminescence from strain B103 at t9 was 5.80 ± 0.54 fold higher than from strain I17 (Fig. 6.7c).

The pattern of *phzB-luxAB* expression from strain B103 followed closely HHL production. Both light output and HHL concentration increased at the same rate during the first 9 h, and then started to decrease simultaneously (Fig. 6.8a). However, luminescence declined at a lower rate, and at t24, relative values of luminescence and HHL concentration showed a 40% difference (Fig. 6.8b). Bioluminescence cell⁻¹ and HHL accumulation cell⁻¹ were also plotted as a function of growth (Fig. 6.8c). *PhzB-luxAB* activity and HHL accumulation from strain B103 increased in parallel from $3.43 \times 10^6 \pm 1.39 \times 10^6$ to $6.64 \times 10^7 \pm 1.26 \times 10^7$ cells colony⁻¹. After this cell density, both luminescence and HHL concentration decreased, but HHL did so more rapidly.

6.6. CONCLUSIONS AND DISCUSSION

Studies of colony formation in *E. coli* or *Pseudomonas* spp. indicated that colonies expand outwards by adding new cells in a relatively narrow zone at the periphery rather than generalised expansion, and thickens by adding cells at the bottom, pushing older cells up. Thus, cell division is likely to be mainly localised at the edge of the colony throughout its morphogenesis (Shapiro, 1983; Emerson, 1999; Newman and Shapiro, 1999). Consequently, as the colony expands, a dominant proportion of cells – between

Fig. 6.7a

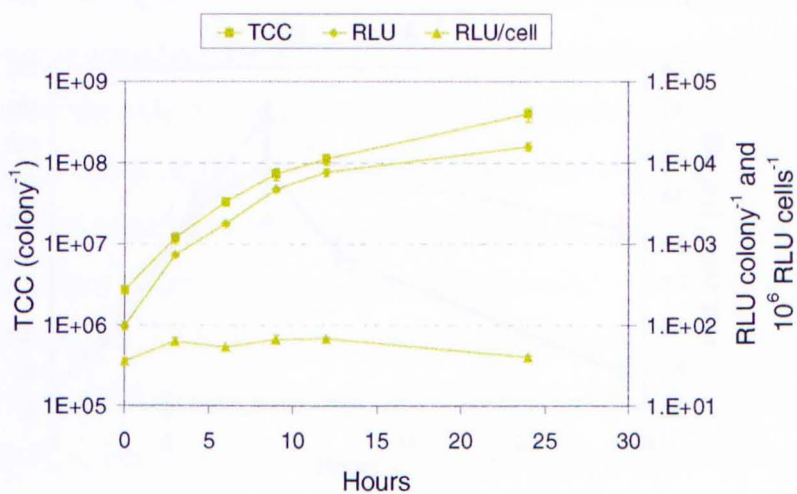


Fig. 6.7b

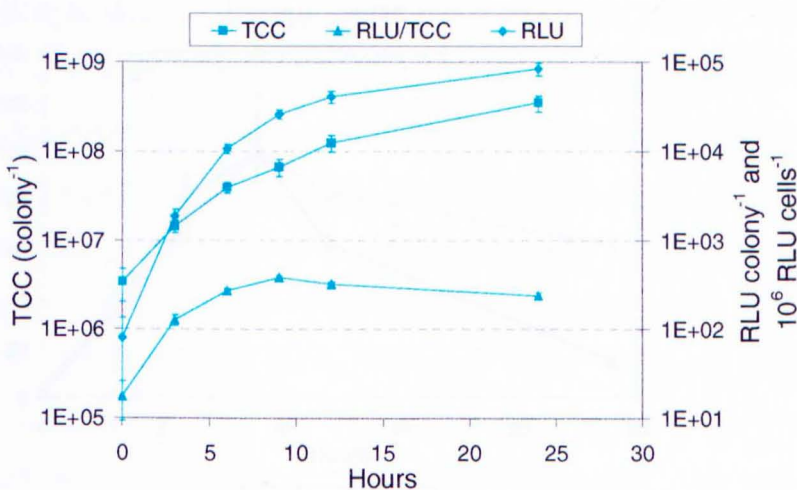


Fig. 6.7c

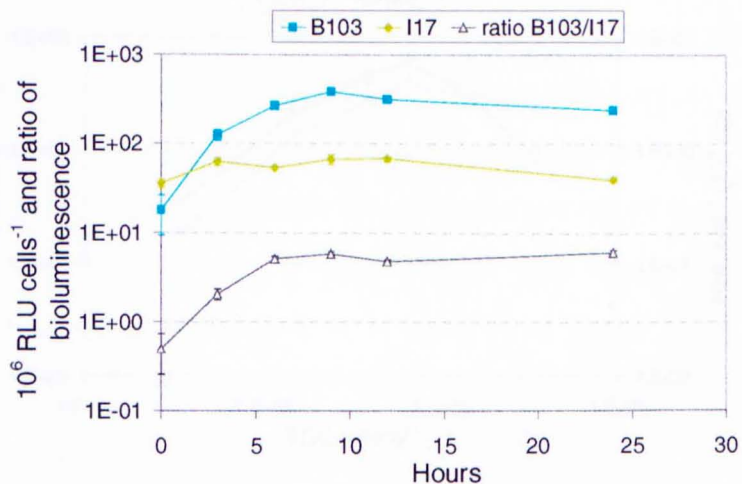


Fig. 6.7. Bioluminescence per ml and per cell from *P. aureofaciens* strain I17 (Fig. 6.7a) and strain B103 (Fig. 6.7b) in colonies growing on NA at 21°C and ratio of luminescence from strain B103 over I17 (Fig. 6.7c).

The time point t0 corresponded to a pre-incubation of 17 h. Standard errors of means shown ($n = 5$).

Fig. 6.8a

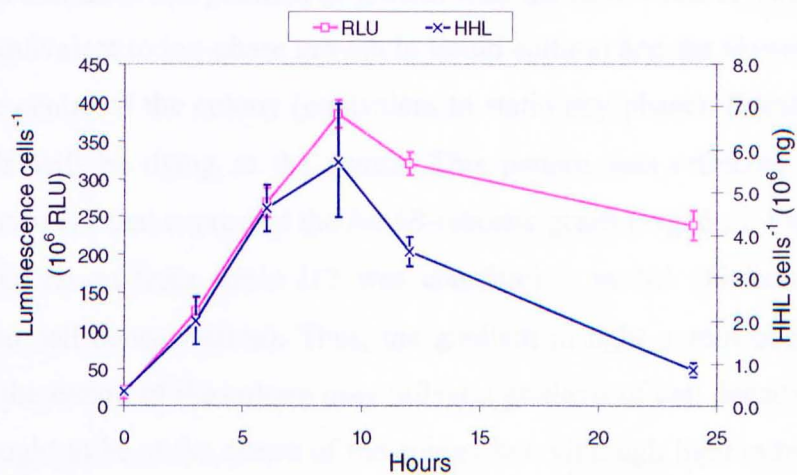


Fig. 6.8b

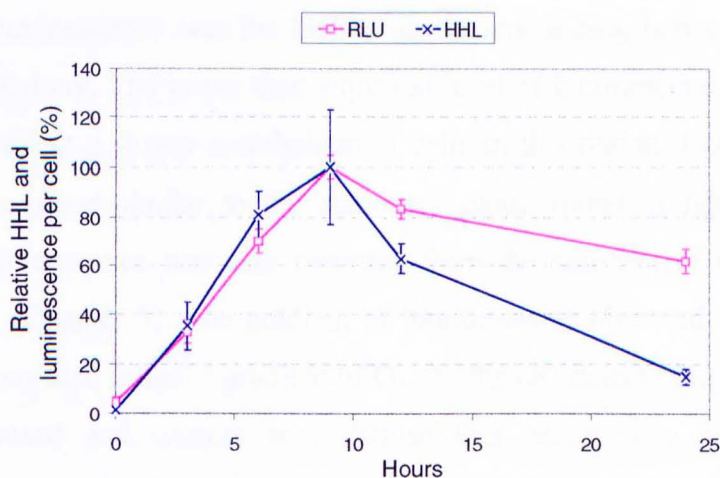


Fig. 6.8c

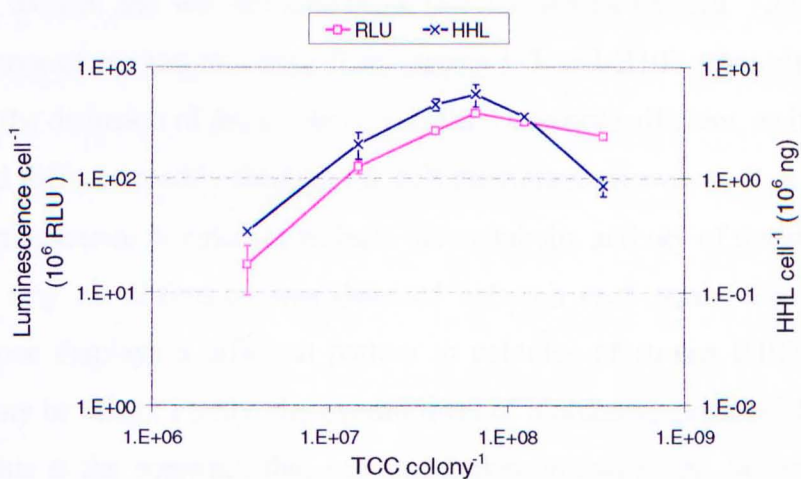


Fig. 6.8. Luminescence and HHL accumulation by *P. aureofaciens* B103 on NA per cell as a function of time (Fig. 6.8a and Fig. 6.8b with relative values) and as a function of cell density (Fig. 6.8c).

The relative values were normalised to the maximum values obtained during the experiment. The time t₀ corresponded to a 17 h pre-incubation. Standard errors of means shown ($n = 5$).

the inside edge and the centre of the colonies – are in a transition phase of growth. It is quite probable that there is a gradient of growth with the fastest cell division taking place at the edge (equivalent to log-phase growth in liquid culture) and the slowest cell division located in the centre of the colony (equivalent to stationary phase). Eventually, in older colonies, cells will be dying at the centre. This pattern was reflected in pictures of colonies of strain I17 that expressed the *luxAB*-reporter genes (Fig. 6.6). Fig. 6.7a showed that *luxAB* expression from strain I17 was constitutive on NA (bioluminescence was proportional to cell concentration). Thus, the gradient in light output observed between the edge and the centre of the colony may reflect a gradient of cell density. The highest cell density ought to be at the centre of the colony but, although light output was high in this region, luminescence was the highest in the inside ring between the edge and the centre of the colony. The lower than expected level of luminescence at the centre of the colony may reflect a slower metabolism of cells in this region. Cells are probably in a stationary-like phase similar to the stationary phase found in liquid culture where a decline in luminescence was also recorded from the constitutive strain as the growth slowed down (Chapter 5). The gradient of luminescence observed in the colonies from both strains may also reflect a gradient of O₂. As the cell density increases, layers of cells are superimposed and oxygen may diffuse less easily. The luciferase reaction is dependent on oxygen and will not take place in cells lacking oxygen. This could explain why the patterns of bioluminescence from strains I17 and B103 were similar. It is not assumed that the diffusion of the aldehyde substrate was not sufficient, as it is known that the compound diffuses readily through the cell membrane. However, it is likely that the pattern of luminescence in colonies reflects the metabolic activity of the strains and, this may explain why no difference was detected between each strain. To study whether bioluminescence displays a different pattern in colonies of strains B103 and I17, two approaches may be taken: Firstly, the overall level of bioluminescence of the colony may be studied. This is the approach that was undertaken in this study. Secondly, a ratio of bioluminescence between the level at the edge and the level within the inside ring of the colony may be calculated. This approach is further developed in the Future Work section.

The overall growth rate slowed down throughout the experiment, and this was also reflected by a continual decrease in cell diameter (Fig. 6.1a and 6.1b). Eventually, at t24, the population had a cell diameter corresponding to stationary phase-like cells (1.02

$\pm 0.002 \mu\text{m}$). This represented the mean cell size of the overall cell population within a colony. However, even if growth had slowed down at t_{24} , it had not stopped, and growth continued with the cell division probably restricted to the edge of the colony. Hence at t_{24} , the sub-population of cells dividing represented a small percentage of the overall population whereas the stationary phase-like cells represented the largest proportion, and the mean cell size of the population had a diameter corresponding to stationary phase-like cells. Between t_3 and t_{12} , the cell diameter corresponded to the cell size found in transition phase in NB. In NB, the transition phase lasted around 4 h. the generation time (g) of strain PGS12, from entry into transition phase to entry into stationary phase, was not significantly different in liquid culture and on NA (T-test_{0.05}; assuming that entry into stationary phase occurred at t_{24} on NA). The generation time was equal to 3.26 ± 0.23 h in NB (from $r_{\text{max}-1}$ to $r_{\text{max}+1}$) and 3.46 ± 0.15 h on NA (from t_3 to t_{24}). It can therefore be assumed that cells were in a transition phase of growth for at least 9 h on NA. The fastest generation time in NB was 0.56 ± 0.01 h (k_{max}) and 1.38 ± 0.06 h on agar (between t_0 and t_3). This indicated that the maximal rate of cell division either occurred before t_0 , or was generally lower on NA.

Although it is relatively easy to measure cell numbers, light output and the concentration of HHL and PCA in a unit of agar, it is more difficult to assess the actual cell density and chemical concentration within the colony. A gradient is expected to exist from the centre outwards. Using measurements of colony depth and width (section 6.3), the volume of colonies was estimated to vary between $0.2 \mu\text{l}$ (at t_0) and $5.5 \mu\text{l}$ (at t_{24}). If the volume of a colony was calibrated to 1 ml, then the cell density within this theoretical colony would vary between 1.5×10^{10} cell ml^{-1} at t_0 and 5.5×10^{10} cell ml^{-1} at t_{24} . Hence, the cell density was 55 to 75 times higher within colony than in liquid culture (comparing cell density at the entry into transition and stationary phase; Table 1).

The maximal concentration of HHL (HHL_{max}) produced by strain PGS12 (average from 3 cultures grown simultaneously at 3 different inoculum concentrations) was $32 \times 10^6 \pm 24 \times 10^6$ ng cell⁻¹ in NB. On NA, HHL_{max} reached $6.07 \times 10^6 \pm 0.65 \times 10^6$ ng cell⁻¹ at t_9 . Hence, there was 5.3 times more HHL produced per cell in broth than in colonies (values significantly different; T-test_{0.05}), but the standard deviation associated with these values

Table 6.1. Comparison of values obtained in NB and on NA.

	NB	NA	Difference NA/NB
Cell density⁽¹⁾	2×10 ⁸ to 1×10 ⁹ ml ⁻¹ 4×10 ⁴ in 0.2 µl to 5.5×10 ⁶ in 5.5 µl	3×10 ⁶ to 3×10 ⁸ colony ⁻¹ 1.5×10 ¹⁰ to 5.5×10 ¹⁰ ml ⁻¹	75 to 55 times more cells
[HHL] at induction⁽²⁾	0.63×10 ⁻⁶ ± 0.3×10 ⁻⁶ ng cell ⁻¹ 210 ± 176 ng ml ⁻¹ 0.16 ± 0.05 ng in 0.2 µl	0.34×10 ⁻⁶ ng cell ⁻¹ 2 ng colony ⁻¹⁽²⁾ 10×10 ³ ng ml ⁻¹	<i>a priori</i> not significant 50 times more HHL on NA
Maximal HHL concentration⁽³⁾	32×10 ⁻⁶ ± 24×10 ⁻⁶ ng cell ⁻¹ 3×10 ³ ± 2×10 ³ ng ml ⁻¹ 6.75 ± 5.09 ng per 2.25 µl	6.07×10 ⁻⁶ ± 0.65×10 ⁻⁶ ng cell ⁻¹ 404 ± 68 ng colony ⁻¹ 17.9×10 ⁴ ± 31×10 ³ ng ml ⁻¹	5.3 times more HHL on NA; significantly different (T-test _{0.05}) 60 time more HHL on NA
Maximal luminescence per cell⁽³⁾	476×10 ⁻⁶ ± 330×10 ⁻⁶ RLU cell ⁻¹ 2.1×10 ⁵ ± 8.5×10 ⁴ RLU ml ⁻¹ 525 ± 240 RLU per 2.25 µl	491×10 ⁻⁶ ± 209×10 ⁻⁶ RLU cell ⁻¹ 3.27×10 ⁴ ± 6.5×10 ³ RLU colony ⁻¹ 14.5×10 ⁶ ± 2.9×10 ⁶ RLU ml ⁻¹	Not significantly different (T-test _{0.05}) 63 times light output on NA
PCA concentration⁽⁴⁾	5.3×10 ⁻⁶ ± 1.4×10 ⁻⁶ ng cell ⁻¹ 7.1×10 ³ ± 1.4×10 ³ ng ml ⁻¹ 35 ± 7 ng per 5.5 µl	36×10 ⁻⁶ ± 5.5×10 ⁻⁶ ng cell ⁻¹ 1.26×10 ⁴ ± 2.14×10 ³ ng colony ⁻¹ 2.2×10 ⁶ ± 3.9×10 ⁶ ng ml ⁻¹	6.8 times more PCA on NA; significantly different (T-test _{0.05}) 360-fold more PCA

¹ The values were taken in NB and on NA from entry into transition phase to entry into stationary phase. These time points corresponded to $r_{\max-1}$ and $r_{\max+1}$ in NB and to t_0 and t_{24} on NA.

² The time of induction of the phenazine operon was defined as the moment from which the activity of the *phzB::luxAB* reporter increased. In colonies this moment was estimated to occur 2 h before t_0 . The comparisons were made here from the values obtained at t_0 on NA. These values are therefore likely to be overestimated (and the comparison stands as a maximal value). At t_0 , HHL could only be detected in one colony of the strain B103.

³ The maximal HHL concentration and bioluminescence level occurred at r_{\max} in liquid culture and at t_9 on NA.

⁴ PCA concentration was measured at the entry in stationary phase which was estimated to occur at t_9 on NA and at t_{13} in NB.

was high. The estimated colony volume at t_9 was $2.5 \mu\text{l}$ and HHL_{max} reached $3000 \pm 2000 \text{ ng ml}^{-1}$ in NB. This was equivalent to $6.75 \pm 5.09 \text{ ng}$ in $2.25 \mu\text{l}$. On NA, HHL accumulated to $404 \pm 68 \text{ ng colony}^{-1}$. This means that for an equivalent volume, there was 60 times more HHL in colonies than in liquid culture. The average cell density at t_9 in NA was ca. 50 times higher than the average cell density at r_{max} in NB. Therefore, the difference in HHL concentration on each medium, when considering equivalent volume, may be due mainly to an increase in cell density in colonies.

The maximal *phzB::luxAB* activity per cell was not significantly different (T-test_{0.05}) when taking into account the values obtained from 3 growth curves in NB ($476 \times 10^{-6} \pm 330 \times 10^{-6} \text{ RLU cell}^{-1}$) and from two replicate experiments on NA ($491 \times 10^{-6} \pm 209 \times 10^{-6} \text{ RLU cell}^{-1}$). In liquid culture, the maximum luciferase activity per ml was $2.1 \times 10^5 \pm 8.5 \times 10^4 \text{ RLU}$ and, on NA bioluminescence reached $3.27 \times 10^4 \pm 6.5 \times 10^3 \text{ RLU}$ per colony with a volume of $2.5 \mu\text{l}$ (at t_9). Hence bioluminescence in NB in the equivalent $2.5 \mu\text{l}$ would be $525 \pm 240 \text{ RLU}$. This result represented a 63-fold increase in transcriptional activity in colonies when compared to NB. The cell density in the colony was ca. 50 times higher than in broth. Therefore, the difference in the level of bioluminescence on each medium, when considering equivalent volumes, was possibly mainly due to a higher cell density in colonies.

PCA production from *P. aureofaciens* PGS12 was compared between NB and NA. Growth was stationary after 13 h in NB and after 24 h on NA, and the cell diameter was not significantly different between both media (T-test_{0.05}) ($1.01 \pm 0.023 \mu\text{m}$ in NB and 1.02 ± 0.003 on NA). Therefore, growth may be considered at early stationary phase at these time points and they were chosen to compare PCA production from each medium. PCA accumulation per cell after 24 h on NA reached a maximum of $36 \times 10^{-6} \pm 5.5 \times 10^{-6} \text{ ng cell}^{-1}$ and $5.3 \times 10^{-6} \pm 1.4 \times 10^{-6} \text{ ng cell}^{-1}$ in NB after 13 h of growth. Hence, PCA production per cell on NA was 6.8 times higher than in broth (difference significant, T-test_{0.05}). Such levels of PCA accumulation were never found in NB, even after 96 h of incubation. The colony volume at t_{24} was estimated to be around $5.5 \mu\text{l}$. Accumulation of PCA reached a maximum of $7100 \pm 1400 \text{ ng ml}^{-1}$ in NB, equivalent to $39 \pm 7.7 \text{ ng}$ in $5.5 \mu\text{l}$ and, per colony, PCA reached $1.26 \times 10^4 \pm 2.14 \times 10^3 \text{ ng}$. For an equivalent volume,

PCA was 360 more concentrated in colony than in broth. At these time points, the cell density was approximately 55 times higher in colonies than in broth. Therefore, the higher PCA concentration in colonies cannot be explained solely on the basis of an increase in cell density in colonies. The higher production per cell could be the result of another feature observed in colony: The presence of HHL within a colony, and per cell, for a prolonged period of time compared to the burst seen in NB. The presence of an autoinducer per cell for a longer period of time may have sustained larger production and accumulation of PCA in colonies. Unlike the sharp decline of HHL after maximal expression in NB, HHL was detected at a constant and maximal level for at least 3 h. Similarly the transcriptional activity of the phenazine operon, as reflected by *phzB::luxAB* expression in strain B103, remained maximal during this time. Overall the transition phase of growth in colonies was longer than in NB. This resulted in a uniform production of HHL and phenazine for a long period of colony development. This form of regulated synthesis of HHL and phenazine gives any individual colony the appearance of a constitutive system for the production of these compounds. The efficient synthesis of PCA in a colony may represent the normal pattern of expression of these chemicals in cells growing attached to a surface in the environment. Because PCA is a stable antifungal compound, a prolonged production of PCA might be followed by an increase PCA concentration in the vicinity where it is produced.

The beginning of the induction of transcription of the phenazine operon was difficult to estimate. Because light from strain I17 was proportional to cell concentration, the ratio of bioluminescence per colony from strain B103 over the bioluminescence per colony from strain I17 should not be very different from the ratio of bioluminescence from strain B103 over the cell concentration per colony. Therefore, an increase in the ratio of bioluminescence from strain B103 over bioluminescence from strain I17 ought to represent an increase in transcriptional activity of the phenazine operon. If the increase took place after this ratio was linear or decreasing, then the increase could reflect the beginning of the induction of transcription of the phenazine operon. In the experiment run with a CCD-camera, the ratio of luminescence started to increase at t24 (Fig. 6.5). At t26, the light output from both strains was not significantly different ($T\text{-test}_{0.05}$); The light output from strain B103 was equal to 1.0 ± 0.04 photon colony⁻¹ second⁻¹ and light output

from strain I17 was equal to 0.87 ± 0.15 photon colony⁻¹ second⁻¹. In the experiment where bioluminescence was measured with a luminometer, light output from both strains was not significantly different at t₀. It is probable, therefore, that the induction of the phenazine operon in this experiment started 2 h earlier, at t-2. If this was the case, it would not be possible to estimate the minimal HHL concentration needed for induction of the phenazine operon using the *luxR*-bioassay, as at t₀, HHL was already at the limit of detection. At t₀, HHL was detected in only one colony (of strain B103) at the concentration of 0.34×10^{-6} ng cell⁻¹. At the moment of induction in NB, HHL concentration was at $0.63 \times 10^{-6} \pm 0.3 \times 10^{-6}$ ng cell⁻¹. These values may not be significantly different but the value obtained on NA may be overestimated (It was not possible to analyse statistically the difference as only one value was available for the experiment on NA). The volume of the colonies at t₀ was estimated around 0.2 µl and there was 2 ng of HHL detected in one colony. HHL accumulation in NB was at 210 ± 176 ng ml⁻¹ or 0.04 ± 0.03 in 0.2 µl. Hence, for the same volume, HHL at the moment of induction might have been up to 50 times more concentrated on NA than in NB.

HHL is a short chain acyl compound and is thought to diffuse freely from cells to cells as does OHHL (Kaplan and Greenberg, 1985). Therefore, the threshold HHL concentration for induction of the phenazine operon represents the 1/K_m value for the formation of the PhzR-HHL complex. This value should remain the same per cell whatever the medium. Although the exact value of HHL was not obtained at the time of induction, it is hypothesised that the leading parameter for HHL concentration within colonies will be the concentration per cell. In this model, samples with higher cell concentration need a higher HHL concentration per volume in order to sustain the internal concentration of autoinducer needed for induction of the operon. Moreover, if the signal molecule were to diffuse from colonies, then even more HHL would need to be produced. In this study, HHL concentration per cell might not have been different on NA and in NB showing that diffusion of the autoinducer from colonies was not necessarily significant.

Researchers have shown that the recovery of ammonia-oxidising bacteria from ammonia starvation in biofilms is significantly enhanced (i.e., the lag phase is significantly decreased) by the addition of 3-oxo-C6-HSL (Bachelor *et al.*, 1997). They

speculated that the higher cell densities achieved in a biofilm might result in a greater concentration of AHL, which in turn may induce the expression of genes whose products promote a more rapid recovery from ammonia starvation. In our model, higher HHL concentration per cell was not achieved although it was calculated that HHL concentration in an equivalent calibrated volume was significantly higher in colonies than in NB. The calculated increase in HHL concentration at induction of transcription of the phenazine operon, at the maximal HHL concentration, and maximal bioluminescence in NA compare to NB corresponded to the increase calculated in cell density in NA. It is, therefore, possible that the higher values in colony may be mainly due to an increase in cell density. Table 6.1 summarises all these comparisons. The production of HHL and the transcriptional activity remained maximal for a longer period of time compared to liquid culture, and this led to an increased production of phenazine by 360-fold in colonies compared to broth. Therefore, it seems that in colonies phenazine production was higher than from planktonic cells because the cells remained in a transition phase of growth for a longer period of time. This resulted in a prolonged presence of the unstable HHL in colonies and the synthesis of a larger amount of the antibiotic PCA.

6.7. FUTURE WORK

1. The ratio of bioluminescence within colonies between the edge and the inside ring may be calculated. For this, colonies need to be observed with a microscope (10 time enlargement) attached to a CCD-camera (this support was not available for this study). In strain I17, this ratio would give a measurement of the difference in cell concentration between the edge and inside ring of a colony. In strain B103, the ratio would give a measurement of the *phzB::luxAB* activity as well as the measurement of difference in cell density. By comparing both ratios, a measurement of *phzB::luxAB* activity would be obtained.
2. The same strains could be grown with different concentration of carbon. The percentage of carbon in the agar medium is proportional to cell density. Cells would be grown in a minimum medium which would allow for PCA and HHL production and the variation in carbon concentration would result in a controlled variation of cell density.

CHAPTER SEVEN

**TRANSCRIPTIONAL ACTIVITY OF THE
PHENAZINE OPERON STUDIED
WITH *LUXAB*-REPORTERS
ON BEAN ROOTS AND WHEAT SEEDLINGS**

CHAPTER SEVEN

TRANSCRIPTIONAL ACTIVITY OF THE PHENAZINE OPERON STUDIED WITH *LUXAB*-REPORTERS ON BEAN ROOTS AND WHEAT SEEDLINGS

7.1. INTRODUCTION

To provide effective biocontrol, rhizosphere bacteria need to be present on roots at the right place (down to the root tip), at the right time (before the pathogen has caused extensive damage), and in sufficient numbers (Bull *et al.*, 1991; Haas *et al.*, 2000). Populations of introduced fluorescent pseudomonads associated with root systems are usually log-normally distributed along the roots, with the population highest near the seed and declining toward the root tip (Bull *et al.*, 1991; Loper, J.E. *et al.*, 1984; Weller, 1984). Typically, colonisation of roots by introduced pseudomonads is quite variable from plant to plant within an experiment (Weller, 1988). The size of the bacterial population is directly related to the size of the inoculum applied to the seed, hence, one approach to increasing root colonisation is to increase the dose of the bacteria applied to the seed. However, increasing root colonisation by increasing the initial dose of bacteria on the seed has limitations. In wheat, populations of introduced fluorescent pseudomonads above a certain concentration (approximately 10^9 per seed) sometimes were phytotoxic (Weller, 1988). Bull *et al.* (1991) demonstrated that there was an inverse linear relationship between the dose of *P. fluorescens* 2-79 on the seed and the number of lesions caused by *Gaeumannomyces graminis* var. *tritici* (Ggt) on the entire root system. This relation was not true with Phz⁻ mutant, showing that the amount of phenazine produced was involved in disease inhibition. Foster *et al.* (1975) studied by SEM the ultra-structure of the root-soil interface and showed that bacteria growing on roots form discrete microcolonies that occupy preferentially grooves between cell walls. Roots are embedded in a mucigel (consisting mainly of pectins and hemicelluloses) itself enclosed in a fine cuticle. The gel on roots grown in nutrient solutions or on agar has a uniform texture of granules or fine fibrils or both. By contrast, in field-grown plants, the gel may

be multi-lamellate, with layers that stain densely (Foster *et al.*, 1975). Bacteria produce exoenzymes such as pectinases and hemicellulases that lyse troughs through the mucilage. In roots infected by some pathogens such as the take-all fungus, the root surface bacteria proliferate because pathogens make the plant cell membranes leaky and on such lesions the mucilage is destroyed and metabolised by bacteria (Foster *et al.*, 1975). In suppressive soils, pseudomonads colonise fungal hyphae and may cause holes about 1 μm in diameter in the fungal cell wall. The hyphae collapse, lyse, and eventually may be completely destroyed (Foster *et al.*, 1975). PCA can be detected directly on plant roots (Thomashow *et al.*, 1990), however PCA detection involves a laborious extraction method and multiple replications of many samples. Gene fusion offers a simpler and faster experimental approach, especially *in situ*. Wood *et al.* (1997), using a *phzI* 'phzB::inaZ' reporter strain that expressed the ice nucleation protein only in the presence of exogenous AHL signals, showed that HHL is involved *in situ* on wheat roots in the expression of the *phzFABCD* operon from *P. aureofaciens* 30-84.

The work presented in this chapter is the first attempt to study the dynamics of expression of the phenazine operon throughout the first days of seedlings colonisation by *P. aureofaciens*. The expression of the phenazine operon was studied in relation to population density on plant roots beans and wheat seedlings. For this, *P. aureofaciens* PGS12, and the isogenic strains B103 and I17, were inoculated onto wheat or bean seedlings. The inoculated bean roots and entire wheat seedlings were monitored by measuring cell counts and density, phenazine production, HHL production, and luciferase activity by strains B103 and I17. The *luxAB* reporter system was chosen because it allows detection of very low levels of gene expression and real time monitoring without extraction of cells from the samples. The system also provides the ability to localise the activity of specific organisms using CCD imaging techniques. Furthermore, other studies have demonstrated that direct measurement of luminescence from a constitutive reporter from non-amended environmental samples provides a measure of the *in situ* metabolic activity of the marked organism (Prosser, 1994).

7.2. AIMS

1. Determine if the marked strains were impeded in root colonisation compared to the wild-type strain.

2. Study the dynamics (level, rate, and timing) of the transcription of the phenazine operon by strain B103 on 2 different plant roots (wheat and bean seedlings).
3. Compare the dynamics of phenazine gene expression with the constitutive expression of luciferase by strain I17 in order to gain information on the overall metabolic activity of the strains during the experiments.
4. Monitor HHL and phenazine on plant roots

7.3. COLONISATION AND LUCIFERASE ACTIVITY ON BEAN SEEDLINGS

The experiment was repeated twice (experiment 1 and 2) and data from both experiments were analysed, and are presented and discussed in this chapter.

7.3.1. Colonisation of bean roots

7.3.1.1. Total cell counts and density

In Expt. 1, the bacterial inoculum on plant roots (average for all strains) was at $1.45 \times 10^9 \pm 4.2 \times 10^8$ cells root⁻¹ and at $3.12 \times 10^7 \pm 8.9 \times 10^6$ cells root⁻¹ in Expt. 2 (Fig. 7.1). The bacterial density reached $1.36 \times 10^8 \pm 2.7 \times 10^7$ cell per mg of dry root at the end of expt. 1 and $2.10 \times 10^7 \pm 1.26 \times 10^6$ at the end of Expt. 2. In both experiments, the cell number (on average for all strains) increased significantly by 12.3 ± 8.6 (in Expt. 1) and by 17 ± 2.8 (in Expt. 2) throughout the 9 days of the experiments. However, in Expt. 1, the density did not increase significantly (T-test_{0.05}) but it did increase significantly in Expt. 2 (by 3.5 ± 1.4).

7.3.1.2. Colonisation as seen with a CCD-camera

Bioluminescence from bacteria on the root surface was examined to detect which part of the roots was being colonised preferentially. It was not possible to distinguish any difference in the pattern of root colonisation between strains B103 and I17. The pictures in Fig. 7.2 refer to strain B103 but similar pictures were obtained with strain I17. During the first days, bioluminescence was present on the whole seedling showing that it was entirely colonised by the strains. Bioluminescence was especially high, on young seedlings up to 3 days, on the young cotyledons and on the root, and less on the shoot

Fig. 7.1a

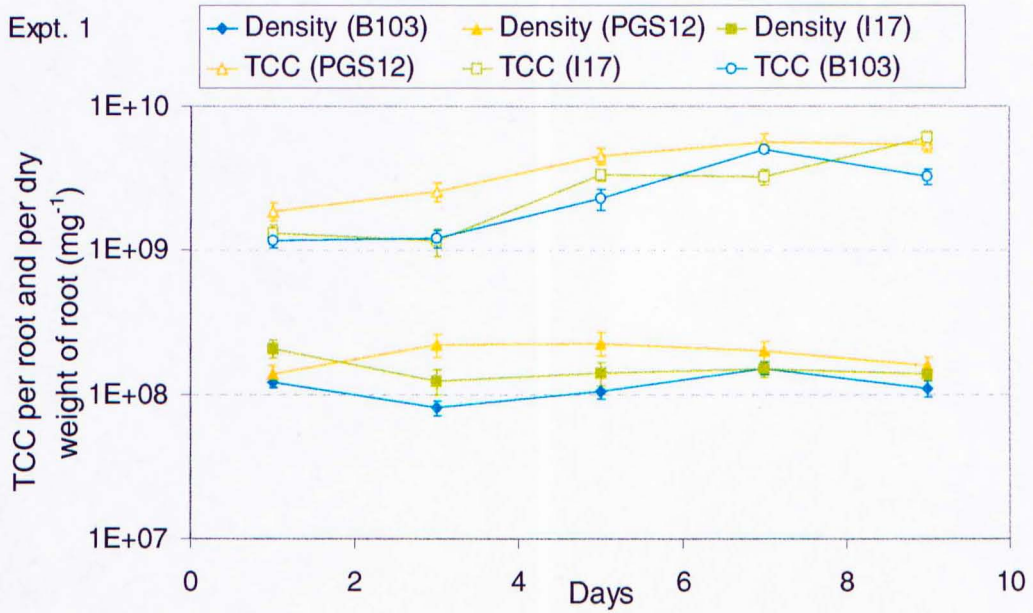


Fig. 7.1b

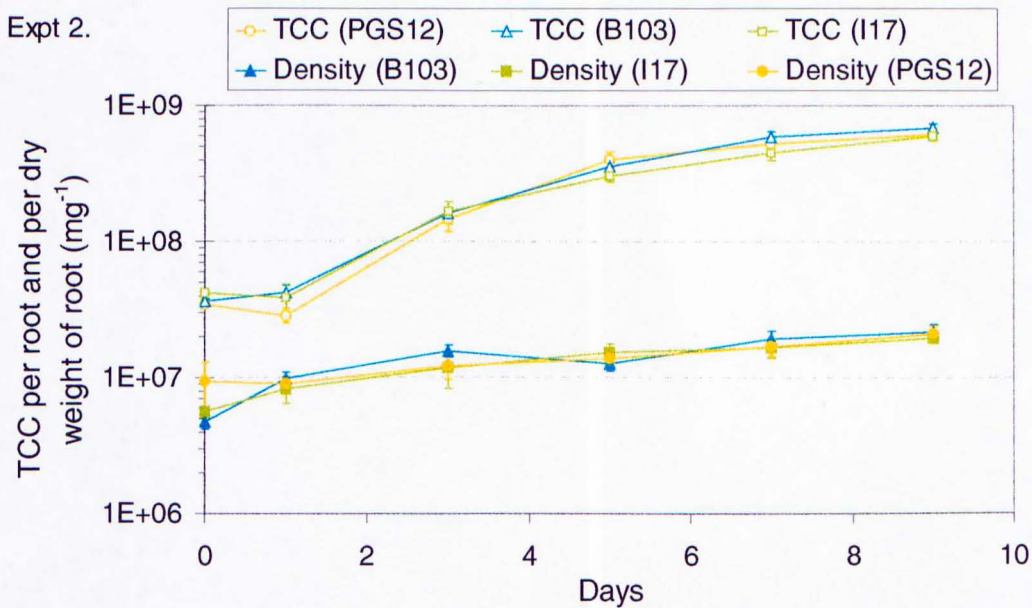


Fig. 7.1. Colonisation of bean roots in sterile vermiculite by *P. aureofaciens* strains PGS12, B103 and I17.

The total cell counts (TCC) were measured per unit of 1 ml. The density was obtained by dividing the cell counts per the dry weight of roots. Expt.1 and Expt. 2 correspond to 2 independent repeats. Standard error of means shown ($n = 9$ for each experiment).

Fig. 7.2a

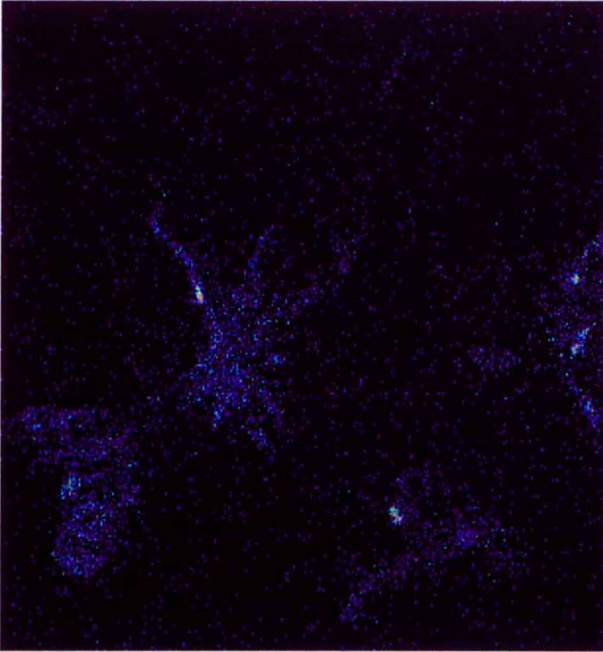


Fig. 7.2aref

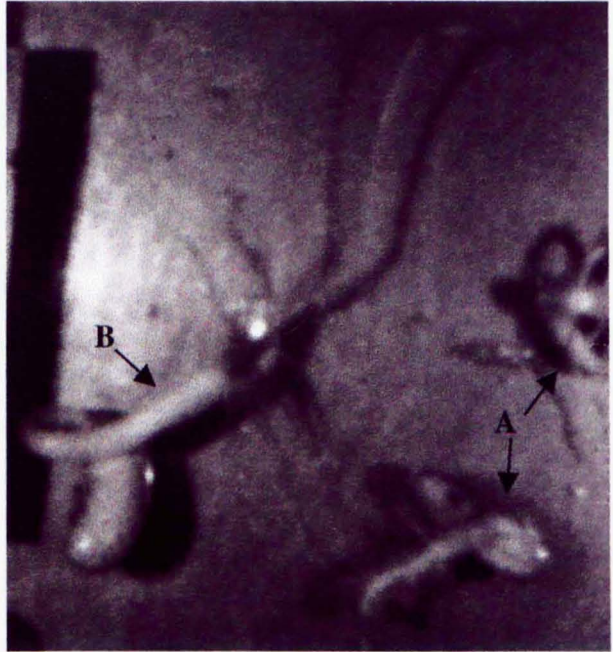


Fig. 7.2b

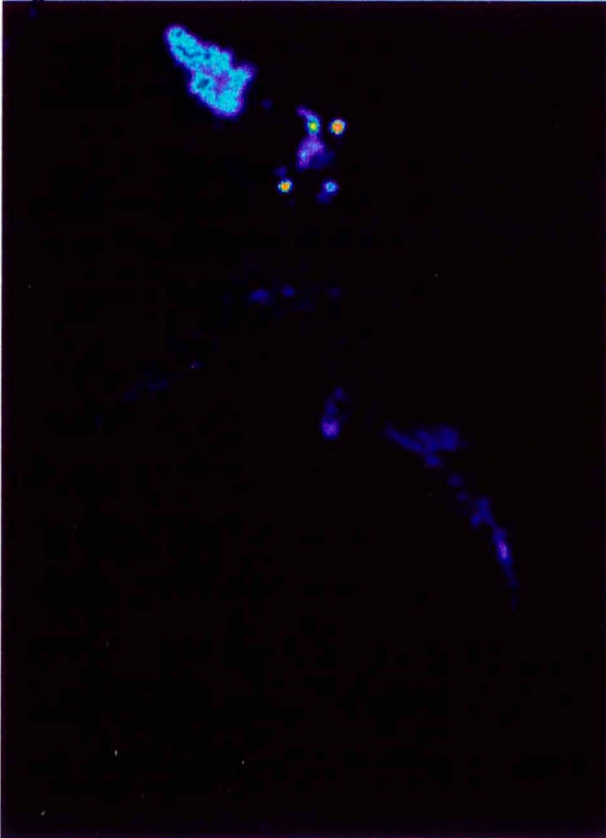


Fig. 7.2bref

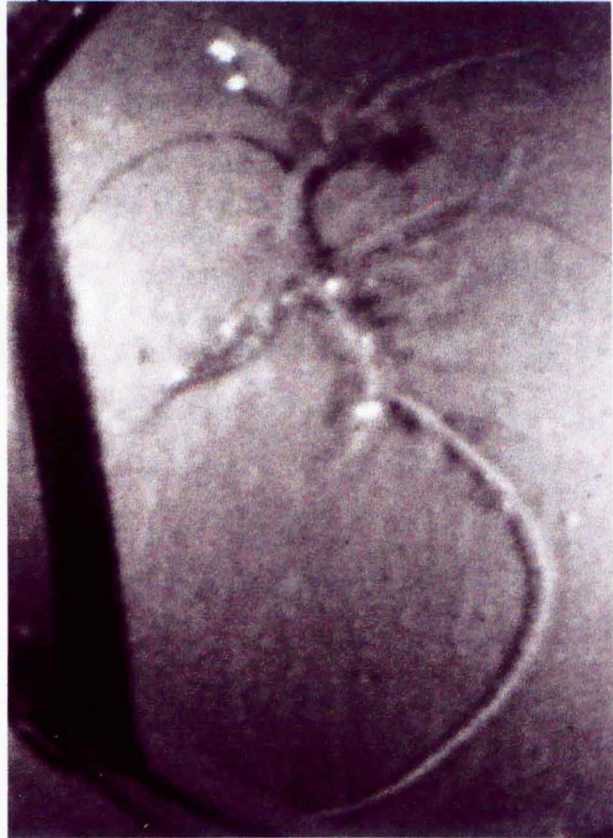


Fig. 7.2c

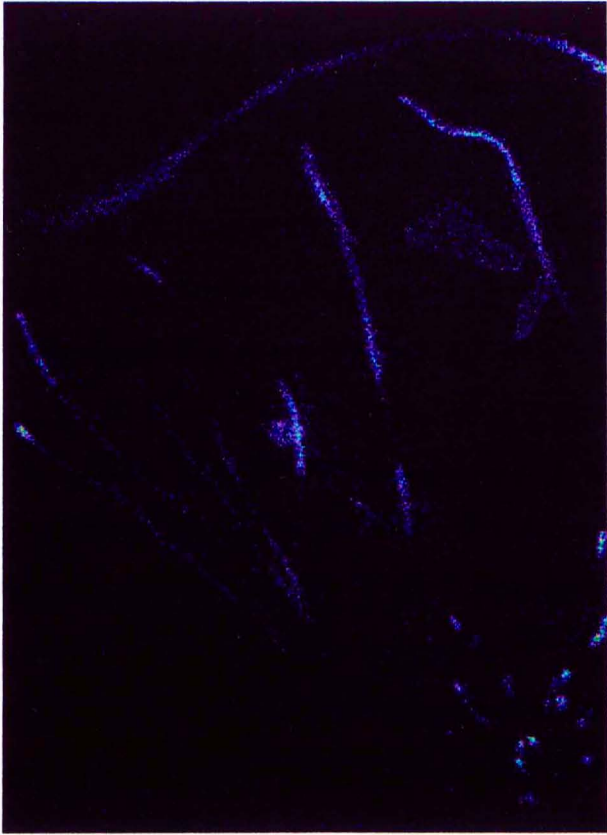


Fig. 7.2c**ref**



Fig. 7.2. Colonisation of bean roots by strain B103 carrying a *phzB::luxAB* gene fusion taken with a CCD-camera after 24 h (A) and 3 days (B) (Fig. 7.2a, Fig. 7.2a**ref**), after 5 days (Fig. 7.2b, 7.2b**ref**), and after 9 days (Fig. 7.2c, 7.2c**ref**).

Bean roots were grown from surface inoculated seedlings under sterile conditions in vermiculite. Aldehyde was added and seedlings or excised roots were viewed by (Fig. 7.2a**ref**, 7.2b**ref**, 7.2c**ref**) bright-field illumination or by CCD dark-field exposure for 25 min (Fig. 7.2a, 7.2b, 7.2c).

(Fig. 7.2a). As the plant grew older and the cotyledons shrunk and eventually fell (after 5-6 days), luciferase activity was found mainly on the crown of the plant (where a large number of roots emerged) and on the roots (Fig. 7.2b, 7.2c). The whole root system was otherwise uniformly colonised and bioluminescence was not found preferentially on the root tips.

7.3.2. Luciferase activity and cell diameter on bean roots

7.3.2.1. Luciferase activity per TCC

A peak of activity of the *phzB::luxAB* marker from strain B103 was recorded at day 3 (15.5 ± 1.95 RLU TCC⁻¹) in Expt. 1 (Fig. 7.3a) and at day 1 (38.6 ± 9.05 RLU TCC⁻¹) in Expt. 2 (Fig. 7.3b). Bioluminescence from strain B103 remained higher than from strain I17 until day 3 in each experiment. The ratio of bioluminescence from strain B103 over strain I17, between day 0 and day 3 from both experiments, averaged 1.18 ± 0.93 . The maximum value of the ratio was recorded at day 0 in Expt. 2 (5.35 ± 2.97) and at day 3 in Expt. 1 (1.8 ± 0.5 ; Fig. 7.3c). At day 0, light from both strains was low, on average around 0.8 ± 0.6 RLU cell⁻¹. During the first 24 h (Expt. 2), bioluminescence from strain B103 increased 68 ± 27.5 times and from strain I17 increased 87.7 ± 13.9 and the difference in the increase between the 2 strains was not significantly different (T-test_{0.05}). Between day 1 and day 3 (Expt. 1), bioluminescence from strain B103 increased 455 ± 56 times, and from strain I17 it increased 33 ± 3.4 times (significant difference between the 2 strains; T-test_{0.05}).

After this, bioluminescence from strain B103 decreased first dramatically (up to day 5) and then decreased more slowly in Expt. 1 or remained constant in Expt. 2. At day 9 in Expt. 2, light output from strain B103 was not significantly different (T-test_{0.05}) from day 0. In Expt. 1, the difference was significant but the light output at day 1 was very low (0.04 ± 0.006 RLU TCC ml⁻¹ in average). After day 1 and day 3, light output from I17 decreased slowly apart from between day 7 and day 9 where it decreased sharply in Expt. 1. In each experiment, the level of luminescence from strain B103 became lower than the level from strain I17 between day 3 and day 4.

Fig. 7.3a

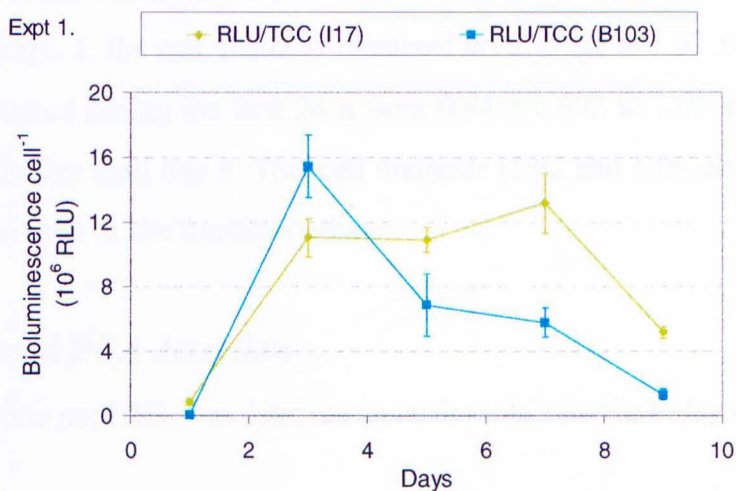


Fig. 7.3b

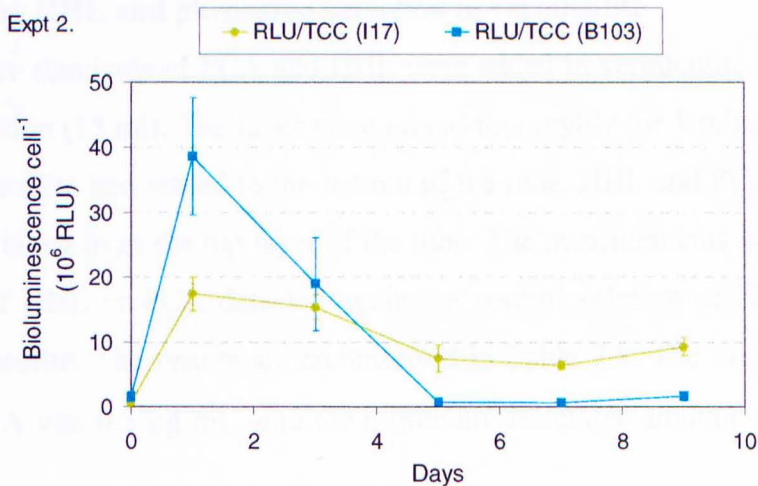


Fig. 7.3c

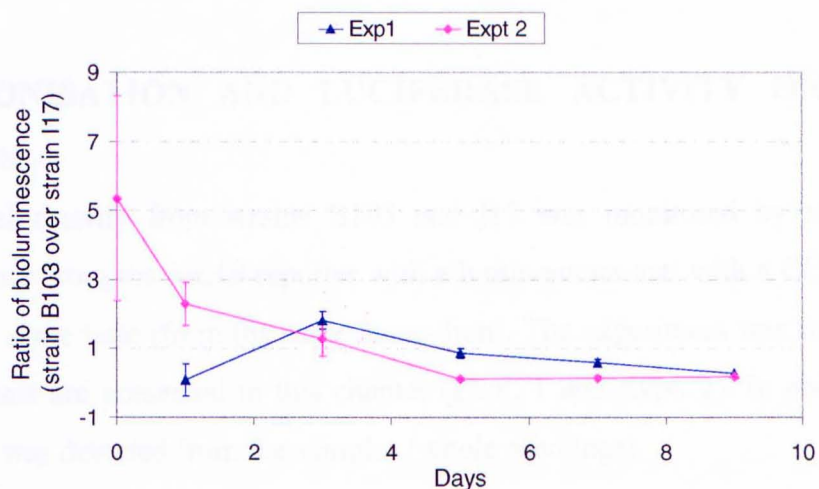


Fig. 7.3. *LuxAB*-reporter activity from *P. aureofaciens* strains B103 and I17 on bean roots and ratio of bioluminescence from strain B103 over the average value of bioluminescence from strain I17 (Fig. 7.3c).

Standard error of means shown ($n = 9$ for each experiment).

7.3.2.2. Cell diameter

There was not much variation in cell diameter during the 9-day experiments (Fig. 7.4a, Fig. 7.4b). In Expt. 1, the cell diameter remained on average at $1.02 \pm 0.009 \mu\text{m}$, and in Expt. 2, it increased during the first 24 h from 0.94 ± 0.002 to $1.06 \pm 0.004 \mu\text{m}$, and it remained at this size until day 9. This cell diameter (1.02 and $1.06 \mu\text{m}$) corresponded in liquid culture to cells in late transition phase.

7.3.3. HHL and PCA detection

Neither phenazine nor HHL was detected on bean roots over the 9-day experiments.

7.3.3.1. Testing HHL and phenazine detection in vermiculite

A range of pure standards of PCA and HHL were added to vermiculite (3 g) mixed with Hoagland solution (15 ml). The tubes were mixed thoroughly for 1 min, and left to stand until the vermiculite had settled to the bottom of the tube. HHL and PCA were measured from samples taken from the top layer of the tube. The measurements were calculated as percentages of HHL or PCA detected against a control solution of Hoagland solution without vermiculite. The results are summarised in Table 7.1. The minimum detectable amount of PCA was $0.5 \mu\text{g ml}^{-1}$ and the minimum detectable amount of HHL was $0.05 \mu\text{g ml}^{-1}$.

7.4. COLONISATION AND LUCIFERASE ACTIVITY ON WHEAT SEEDLINGS

Transcriptional activity from strains B103 and I17 was monitored by recording the bioluminescence from the *luxAB* reporter with a luminometer and with a CCD-camera in parallel at the same time (from the same inoculum). The experiment was repeated twice and both repeats are presented in this chapter (Expt. 1 and Expt. 2). In each repeat, no PCA or HHL was detected from the samples (whole seedlings).

Fig. 7.4a

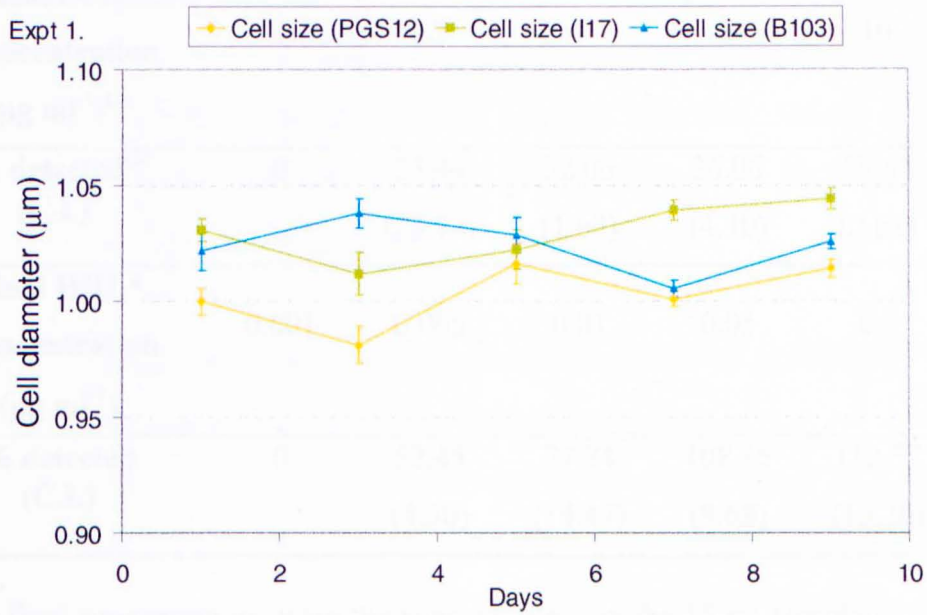


Fig. 7.4b

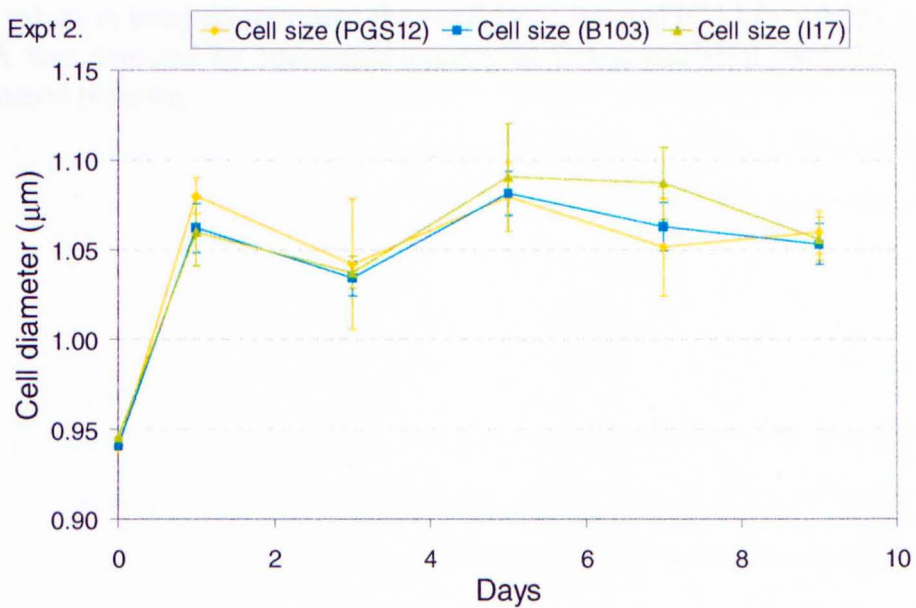


Fig. 7.4. Average cell diameter of *P. aureofaciens* strains PGS12, B103, and I17 colonising sterile bean roots over 9 days.

The measurements were obtained with a CellFacts Instrument. Standard error of means shown ($n = 9$ for each experiment).

Table 7.1. Detection of PCA and HHL in Hoagland solution mixed with vermiculite.

Final PCA*						
Concentration	0.1	0.5	1	5	10	50
($\mu\text{g ml}^{-1}$)⁽¹⁾						
% detected⁽²⁾	0	35.44	32.06	36.06	58.86	51.98
(C.I.)³		(22.92)	(1.62)	(4.30)	(2.62)	(1.33)
Final HHL*						
Concentration	0.001	0.005	0.01	0.05	0.1	
($\mu\text{g ml}^{-1}$)						
% detected	0	52.45	77.74	108.35	112.57	
(C.I.)		(4.30)	(14.47)	(9.68)	(15.36)	

¹ The final concentrations were the concentrations in the 15 ml Hoagland solution (with or without vermiculite).

² The percentages were calculated against what was detected in Hoagland solution without vermiculite (100% values).

³ The values in brackets represent the confidence interval (C.I.) ($p = 0.05$).

* PCA was detected by spectrophotometry at OD₃₆₉ and HHL was detected using the *luxR*-based bioassay.

7.4.1. Colonisation of wheat seedlings

7.4.1.1. Total cell counts

In both experiments, bacterial growth was observed on wheat seedlings. Cell numbers increased by 4.2 ± 0.9 fold (Expt. 1) and by 8.4 ± 0.09 (Expt. 2) in average for all 3 strains over the 72-h experiment. Cell numbers increased linearly throughout the experiment from ca. 2×10^7 cells seedling⁻¹ (at day 0) to 8×10^7 (Expt. 1; Fig. 7.5a) and 1×10^8 (Expt. 2; Fig. 7.5b) cells seedling⁻¹.

7.4.2. Luciferase activity and cell diameter on wheat seedlings

7.4.2.1. Luciferase activity measured with a luminometer

Before bacterial inoculation of the seedlings, bacteria were grown in 1/5 NB for 18 h which resulted in low gene expression for both strains. However, on wheat seedlings luminescence from both strains decreased further and reached at t72 $1.28 \pm 0.17 \times 10^{-6}$ RLU cell⁻¹ for strain B103 (average from both repeats) and for strain I17, $0.45 \pm 0.06 \times 10^{-6}$ RLU cell⁻¹ in Expt. 1 (Fig. 7.6a) and 4.34 ± 1.19 RLU cell⁻¹ in Expt. 2 (Fig. 7.6b). During both experiments, bioluminescence per cell from strains B103 and I17 decreased similarly except in Expt. 2 where bioluminescence per ml and per cell from strain I17 increased significantly after 24 h. Bioluminescence from strain B103 during the first 24 h was twice the level from strain I17 as indicated by the ratio of bioluminescence (Fig. 7.7a).

7.4.2.2. Cell diameter

Throughout Expt. 2, the bacterial cell diameter, on average for strains B103 and I17, decreased from 1.004 ± 0.003 μm to 0.94 ± 0.001 (Fig. 7.7b). The former diameter was the size of the cells in the inoculum whereas the latter diameter corresponded in liquid culture to cells in stationary phase for 48 h or more.

7.4.2.3. Bioluminescence measured with a CCD-camera

Gene expression from strain B103 and I17 growing on wheat seedling was also video-imaged with a CCD-camera and the experiment was repeated twice (Fig. 7.8). Overall, bioluminescence from both strains decreased throughout each experiment.

Fig. 7.5a

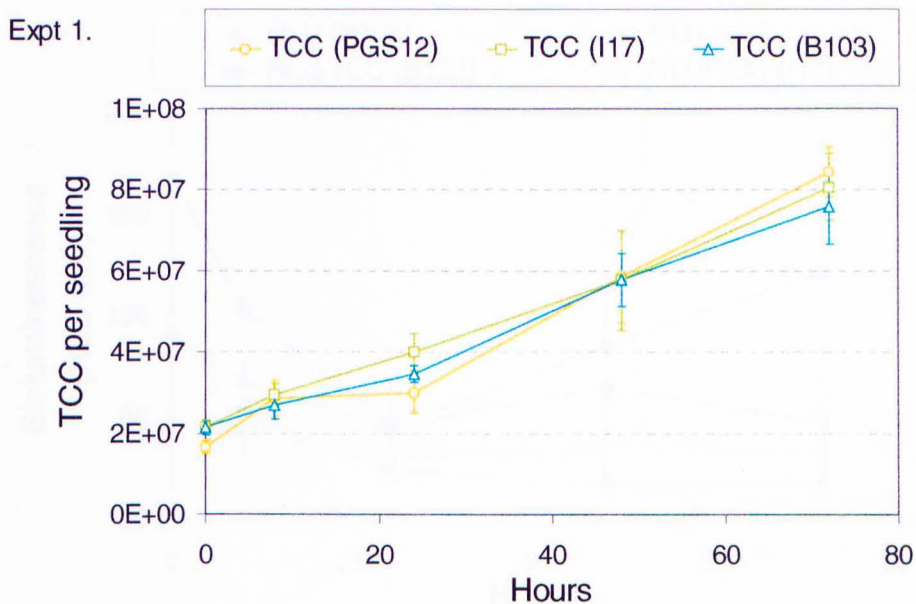


Fig. 7.5b

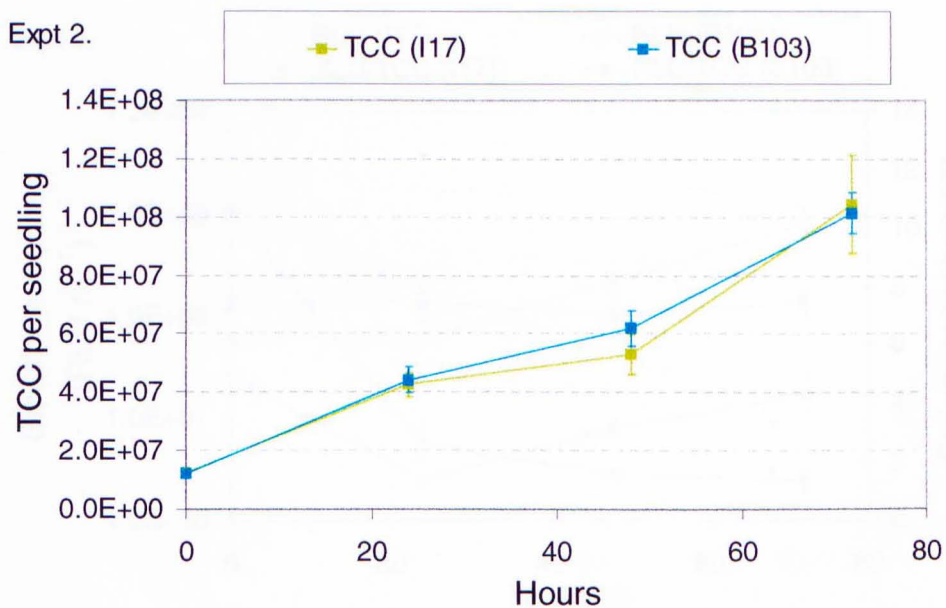


Fig. 7.5. Colonisation of wheat seedlings by *P. aureofaciens* strain B103, I17, and PGS12.

Experiment 1 and 2 correspond to 2 repeats. The cell numbers were obtained with a CellFacts instrument. Standard error of means shown ($n = 9$ for each experiment).

Fig. 7.6a

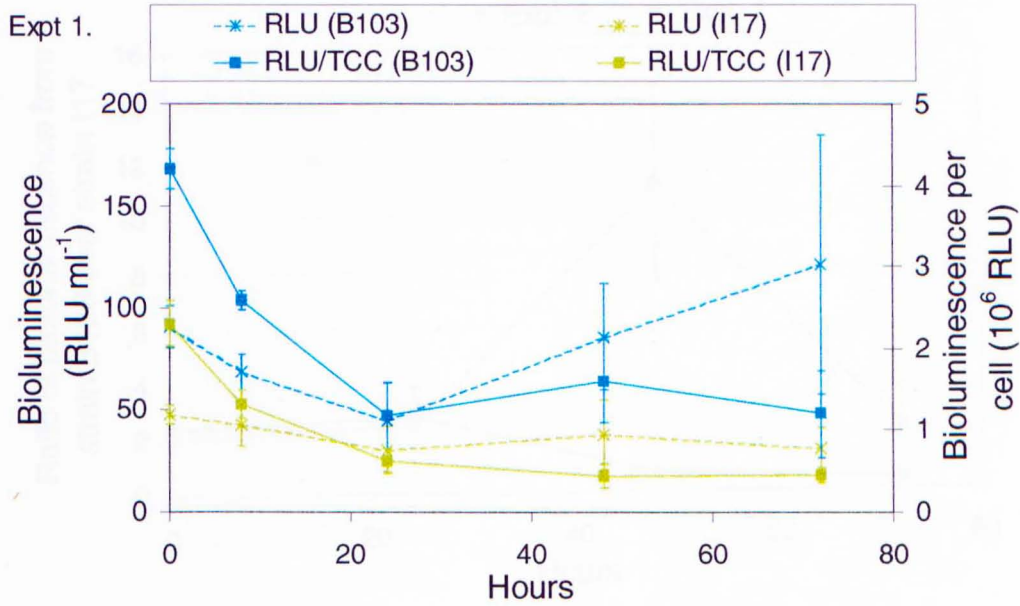


Fig. 7.6b

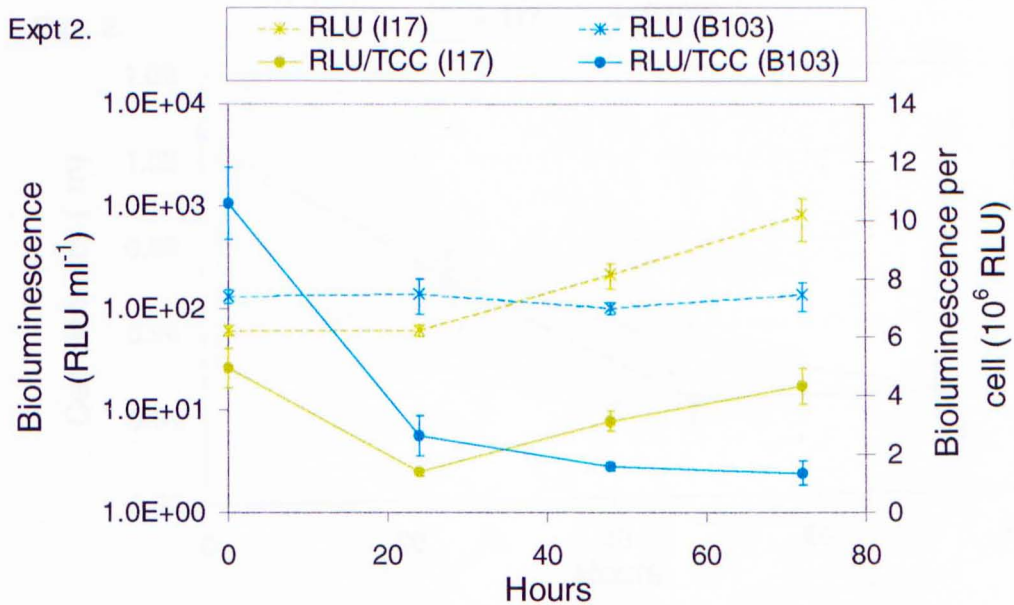


Fig. 7.6. Bioluminescence from *P. aureofaciens* strains B103 and I17 on wheat seedlings.

Standard error of means shown ($n = 9$ for each experiment).

Fig. 7.7a

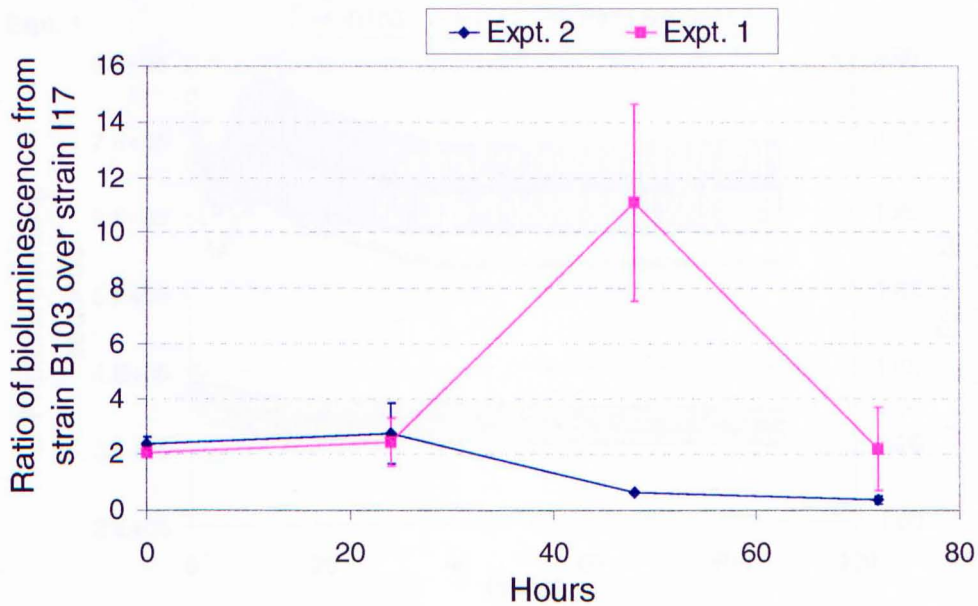


Fig. 7.7b

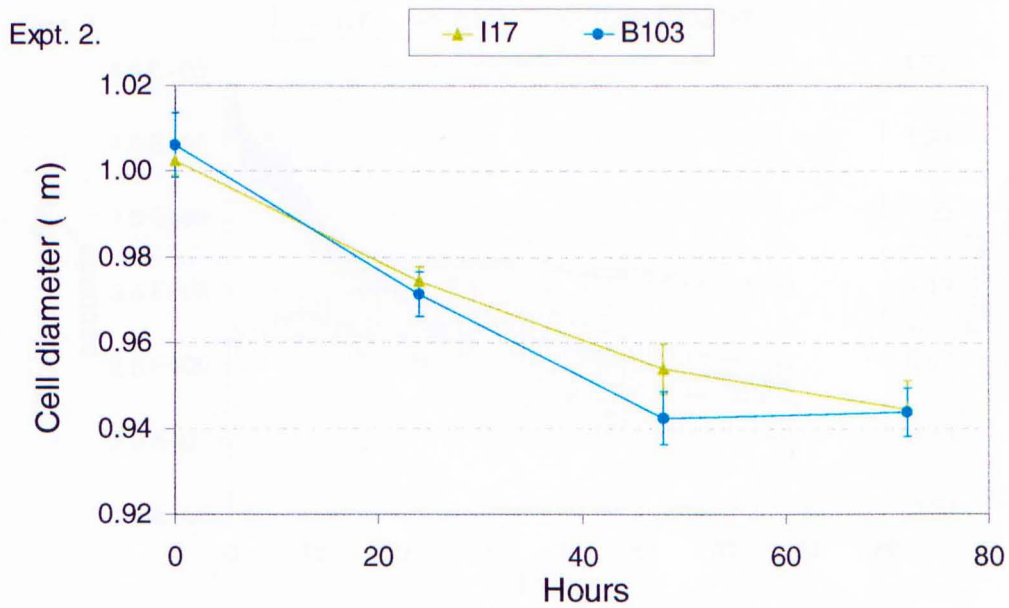


Fig. 7.7. Ratio of bioluminescence (Fig. 7.7a) from *P. aureofaciens* strain B103 over the average bioluminescence level from strain I17 and cell diameter (Fig. 7.7b) on wheat seedlings.

The cell size measurements were obtained with a CellFacts instrument. Standard error of means shown ($n = 9$ for each experiment).

Fig. 7.8a

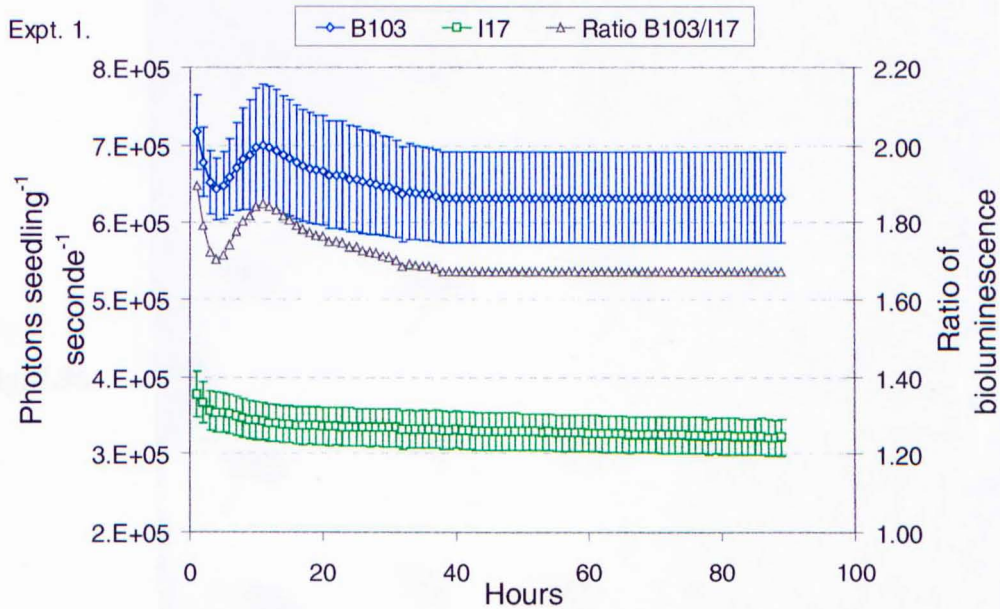


Fig. 7.8b

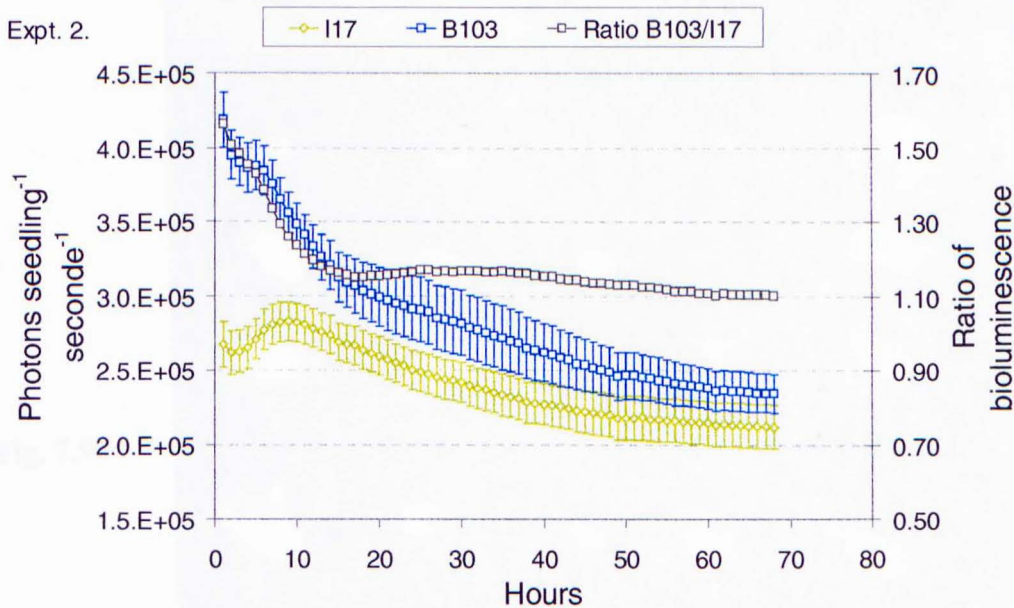


Fig. 7.8. *luxAB*-reporter activity from *P. aureofaciens* B103 and I17 on wheat seedlings video-imaged with a CCD-camera.

The ratio of bioluminescence was obtained by dividing all the data from strain B103 by the averaged light output from strain I17. Experiment 1 and 2 correspond to 2 repeats. Standard error of means shown ($n = 8$ in Expt. 1, and $n = 15$ in Expt. 2).

Fig. 7.9a



Fig. 7.9b

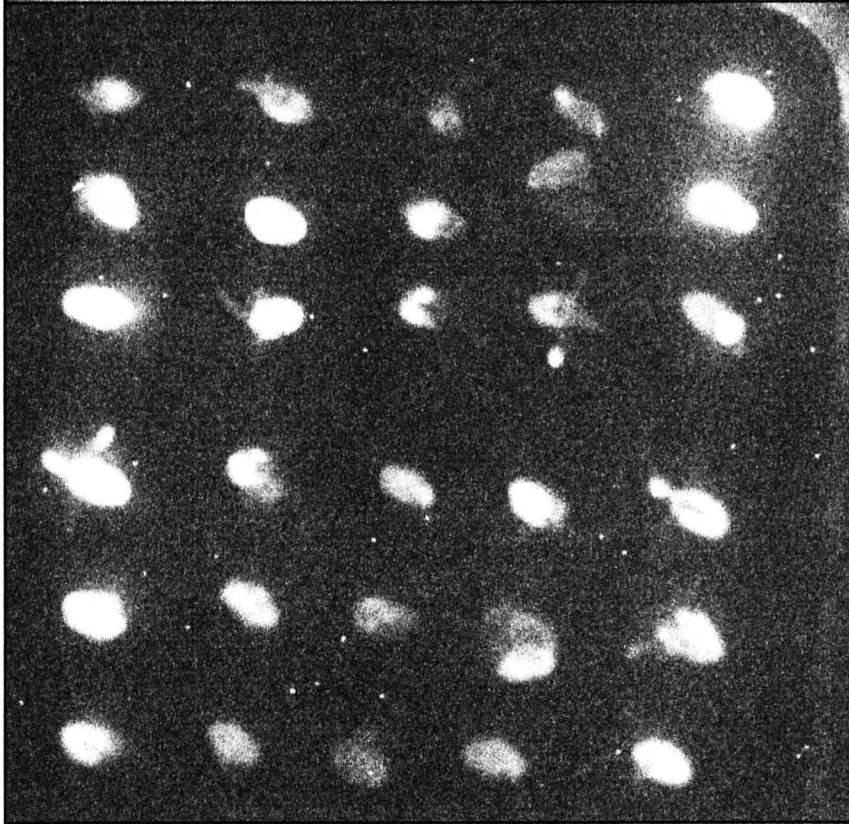


Fig. 7.9c

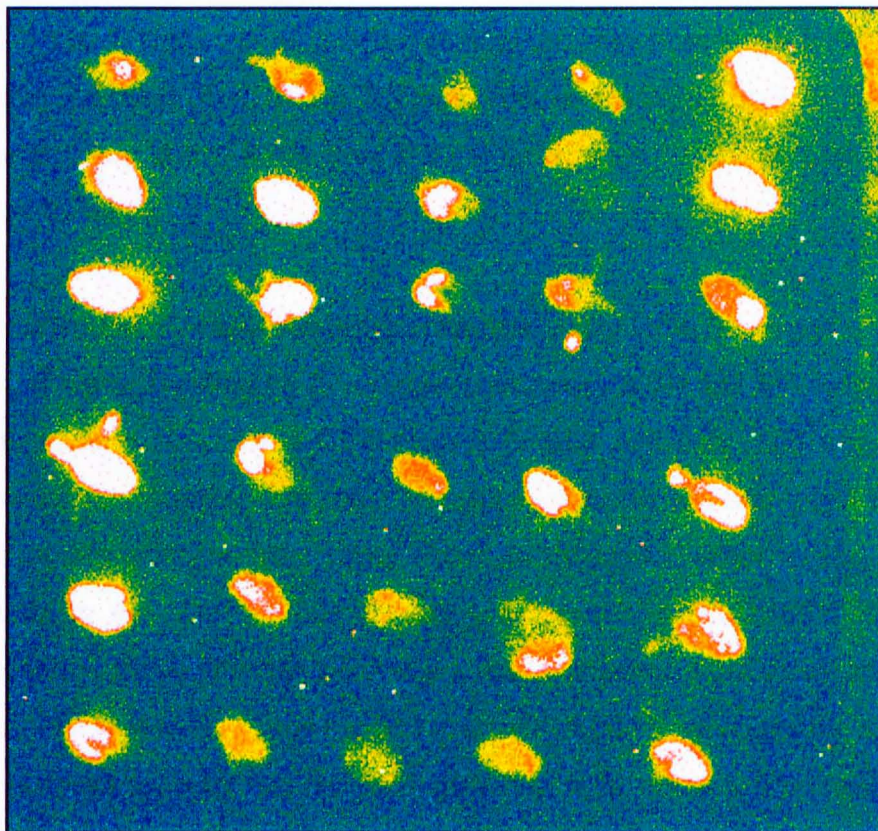


Fig. 7.9. Wheat seedlings after 68 h of colonisation by *P. aureofaciens* strain B103 (top 15 seedlings) and strain I17 (bottom 15 seedlings) as seen by a CCD-camera.

Fig. 7.9a is the reference picture (bright-field imaging). Bioluminescence (dark-field imaging) is represented in black and white (Fig. 7.9b) and in a grade of colour where white represents the highest intensity (Fig 7.9c). The level of bioluminescence from these pictures is plotted in Fig. 7.8b and corresponds to the time point 68.

Luminescence from I17 decreased by 15.0% in Expt. 1 and by 20.8% in Expt. 2 (between the end and the beginning of the experiment). The decrease in bioluminescence from B103 was more variable; bioluminescence decreased by 11.8% in Expt. 1 and by 44.1% in Expt. 2. In Expt. 1, there was an increase in luminescence from strain B103 after 12 h whereas bioluminescence from strain I17 increased momentarily at 9 h. The ratio of bioluminescence from strain B103 over I17 varied between 1.10 and 1.90 in average during both experiments.

7.4.2.4. Colonisation of wheat seedlings visualised using a CCD-camera

Colonisation of wheat seedling by *P. aureofaciens* strains B103 and I17 is illustrated in Fig. 7.9 with pictures taken by a CCD-camera (bright- and dark-field imaging). The moment at which the pictures were taken corresponded to the last time point in Expt. 2. Three major points emerged from them. First, no difference either in the pattern of colonisation or in the level of bioluminescence between strain B103 and I17 was detected. Secondly, for each strain there was a large variation in bioluminescence; from some seedlings there was very little luciferase activity while from others the light output was sufficient to be reflected on the petri dish (top right corner). The seed coat was always covered with bacteria and the maximal activity was at each extremity of the seed but especially where the roots and the first shoot emerged. The third point noted was that of the first 3 seminal roots, the number of roots coated with bacteria was variable.

7.5. COMPARISON OF BIOLUMINESCENCE FROM CELLS GROWING IN LIQUID CULTURE, COLONIES, ON BEAN ROOTS, AND ON WHEAT SEEDLINGS

The maximal and minimal values of bioluminescence from strain B103, the average level of bioluminescence from strain I17, and the ratio of bioluminescence obtained on laboratory growth media and plant roots are given in Table 7.2. These values are averages from multiple experiments, however, because measurements were discrete, higher values could have occurred between the chosen time points. The levels of bioluminescence from planktonic cells and from cells in colonies from strain B103 were the highest and were not significantly different ($T\text{-test}_{0.05}$). These values were approximately 12.5 times higher than the maximum values obtained on bean roots and 47 times the maximum values

Table 7.2. Bioluminescence per cell from strains B103 and I17 on laboratory media and on plant roots.

Bioluminescence (RLU cell⁻¹ ± CI⁽¹⁾)	In NB⁽²⁾	In colonies on NA⁽³⁾	On bean roots⁽⁴⁾	On wheat seedlings⁽⁵⁾
Minimum level from strain B103	2.99×10 ^{-6†} ± 0.20×10 ⁻⁶	17.7×10 ^{-6†} ± 16.5×10 ⁻⁶	0.6×10 ^{-6¶} ± 0.4×10 ⁻⁶	1.37×10 ^{-6†¶} ± 0.82×10 ⁻⁶
Maximum level from strain B103	476×10 ⁻⁶ ± 330×10 ^{-6*}	491×10 ⁻⁶ ± 209×10 ^{-6*}	39×10 ⁻⁶ ± 18×10 ⁻⁶	10.57×10 ⁻⁶ ± 2.43×10 ⁻⁶
Average level from strain I17	14.5×10 ^{-6‡} ± 2.0×10 ⁻⁶	54.2×10 ⁻⁶ ± 11.0×10 ⁻⁶	9.5×10 ^{-6§‡} ± 4.9×10 ⁻⁶	3.45×10 ^{-6§} ± 1.54×10 ⁻⁶
Ratio (strain B103 over strain I17)	0.2 ⁽⁶⁾ to 55 ⁽⁷⁾	0.33 to 7.10	0.06 to 4.11	0.40 to 3.06

¹ Confidence intervals ($p = 0.05$).

² Average values from 3 growth cultures started with 3 different inoculum concentrations

³ Average values from 2 repeated experiments

⁴ Average values from experiment 2 where the highest values of bioluminescence were recorded

⁵ Average values from experiment 2 where the highest values of bioluminescence were recorded

^{6, 7} Respectively, the ratio of the minimal level and maximal level of bioluminescence from strain B103 over the average level from strain I17.

* † ¶ § ‡ Values not significantly different from one another (T-test_{0.05}).

obtained on wheat seedlings. All minimum values of bioluminescence grouped within a close range and many were not significantly different from each other (T-test_{0.05}). The highest level of bioluminescence from strain I17 was recorded on NA and it represented 3.8 times the level found in NB. The levels in NB and on bean roots, and the levels on bean roots and on wheat seedlings, were two by two not significantly different (Table 7.2; T-test_{0.05}). The largest difference between the lower and higher ratio of bioluminescence from strain B103 over strain I17 was found in NB. The ratio of the maximal values obtained from NA and plant roots were similar.

7.6. CONCLUSIONS AND DISCUSSION

In contrast to laboratory culture studies, all experiments monitoring *P. aureofaciens* PGS12 on roots failed to detect HHL and PCA. This can not be explained by the inability of cells to colonise the roots or plant systems, as cell numbers increased throughout each experiment. For inoculation of the wheat seedlings, cells were grown in 1/5 NB to reduce their metabolism, the effect being that an increase in metabolism ought to generate a detectable increase in bioluminescence. On wheat seedlings, bioluminescence per cell from strain I17 decreased or remained constant. A decrease in bioluminescence per cell from the constitutive *luxAB*-reporter may imply that the cell metabolism was slowing down and that cells were getting further into stationary phase than they were already in the inoculum. Both luminometry and cell diameter may provide a measure of metabolic activity (Ratray *et al.*, 1992; Neidhardt, 1990). Cell diameter decreased throughout the experiment also indicating that the cell metabolism was slowing down. More precisely, cell diameter is related to growth rate, hence if the diameter is reducing, the growth rate is slowing down. At the limit of this relation, the minimum cell size corresponds to the minimum growth rate. Thus, the smaller cell diameters refer generally to cells in stationary-phase like or to dormant cells. However, the cell numbers on the wheat seedlings increased significantly throughout the experiments and it is improbable that division of stationary-phase like cells could result in such an increase. Therefore, a sub-population must have been dividing actively to enable colonisation but this did not affect the general trend of the cell population. Bioluminescence per cell from strain B103 decreased also throughout each experiment indicating that transcription of the phenazine

operon was not induced on wheat seedlings. Neither HHL nor PCA was detected although the cell density was high enough for production to occur. For example, Pierson *et al.* (1998) showed inter-population signalling via AHLs among bacteria in the wheat rhizosphere that had a lower inoculum than the ones used in this study. Pierson *et al.* (1998) did their experiments with wheat grown in sterile sand whereas the seedlings in our experiments were grown on agar. To sterilise the seeds, they were washed with high concentrations of hydrochloride acid. Although, the agar provided a well-moisturised surface (only 0.7% w/v agar was used for this effect), it is possible that this was not the right physical environment for the seedlings and consequently for the bacteria to produce secondary metabolites. However, good bacterial growth was recorded.

On bean roots, the cell number increased in both experiments but the density may have reached its maximum in Expt. 1 as the cell numbers per dry weight of root did not increase significantly throughout this experiment. This indicated that the maximum root coverage might have been reached. Examination of root colonisation by *P. aureofaciens luxAB*-marked strains (I17 and B103) showed a good coverage of the entire root system by the bacteria; bioluminescence was present on all parts of the roots. Bioluminescence per cell from strains I17 and B103 increased by 25-fold during the first 3 days and then remained constant or decreased. This peak of luciferase activity by both strains may represent an increase in metabolic activity. Moreover, during that time the cell diameter increased from 0.94 to between 1.02 and 1.06 μm . This indicated that the cell population on bean roots during the first 3 days was metabolically active, dividing and colonising the roots. The ratio of bioluminescence from strains B103 over I17 gives a representation of the transcriptional activity of the phenazine operon compare to a general cell metabolism. Therefore, in Expt. 1, there was up to 1.81 ± 0.47 , and in Expt. 2 up to 5.35 ± 2.97 times more transcriptional activity from strain B103 than from strain I17 during the first 3 days.

However, neither PCA nor HHL were detected on bean roots. The compounds may not be produced or produced in too low amounts to allow for their detection. The minimal amount of HHL detectable in vermiculite mixed with $\frac{1}{2}$ Hoagland solution was 50 ng ml^{-1} . In NB, when full transcription of the phenazine operon occurred, strain B103 produced $5.25 \times 10^{-6} \pm 0.26 \times 10^{-6} \text{ ng cell}^{-1}$ of HHL. The cell density reached, in Expt. 1 at day 9, 3.2×10^9 cells per root. To obtain 50 ng ml^{-1} of HHL, each cell needed to produce

on average 1.56×10^{-8} ng of HHL. Hence, the production in NB was 336 times higher. In Expt. 2 at day 9, the cells reached 6.89×10^8 per root. To obtain 50 ng ml^{-1} , each cell needed to produce 7.26×10^{-8} ng of HHL. This was 72 times less than the production in NB. In conclusion, if the transcription of the operon on bean roots was from 72 to 336 times less than in NB, this was still sufficient to produce a minimum concentration detectable of 50 ng ml^{-1} of HHL. The highest level of bioluminescence from strain B103 on bean roots was about 12.5 times less than what was recorded on NA and in NB (Table 7.2). Thus, it is probable that the level of transcription on bean roots was also 10-fold less than in NB, and it may follow that the amount of HHL produced on plant roots were also 10 fold less than in NB. Nevertheless, production per cell was 7.2 to 33.6 times less than in NB, ought to have been sufficient for HHL to accumulate to a detectable level. Despite the fact that (i) theoretically HHL was detectable (if produced in the range described above), and (ii) transcription of the phenazine operon was recorded, no HHL was detected. Therefore several hypotheses may be stated: first, HHL was produced in lower amounts than between 1.56 and $7.25 \times 10^{-8} \text{ ng cell}^{-1}$; secondly, HHL was degraded too quickly to be detected; thirdly, HHL was also adsorbed onto the plant material lowering the detection limit.

The minimum detectable level of PCA was 500 ng ml^{-1} . For the cells at day 9 to accumulate this amount, they needed to produce, in Expt. 1, $1.56 \times 10^{-7} \text{ ng cell}^{-1}$, and in Expt. 2, $7.25 \times 10^{-7} \text{ ng cell}^{-1}$. In NB, cells produced after 12 h, ca. $10 \times 10^{-6} \text{ ng cell}^{-1}$. Thus, if cells produced on bean roots over 9-days 13.8 to 64 times less PCA than in NB, the amount produced would have still been sufficient for detection. PCA production per cell on nutrient agar was 6.8 ± 1.85 times higher than in NB. So if cells produced 94 to 435 times less PCA than on NA, the compound could still have been detected on bean roots. However, PCA was not detected. Thus, the compound was either produced in very low amounts, compared to the production on NA and in NB, or not produced at all.

It would therefore seem that not all the conditions that support bacterial growth lead to the production of HHL and PCA on plant roots. On bean roots, bioluminescence per cell from strains I17 and B103 increased by 25-fold during the first 3 days. The ratio of bioluminescence from strains B103 over I17 was up to 5.35 ± 2.97 showing that transcriptional activity of the phenazine operon from strain B103 was induced on bean

roots. Growth was recorded and the cell density was close to the capacity of the bean root system. The physical conditions used in this study led to a very good plant and root growth (for both bean and wheat). The plants were grown at 26°C which was only 1°C below the optimal condition for PCA (Slininger and Shea-Wilbur, 1995), and during the 9-day experiment the vermiculite was kept moist by wrapping the plants in a plastic bag. Therefore, all experimental conditions monitored were met for production of PCA and HHL, and it is possible that production occurred but a level too low to enable detection. Gurusiddaiah *et al.* (1986) showed that minimum inhibitory concentrations below 1 µg ml⁻¹ failed to inhibit growth of many different fungi. Therefore, it is likely that if PCA was produced at levels lower than 500 ng ml⁻¹, this would not have been sufficient to suppress fungal growth *per se*.

7.7. FUTURE WORK

Georgakopoulos *et al.* (1994a) studied phenazine gene expression on several seeds with a *phz::InaZ* reporter strain. The inoculation was performed on non-sterilised seeds that were subsequently grown in soil. They did not monitor phenazine or HHL production. They obtained high levels of gene expression from bacteria growing on wheat seedlings over 48 h experiments. It is possible that in a sterile system, bacteria are not challenged to produce antibiotics as much as they would be in a non-sterile environment. The next experiment following this study could be to inoculate *P. aureofaciens* on non-sterilised wheat and bean seedlings and to grow them otherwise in the same conditions. To count cell numbers, it would not be possible to use the CellFacts instrument since it would not give a specific count for the strain of interest. Cell count could be obtained by plating dilution technique using the natural resistance to tetracycline in *P. aureofaciens* PGS12 and the *luxAB* in *P. aureofaciens* B103 and I17 as marker genes.

CHAPTER EIGHT

CONCLUDING DISCUSSION

CHAPTER EIGHT

CONCLUDING DISCUSSION

It has been over a decade since multicellularity was proposed as a general bacterial trait (Newman and Shapiro, 1999). Intercellular communication and multicellular coordination are now known to be widespread among prokaryotes and to affect multiple phenotypes (Gray, 1997; Kaiser and Losick, 1993). This change in thinking is due mainly to the discovery that quorum-sensing signal molecules (AHLs) are used throughout the eubacterial kingdom to regulate the expression of a wide variety of phenotypes (Shapiro and Dworkin, 1997; Dunny and Winans, 1999; England *et al.*, 1999). Microorganisms isolated from the rhizosphere of plants have potential value as supplements or alternatives to chemical pesticides for disease control of soilborne fungal plant pathogens. Pseudomonads like *P. aureofaciens* are potential biological control agents. The wild-type strain PGS12 used in this research produces the antibiotic phenazine that inhibits growth of many different fungal pathogens. Understanding the genetic and physiological processes that underpin antibiotic production can only aid the development of bacterial biocontrol agents. Phenazine antibiotic biosynthesis in *P. aureofaciens* is under quorum sensing control (Pierson III *et al.*, 1994). This research project focused on the regulation of the phenazine operon by *P. aureofaciens* PGS12 which was originally isolated from a field of maize (Georgakopoulos, 1994a). The aim was to study the role of the autoinducer HHL and cell density in regulating phenazine production when the bacteria are growing under different conditions, in liquid culture, on a solid surface as colonies, and on plant roots. Two approaches were undertaken to monitor production of phenazine antibiotics. The production of the antibiotics was quantified *in vitro* and *in situ* and the reporter genes *luxAB* were fused to a phenazine gene to study the transcriptional activity of the operon and its regulation by HHL. Chromosomal random gene fusions were generated using a mini-Tn5-*luxAB* transposon into *P. aureofaciens* PGS12. Strains were screened for insertion of the *luxAB* gene within the *phzFABCD*, the biosynthetic cluster of the phenazine operon, and a strain expressing constitutive luciferase activity was also selected.

After transposon mutagenesis, the resulting transconjugants had a single, stably integrated chromosomal copy of the *luxAB* genes. Mutants defective in phenazine antibiotic production [Phz⁻] were recovered after transposon mutagenesis. Of these mutants, the majority (80%) were also deficient in HHL production [HHL⁻] and only 15.4% were [HHL⁺, Phz⁻]. Yet, 5 genes code for phenazine biosynthesis (*phzFABCD*) and only one gene (*phzI*) codes for the HHL synthetase. It was expected, since *Tn5* transposon mutagenesis occurs at random, that 5 times more [HHL⁺, Phz⁻] mutants than [HHL⁻, Phz⁻] mutants ought to have been recovered. Two reasons may explain these results. First, transposon mutagenesis may not occur completely at random and there may be some “hot spots” for *Tn5* insertion. Secondly, the [HHL⁻] phenotype may result from several genotypes, including mutation in global regulatory systems such as the GacA/GacS system, which may give a [HHL⁻] phenotype (Chancey *et al.*, 1999). The [HHL⁻, Phz⁻] strains were tested for *Tn5* insertion in *phzI* by PCR and only one strain (strain B21) may have an insertion in *phzI*. Furthermore, 3 [HHL⁻, Phz⁻] strains (strains B105, I18Y, and A5Y) were generated spontaneously from [HHL⁺, Phz⁻] strains by subculturing the bacteria on NA. These strains may have undergone a second mutation. Therefore, there may be some double mutants among the 80% of [HHL⁻, Phz⁻]. These strains may have a *luxAB* insert within the phenazine biosynthetic genes and a second mutation leading to the [HHL⁻] phenotype. These mutants characterised briefly in this study are now available to continue working in this direction.

The selected [HHL⁺, Phz⁻] strains were all prototrophs and produced fluorescent siderophores. While strains were tested for pyoverdinin production on KB medium, a new phenotype seemingly associated with HHL production was discovered. All [HHL⁻] strains were also deficient in the excretion of mucus whereas [HHL⁺] strains produced normal amounts of mucus on KB medium. Although it has never been reported that the PhzI/PhzR system is involved in regulation of other phenotypes than phenazine biosynthesis, this cannot be excluded. In many species, quorum-sensing systems do regulate more than one phenotypes in the same species. In *P. aeruginosa*, LasR-3-oxo-C12-HSL has been shown to activate the *xcpP* and *xcpR* genes, which encode proteins of the *P. aeruginosa* general secretory pathway (Chapon-Herve *et al.*, 1997). Further characterisation of these strains to determine the insert position is required.

Strain B103 was shown to have a single insert in *phzB* and was used in this research to study the transcription of the phenazine operon. The selected strains were tested for HHL production using a *luxRI'-luxABCDE* biosensor. After optimisation of the bioassay, high sensitivity to HHL was achieved: levels as low as 0.1 ng ml^{-1} were detected. Higher sensitivity for the detection of HHL might be achieved by using strain B103I that would have a mutated *phzI* gene. PCA was quantified preferentially by spectrophotometry that had the advantage of not necessitating extraction of PCA from the samples, and sensitivity was reasonable (50 ng ml^{-1}).

Georgakopoulos (1994) cloned the phenazine biosynthetic locus of *P. aureofaciens* PGS12 and analysed its expression *in vitro* with the ice nucleation reporter gene. However, the regulation of phenazine production by AHLs in liquid culture has never been thoroughly investigated. Pierson III (1994) showed that phenazine accumulated in response to cell density and HHL accumulation by growing an HHL-deficient strain in a cell-free conditioned medium (medium in which strain 30-84 had grown). In this present research, growth of *P. aureofaciens* was monitored using an electronic counter (CellFacts instrument, Microbial Systems) that also provided measurement of the cell diameters producing a cell size distribution profile. Study of *P. aureofaciens* PGS12 showed that HHL production is first detected in the mid-log phase probably due to activity of the previously produced PhzI protein (the HHL synthase), and to activity of a small amount of newly produced PhzI. The point from which HHL per cell accumulated faster than growth is an indicator of the beginning of the autoinduction process. At this point, HHL concentration may have reached a threshold concentration that enabled the formation of active PhzR-HHL complexes (i.e. the substrate HHL had reached $1/K_m$, the affinity concentration for PhzR). The transcriptional regulator can then activate transcription of the phenazine operon comprising the biosynthetic genes and *phzI*. This resulted in the autoinduction of HHL and a 100-300-fold increase in concentration over pre-induction levels. The autoinduction process was calculated to be initialised upon accumulation of HHL to a threshold concentration of $0.63 \times 10^{-6} \pm 0.3 \times 10^{-6} \text{ ng cell}^{-1}$. At this moment, the cell density was at ca. $2 \times 10^8 \text{ cells ml}^{-1}$. The transcriptional activity of the phenazine operon from strain B103 was at its minimum with a level of ca. $3 \times 10^{-6} \text{ RLU cell}^{-1}$. The growth was in the region of the maximal specific growth rate (k_{\max}) and the cell diameter was also maximal at ca. $1.30 \text{ }\mu\text{m}$.

After k_{\max} , the growth rate deceleration was accompanied by a significant decrease in cell diameter; cells measured about 1.15 μm in the transition between the exponential and stationary phase. HHL accumulation was maximal in the transition phase and more specifically between $r_{\max-1}$ and r_{\max} (r_{\max} , the maximal volumetric growth rate). Up to 38% more HHL was produced than cell biomass. In strain B103, the maximal HHL concentration and the maximal transcriptional activity from the *phzB::luxAB* reporter ($233 \times 10^{-6} \pm 10.5 \times 10^{-6}$ RLU cell⁻¹) occurred simultaneously in transition phase. In late transition phase and early stationary phase (between r_{\max} and $r_{\max+1}$), HHL decreased rapidly while the production of PCA was maximal. PCA was first detected in the medium in transition phase at r_{\max} . HHL concentrations and luciferase activity from the *phzB::luxAB* fusion in strain B103 decreased simultaneously. In the stationary phase, HHL concentration continued to decrease at a low rate whereas PCA continued to accumulate. After 13 h of growth, PCA production reached $4.35 \times 10^{-6} \pm 0.65 \times 10^{-6}$ ng cell⁻¹. Eventually, at 24 h, cells measured 0.98 ± 0.009 μm .

During liquid culture of *P. aureofaciens* PGS12, the production of HHL coincided with a decrease in growth rate and its production abruptly dropped as cells entered stationary phase and growth stopped. When growth was monitored on nutrient agar, the transition phase was much longer than in nutrient broth and this resulted in a prolonged production of the autoinducer. In colonies, the production of HHL also stopped as cells entered stationary phase. Until a recent publication by Whiteley *et al.* (2000), it was thought that in *P. aeruginosa* the RhIR-RhII system influenced *rpoS* expression (Latifi *et al.*, 1996) and that stationary-phase-specific genes regulated by RpoS might be partly under quorum-sensing control. However, Whiteley *et al.* (2000) showed that it is RpoS that can function to repress *rhII*. They hypothesised that there is a regulatory loop in which RhIR-RhII activates *rpoS* and the *rpoS* product, in turn, represses *rhII*. However, the RhIR-RhII quorum-sensing system did not regulate *rpoS* transcription under their experimental conditions. Pyocyanine is a phenazine compound produced by *P. aeruginosa* which is under the control of the RhIR/RhII quorum-sensing system. Therefore, quorum-sensing regulation between both strains may share some homology. It is, therefore, tempting to hypothesise that in *P. aureofaciens* HHL also induces *rpoS* transcription which product in its turn may repress *phzI*. A direct linkage between a two-component sensory transduction system and a quorum-sensing system was shown to

control gene expression in *P. aureofaciens* (Chancey *et al.*, 1999) and in *P. aeruginosa* PAO1 (Reimann *et al.*, 1997). GacA/GacS may control AHL production via positive transcriptional regulation of *phzI* (Chapter 1). Recent evidence suggests that regulatory systems, such as two-component and quorum-sensing systems, are part of integrated regulatory networks (Latifi *et al.*, 1996; Chancey *et al.*, 1999). It is becoming clear that quorum sensing is a core and global regulatory system governing the gene expression of many crucial metabolic functions. In Table 8.1, a model incorporating known and hypothetical controls for the regulation of phenazine production in *P. aureofaciens* PGS12 is proposed.

The expression of *phzB::luxAB* gene fusion from strain B103 followed a pattern characteristic of genes under the influence of an autoinducer such as that found in *V. fischeri* (Nealson, 1977). The bioluminescence profile of the organism varied with cell density and with the phases of growth. As described in Fig. 5.8, luciferase activity in strain B103 reflected the transcription and regulation of the phenazine operon. Upon accumulation of HHL to $0.63 \times 10^{-6} \pm 0.3 \times 10^{-6}$ ng cell⁻¹, the autoinduction process began and the transcription of the *luxAB* genes inserted into *phzB* occurred simultaneously to the transcription of *phzI*. Therefore, in strain B103, light formation reported in real time the accumulation of HHL. The dramatic decline of HHL concentration at the entry into stationary phase may be attributed to either its degradation, its binding to other molecules in the media, or to the negative autoregulation via PhzR. HHL together with PhzR represses *phzR* expression post-transcriptionally and transcriptionally. In *Vibrio fischeri*, the regulation can be positive or negative, depending upon the level of cellular LuxR and OHHL, and the presence or absence of a downstream element in the *luxD* open reading frame (Dunlap and Ray, 1989; Engebrecht and Silverman, 1986; Shadel and Baldwin, 1992). The decline in HHL concentration in culture of *P. aureofaciens* B103 was slower than in the wild-type strain. The discrepancy between B103 and the parental strain PGS12 regarding HHL decline may be attributed to changes in expression of coding regions downstream of the *luxAB*-insert, such as the *phzC* and *phzD* genes which might be involved in the down regulation of the phenazine operon. In strain B103, this downstream factor may not be transcribed, and the transcription of the whole operon may not be down regulated as efficiently as found for the wild-type strain. A newly identified protein may be involved in HHL degradation. AHL-dependent synthesis of RpoS was prevented by

Fig. 8.1.

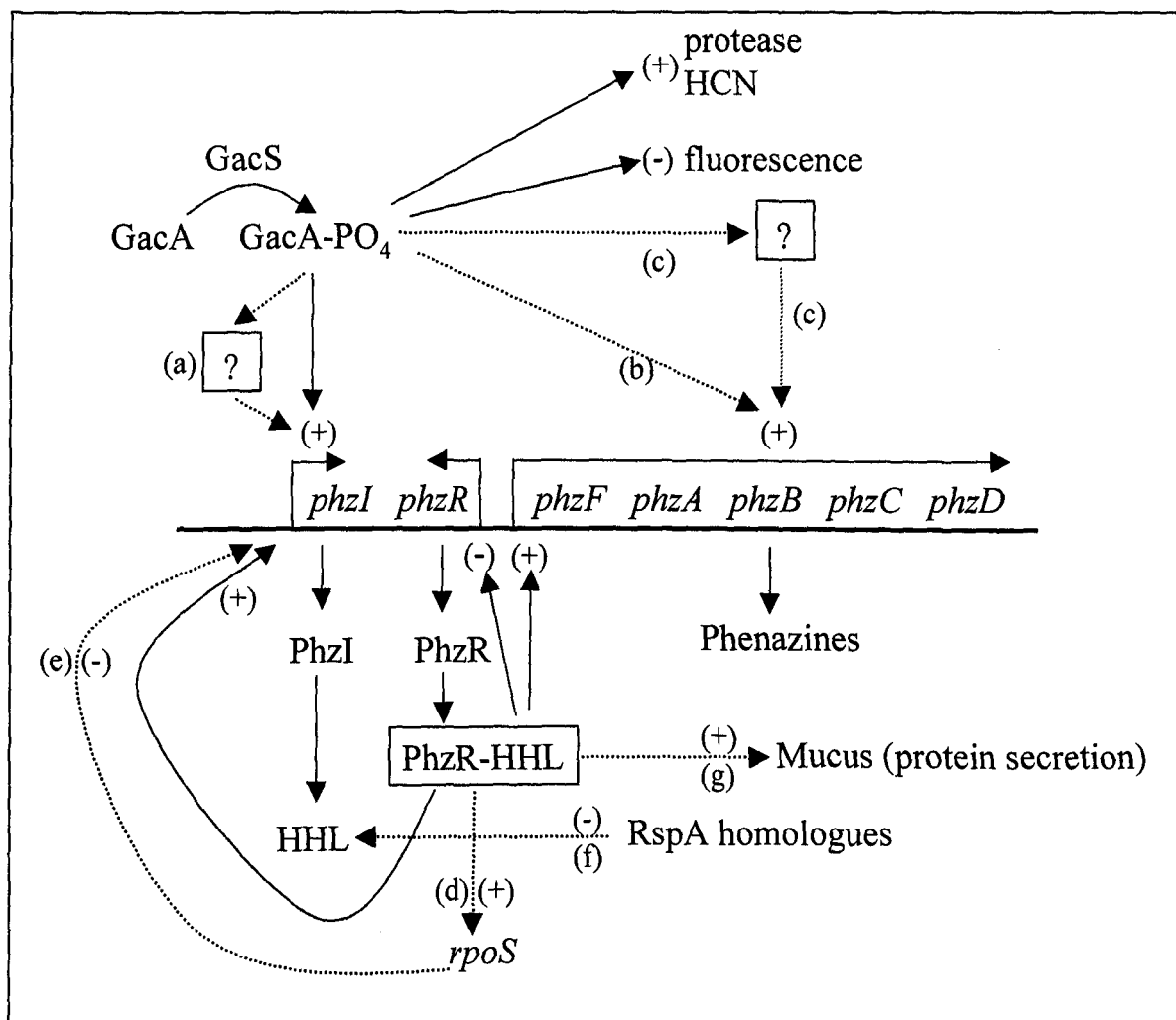


Fig. 8.1. Model for control of phenazine regulation in *P. aureofaciens* PSG12 (adapted from Chancey *et al.*, 1999).

GacS responds to the presence of an unknown signal by transphosphorylating GacA. GacA may control phenazine production by regulating AHL synthesis through transcriptional control of *phzI* either directly or indirectly (reaction a). GacA may also control phenazine production at a second level, possibly by direct binding of GacA (reaction b) or by some unidentified regulatory protein controlled by GacA (reaction c). Latifi *et al.* (1996) showed that the transcriptional regulator complex RhlR-HHL activated *rpoS* transcription in *P. aeruginosa* (reaction d). Whiteley *et al.* (2000) could not show that this was true and they showed that *rpoS* repressed *rhII* (reaction e). RspA was shown in *E. coli* to be involved in AHL degradation (Huisman and Kolter, 1994; reaction f). In *P. aureofaciens* PGS12, [HHL] mutants were deficient in mucus production, and in *P. aeruginosa*, LasR-3-oxo-C12-HSL has been shown to activate the *xcpP* and *xcpR* genes, which encode proteins of general secretory pathway (Chapon-Herve *et al.*, 1997; reaction g). The solid arrows indicate known regulatory controls, and the dashed arrows possible regulatory controls. Plus and minus signs indicate positive and negative regulation respectively.

over-expression of RspA (Huisman and Kolter, 1994). The similarity of the RspA sequence to that of catabolic enzymes led to hypothesise that the effect of RspA on *rpoS* transcription could result from a degradation of homoserine lactones.

As shown in Chapter 4, in cultures of the wild-type strain, PCA was first detected in the transition phase around r_{\max} , and the maximal rate of PCA production corresponded to the sharp decrease in HHL concentration. Therefore, PCA was produced after the burst of HHL synthesis, after full autoinduction of the operon. PCA synthesis carried on during stationary phase, and because it is stable (Turner and Messenger, 1986), it accumulated in the media. The *luxAB* reporter system in the phenazine operon in strain B103 followed HHL production; this indicated that production of phenazine operon transcripts and promoter activity declined quickly after the peak of HHL production. Since PCA was still produced beyond this point, the protein products would appear to be relatively stable and continued to produce phenazine after the operon promoter had been silenced. If the PhzI protein behaved in a similar fashion, HHL synthesis would be expected to continue likewise for a longer period. Therefore, either PhzI is silenced or degraded in the cell relatively quickly.

The luciferase expression from strain I17 was proportional to cell density during the exponential growth of the organism and strain I17 may be referred to as a *luxAB* constitutive reporter. However, bioluminescence per cell declined when cells entered stationary phase. Rattray (1992) showed that luminometry could provide a measure of microbial activity by comparing activity provided by radiorespirometric and bioluminescence measurements. Luciferase activity may provide a direct assessment of the level of reducing equivalents (FMNH₂) in cells (Jablonski and DeLuca, 1978; Rattray, 1992). Hence, the decrease in bioluminescence during stationary phase reflects a general slow down of cell metabolism. Because in constitutive *luxAB*-reporter, bioluminescence is proportional to cell number, luminometry may be used to measure microbial biomass. Luminescence of dilutions of cells dividing exponentially is proportional to cell concentration over several orders of magnitude and the lower detection limit for cells of strain I17 by luminometry was around 345 cells ml⁻¹. Therefore, the *luxAB* reporter genes permitted a very sensitive detection of cells.

Bioluminescence per cell from strain I17 can also be used to compare the transcriptional activity from other non-constitutive *lux*-reporters. When cells entered stationary phase, light output from both strains decreased but the decline in bioluminescence from strain B103 was approximately 6.8 times higher than the decline in bioluminescence from strain I17. If the decrease in bioluminescence from strain I17 represented a decrease in cell metabolism, then the difference in decrease between the 2 strains may represent more specifically a decrease in transcriptional activity from strain B103. This phenomenon may result from a down-regulation of the transcriptional activity of the phenazine operon by PhzR or other regulatory mechanisms. In contrast, when cells were dividing exponentially in NB at 28°C, the bioluminescence per cell from strain I17 was maximal and constant at ca. 14.5×10^{-6} RLU cells⁻¹. In transition phase, the level of bioluminescence from strain B103 was maximal and the level was up to 55 times the level from the constitutive reporter. When the growth rate was maximal, the level of bioluminescence from strain B103 was only 0.2 ± 0.01 times the levels from strain I17. All together, between $r_{\max-1}$ to $r_{\max+1}$, bioluminescence per cell increased 57 ± 5 times. These values showed clearly the power of the autoinduction process. The shift in the transcriptional activity of the phenazine operon happened in only 3 h.

In the environment, bacteria proliferate and survive mainly attached to surfaces. Colony development by bacteria holds many parallels with the formation and development of biofilms (Costerton *et al.*, 1995). The high cell concentration typically found in biofilms has led to the suggestion that AHL activity may be essential components of their physiology. The production of HHL and phenazine was also monitored for colonies of *P. aureofaciens* PGS12, B103 and I17 growing on nutrient agar (Chapter 6). The transcriptional activity of the *phzB::luxAB* genes fusion from strain B103 was studied and compared to the constitutive luciferase activity from strain I17. The aim of this study was to provide information on the activity of the phenazine operon from cells growing in colonies. This study provided the first attempt to study phenazine production from cells growing on solid surface agar.

Studies of colony formation by *E. coli* or *Pseudomonas* species indicates that colonies expand outwards by adding new cells in a relatively narrow zone at the periphery, thus, cell division is likely to be mainly localised at the edge of the colony

throughout its morphogenesis (Shapiro, 1983; Emerson, 1999; Newman and Shapiro, 1999). Consequently, as the colony expands, a dominant proportion of cells – between the inside edge and the centre of the colonies – may be in a transition phase of growth. This pattern was reflected in colonies of strain I17 that expressed the *luxAB*-reporter genes. Luminescence was the highest in the inside ring between the edge and the centre of the colony. The lower than expected luminescence levels at the centre of the colony may reflect a slower metabolism of cells in this region. Cells may be in a stationary-like phase similar to the stationary phase found in liquid culture where a decline in luminescence from the constitutive strain was also recorded (Chapter 5).

In NB, the transition phase lasted a maximum of 4 h whereas it was estimated that cells were in a transition phase of growth for at least 9 h on NA. The colony volume was estimated from measurements made throughout the experiments and from measurements of colony depth established by Newman and Shapiro (1999). It was estimated that the cell density was 55 to 75 times higher within a colony than in liquid culture. The maximal volumetric production – for calibrated equivalent volumes on NA and in NB – of HHL, and light output were also between 50 and 65 times higher on NA and in liquid culture. The maximal light output and maximal HHL accumulation per cell was similar on both media. Therefore, these values could be mainly the result of the increased cell density in colonies compared to NB. The production of the antibiotic PCA was per cell ca. 7 times higher in colonies than in NB and the production in an equivalent volume was estimated to be 360 times higher in a colony. Therefore, the higher PCA concentration in colonies cannot be explained solely on the basis of an increase in cell density in colonies. The autoinducer was present within colonies for a prolonged period of time (at least 3 h) compared to the burst seen in NB. Similarly the transcriptional activity of the phenazine operon, as reflected by *phzB::luxAB* expression in strain B103, remained maximal during this time. High concentrations of HHL per cell for a longer period of time may have sustained large production and accumulation of PCA in the colony. The efficient synthesis of PCA in a colony may represent the normal pattern of expression of these chemicals in cells growing attached to a surface in the environment. Because PCA is a stable antifungal compound, a prolonged production of PCA might lead to an increase PCA concentration in the vicinity where it is produced.

In the proposed model, higher HHL concentration per cell was not achieved although HHL concentration in equivalent calibrated volumes was significantly higher in colonies than in NB. The calculated increase in HHL concentration at induction of transcription of the phenazine operon, in the maximal HHL concentration, and maximal bioluminescence in NA compare to NB corresponded to the increase calculated in cell density in NA. Therefore the higher values in the colony may be the result of an increase in cell density. The production of HHL and the transcriptional activity remained maximal for a longer period of time compared to liquid culture, and this led to an increased production of phenazine (360-fold) in the colony compare to broth. This is the first time detailed studies on this strain have been conducted on nutrient agar, and for many other bacteria colony growth and autoinduction have not been studied. This work illustrates how basic principles of the system operate and such studies can fill a gap between studies in nutrient broth and biofilms.

The dynamics of expression of the phenazine operon were also studied throughout the first days of seedling colonisation by *P. aureofaciens* PGS12. Wood *et al.* (1997) using a *phzI**phzB::inaZ* reporter strain that expressed the ice nucleation protein only in the presence of exogenous AHL signals, showed that HHL was present *in situ* on wheat roots. They linked HHL production with the expression of the *phzFABCD* operon from *P. aureofaciens* 30-84. *P. aureofaciens* PGS12, and the isogenic strains B103 and I17, were inoculated onto wheat or bean seedlings. The inoculated bean roots and entire wheat seedlings were monitored by measuring cell counts and density, phenazine production, HHL production, and luciferase activity by strains B103 and I17. The system also provides the ability to localise specific activity on the root system using CCD imaging techniques.

In contrast to laboratory culture studies, all experiments monitoring *P. aureofaciens* PGS12 on roots led to the lack of detection of HHL and PCA. This could not be explained by the inability of cells to colonise the roots or plant systems, as cell numbers increased throughout each experiment. On wheat seedlings, bioluminescence per cell from strain I17 and cell diameter decreased throughout the experiment. This indicated that the cell metabolism was slowing down. On bean roots, the cell number increased in both experiments. Examination of the root indicated that *P. aureofaciens*

luxAB-marked strains (I17 and B103) had colonised the entire root system; bioluminescence was present on all parts of the roots. Bioluminescence per cell from strains I17 and B103 increased (25-fold) during the first 3 days and then remained constant or decreased. This peak of luciferase activity by both strains may represent an increase in metabolic activity. The ratio of bioluminescence from strains B103 over I17 gives a representation of the transcriptional activity of the phenazine operon compared to general cell metabolism. There was up to 5.35 ± 2.97 times more transcriptional activity from strain B103 than from strain I17. However, neither PCA nor HHL were detected on bean roots. It is possible that the compounds were not produced, or were produced in too low amounts to allow for their detection. It is also possible that HHL was degraded too quickly to be detected or that it was adsorbed onto the plant material lowering the detection limit. Similarly PCA production was not detected although the minimum detectable level of cell was present. Thus, the compound was either produced in very low amounts, compared to the production on NA and in NB, or not produced at all. It would therefore seem that not all the conditions that support bacterial growth lead to the production of HHL and PCA on plant roots. *In vitro*, minimum inhibitory concentrations below $1 \mu\text{g ml}^{-1}$ failed to inhibit growth of many different fungi (Gurusiddaiah *et al.*, 1986). It is likely that if PCA was produced at levels lower than 500 ng ml^{-1} , then, the levels would not be sufficient *per se* to suppress fungal growth.

From an ecological point of view, the population is the key biological entity. Its survival depends upon having the right cell type when confronted by phage attack, antibiotics, desiccation, or the need to utilise novel growth substrates. In *E. coli*, survival in stationary phase involves several factors, including the RpoS sigma factor (Kolter *et al.*, 1993), which is subject to quorum-sensing control in *P. aeruginosa* (Pesci and Iglewski, 1999) and possibly in *E. coli* (Huisman and Kolter, 1994). Monocultures may display large-scale functional differentiation of various cell groups, such as the stalks and sporangia in Myxobacterial fruiting bodies and substrate and aerial mycelia in *Streptomyces* (Shapiro and Dworking, 1997). It appears to be a general rule that organisation in biofilms and colonies provides enhanced resistance to a wide range of antibacterials (Costerton *et al.*, 1995). In *P. aureofaciens* a division of labour within the colony and during the development of the colony was observed. HHL and phenazine production occurred only when a critical cell

density was achieved. Within the colony, a clear delimitation in the level of transcription was observed. The lowest transcriptional activity was at the periphery of the colonies where cells were dividing actively. The highest level of bioluminescence was found in the inside ring of the colony and there was a lower expression in the centre. Therefore, a co-ordinated regulation of phenazine gene expression occurred at the population level within the colony but also in liquid culture. On plant root, a co-ordinated expression of the phenazine operon might have happened although production of the autoinducer and the antibiotic was not detected. Therefore, to study phenazine production on plant root, different conditions would need to be tested. Although sterile systems can facilitate study by avoiding the need for selection of the strain of interest, this may lead to conditions that are unfavourable for antibiotic production.

CHAPTER NINE

REFERENCES

CHAPTER NINE

REFERENCES

- Agrios G.N.** 1988. *Plant Pathology* (3rd ed.). San Diego: Academic Press.
- Amin-Hanjani S., Meikle A., Glover L.A., Prosser J.I., and Killham K.** 1993. Plasmid and chromosomally encoded luminescence marker systems for detection of *Pseudomonas fluorescens* in soil. *Mol. Ecol.* **2**:47-54.
- Anderson J.P.E. and Domsch K.H.** 1978. A physiological method for the quantitative measurement of microbial biomass in soils. *Soil Biol. Biochem.* **10**:215-221.
- Bailey M.J., Lilley A.K., Thompson I.P., Rainey P.B., and Ellis R.J.** 1995. Site-directed chromosomal marking of a fluorescent pseudomonad isolated from the phytosphere of field grown sugar beet; stability and potential for marker gene transfer. *Mol. Ecol.* **4**:755-763.
- Bainton N.J., Bycroft B.W., Chhabra S.R., Stead P., Gledhill L., Hill P.J, Rees C.E.D., Winson M.K., Salmond G.P.C., Stewart G.S.A.B., and Williams P.** 1992. A general role for the *lux* autoinducer in bacterial cell signalling: Control of antibiotic biosynthesis in *Erwinia*. *Gene* **116**:87-91.
- Batchelor S.E., Cooper M., Chhabra S.R., Glover L.A., Stewart G.S., Williams P., and Prosser J.I.** 1997. Cell density-regulated recovery of starved biofilm populations of ammonia-oxidizing bacteria. *Appl. Environ. Microb.* **63**:2281-2286.
- Beauchamp C.J., Kloepper J.W., Lemke P.A.** 1993. Luminometric analysis of plant root colonisation by luminescent pseudomonads. *Can. J. Microbiol.* **39**:434-441.
- Becker J.O., Hepfer C.A., Yuen G.Y., van Gundy S.D., Schroth M.N., Hancock J.G., Weinhold A.R., and Bowman T.** 1990. Effect of rhizobacteria and metham-sodium on growth and root microflora of celery cultivars. *Phytopathol.* **80**:206-211.
- Berkeley R.C.W., Lynch J.M., Melling J., Rutter P.R., and Vincent B. (eds.)** 1980. *Microbial Adhesion to Surfaces*. Ellis Horwood, Chichester.
- Bloomfield S.F., Stewart G.S.A.B., Dodd C.E.R., Booth I.R., and Power E.G.M.** 1998. The viable but non-culturable phenomenon explained? *Microbiol.* **144**:1-3.
- Bowen G.D.** 1979. Integrated and experimental approaches to the study of growth of organisms around roots. In *Soil-borne Plant Pathogens* (Schippers, B., and Gams W., eds.), pp. 207-227. Academic Press, London.
- Bowen G.D.** 1980. Misconception, concepts and approaches in rhizosphere biology. In *Contemporary Microbial Ecology* (Elwood, D.C., Hedger J.N., Latham M.J., Lynch J.M., and Slater J.H., eds.), pp. 283-304. Academic Press, London.

- Brisbane P.G., Janik J.L., Tate M.E. and Warren R.F.O.** 1987. Revised structure for the phenazine antibiotic from *Pseudomonas fluorescens* 2-79 (NRRL B-15132). *Antimicrob. Agents Chemother.* **31**:1967-1971.
- Brock T.D.** 1997. Microbial growth. In *Biology of Microorganisms*, 8th ed. (Madigan M.T., Martinko J.M., Parker J., eds.). Printice Hall International Limited, London.
- Bull C.T., Weller D.M., Thomashow L.S.** 1991. Relation between root colonisation and suppression of *Gaeumannomyces graminis* var. *tritici* by *Pseudomonas fluorescens* strain 2-79. *Phytopathol.* **81**:954-959.
- Caldwell D.E. and Lawrence J.R.** 1986. Growth kinetics of *Pseudomonas fluorescens* microcolonies within the hydrodynamic boundary layers of surface microenvironments. *Microb. Ecol.* **12**:299-312.
- Campbell I.M.** 1984. Secondary metabolism and microbial physiology. *Advances in Microbial Physiology* **25**:1-17.
- Chancey S.T., Wood D.W., and Pierson III L.S.** 1999. Two-component transcriptional regulation of *N*-acyl-homoserine lactone production in *Pseudomonas aureofaciens*. *Appl. Environ. Microbiol.* **65**:2294-2299.
- Chapon-Herve V.M., Akrim M., Latifi A., Williams P., Lazdunski A., and Bally M.** 1997. Regulation of the *xcp* secretion pathway by multiple quorum-sensing modulons in *P. aeruginosa*. *Mol. Microbiol.* **24**:1169-1178.
- Clerc A., Manceau C., and Nesme X.** 1998. Comparison of randomly amplified polymorphic DNA with amplified fragment length polymorphism to assess genetic diversity and genetic relatedness with genospecies III of *Pseudomonas syringae*. *Appl. Environ. Microbiol.* **64**:1180-1187.
- Cooper S.** 1991. *Bacterial growth and division: biochemistry and regulation of prokaryotic and eukaryotic division cycles*. Academic Press: San diego, California.
- Costerton J.W., Lewandowski Z., Caldwell D.E., Korber D.R., and Lappin-Scott H.M.** 1995. Microbial Biofilms. *Ann. Rev. Microbiol.* **49**:711-745.
- Cui Y., Chatterjee A., Liu Y., Dumenyo C.K., and Chatterjee A.K.** 1995. Identification of a global repressor gene, *rsmA*, of *Erwinia carotovora* subsp. *carotovora* that controls extracellular enzymes, OHHL, and pathogenicity in soft-rotting *Erwinia* spp. *J. Bacteriol.* **177**: 5108-5115.
- Chatterjee A., Cui Y., Liu Y., Dumenyo C.K., Chatterjee A.K.** 1995. Inactivation of *rsmA* leads to overproduction of extracellular pectinases, cellulases, and proteases in *Erwinia carotovora* subsp. *carotovora* in the absence of the starvation / cell density-sensing signal, OHHL. *Appl. Environ. Microbiol.* **61**:1959-1967.
- Davies D.G., Parsek M.R., Pearson J.A., Iglewski B.H., Costerton J.W., and Greenberg E.P.** 1998. The involvement of cell-to-cell signals in the development of a bacterial biofilm. *Science* **280**:295-298.

- Defago G., and Haas D.** 1990. Pseudomonads as antagonists of soilborne plant pathogens: Modes of action and genetic analysis. In: *Soil Biochemistry*, Vol.6 (Bollag J.-M., and Stotzky G., eds.), pp. 249-291. Marcel Dekker, New York.
- Devine J.H., Countryman C., and Baldwin T.O.** 1988. Nucleotide sequence of the *luxR* and *luxI* genes and structure of the primary regulatory region of the *lux* regulon of *Vibrio fischeri* ATCC 7744. *Biochemistry* **27**:837-842.
- Dowling D.N. and O'Gara F.** 1994. Metabolites of *Pseudomonas* involved in the biocontrol of plant disease. *Trends in Biotech.* **12**:133-141.
- Drahos D., Hemming B.C., McPherson, S.** 1986. Tracking recombinant organisms in the environment: b-galactosidase as a selectable non-antibiotic marker for fluorescent pseudomonads *Bio/Technol.* **4**:439-444.
- Duke S.O., Menn J.J., and Plimmer J.R.** 1993. Challenges of pest control with enhanced toxicological and environmental safety. In: *Pest Control with Enhanced Environmental Safety* (Duke S.O., Menn J.J., and Plimmer J.R., eds.), pp. 1-13. American Chemical Society, Washington, DC.
- Dunlap P.V., and Greenberg E.P.** 1988. Control of *Vibrio fischeri lux* gene transcription by a cyclic AMP receptor protein-LuxR protein regulatory circuit. *J. Bacteriol.* **170**:4040-4046.
- Dunlap P.V., and Greenberg E.P.** 1991. Role of intercellular chemical communication in the *Vibrio fischeri*-monocentrid fish symbiosis. In: *Microbial Cell-Cell Interactions* (Dworkin M., ed.), pp. 219-240. American Society for Microbiology, Washington, DC.
- Dunlap P.V.** 1997. *N*-acyl-L-homoserine lactone autoinducers in bacteria. In: *Bacteria as Multicellular Organisms* (Shapiro J.A., and Dworkin M., eds.), pp.69-106. Oxford University Press, (UK).
- Dunlap P.V., and Ray J.M.** 1989. Requirement for autoinducer in transcriptional negative autoregulation of the *Vibrio fischeri luxR* gene in *E. coli*. *J. Bacteriol.* **171**:3549-3552.
- Dunny G.M., and Winans S.C. (eds.).** 1999. *Cell-Cell Signalling in Bacteria*. American Society for Microbiology, Washington, DC.
- Eberhard A., Burlingame A.L., Eberhard C., Kenyon G.L., Nealson K.H., and Openheimer J.J.** 1981. Structural identification of autoinducer of *Photobacterium fischeri* luciferase. *Bioch.* **20**:2444-2449.
- Elmholt, S.** 1991. Side effects of propiconazole (Tilt 250 EC) on non-target soil fungi in a field trial compared with natural stress effects. *Microb. Ecol.* **22**:99-108.
- Emmert E.A.B., and Handelsman J.** 1999. Biocontrol of plant disease: a (Gram-) positive perspective. *FEMS Microbiol. Lett.* **171**:1-9.
- Emerson D.** 1999. Complex pattern formation by *Pseudomonas* strain KC in response to nitrate and nitrite. *Microbiol.* **145**:633-641.
- Engbrecht J., and Silverman M.** 1986. Regulation of expression of bacterial genes for bioluminescence. In: *Genetic Engineering: Principles and Methods*, Vol.8 (Setlow J.K. and Hollaender A., eds.) pp. 31-44. Plenum Publishing, New York.

- England R.R., Hobbs G., Bainton N.J., and Roberts D.McL.** (eds.). 1999. *Microbial Signalling and Communication*. 57th symposium of the Society for General Microbiology. Cambridge University Press, Cambridge (UK).
- Flavier A.B., Ganova-Raeva L.M., Schell M.A., and Denny T.P.** 1997. Hierarchical autoinduction in *Ralstonia solanacearum*: Control of acyl-homoserine lactone production by a novel autoregulatory system responsive to 3-hydroxypalmitic acid methyl ester. *J. Bacteriol.* **179**:7089-7097.
- Fravel D.R.** 1988. Role of antibiosis in the biocontrol of plant diseases. *Ann. Rev. Phytopathol.* **26**:75-91.
- Foster R.C., Rovira A.D., and Cock T.W.** (eds.) 1975. *Ultrastructure of the Root-Soil Interface*. The American Phytopathological Society, St Paul, Minnesota (USA).
- Fujita M., Tanaka K., Takahashi H., and Amemura A.** 1994. Transcription of the principal sigma-factor genes, *rpoD* and *rpoS*, in *Pseudomonas aeruginosa* is controlled according to the growth phase. *Mol. Microbiol.* **13**:1071-1077.
- Fuqua C., Winans S.C., and Greenberg E.P.** 1994. Quorum sensing in bacteria: the LuxR-LuxI family of cell density-response transcriptional regulators. *J. Bacteriol.* **176**:269-75.
- Fuqua C., Burbea M., and Winans S.C.** 1995. Activity of the *Agrobacterium* Ti plasmid conjugal transfer regulator TraR is inhibited by the product of the *TraM* gene. *J. Bacteriol.* **177**:1367-1373.
- Georgakopoulos D.G., Henson M., Panopoulos N.J., and Schroth M.N.** 1994a. Cloning of a phenazine biosynthetic locus of *Pseudomonas aureofaciens* PGS12 and analysis of its expression in vitro with the ice nucleation reporter gene. *Appl. Environ. Microbiol.* **60**:2931-2938.
- Georgakopoulos D.G., Henson M., Panopoulos N.J., and Schroth M.N.** 1994b. Analysis of expression of a phenazine biosynthetic locus of *Pseudomonas aureofaciens* PGS12 on seeds with a mutant carrying a phenazine biosynthetic locus-Ice nucleation reporter gene fusion. *Appl. Environ. Microbiol.* **60**:4573-4579.
- Gessard M.C.** 1892. Sur la fonction fluorescigène des microbes. *Ann. Inst. Pasteur* **6**:801-823.
- Grant F.A., Glover L.A., Killham K., and Prosser J.I.** 1991. Luminescence-based viable cell enumeration of *Erwinia carotovora* in the soil. *Soil. Biol. Biochem.* **23**:1021-1024.
- Gray K.M.** 1997. Intercellular communication and group behaviour in bacteria. *Trends Microbiol.* **5**:184-188.
- Gurusiddiah S., Weller D.M., Sarkar A., and Cook R.J.** 1986. Characterization of an antibiotic produced by a strain of *Pseudomonas fluorescens* inhibitory to *Gaeumannomyces graminis* var. *tritici* and *Pythium* spp. *Antimicrob. Agents Chemother.* **29**:488-95.
- Hale M.G., Lindsey D.L., and Hameed K.M.** 1973. Gnotobiotic culture of plants and related research. *The Botanic. Rev.* **39**:261-73.
- Hamdan H., Weller D.M., and Thomashow L.S.** 1991. Relative importance of fluorescent siderophores and other factors in biological control of *Gaeumannomyces graminis* var. *tritici* by *Pseudomonas fluorescens* 2-79 and M4-80R. *Appl. Environ. Microbiol.* **57**:3270-77.

- Haas D., Blumer C., and Keel C.** 2000. Biocontrol ability of fluorescent pseudomonads genetically dissected: importance of positive feedback regulation. *Curr. Opin. Biotechnol.* **11**:290-297.
- Haynes W.C., Stodola F.H., Locke J.M., Pridham T.G., Conway H.F., Sohns V.E., and Jackson R.W.** 1956. *Pseudomonas aureofaciens* Kluver and phenazine- α -carboxylic acid, its characteristic pigment. *J. Bacteriol.* **72**:412-17.
- Hengge-Aronis R.** 1993. Survival of hunger and stress: the role of *rpoS* in early stationary phase gene regulation in *E. coli*. *Cell* **72**:165-168.
- Henrici A.T.** 1928. *Morphologic Variation and Rate of Growth of Bacteria*. Microbiology Monographs. Bailliere, Tindall and Cox, London.
- Herrero M., de Lorenzo V., and Timmis K.N.** 1990. Transposon vectors containing non-antibiotic resistance selection markers for cloning and stable chromosomal insertion of foreign genes in gram-negative bacteria. *J. bacteriol.* **172**:6557-6567.
- Hewitt W.** 1977. *Microbiological Assay: An Introduction to Quantitative Principles and Evaluation*. Academic Press, New York.
- Hoagland D.R. and Arnon K.I.** 1950. The water-culture method for growing plants without soil. *Univ. Calif. Agric. Exp. Sta. Circ.* 347 rev.ed.
- Holden M.T.G., Ram Chhabra S., de Nys R., Stead P. Bainton N.J., Hill P.J. Manefield M., Kumar N., Labatte M., England D., Rice S., Givskov M., Salmond G.P., Stewart G.S., Bycroft B.W., Kjelleberg S., and Williams P.** 1999. Quorum-sensing cross talk: isolation and chemical characterisation of cyclic dipeptides from *Pseudomonas aeruginosa* and other Gram-negative bacteria. *Mol. Microbiol.* **33**:1254-1266.
- Holden M.T.G., Swift S., and Williams P.** 2000. New signal molecules on the quorum-sensing block. *Trends Microbiol.* **8**:101-103.
- Holliday P.** 1989. *A dictionary of plant pathology*. New York: Cambridge University Press, Inc.
- Horinouchi S. and Beppu T.** 1992. Autoregulatory factors and communication in Actinomycetes. *Annu. Rev. Microbiol.* **46**:377-398.
- Huisman G.W. and Kolter R.** 1994. Sensing starvation: a homoserine lactone-dependent signalling pathway in *Escherichia coli*. *Science.* **265**:537-539.
- Jablonski E. and DeLuca M.** 1978. Studies of the control of luminescence in *Beneckea harveyi*: Properties of the NADH and NADPH:FMN oxidoreductases. *Biochem.* **17**:672-678.
- Janse J.D., Derks J.H.J., Spit B.E., and van der Tuin W.R.** 1992. Classification of fluorescent soft rot *Pseudomonas* bacteria, including *P. marginalis* strains, using whole cell fatty acid analysis. *Syst. Appl. Microbiol.* **15**:538-553.
- Jansson J.K. and Prosser J.I.** 1997. Quantification of the presence and activity of specific microorganisms in nature. *Mol. Biotech.* **7**:103-120.
- Kaiser D. and Losick R.** 1993. How and why bacteria talk to each other. *Cell* **73**:873-885.

- Kaplan H.B. and Greenberg E.P.** 1985. Diffusion of autoinducer is involved in regulation of the *Vibrio fischeri* luminescence system. *J. Bacteriol.* **163**:1210-1214.
- Kersters K., Ludwig W., Vancanneyt M., De Vos P., Gillis M., and Schleifer K-H.** 1996. Recent changes in the classification of the Pseudomonads, an overview. *System. Appl. Microbiol.* **19**:465-477.
- Killham K.S., White D., and Leifert C.** 1998. Lux-marked bacteria and biological control in the rhizosphere. Joint Meeting of the Society for Applied Microbiology on Detection, Isolation and Manipulation of Soil and Rhizosphere Microorganisms. University of Warwick, UK.
- King J.M.H., Digrazia P.M., Applegate B.** 1990. Rapid, sensitive bioluminescent reporter technology for naphthalene exposure and biodegradation. *Science.* **249**:778-781.
- Kluyver A.J.** 1956. *Pseudomonas aureofaciens* nov. spec., and its pigments. *J. Bacteriol.* **72**:406-11
- Kolter R., Siegele D.A., Tormo A.** 1993. The stationary phase of the bacterial life cycle. *Annu. Rev. Microbiol.* **47**:855-874.
- Korth H.** 1974. Mixed carbon source effect in the phenazine- α -carboxylic acid synthesis and the aromatic pathway in *Pseudomonas* spp. *Arch. Microbiol.* **97**:245-52.
- Latifi A., Foglino M., Tanaka K., Williams P., and Lazdunski A.** 1996. A hierarchical quorum-sensing cascade in *Pseudomonas aeruginosa* links the transcriptional activators LasR and RhIR (VsmR) to expression of the stationary phase sigma factor RpoS. *Mol. Microbiol.* **21**:1137-1146.
- Laville J., Voisard C., Keel C., Maurhofer M., Defago G., and Haas D.** 1992. Global control in *P. fluorescens* mediating antibiotic synthesis and suppression of black rot of tobacco. *Proc. Natl. Acad. Sci. USA* **89**:1562-1567.
- Lazazzera B.A.** 2000. Quorum sensing and starvation: signals for entry into stationary phase. *Curr. Opin. Microbiol.* **3**:177-182.
- Lee S. and Fuhrman J.A.** 1990. DNA hybridisation to compare species compositions of natural bacterioplankton assemblages. *Appl. Environ. Microbiol.* **56**:739-746.
- Levy S.B.** 1978. Emergence of antibiotic-resistant bacteria in the intestinal flora of farm inhabitants. *J. Infect. Dis.* **137**:688-690.
- Lindow S.E.** 1995. The use of reporter genes in the study of microbial ecology. *Microbiol. Ecol.* **4**:555-566.
- van Loon L.C., Bakker P.A.H.M., Pieterse C.M.J.** 1998. Systemic resistance induced by rhizosphere bacteria. *Annu. Rev. Phytopathol.* **36**:453-483.
- Loper J.E., Suslow T.V., and Schroth M.N.** 1984. Lognormal distribution of bacterial populations in the rhizosphere. *Phytopathol.* **74**:1454-1460.

- de Lorenzo V., Herrero M., and Timmis K.N.** 1990. Mini-Tn5 transposon derivatives for insertion mutagenesis, promoter probing and chromosomal insertion of cloned DNA in Gram-negative bacteria. *J. Bacteriol.* **172**:6568-6572.
- de Lorenzo V., Herrero M., and Timmis K.N.** 1998. Mini-transposons in microbial ecology and environmental biotechnology. *FEMS Microbiol. Ecol.* **27**:211-224.
- Lowen P.C. and Heggen-Aronis R.** 1994. The role of the sigma factor RpoS (KatF) in bacterial global regulation. *Annu. Rev. Microbiol.* **48**:53-80.
- Lugtenberg B.J.J., and Dekkers L.C.** 1999. What makes *Pseudomonas* bacteria rhizosphere competent? *Environ. Microbiol.* **1**:9-13.
- Mazzola M., Cook R.J., Thomashow L.S., Weller D.M., and Pierson III L.S.** 1992. Contribution of phenazine antibiotic biosynthesis to the ecological competence of fluorescent pseudomonads in soil habitats. *Appl. Environ. Microbiol.* **58**:2616-24.
- Mazzola M., Fujimoto D.K., Thomashow L.S., and Cook R.J.** 1995. Variation in sensitivity of *Gaeumannomyces graminis* to antibiotics produced by fluorescent *Pseudomonas* spp. and effect of biological control of take-all of wheat. *Appl. Env. Microbiol.* **61**:2554-2559.
- McLean R.J.C., Whiteley M., Stickler D.J., and Fuqua W.C.** 1997. Evidence of autoinducer activity in naturally occurring biofilms. *FEMS Microbiol. Letters* **154**:259-263.
- Meikle A., Glover L.A., Kilham K., and Prosser J.I.** 1994. Potential luminescence as an indicator of activation of genetically-modified *Pseudomonas fluorescens* in liquid culture and in soil. *Soil Biol. Biochem.* **26**:747-755.
- Migula W.** 1894. Uber ein neues system der bakterien. *Arb. Bakteriolog. Inst. Karlsruhe* **1**:235-38
- Miller V.L., and Mekalanos J.J.** 1988. A novel suicide vector and its use in construction of insertion mutations: osmoregulation of outer membrane proteins and virulence determinants in *Vibrio cholerae* requires *toxR*. *J. Bacteriol.* **170**:2575-2583.
- Moore E.R.B., Mau M., Arnscheidt A., Van de Peer Y., De Wachter R., Collins M.D., Boettger E.C., and Timmis K.N.** 1996. Determination and comparison of the 16S rRNA gene sequences of species of *Pseudomonas* (*sensu stricto*) and estimation of intrageneric relationships. *System. Appl. Microbiol.* **19**:478-92.
- Morgan J.A.W., Winstanley C., Pickup K.W., Jones J.G., and Saunders J.K.** 1989. Direct phenotypic and genotypic detection of a recombinant pseudomonad population released into lake water. *Appl. Environ. Microbiol.* **55**:2537-3544.
- Muffler A., Traulsen D.D., Fischer D., Lange R., and Hengge-Aronis R.** 1997. The RNA-binding protein HF-I plays a role which is largely, but not exclusively, due to its role in expression of the sigmaS subunit of RNA polymerase in *Escherichia coli*. *J. Bacteriol.* **179**:297-300.
- Nealson K.H.** 1977. Autoinduction of bacterial luciferase. Occurrence, mechanism and significance. *Arch. Microbiol.* **112**:73-79.

- Nealson K.H.** 1999. Early observations defining quorum-dependent gene expression. In: *Cell-Cell Signalling in Bacteria*, (Dunny G.M. and Winans S.C.), pp.277-290. American Society for Microbiology, Washington D.C.
- Neidhardt F.C., Ingraham J.L., and Schaechter M.** (eds.). 1990. *Physiology of the Bacterial Cell: A molecular Approach*. Sinauer Associates, Sunderland, U.S.A.
- Newman D.L. and Shapiro J.A.** 1999. Differential *fiu-lacZ* regulation linked to *Escherichia coli* colony development. *Mol. Microbiol.* **33**:18-32.
- Nogueira T. and Springer M.** 2000. Post-transcriptional control by global regulators of gene expression in bacterial. *Curr. Opin. Microbiol.* **3**:154-158.
- Palleroni N.J., Kunisawa R., Contopoulos R., and Doudoroff M.** 1973. Nucleic acid homologies in the genus *Pseudomonas*. *Int. J. Syst. Bacteriol.* **23**:333-339.
- Palleroni N.J.** 1984. *Pseudomonadaceae*. In: *Bergey's Manual of Systematic Bacteriology*, Vol.1 (Krieg N.R., and Holt J.G., eds.), pp. 141-199. Williams and Wilkins, Baltimore.
- Palleroni N.J.** 1992. Present situation in the taxonomy of aerobic pseudomonads. In: *Pseudomonas Molecular Biology and Biotechnology*, (Galli E., Silver S., and Witholt B.), pp.105-115. American Society for Microbiology, Washington D.C.
- Palleroni N.J.** 1993. *Pseudomonas* classification. A new case history in the taxonomy of Gram-negative bacteria. *Antonie van Leeuwenhoek Int. J. Gen. Mol. Microbiol.* **64**:231-251.
- Perrin L.C., Wilson W.R., Denny W.A., and McFadyen W.D.** 1999. The design of cobalt(III) complexes of phenazine-1-carboxamides as prointercalators and potential hypoxia-selective cytotoxins. *Anticancer Drug Des.* **14**:231-241.
- Pesci E.C., and Iglewski B.H.** 1997. The chain of command in *Pseudomonas* quorum sensing. *Trends Microbiol.* **5**:132-134.
- Pesci E.C., Pearson J.P., Seed P.C, and Iglewski B.H.** 1997. Regulation of *las* and *rhl* quorum sensing in *Pseudomonas aeruginosa*. *J. Bacteriol.* **179**:3127-3132.
- Pesci E.C., and Iglewski B.H.** 1999. Quorum sensing in *Pseudomonas aeruginosa*. In: *Cell-Cell Signalling in Bacteria* (Dunny G.M., and Winans S.C., eds.), pp.147-155. American Society for Microbiology, Washington, U.S.A.
- Pesci E.C., Millbank J.B., Pearson J.P., McKnight S., Kende A.S., Greenberg E.P., Iglewski B.H.** 1999. Quinolone signalling in the cell-to-cell communication system of *Pseudomonas aeruginosa*. *Proc. Natl. Acad. Sci. USA.* **96**:11229-11234.
- Pesci E.C.** 2000. New signal molecules on the quorum-sensing block: Response. *Trends Microbiol.* **8**:103-104.
- Picker S.D., and Fridovich I.** 1984. On the mechanism of production of superoxide radical by reaction mixtures containing NADH, phenazine methosulfate, and nitroblue tetrazolium. *Arch. Biochem. Biophys.* **228**:155-158.

- Pierson E.A., Wood D.W., Cannon J.A., Blachere F.M., and Pierson III L.S.** (1998). Interpopulation signalling via *N*-acyl-homoserine lactones among bacteria in the wheat rhizosphere. *Mol. Plant Microb. Interact.* **11**:1078-1084.
- Pierson III L.S., and Thomashow L.S.** 1992. Cloning and heterologous expression of the phenazine biosynthetic locus from *Pseudomonas aureofaciens* 30-84. *Mol. Plant Microb Interact.* **5**:330-339.
- Pierson III L.S., Keppenne V.D., and Wood D.W.** 1994. Phenazine antibiotic biosynthesis in *Pseudomonas aureofaciens* 30-84 is regulated by PhzR in response to cell density. *J. Bacteriol.* **176**:3966-3974.
- Pierson III L.S., Gaffney T., Lam S., and Gong F.** 1995. Molecular analysis of genes encoding phenazine biosynthesis in the biological control bacterium *Pseudomonas aureofaciens* 30-84. *FEMS Microbiol. Letters* **134**:299-307.
- Pierson III L.S., and Pierson E.A.** 1996. Phenazine antibiotic production in *Pseudomonas aureofaciens*: Role in rhizosphere ecology and pathogen suppression. *FEMS Microbiol. Letters* **136**:101-08.
- Pierson III L.S., Wood D.W., and von Bodman S.B.** 1999. Quorum sensing in plant-associated bacteria. In: *Cell-Cell Signalling in Bacteria*. Dunny G.M., and Winans S.C. (eds.). Washington: American Society for Microbiology, pp. 101-115.
- Prescott L.M., Harley J.P., and Klein A.D.** (eds.). 1996. *Microbiology*, 3rd ed. WCB, London.
- Prosser J.I.** 1994. Molecular marker systems for detection of genetically engineered microorganisms in the environment. *Microbiol.* **140**:5-17.
- Prosser J.I., Killham K., L.A. Glover, and Rattray E.A.S.** 1996a. Luminescence-based systems for detection of bacteria in the environment. *Crit. Rev. Biotech.* **16**:157-183.
- Prosser J.I., Rattray E.A.S., Killham K., and L.A. Glover.** 1996b. *lux* as a marker gene to track microbes, chapter 6. In: *Molecular Microbiol Ecology Manual*. Kluwer Academic Publishers, The Netherlands.
- Rattray E.A.S., Prosser J.I., Killham K., and Glover L.A.** 1990. Luminescence-based non-extractive technique for in situ detection of *Escherichia coli* in soil. *Appl. Environ. Microbiol.* **56**:3368-3374.
- Rattray E.A.S.** 1992. Development of a bioluminescence-based detection system for a genetically modified microorganism [dissertation]. Aberdeen (UK): University of Aberdeen.
- Rattray E.A.S., Glover L.A., Prosser J.I., and Killham K.** 1995. Characterisation of rhizosphere colonisation by a luminescent construct of *Enterobacter cloacae* at the single cell and population levels. *Appl. Environ. Microbiol.* **61**:2950-2957.
- Reimmann C., Beyeler M., Latifi A., Winteler H., Foglino M., Lazdunski A., and Haas D.** 1997. The global regulator GacA of *Pseudomonas aeruginosa* PAO1 positively controls the production of the autoinducer *N*-butyryl-homoserine lactone and the formation of the virulence factors pyocyanin, cyanide, and lipase. *Mol. Microbiol.* **24**:309-319.
- Ruby E.G., Greenberg E.P., Hastings J.W.** 1980. Planktonic marine luminous bacteria: species distribution in the water column. *Appl. Environ. Microbiol.* **39**:302-306.

- Sarniguet A., Kraus J., Henkels M.D., Muehlchen A.M., and Loper J.E.** 1995. The sigma factor α^s affects antibiotic production in *Pseudomonas fluorescens* Pf-5. *Proc. Natl. Acad. Sci. USA.* **29**:12255-12259.
- Schaechter M., Maaløe, O., and Kjeldgaard N.O.** 1958. Dependency on medium and temperature of cell size and chemical composition during balanced growth of *Salmonella typhimurium*. *J. Gen. Microbiol.* **19**:592-606.
- Schaechter M., Williamson J.P., Hood J.R., and Koch A.L.** 1962. Growth, cell, and nuclear division in some bacteria. *J. Gen. Microbiol.* **29**:421-434.
- Schauer A.T.** 1988. Visualizing gene expression with luciferase fusions. *Trends Biotech.* **6**:23-27.
- Schippers B.** 1993. Exploitation of microbial mechanisms to promote plant health and plant growth. *Phytoparasitica* **21**:275-279.
- Schroth M.N. and Hancock J.G.** 1982. Disease-suppressive soil and root-colonising bacteria. *Science* **216**:1376-81
- Shadel G.S., and Baldwin T.O.** 1991. The *Vibrio fischeri* LuxR protein is capable of bidirectional stimulation of transcription and both positive and negative regulation of the *luxR* gene. *J. Bacteriol.* **173**:568-574.
- Shadel G.S., and Baldwin T.O.** 1992. Identification of a distantly located regulatory element in the *luxD* gene required for negative autoregulation of the *Vibrio fischeri luxR* gene. *J. Biol. Chem.* **267**:7690-7695.
- Shapiro J.A.** 1983. The use of *Mudlac* transposons as tools for vital staining to visualize clonal and non-clonal patterns of organisation in bacterial growth on agar surfaces. *J. Gen. Microbiol.* **130**: 1169-1181.
- Shapiro J.A., and Dworkin M.** (eds.). 1997. *Bacteria as Multicellular Organisms*. Oxford University Press, Oxford (UK).
- Simons M., van der Bij A.J., Brand I., de Weger L.A., Wijffelman C.A., and Lugtenberg B.J.** 1996. Gnotobiotic system for studying rhizosphere colonisation by plant growth-promoting *Pseudomonas* bacteria. *Mol. Plant Microb. Interact.* **9**:600-07.
- Slininger P.J., and Jackson M.A.** 1992. Nutritional factors regulating growth and accumulation of phenazine-1-carboxylic acid by *Pseudomonas fluorescens* 2-79. *Appl. Microbiol. Biotech.* **37**:388-92.
- Slininger P.J., and Shea-Wilbur M.A.** 1995. Liquid-culture pH, temperature, and carbon (not nitrogen) source regulate phenazine productivity of the take-all biocontrol agent *Pseudomonas fluorescens* 2-79. *Appl. Microbiol. Biotech.* **43**:794-800.
- Smit E., van Elsas J.D., and van Veen J.A.** 1992. Risks associated with the application of genetically modified microorganisms in terrestrial ecosystems *FEMS Microbiol. Rev.* **88**:263-278.
- Stead P., Rudd B.A.M., Bradshaw H., Noble D., and Dawson M.J.** 1996. Induction of phenazine biosynthesis in cultures of *Pseudomonas aeruginosa* by *N*-(3-oxohexanoyl) homoserine lactone. *FEMS Microbiol. Letters* **140**:15-22.

- Stewart G.S.A.B., and Williams P.** 1992. *lux* genes and the applications of bacterial bioluminescence. *J. Gen. Microbiol.* **138**:1289-1300.
- Strange R.N.** 1993. *Plant Disease Control: Towards Environmentally Acceptable Methods*, 354 pp. Chapman and Hall, New York.
- Surette M.G., Miller M.B., and Bassler B.L.** 1999. Quorum sensing in *Escherichia coli*, *Salmonella typhimurium*, and *Vibrio harveyi*: a new family of genes responsible for autoinducer production. *Proc. Natl. Acad. Sci. USA.* **96**:1639-1644.
- Swift S., Winson M.K., Chan P.F., Bainton N.J., Birdsall M., Reeves P.J., Rees C.E.D., Chhabra S.R., Hill P.J., Throup J.P., Bycroft B.W., Salmond G.P.C., Williams P., and Stewart G.S.A.B.** 1993. A novel strategy for the isolation of luxI homologues: Evidence for the widespread distribution of a LuxR:LuxI superfamily in enteric bacteria. *Mol. Microbiol.* **10**:511-20.
- Swift S., Throup J., Williams P., Salmond G.P.C., Stewart G.S.A.B.** 1996. Quorum sensing: A population-density component in the determination of bacterial phenotype. *Trends Biochem. Sci.* **21**:214-219.
- Swift S., Williams P., and Stewart G.S.A.B.** 1999. *N*-acylhomoserine lactones and quorum sensing in proteobacteria. In: *Cell-Cell Signalling in Bacteria* (Dunny G.M. and Winans S.C., eds.), pp.291-313. American Society for Microbiology, Washington, D.C.
- Tang C-S., and Young C-C.** 1982. Collection and identification of allelopathic compound from the undisturbed root system of Bigalta Limpograss (*Hemarthria altissima*). *Plant Physiol.* **69**:155-60.
- Telford G., Wheeler D., Williams P., Tomkins P.T., Appleby P., Sewell H., Stewart G.S.A.B., Bycroft B.W., and Pritchard D.I.** 1998. The *Pseudomonas aeruginosa* quorum-sensing signal molecule, *N*-(3-oxododecanoyl)-L-homoserine lactone has immunomodulatory activity. *Infect. Immun.* **66**:36-42.
- Teplitski M., Robinson J.B., and Bauer W.D.** 2000. Plant secretes substances that mimic bacterial *N*-acyl homoserine lactone signal activities and affect population density-dependent behaviours in associated bacteria. *Mol. Plant Microb. Interact.* **13**:637-648.
- Thomashow L.S., and Weller D.M.** 1988. Role of a phenazine antibiotic from *Pseudomonas fluorescens* 2-79 in biological control of *Gaeumannomyces graminis* var. *Tritici*. *J. Bacteriol.* **170**:3499-508.
- Thomashow L.S., and Weller D.M.** 1990. In: *Biological Control of Soil-Borne Plant Diseases – Progress and Challenges for the Future* (Hornby D., Cook R.J., Henis Y., Ko W.H., Rovira A.D., Schippers B., and Scott P.R. (eds.) pp.109-122. CAB International, Wallingford, UK.
- Thomashow L.S., Weller D.M., Bonsall R.F., and Pierson III L.S.** 1990. Production of the antibiotic phenazine-1-carboxylic acid by Fluorescent *Pseudomonas* species in the rhizosphere of Wheat. *Appl. Environ. Microbiol.* **56**:908-12.
- Thomashow L.S., and Pierson III L.S.** 1991. Genetic aspects of phenazine antibiotic production by fluorescent pseudomonads that suppress take-all disease of wheat. In: *Advances in Molecular Genetics of Plant-Microbe Interactions, Vol. 1* (Hennecke H. and Verma D.P.S., eds.), pp. 443-449. Kluwer Academic Publishers, Netherlands.

- Thomashow L.S.** 1996. Biological control of plant root pathogens. *Curr. Opin. Biotech.* **7**:343-347.
- Throup J.P., Camara M., Briggs G.S., Winson M.K., Chhabra S.R., Bycroft B.W., Williams P., and Stewart S.A.B.** 1995. Characterisation of the *yenI/yenR* locus from *Yersinia enterocolitica* mediating the synthesis of two *N*-acyl homoserine lactone signal molecules. *Mol. Microbiol.* **17**:345-56.
- Toohey J.I., Nelson C.D., and Krotkov G.** 1965. Toxicity of phenazine carboxylic acid to some bacteria, algae, higher plants, and animals. *Can. J. Bot.* **43**:1151-1155.
- Torsvik V., Goksoyr J., and Daae F.L.** 1990. High diversity in DNA of soil bacteria. *Appl. Environ. Microbiol.* **56**:782-787.
- Turner J.M., and Messenger A.J.** 1986. Occurrence, biochemistry and physiology of phenazine pigment production. *Adv. Microb. Physiol.* **27**:211-75.
- Vancanneyt M., Witt S., Abraham W.R., Kersters K., and Fredrickson H.L.** 1996. Fatty acid content in whole-cell hydrolysates and phospholipid fractions of pseudomonads: A taxonomic evaluation. *Syst. Appl. Microbiol.* **19**:528-540.
- de Weger L.A., van der Vlugt C.I.M., Wijffes A.H.M., Bakker P.A.H.M., Schippers B., and Lugtenberg B.J.J.** 1987. Flagella of a plant growth stimulating *Pseudomonas fluorescens* strain are required for colonisation of potato roots. *J. Bacteriol.* **169**:2769-2773.
- de Weger L.A., Dunbar P., Mahafee W.F., Lugtenberg B.J.J., and Sayler G.S.** 1991. Use of bioluminescence makers to detect *Pseudomonas* spp. in the rhizosphere. *Appl. Environ. Microbiol.* **57**:3641-3644.
- Weller D.M.** 1984. Distribution of a take-all suppressive strain of *Pseudomonas fluorescens* on seminal roots of winter wheat. *Appl. Environ. Microbiol.* **48**:897-899.
- Weller D.M.** 1988. Biological Control of soilborne plant pathogens in the rhizosphere with bacteria. *Ann. Rev. Phytopathol.* **26**:379-407.
- Whiteley M., Parsek M.R., and Greenberg E.P.** 2000. Regulation of quorum sensing by RpoS in *Pseudomonas aeruginosa*. *J. Bacteriol.* **182**:4356-4360.
- White D., Leifert C., Ryder M.H. and Killham K.** 1996. *Lux* gene technology – a strategy to optimise biological control of soil-borne diseases. *New Phytol.* **133**:173-181.
- Whiteley M., Parsek M.R., and Greenberg E.P.** 2000. Regulation of quorum sensing by RpoS in *Pseudomonas aeruginosa*. *J. Bacteriol.* **182**:4356-4360.
- Willis D.K., Hrabak E.M., Rich J.J., Barta T.M., Lindow S.E., and Panopoulos N.J.** 1990. Isolation and characterisation of a *Pseudomonas syringae* pv. *syringae* mutant deficient in lesion forming ability on bean. *Mol. Plant Microb. Interact.* **3**:149-156.
- Wilson K.J.** 1995. Molecular techniques for the study of rhizobial ecology in the field. *Soil. Biol. Biochem.* **27**:501-514.
- Wilson M. and Lindow S.E.** 1993. Phenotypic plasticity affecting survival in *Pseudomonas syringae*. *Appl. Env. Microb.* **59**:410-416.

Wilson K.J., Sessitsch A., Corbo J.C., Giller K.E., Akkermans A.D.L., and Jefferson R.A. 1995. β -Glucuronidase (GUS) transposons for ecological and genetic studies of rhizobia and other Gram-negative bacteria. *Microbiol.* **141**:1691-1705.

Winson M.K., Swift S., Fish L., Throup J.P., Jørgensen F., Chhabra S.R., Bycroft B.W., Williams P., and Stewart G.S.A.B. 1998. Construction and analysis of *luxCDABE*-based plasmid sensors for investigating *N*-acyl homoserine lactone-mediated quorum sensing. *FEMS Microbiol. Letters* **163**:185-192.

Wood D.W., and Pierson III L.S. 1996. The *phzI* gene of *Pseudomonas aureofaciens* 30-84 is responsible for the production of a diffusible signal required for phenazine antibiotic production. *Gene* **168**:49-53.

Wood D.W., Gong F., Daykin M.M., Williams P., and Pierson III L.S. 1997. *N*-acyl-homoserine lactone-mediated regulation of phenazine gene expression *Pseudomonas aureofaciens* 30-84 in the wheat rhizosphere. *J. Bacteriol.* **179**:7663-7670.

Yanisch-Peron C., Viera J., and Messing J. 1985. Improved M13 phage cloning vectors and host strains: nucleotide sequences of the M13mp18 and pUC19 vectors. *Gene* **33**:103-109.

You Z., Fukushima J., Tanaka K., Kawamoto S., and Okuda K. 1998. Induction of entry into the stationary growth phase in *Pseudomonas aeruginosa* by *N*-acylhomoserine lactone. *FEMS Microbiol. Lett.* **164**:99-106.